Sudan University of Science and Technology
College of Graduate Studies

Synthesis and Characterization of Vanadium Complexes as Insulin Mimics for Diabetes Types 2 and Their Impact on Rats

تحضير وتوصيف معقدات الفاناديوم مقلدات للأنسيولين في مرض السكري من النوع الثاني وأثرها على الفئران

AThesis Submitted in Fulfillment of the Requirements for the Degree of Doctor of Philosophy in Chemistry

By

Enas Salah Aldin Mohammed Dafalla

Supervisor

Dr. Hassan Ibrahim Nimir

Co-Supervisor

Professor Elmugdad Ahmed Ali

April 2018

DEDICATION

To my Father, whose love for me has no boundaries who taught me the value of hard work. Thank you so much Father.

To my Family for their continuous support and unwavering belief that encourage me to work hard.

I would like to thank all my Friends, my Colleagues for their undying support.

ACKNOWLEDGMENTS

First and foremost, I thank **Allah** (almighty) for helping me to accomplish this work.

I would like to express deep thanks to my supervisors, **Dr. Hassan Ibrahim Nimir** and **Prof .Elmugdad Ahmed Ali**, for their guidance, encouragement and gracious support throughout the research, their expertise in the field that motivated me to work in this area and their faith in me at every stage of this research.

I am very much indebted to **Dr. Mohamed Refaat Shehata**-Cairo University-Department of Chemistry for his useful directions during the stages of preparation of solution, analytical procedures and interpretation of the results.

I would like to thank **Dr. Dalia Fayed,** Department of Therapeutic Chemistry, National Research Centre, Cairo, for helping me and advising in the bioactivity work.

I would like to thank Alzaeim Alazhari University for providing the financial support.

ABSTRACT

In this research oxovanadium complexes and di oxovanadium complexes (C1-C15) and ligands (L1-L16), specifically, organic ligands considered to be of biological importance, as insulin mimics. They were synthesized, and divided in four groups: vanadium salts with amino acids, carboxylic acids, thiosemicarbazone, 1.10 phenanthoroline, 3-Hydroxypyridine and Schiff-base ligands. The complexes were characterized by conductivity measurements; magnetic susceptibility, UV-Vis, IR, thermal gravimetric analysis TGA, ^{1}H and ^{13}C NMR.The molecular structure of the complexes (C1- C15) were confirmed using the DFT calculation to obtain the optimized geometries using the Gaussian 09 program at the B3LYP/LANL2DZ level of theory. The vanadium atoms in the complexes were coordinated in different distorted geometries with ligands (L1- L16), acting as a bi-dentate and tridentate ligands through the amino nitrogen atoms, sulfur atom, phenol oxygen atom and carboxylate oxygen atom.

The total energies for the highest occupied molecular orbital (HOMO) energies, the lowest unoccupied molecular orbital (LUMO) energies and the dipole moment for the ligands (L1-L16), and their complexes (C1-C15), were calculated, It was found that the more negative value of total energy of the complexes than that of free ligands indicates their extra stability polarity, much larger enhance than those of free ligands.

As vanadium compounds insulin sensitivity and act as insulin mimetic and has anti-diabetic effects, complexes of C1, C6, C10, C13 were further tested on rats after they had been injected by streptozotocin, that causes a type 2 diabetes. In this study intra-peritoneal administration active anti-diabetic organic vanadium complexes. After four weeks of complexes treatment, the result showed significant

hyperglycemia improvement indicating that vanadium complexes had anti-diabetic and insulin-sensitizing effects on the diabetic rats.

المستخلص

في هذا البحث تم تحضير خمسة عشر معقد للفاناديوم ،معقدات أوكسوفاناديوم ومعقدات ديوكسوفاناديوم مع عدد من اللواقط العضوية ذات الفعالية البيولوجية كمركبات مقلدة للأنسولين، تم تحضيرها وتقسيمها إلى أربع مجموعات:أملاح الفاناديوم التي ترتبط فيها ذرة فانديوم مع لواقط الأحماض الأمينية والأحماض الكاربوكسيلية، ومركبات الثيوسيمي كاربازون وقواعد شيف . تم تحليل المعقدات عن طريق قياس التوصيلية والمغناطيسية والتحليل المثقالي الحراري. وتوصيفها بإستخدام جهاز الأشعة فوق البنفسجية، الأشعة تحت الحمراء، الرنين المغناطيسي. تم التأكد من التركيب الجزيئي للمعقدات(C1- C15) باستخدام برنامج Gaussian09 بتطبيق نظرية الكثافة الوظيفية على مستوى B3LYP / LANL2DZ للحصول على الشكل الهندسي الأمثل للمعقدات الناتجة من أرتباط فاناديوم بذرة الكبريت والنيتروجين والأكسجين في اللواقط أحادية السن وثنائية السن.

تم حساب الطاقات الكلية ،طاقة أعلى مدارات جزيئية ،طاقة أقل مدارات جزيئية، والعزم المغناطيسي للواقط والمعقدات ،وجدت أن المعقدات ذات طاقة سلبيه عاليه أعلى من الطاقة السلبية للواقط مما يثبت أستقرارية هذه المعقدات .

بما أن مركبات الفاناديوم تعتبر معززه لحساسية الأنسولين وتعمل كموادمقلدة له وكمضاد لمرض السكري تم أختبار معقدات C1, C6, C10, C13 على فئران التجارب المصابة بمرض السكري من النوع الثاني بعد حقنها بمادة STZ المسببه للمرض. بعد أربع أسابيع من حقن المعقدات لوحظ التحسن في أرتفاع سكر الدم. وأثبتت المعقدات فعاليتها كمواد مضاده للسكرومعززه للأنسلين في فئران التجارب .

List of Contents

List of Tables

List of Figures

LIST OF ABBREVIATIONS

gly	Glycine
tyro	L-Tyrosine
cys	L-Cysteine
homo	L-Homoserine
tart	Tartaric acid
2-Pico	2-picolinic acid
2.6Py	2.6pyridine carboxalic acid
phen	1.10phenanthrolin
SALTSC	Salicylsaldehyde Thiosemicarbazone
ClBTSC	2-Chlorobenzaldehyde Thiosemicarbazone
3-APTSC	3-Amino pyridine Thiosemicarbazone
3-HyP	3-Hydroxypyridine
DMEDA	N. N Dimethylethelynediamine
DAP	1.2 Diamine propane
2-PA	2-Picolylamine
STZ	Streptozotocin
IR	Infrared Spectrophotometer
UV	Ultra Violet Spectrophotometer
NMR	Nuclear Magnetic Resonance Spectrophotometer
TGA	Thermo gravimetric studies
DFT	Density Functional Theory
HOMO	Highest Occupied Molecular Orbital
LUMO	Lowest Unoccupied Molecular Orbital
SPSS	Statistical Package for the Social Sciences
EPR	Electron Paramagnetic Resonance

kDa.	kilodalton
DM	Diabetes Mellitus
DMF	Dimethyleformamide
Dmso	Dimethyl Sulfoxide
ppt	Precipitate

1.1 History of vanadium

In 1802, the mineralogist Andres Manuel del Rio (1764-1849) believed that he discovered a new metal similar to chromium and uranium in a brown lead mineral from Mexico. He first named it *panchromium,* because of the varied colours of its salts, but changed the name later on in *erythronium* (‘red’) as a reference to the red colour of its salts when treated with acids. However, soon he withdrew his discovery, since a French chemist incorrectly declared that this new element was only impure chromium. Vanadium was rediscovered in 1831 by the Swedish chemist Nils Gabriel Sefström (1787-1845) in remnants of iron ore quarried at the Taberg in Småland. He named the element *vanadin*, after the goddess of beauty, youth and love, Vanadis, referring to the beautiful multicoloured compounds. Vanadis is a common name for Freyja according to the Northern Germanic tribes. After Sefström announced the discovery of vanadium, the brown lead ore from Mexico was reanalysed and it was shown that it really contained vanadium instead (Ligtenbarg, 2011).

1.2 Occurrence, Distribution and Impact

Vanadium (Atomic No. 23) is comparatively abundant in the universe. At 0.0001%, its cosmic abundance is comparable to that of copper and zinc. The cosmic abundance is, e.g., reflected in chondritic meteorites, which contain 220 atoms of the isotope ^{51}V in relation to 106 silicium atoms. Cosmic formation of vanadium is based on the (α, γ) cascade up to ^{52}Cr, followed by the reaction (Kanamori and Tsuge, 2012).

$$^{52}Cr\ (n,\ \alpha)\ ^{53}Cr\ (n,\ \gamma)\ ^{51}Ti\ (\beta^-,\ \gamma)\ ^{51}V$$

The isotope ^{51}V accounts for 99.75% of the naturally occurring isotopes. The remaining 0.25% is supplied by the isotope ^{50}V, whose cosmic formation is due to an electron-capture process by ^{50}Cr

$$^{50}_{24}Cr + {}_{-1}^{0}e \quad \beta^{-}_{23} \rightarrow {}^{50}V$$

^{50}V is *very* mildly radioactive, decaying with a half life of 1.4×10^{17} years either by electron capture/positron emission (to generate ^{50}Ti; 83%) or via β^- decay (to form ^{50}Cr; 17%):

$$^{50}_{23}V + \beta^{-} \rightarrow {}^{50}_{22}Ti \,/\, {}^{50}_{23}V \rightarrow {}^{50}_{22}Ti + \beta^{+} \text{ and } {}^{50}_{23}V \rightarrow {}^{50}_{24}Cr + \beta^{-}$$

In the Earth's crust, vanadium is 22nd in abundance (0.013% w/w) and thus more abundant than copper and zinc. In sea water, commonly considered the cradle of life on our planet, the average concentration of vanadium, which is present mainly in the form of ion pairs $Na^{+}H_2VO_4^{-}$, is around 30 nM. Vanadium is thus the second most abundant transition element in marine environments, outmatched only by molybdenum [ca 100 nm molybdate(VI)]. Vanadium is supplied by riverine input; scavenging by vent-derived iron oxides helps to control the concentration and cycling of vanadium in the oceans. The vanadium content of human blood plasma is around 200 nM this ca 10-fold increase with respect to sea water points to its possible biological function. The vanadium level in tissue is even higher, averaging $0.3 mgkg^{-1}$ (ca 6μg). Vanadium accumulates in bones, liver and kidneys.
Vanadium is a ubiquitous trace element. The average content in shales, which are particularly rich in vanadium, is 0.012% w/w. In sandstone and carbonate-based and magmatic rock, the vanadium content is lower by one order of magnitude

More than 120 vanadium-based minerals are known, containing the element in cationic and anionic form, and in the oxidation states III, IV and V. A cross-section representing these characteristics and the general inorganic chemistry of vanadium is provided in **Table 1.1**. The most common minerals are vanadinite **Figure 1.1**, patronite, roscoelite (vanadium mica), carnotite and descloizite. Vanadium minerals are essentially formed in the course of geological processes. An epigenic formation of specific minerals is, however, conceivable: certain bacteria, such as *Pseudomonas vanadiumreductans* and *Shewanella oneidensis* (Rehder, 2008).

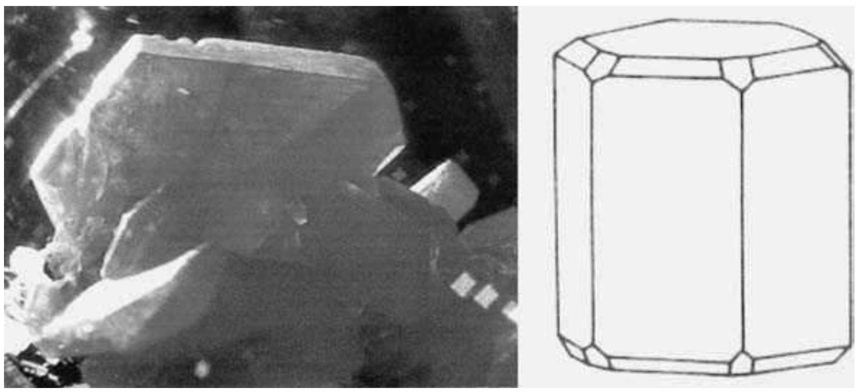

Figure 1.1 Crystals and crystal habit of (hexagonal) vanadinite, $Pb_5[VO_4].Cl$ The crystals are deep orange–red.

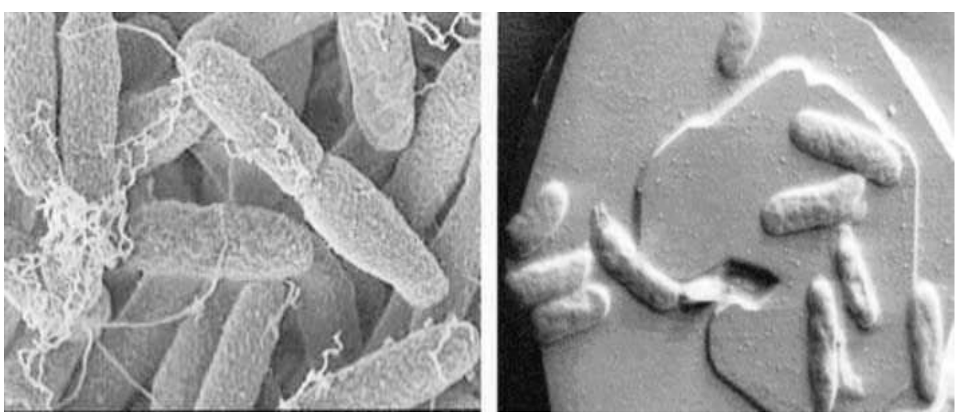

Figure 1.2 Scanning electron microscopy images of the soil bacterium *Shewanella oneidensis*(strain MR-1). The picture on the right shows the bacterium on haematite (Fe_2O_3).

Table 1.1 Selection of vanadium minerals with information on the nature of vanadium.

Minerals name	Formula	Oxidation state of vanadium
Karelianite	V_2O_3	III
Roscoelite	$K(Al, V)_2(OH, F)_2[AlSi_3O_{10}]$	III
Haggite	$VO(OH).VO(OH)_2$	III and IV
Minasrsgrite	$VOSO_4.5H_2O$	IV
Simplotite	$Cu[V_4O_9]$	IV
Patronite	$S_4V= V(S_2)_2$	IV
Vanoxite	$2V_2O_4.V_2O_5.8H_2O$	IV, V
Sherwoodite	$Ca_9Al_2V_4V_{24}O_{80}.56H_2O$	IV, V
Navajoitite	$V_2O_5.3H_2O$	V
Munirite	Na[VO3]	V
Steigerite	$Al[VO4].3H_2O$	V
Carnotite	$K(UO_2)[VO_4]$	V
Vanadinite	$Pb_5[VO_4].Cl$	V
Descloizite	$Pb(Zn, Cu) OH[VO_4]$	V
Chervetite	$Pb_2[V_2O_7]$	V
Barnesite	$Na_2[V_6O_{16}]$	V
Hummerite	$K_2Mg_2[V_{10}O_{28}]$	V
Sulvanite	$Cu_3[VS_4]$	V

A high vanadium content is often associated with high sulfur contents. The reasons for the notable enrichment of vanadium in fossils compared with bio-mass precursors such as bacteria, protozoans, algae, plants and animals are still under debate. Possible mechanisms for a secondary input of vanadium in decaying material include accumulation by phenolic compounds formed by degradation of lignin, by humic substances, and absorption from ground water, in particular in areas where the ground water is enriched by weathering of vanadium containing minerals and rocks. Anoxic conditions appear to promote vanadium absorption, possibly because of the very low solubility of vanadyl (VO^{2+}) [6] hydroxides at a pH of around 7. In the case of crude oil, accumulation of vanadium may also be traced back to vanadium scavenging as oil passes through sediments rich in vanadium.

Crude oil contains various porphinogens, derived from chlorophylls and haems of decayed marine organisms. Porphinogens are excellent complexing agents for the vanadyl cation. Most of the vanadium contained in carbonaceous sedimentary rock, asphaltene/kerogene and geologically young oil is in fact present in the form of vanadyl porphyrins; see, e.g., the chlorophyll-derived complex in **Figure 1.3**. Old oils contain most of the vanadium in non-porphinogenic compounds, examples of which are also shown in **Figure 1.3**.

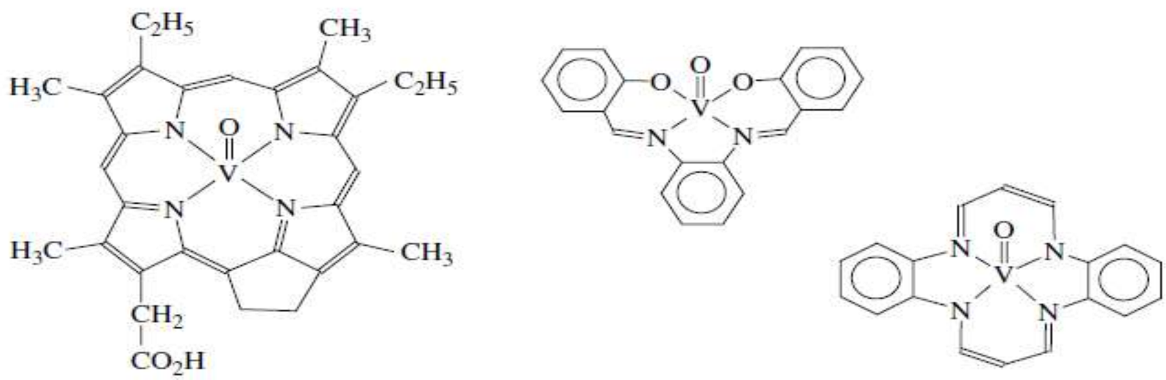

Figure 1.3 Examples of vanadyl compounds in crude oil. Left: porphinogenic (vanadyldesoxiphyllerythrin); middle and right, non-porhinogenic.

Vanadium occurs with an abundance of 0.014% in the earth's crust and is widespread. The element is the second most abundant transition metal in the oceans (50 nM). Some aquatic organisms are known to accumulate vanadium.

For instance, members of an order of tunicates (*Ascidiacea*) concentrate vanadium up to 0.15 M in specialised blood cells. However, the actual function of vanadium and the nature of the vanadium compounds present in these organisms remain unclear. A naturally occurring vanadium-containing enzyme, vanadium 16 bromoperoxidase was discovered in the marine brown alga, *Ascophyllum Nodosum.* Since then, several vanadium haloperoxidases have been isolated and studied. Many of these enzymes have been detected in brown and red seaweeds.

However, the accumulation of vanadium is not restricted to marine organisms, since vanadium containing haloperoxidases have also been isolated from terrestrial fungi and a vanadium compound of low molecular weight (amavadin) has been isolated from the toadstool *Amanita muscaria*(Kanamori and Tsuge, 2012).

1.3 The chemistry of vanadium

Vanadium has an electronic configuration of [Ar] $4s^2$ $3d^3$ and can exist in eight oxidation states ranging from –3 to +5, but with the exception of –2. Only the three highest, +3, +4 and +5, are important in biological systems. Under ordinary conditions, the +4 and +5 oxidation states are the most stable. The coordination chemistry of vanadium is strongly influenced by the oxidation/reduction properties of the metal centre and the chemistry of vanadium ions in aqueous solution is limited to oxidation states of +2, +3, +4 and +5. Vanadium compounds of oxidation state of +2 and +3 are unstable to air and their compounds are predominantly octahedral (NEJO, 2009).

Table 1.2 Halides, oxides, sulfides of Vanadium

Compounds	**Oxidation state**			
	+5	**+4**	**+3**	**+2**
Oxides	V_2O_5	VO_2	V_2O_3	VO
Halides	VF_5	VF_4-VCl_4- VBr_4	VF_3-VCl_3 VBr_3-VI_3	VF_2-VCl_2, VBr_2- VI_2
Sulfides	-	-	V_2S_3	VS

Besides the 4 oxides of vanadium shown, a number of other phases of intermediate composition have been identified and the lower oxides in particular have wide ranges of homogeneity. V_2O_5 is orange yellow when pure and is the final product when the metal is heated in an excess of oxygen but contamination with lower oxides is then common and a better method is to heat: (Greenwood, Earnshaw, 2005).

$$2NH_4VO_3 \rightarrow V_2O_5 + 2NH_3 + H_2O$$

1.3.1 Oxidation States of Vanadium

Vanadium is known as a redox -active element that assumes oxidation states from 1 to -5. Compounds with oxidation states of +2 or higher are more common. Although vanadium compounds with an oxidation number less than +2 may not be relevant to biological systems.

1.3.1.1 Oxidation States Lower Than +I

Most vanadium complexes in lower oxidation states are organometallic ones where the large electron density on the metal center is stabilized by acidic ligand, such as carbonyl or arenes. one of the interesting vanadium (I) complexes.

1.3.1.2 Oxidation State +II

For the +2 oxidation state, an aqua complex cation $[V(H_2O)_6]^{2+}$ is known, the oxidation potential of which is - 0.26 V versus NHE under strongly acidic conditions, demonstrating its strong reducing ability (Cotton, et al, 1998). $[V(H_2O)_6]^{2+}$ is also susceptible to oxygen even in the solid state, especially when it has moisture. An octahedral V(II) complex with two 2,20:600,200-terpyridine (trpy) has also been reported (Dobson and Taube, 1989).

It is reversibly oxidized to V(III) species at 0.46 V versus NHE, showing the considerable stability of $[V(II)(trpy)_2]^{2+}$ under ambient conditions.

1.3.1.3 Oxidation State +III

As mentioned in the previous section, $[V(II)(H_2O)_6]^{2+}$ is oxidized to $[V(III)(H_2O)_6]^{3+}$ at - 0.26 V versus NHE, whereas the edta complex $[V(III)(edta)(H_2O)]^-$

is reduced to $[V(II)(edta)(H_2O)]^{2-}$ at a more negative potential of 1.01 V versus NHE. Related V (III) complexes with tetra (carboxylate)diamine ligands display similar reduction potentials, demonstrating the considerable electron donating nature of carboxylate groups.

1.3.1.4 Oxidation States +IV and +V

Vanadium ions in the +4 and+5 oxidation states widely adopt the oxo ligand(s), Highly charged vanadium ions, such as V(IV) and V(V), being small hard ions, prefer the oxo ligand, O^{2-}, which provides lone pairs not only by δ donation, but also by π donation, to provide a V= O double bond. Donation from the oxo ligand is so prominent that the reduction potentials are almost comparable among dioxo-vanadium(V), oxo-vanadium(IV), and vanadium(III) complexes with the same ligand, in several cases. The redox behaviors of oxo-vanadium complexes tend to be complex in the presence of H^+ because the conversion of an oxo ligand to an aqua ligand often triggers further change in the coordination sphere by ligand substitution.

Vanadium(IV) complexes with an oxo ligand tend to assume square pyramidal coordination geometry with the oxo ligand at the apical position because of its strong *trans* influence. The reduction process of these complexes is usually irreversible and is observed at relatively negative potentials because of the preference of the resulting V(III) species for an octahedral coordination geometry, and because of the strong δ and π electron-donation from the oxo ligand. The acac complex $[V(IV)(O)(acac)_2]$ is irreversibly reduced to a V(III) species at E_{pc} = -2.10 V versus $Ag/AgClO_4$ in the presence of Hacac in an acetonitrile solution, whereas, under the same conditions, the V(III) acac complex, $[V(III)(acac)_3]$ is reversibly reduced at $E_{1\backslash 2}$ = -1.78 V. These results demonstrate that V(IV)=O species are more tolerant of reduction than V(III) species, reflecting the large stabilization of the

V(IV) state by the presence of an oxo ligand. The change in coordination geometry caused by protonation of the oxo ligand is also important in the redox chemistry of oxo vanadium(IV) complexes. Hexacoordinated oxovanadium complexes with glutathione derivatives also show reversible reduction at around -1.3 V .Thus, the reversibility of the reduction process of oxo V(IV) complexes is strongly affected by the coordination geometry.

Most mono-oxovanadium(V) complexes undergo a reversible reduction process when the coordination geometry is intact during the redox processes. The hexacoordinated oxovanadium(V) complexes with catecholato and tridentate Schiff base ligands derived from aminoquinoline are reversibly reduced between -0.24 and - 0.37 V. Reversible reduction is also observed for the oxovanadium(V) complexes with tetradentate Schiff base ligands derived from cyclohexanediamine and salicyladehyde derivatives. Other than an oxo-ligand, anionic and/or strongly electron-onating ligands are known to stabilize V(IV) complexes(Kanamori and Tsuge, 2012).

Many oxovanadium(V) complexes contain the VO_2^+ entity and the *cis* geometry in dioxo complexes have been confirmed by structural determination. The oxo complexes of the halides, alkoxides, peroxides, hydroxamates and amino carboxylates have been characterized. The oxidation of ligands by vanadium(V) prevents the isolation of a larger number of complexes. On the other hand, the oxidizing properties of vanadium(V) compounds are useful for many preparative reactions, namely for the catalysis of oxidations. Important examples are catalyst used for the oxidation of SO_2 to SO_3 in the industrial production of sulphuric acid Vanadium(IV) is the most stable oxidation state under ordinary conditions and majority of vanadium(IV) compounds contain the VO^{2+} unit (oxovanadium(IV) or vanadyl ion) which can persist through a variety of reactions and in all physical states. The VO^{2+} ion forms stable anionic, cationic and neutral complexes with several types of ligands and has one coordination position occupied by the vanadyl oxygen. A wide variety of oxovanaduim(IV) complexes have been prepared and characterized. A square pyramidal geometry has been well established with the oxovanadium(IV) oxygen apical and the vanadium atom lying above the plane defined by the donor atoms of the equatorial ligands. These square pyramidal complexes generally exhibit strong tendency to remain five coordinate.

However, orange polynuclear linear chain structures (···V=O···V=O···) and orange octahedral structures with a weak coordination of a solvent molecule are observed in the solid state for the Schiff base-oxovanadium(IV) complexes which have a six-membered N-N chelate ring. These complexes take a distorted octahedral coordination. The absorption band due to V=O stretching vibration of oxovanadium(IV) complexes is usually observed at a higher wave number compared to those of vanadate(V) complexes. The V=O stretching vibration, however, is susceptible to a number of influences including electron donation from basal plane ligand atoms, solid-state effects, and coordination of additional molecules. Therefore, there has been considerable work done to assign the V=O stretching frequencies in oxovanadium(IV) compounds (Klich *et al.*, 1996) (Hodge and Nordquest, 1971).

Electronic absorption spectra of oxovanadium(IV) complexes are normally interpreted in terms of the energy level scheme derived from a molecular orbital treatment for a square-pyramidal structure with C_{4v} symmetry at the metal center, in which the z-axis is taken as the vanadium–oxygen double bond, and the x- and y-axes are taken along the equatorial bonds. In this scheme, b2 (d_{xy}) < eπ* (d_{xz}, d_{yz}) < b1* ($d_{x^2-y^2}$) < a1* (d_{Z^2}), three electronic transitions are predicted, and indeed three absorption bands due to the d–d transitions are usually observed for oxovanadium(IV) complexes. However, in case of distorted oxovanadium(IV) complex, four absorption bands are observed owing to the splitting of d_{xz} and d_{yz}.

Due to the d^1 configuration of V(IV) ions, vanadium(IV) species are easily identified by EPR spectroscopy. Typical eight-line patterns are observed due to hyperfine interaction of the ^{51}V nucleus (I = 7/2) (NEJO, 2009).

As a consequense of their low radius/charge ratio, vanadium(V) centres are usually strong Lewis acids, which makes them suitable for the activation of peroxidic reagents. Accordingly, vanadium(V) complexes have been found to act as catalyst precursors in various oxidation reactions like bromination reactions, epoxidations of alkenes and allylic alcohols, oxidations of sulfides to sulfoxides and sulfones, hydroxylations of alkanes and arenes, and oxidations of primary and secondary alcohols to the corresponding aldehydes and ketones (Figure 1.4). Examples of these types of oxidations will be discussed below. The active species has been identified in stoichiometric reactions as mononuclear oxoperoxovanadium(V) complexes, some of which have been structurally characterised.Vanadium(IV) complexes can also be used as precursors in these oxidation reactions. In the presence of excess peroxide, they are readily converted to the oxoperoxovanadium(V) complexes.

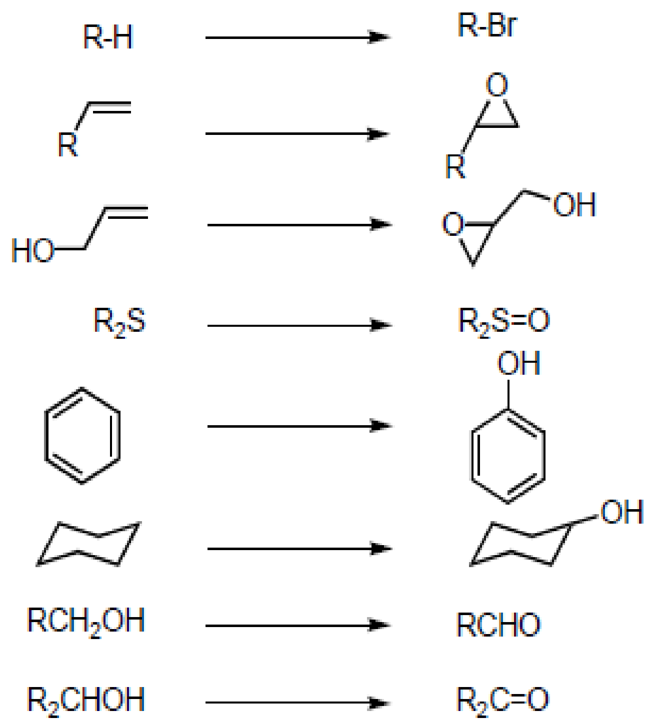

Figure 1.4 Examples of the reaction types mediated by peroxovanadium(V) complexes.

Simple vanadium complexes, *e.g.* vanadyl acetylacetonate [$VO(acac)_2$], are useful catalysts in the epoxidation of allylic alcohols. The actual oxoperoxo catalyst is formed *in situ* by oxidation of V(IV) to V(V) with excess of alkylhydroperoxide, yielding an alkylhydroperoxo vanadium(V) complex. An excellent example of high regioselectivity is the epoxidation of geraniol catalysed by a $VO(acac)_2$–TBHP (tert-butylhydroperoxide) system.

Several vanadium complexes are known to catalyse the oxidation of unfunctionalised olefins. It was proposed that when a vacant site on the vanadium centre is present, the olefins are able to coordinate to the vanadium centre, leading to the formation of epoxides with high selectivity. However, when coordination of the olefin is not possible, one electron oxidation processes often play a role, which proceed in a non-stereoselective manner. Simple vanadium(V) peroxide complexes also are efficient and selective catalysts in the oxidation of prochiral dialkyl, arylalkyl or diaryl sulfides to the corresponding sulfoxides. These complexes are usually generated *in situ* from vanadium salts such as $VO(acac)_2$, sodium *meta*-vanadate ($NaVO_3$), or vanadium pentoxide (V_2O_5) and H_2O_2. The reactions are often nearly quantitative with respect to the peroxide. Two mechanisms may occur, dependent on the nature of the ligand. The reaction pathway proceeds either *via* heterolytic or homolytic cleavage of the peroxidic oxygen-oxygen bond. For example, $VO(O_2)(OCH_3)$ oxidises di-*n*-butyl sulfide as well as methyl phenyl sulfide in a bimolecular, electrophilic reaction. In the proposed mechanism the sulfide does not coordinate to the metal centre, but undergoes nucleophilic addition to the peroxide oxygen, *i.e.* the oxygen is electrophilic in nature. This mechanistic route is common for peroxometal complexes such as Ti(IV) and Mo(VI) derivatives.

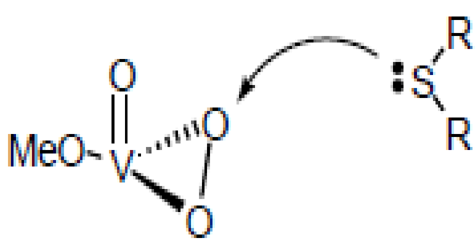

Figure 1.5 Nucleophilic addition of a sulfide to the peroxide oxygen of $VO(O_2)(OCH_3)$.

The electrophilic or nucleophilic character of the peroxide oxygen transfered to the sulfide can be established by using thianthrene 5-oxide (SSO) as a mechanistic probe **Figure 1.15**. This compound has both a sulfide and a sulfoxide site. The sulfide sulfur atom, being electron rich, is expected to undergo preferably electrophilic oxidation giving SOSO, whereas the more electron deficient sulfoxide sulfur is expected to undergo nucleophilic oxidation yielding SSO_2. Consequently, those oxidants that give high amounts of SOSO product are electrophilic in their reactivity, while high yields of sulfone point to a nucleophilic oxidant.

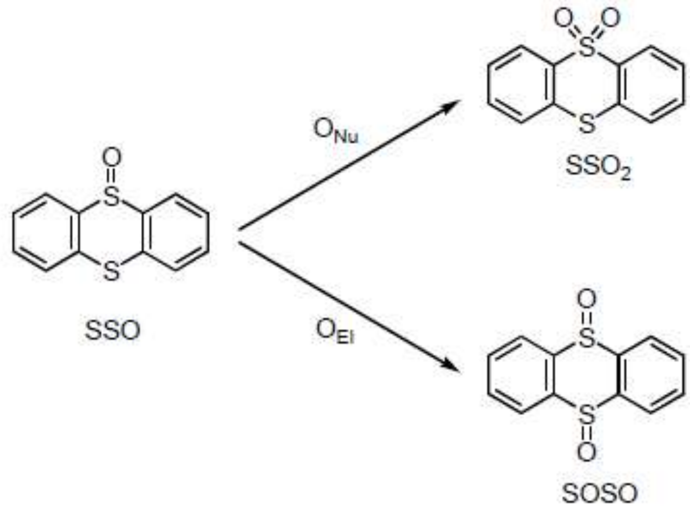

Figure 1.6 Reaction of thianthrene 5-oxide (SSO) with nucleophilic and electrophilic peroxide species.

Given the electrophilic nature of the $VO(O_2)(OCH_3)$ catalyst, the preference for sulfide oxidation over sulfoxide oxidation is obvious. This explains the quantitative yields of sulfoxide found in sulfide oxidation reactions. However, a peroxovanadium(V) complex of picolinic acid (L1), for example, shows low selectivity in sulfide oxidation leading to mixtures of sulfoxides and sulfones. It was proposed that the ligand suppresses the rate of the heterolytic reaction by reducing the electrophilicity of the peroxo oxygen. Here, a competitive homolytic pathway is likely to occur *via* one-electron transfer of the bound sulfide, forming a radical cation- radical anion pair **Figure 1.7**.

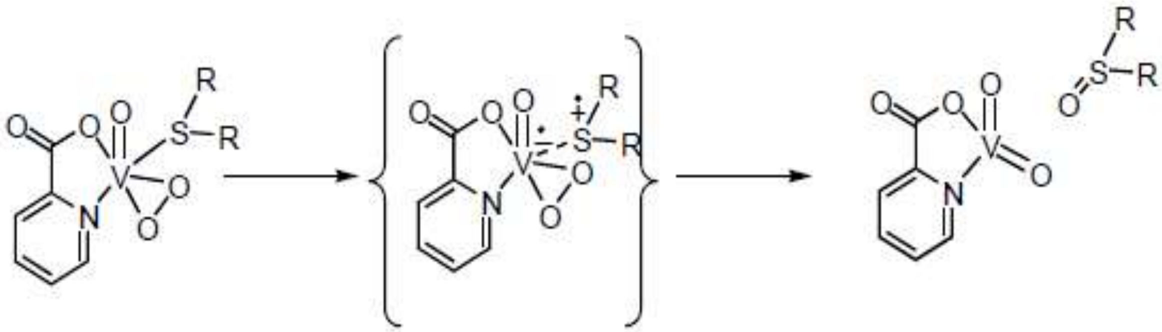

Figure 1.7 Radical mechanism for the sulfide oxidation catalysed by $VO(O_2)(L1)$.

The hydroxylation of aromatic hydrocarbons to the corresponding phenolic compounds forms another type of reaction that peroxovanadium(V) complexes are able to catalyse. Aliphatic hydrocarbons are also hydroxylated, though less easily than arenes, giving alcohols and ketones as the reaction products. Finally, vanadium(V) peroxo complexes are known to catalyse the oxidation of primary and secondary alcohols to aldehydes and ketones. For instance, vanadium(V) oxytriisopropoxide, $VO(OiPr)_3$, catalyses the oxidation of 2-propanol by H_2O_2 to acetone. Similarly, ethanol is oxidised to acetaldehyde (Ligtenbarg, 2001).

1.3.2 Coordination numbers (CN) and coordination geometries of vanadium

Vanadium is a transition metal with a wide range of oxidation states (from -1 to +5) and it can adopt a variety of coordination numbers (CN) and coordination geometries. Among the oxidation states, the +3, +4, and +5 states have been found in biological systems. The coordination stereochemistry of vanadium (III), (IV), and (V) complexes and their redox behaviors, including the lower oxidation states, will be presented as the basis of the biological chemistry of vanadium. Ideal coordination polyhedra from CN 4 through (Kanamori and Tsuge, 2012) are presented in **Fig. 1.8** Although the real coordination geometries adopted by most vanadium complexes are distorted from the ideal polyhedron to some extent, each of the polyhedra, except the square-plane and the square antiprism, has been found in vanadium complexes. This property of vanadium, adopting versatile coordination geometries, is distinct from other first-row transition metals: *e.g.*, Chromium(III) and cobalt(III) give exclusively hexa coordinate octahedral complexes and the stereochemistry of copper(II) is dominated by square planar geometry. Transition metals in biological systems are generally classified as having either a structural role in stabilizing protein structure or a functional role, involved in biological reactions.

However, these roles cannot be separated conclusively because it is believed that the biological function of a transition metal depends on its structure. Generally, coordinating groups of metals in biological systems are supplied by proteins surrounding the metal ion, and the arrangement of coordinating groups in proteins does not always provide ideal coordination geometries for the metal ions. Proteins sometimes fold in a specific manner that forces the metal ion to adopt a largely distorted structure, far from the ideal geometry. This is termed an *entatic state*, which is believed to be closer to a structure in the transition state of the enzymatic reaction involving the transition metal, giving an energetically favorable pathway for the reaction(Korbecki *et al.*, 2012).

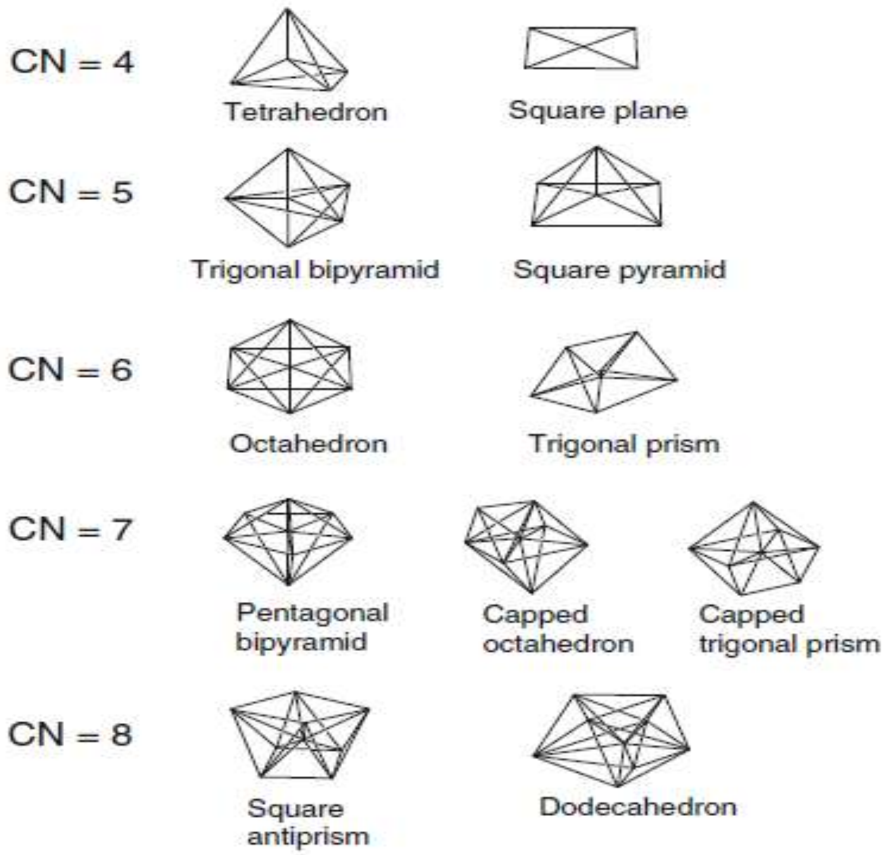

Figure 1.8 Coordination geometries of CN4 through CN8

Thus, flexibility in coordination geometry should be a key factor for metals in biological systems. In the following sections, we will present the variety of coordination geometries adopted by vanadium. Typical organometallic compounds and metal clusters of vanadium will not be discussed here.

1.3.2.1Structural Aspects of Vanadium

- ***a: Coordination Number 4***

Tetra coordination (CN=4) generally adopts tetrahedral or square planar geometries. Square planar geometry is typically found for the d^8 metal complexes, such as Pt(II) and Pd(II), whereas, a square planar vanadium complex has not been found, so far. Tetrahedral complexes are favored for complexes with small central ions coordinated by large ligands, such as halogeno anions; (Shriver and Atkins,

1999) typical examples include $[FeCl_4]^{2-}$ and $[CoCl_4]^{2-}$. However, this is not the case for vanadium complexes because the vanadium atom has a large ionic radius among the first-row transition metals. Another example of a tetrahedral complex is the oxoanion of d^0 metals situated in the left side of the *d* block, such as $[VO4]^{3-}$, $[CrO4]^{2-}$, and $[MnO4]^{-}$. The electron-rich oxo (O^{-2}) anion can donate its electrons to a metal center through two π bonds between *p* orbitals of the oxo ion and *d* orbitals of the metal ion, in addition to a normal coordination bond of δ type, resulting in a bond order of up to three **Fig. 1.9**. This multiple donation of electrons (multiple bonds) results in the stabilization of electron-poor d^0 metals. The oxoanion of vanadium (V) (usually called "vanadate") exhibits a complex behavior in aqueous solution due to protonation equilibria, as well as oligomerization. The simple vanadate $[VO_4]^{3-}$ ion can only exist at very alkaline pH (>12). Below pH 12, various polyoxovanadium(V) species are formed, depending on the total concentration of vanadium and the ionic medium concentration. Speciation of the vanadium (V) oxoanion in aqueous solution has been studied thoroughly using a combination of potentiometric and ^{51}V NMR spectroscopic data (Elvingson, et al 1996). ^{51}V NMR spectroscopy is a powerful tool and has been widely used in the study of vanadium (V) solution chemistry.(Rehder, 2008) Formulations of the species in solution have been presented with their formation constants.Well-characterized structures of the oligomeric species are shown in **Fig. 1.10**. The oligomerization of vanadate occurs by sharing a corner of the tetrahedron of a VO_4 unit. As shown in **Fig. 1.9**, cyclic oligomers are formed in addition to linear ones. This behavior is distinct from that of chromium (neighboring atom of vanadium in the periodic table), in which only linear oligomers, such as $Cr_2O_7{}^{2-}$ and $Cr_3O_{10}{}^{2-}$, are recognized. Instead, vanadate oligomerization more closely resembles that of phosphate, for which the tetracyclo anion, $P_4O_{12}{}^{4-}$, has been found. This similarity in oligomerization behavior between vanadate and phosphate may relate to a biological role of vanadium because phosphate is an inorganic ion found commonly in living systems.

Figure 1.9 π-Bonding between the *p* orbitals of an oxo ligand and vanadium *d* orbitals

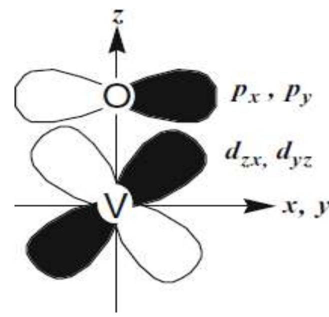

In contrast to polyoxovanadate species with nuclearity from 2 to 5, decavanadate (V_{10}) formed in slightly or moderately acidic solutions, as well as monomeric species formed in very acidic solutions, consist of octahedral units. Tetrahedral vanadium complexes other than oxovanadium(V) species are very rare. R_2N^- ligands have been shown to give tetrahedral vanadium complexes **Fig. 1.11**. Interestingly, the oxidation state of vanadium in changes depending on the R group: $[V(V)(NEt_2)_4]^+$, $[V(IV)(NMe_2)_4]$, and $[V(III)(NPh_2)_4]^-$ although the reason why is unclear.

Although these species will not relate directly to the biological chemistry of vanadium because they are fairly unstable, it should be noted that the R_2N^- ligand has a strong donating ability, like the O_2^- ligand.

A unusual trigonal monopyramidal structure for CN=4 has been found (Fig. 1.7). In this complex, $[V(III)(SC_6H_3\text{-}2,6\text{-}(SiMe_3)_2)_3(THF)]$, the vacant site *trans* to the THF ligand is occupied by an agostic C–H bond from a SiMe group of the thiolate ligand. Thus, the coordination geometry of this complex would be better described as a trigonal bipyramid, by including the agostic interaction (Kanamori and Tsuge, 2012).

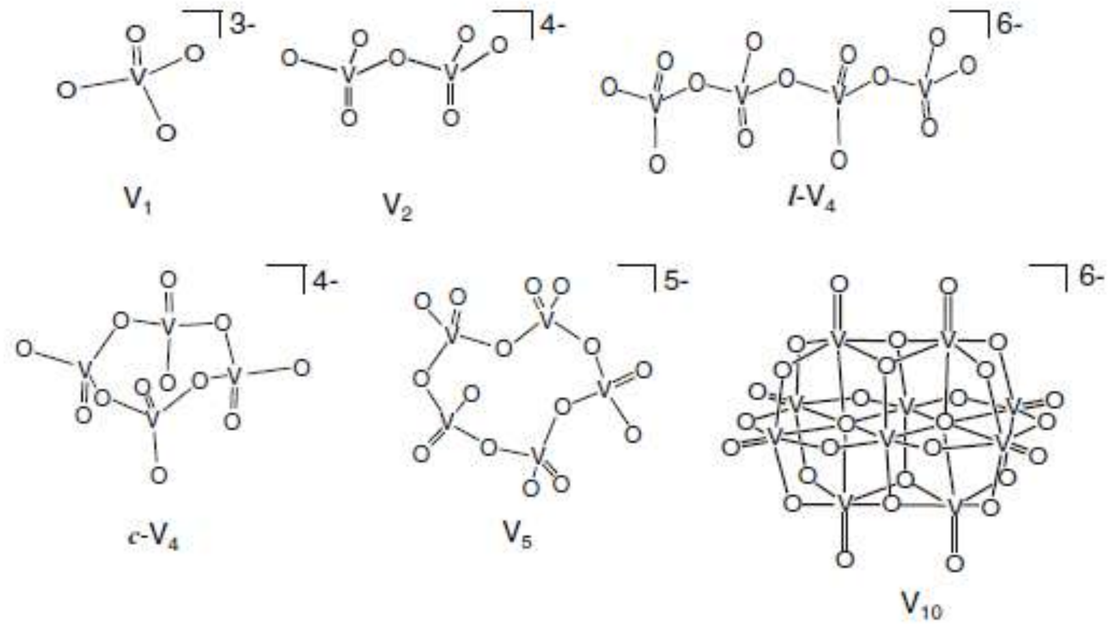

Figure 1.10 Structure of vanadate species formed in solution

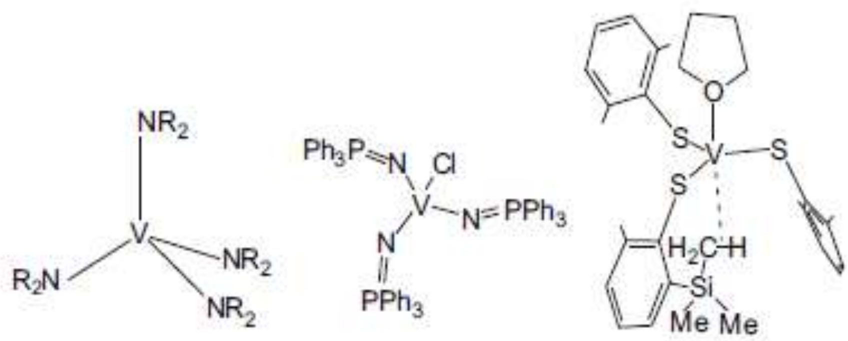

Figure 1.11 Tetrahedral vanadium complexes

- ***b: Coordination Number 5***

Pentacoordinate vanadium is important with regard to the biological chemistry of vanadium because the vanadium ion in the active center of vanadium-dependent haloperoxidases (VHPOs) adopts pentacoordination. The ideal geometries of pentacoordinate metal complexes are trigonal bipyramid and square pyramid. (Shriver and Atkins, 1999) The natural form of VHPO adopts a trigonal bipyramidal structure, whereas the reaction intermediate coordinated by a peroxo ligand forms a square pyramidal structure (Fig. 1.8).(Messerschmidt and Wever, 1996) Because the energies of the trigonal bipyramid and square pyramid differ little from one another, pentacoordinate complexes are often fluxional, as illustrated by the observations that two types of complexes have been obtained with the same ligand or closely related ligands. Examples of such complexes are shown in **Fig. 1.12**.

Although a trigonal bipyramidal structure minimizes ligand-ligand repulsions for pentacoordinate complexes, the stereochemistry of oxovanadium(IV) (usually called "vanadyl") complexes is dominated by square pyramidal geometry, as in [V(IV)O(acac)$_2$]. This preference is thought to be a result of the strong multiple bonding induced by an oxo ligand. In octahedral complexes of oxovanadium(IV), the bond distances *trans* to the oxo group are considerably longer than those *cis* to the oxo group. This phenomenon is called "*trans* influence" (not to be confused with the kinetic "*trans* effect"), which is considered to be a result of the strong V(IV)-O^{2-} bond. Because two ligands situated in *trans* positions with each other use common *d* orbitals for bonding with the central metal ion, strong electron donating from O^{2-} makes an attachment of the ligand *trans* to O^{2-} unfavorable.

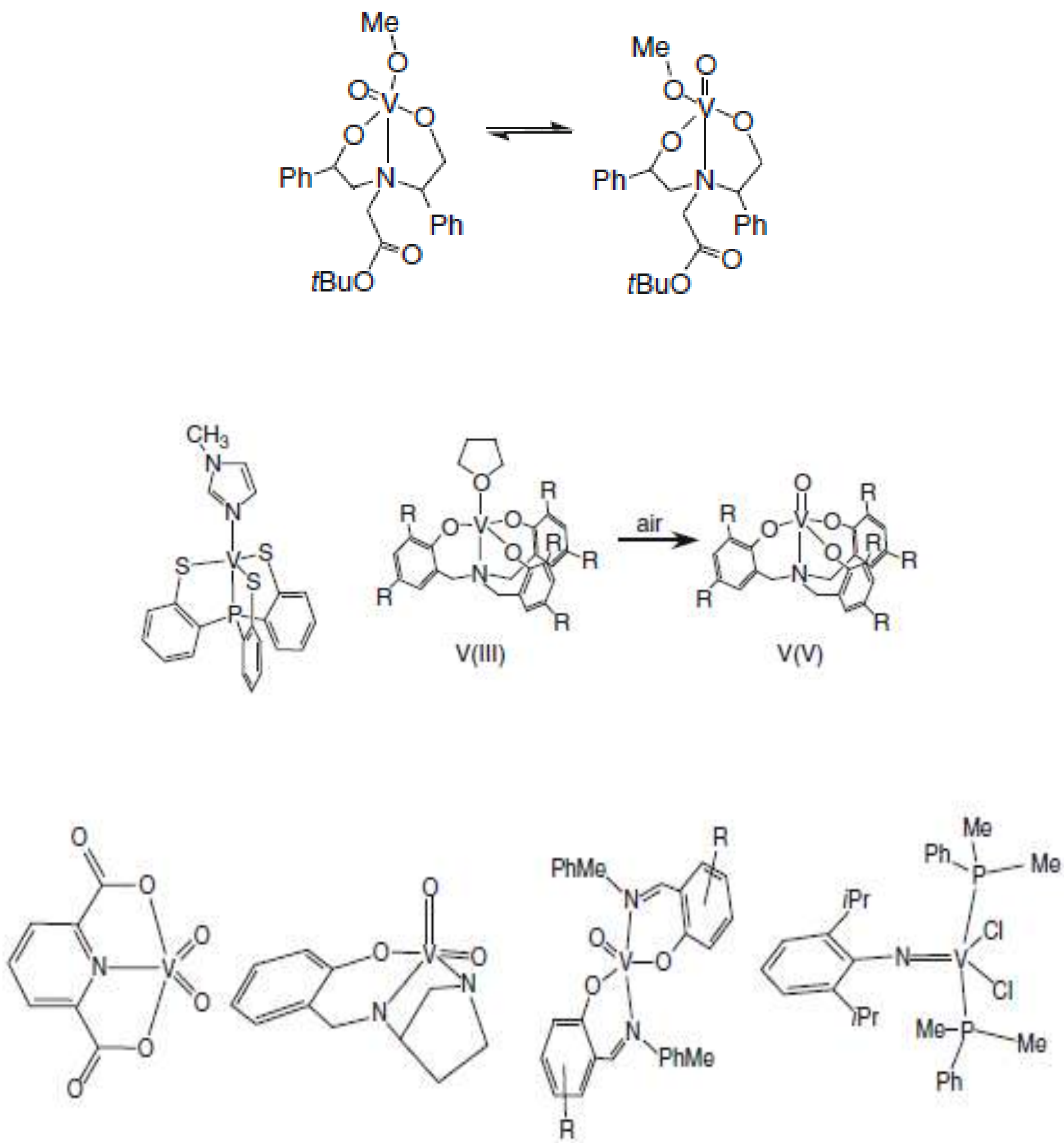

Figure 1.12 pentacoordinate vanadium complexes

Thus, the square pyramidal geometry adopted by vanadyl complexes may be considered to be an extreme case of trans influence where a weakly bound ligand *trans* to the O^{2-} group leaves the coordination sphere (*e.g.*, in crystallization), making a vacant site. Thus, in a solution in which the solvent molecule has a coordinating ability, it is plausible that the solvent molecule weakly coordinates in the sixth position, trans to the O^{2-} group, even if the complex adopts a square planar geometry in the solid state. Square pyramidal and trigonal bipyramidal structures can be formed selectively by designing the ligand structure. For example, tetradentate ligands with high planarity, such as porphyrin, yield exclusively square pyramidal complexes(Kanamori and Tsuge, 2012).

On the other hand, tetradentate tripodal ligands tend to yield a trigonal bipyramidal geometry, as shown in (Fig. 1.8), $[V(III)(P(C_6H_4\text{-}2\text{-}S^-)_3)$(1-methylimidazole)]. (Hsu *et al.*, 2003) $V(III)(N(CH_2C_6H_2R_2O^-)_3)(THF)]$ and $[V(V)O(N(CH_2C_6H_2R_2O^-)_3)]$

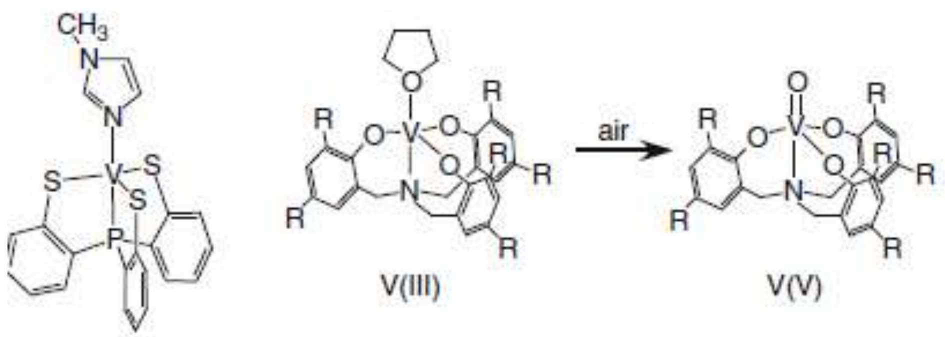

Figure 1.13 Trigonal bipyramidal complexes

Structural similarity among the complexes in different oxidation states is an important factor for constructing a readily accessible pathway in redox reactions. Other examples of pentacoordinate vanadium complexes are shown in **Fig. 1.13**. Compounds, $[V(V)(O)_2(dipic)]^-$ and**,** $[V(V)(O)_2$((*S*)-*N*-salicylidene-3-aminopyrrolidine)] (are examples showing that dioxovnadium(V) complexes with a tridentate ligand can adopt both trigonal bipyramidal and square pyramidal structures. Compound, $[V(IV)O(OC_6H_3(R)CNCHPhMe)]$, (Santoni and Rehder, 2004) Structural $[V(IV)(N\text{-}2,6\text{-}i\text{-}Pr_2C_6H_3)(PMe_2Ph)]$ is a rare example of an arylimido complex of vanadium(IV) (Lorber, et al, 2003).

- ***c: Coordination Number 6***

A hexacoordinate octahedral arrangement is the most common structure for transition metal complexes. This structure is found for vanadium complexes in all biologically relevant oxidation states, +3, +4, and +5. In contrast, trigonal prismatic geometry is unusual.

Although coordination compounds of vanadium (IV) are dominated by oxovanadium (vanadyl) species, several complexes without oxo ligands have been prepared and structurally characterized. This type of complex is called “bare” or “non-oxo” vanadium (IV). To obtain a bare vanadium (IV) complex, a ligand that can serve as a strong π donors must be introduced to the coordination sphere to compensate for the strong electron donation from the oxo group. Representative ligands with such ability are catecholates. In fact, a hexacoordinate bare vanadium (IV) complex, $[V(IV)(cat)_3]^{2-}$ (cat=catecholate) has been obtained **Fig 1.14**. Although, in general, vanadium(V) complexes also contain one or two oxo groups, 3,5-di-*tert*-butylcatecholate yields a bare vanadium(V) complex Na[V(V)(DBcat)3] Vanadium(V) complexes without strongly bound oxo ligands are quite rare. In addition to the above vanadium (IV) and (V) complexes, a vanadium (III) complex, $K_3[V(III)(cat)_3]$ has been obtained and their redox behaviors were examined.(Kanamori and Tsuge, 2012)

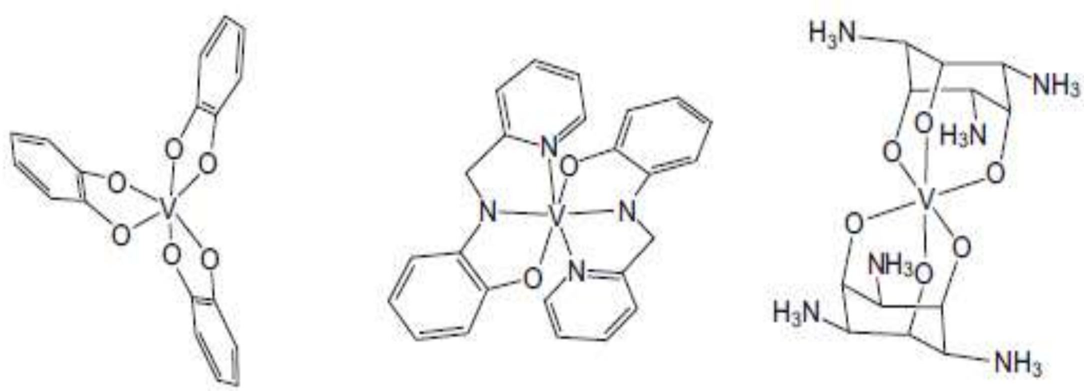

Figure 1.14 Bar or non- oxo vanadium (IV) complexes

Some oxo(peroxo)vanadium(V) complexes adopt a geometry that can be best described as a pentagonal pyramid **Fig. 1.15** (Drew, and Einstein, 1972) This geometry is very unusual for hexacoordinate complexes. Thus, it may be better to consider this geometry as a special case of the pentagonal bipyramidal structure, which is found commonly in oxo(peroxo)vanadium(V) complexes. Specifically the seventh ligand opposite to the oxo group in the pentagonal bipyramidal structure may leave the coordination sphere due to a strong *trans* influence of the oxo group in crystallization, resulting in a pentagonal pyramidal geometry.

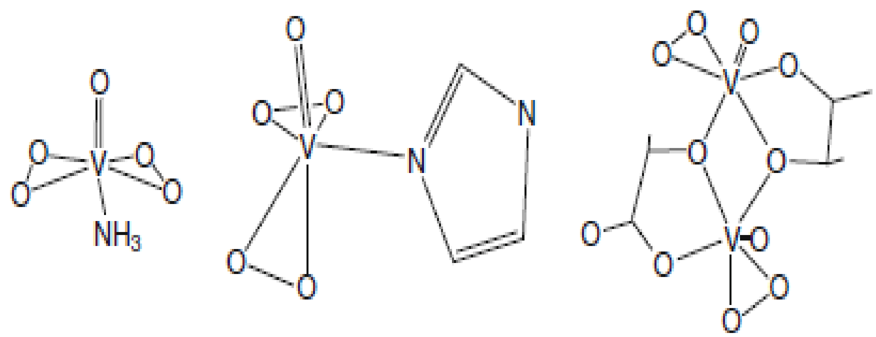

Figure 1.15 Hexacoordinate pentagonal pyramidal complexes

- ***d: Coordination Number 7***

A coordination number greater than six is encountered rarely in first-row transition metal complexes because 3d metal ions do not have an ionic radius large enough to accommodate more than six ligands. Recently, however, heptacoordinate vanadium complexes have become less rare. This may be explained by considering that vanadium ions (especially vanadium (III)) have a slightly larger ionic radius than other first-row transition metal ions. The ideal geometries for heptacoordination include a pentagonal bipyramid, capped octahedron, and capped trigonal prism; these three geometries are, however, similar in energy to heptacoordination (Shriver and Atkins, 2006).

Thus, heptacoordinate vanadium complexes are often fluxional and most of them adopt intermediate structures.

Because cyanide is a small ligand, vanadium (III) can accommodate seven cyano ligands to yield the heptacoordinate vanadium(III) complex, $[V(III)(CN)_7]^{3-}$ with pentagonal bipyramidal geometry, as shown in **Fig. 1.16.** The bent coordination of cyanide found in has been attributed to the interaction of the ligand with the cations surrounding the complex. The pentagonal bipyramidal geometry of this complex has been explained in terms of crystal field stabilization, rather than the size of the vanadium(III) ion. One strategy to obtain pentagonal bipyramidal complexes is to employ a ligand in which five donor atoms are arranged in a pentagonal plane. Examples of this type of complex are illustrated in (Fig. 1.12), Compounds, $[V(III)(teg)Br_2]^+$ (H_2teg=tetraethylene glycol) and $[V(III)_2L(H_2O)_4]^{4+}$ (H_2L=1,7,14,20-tetramethyl-2,6,15,19-tetra-aza[7,7](2,6)-pyridinophane-4,7-diol) have a highly planar structure with regard to the equatorial coordination.

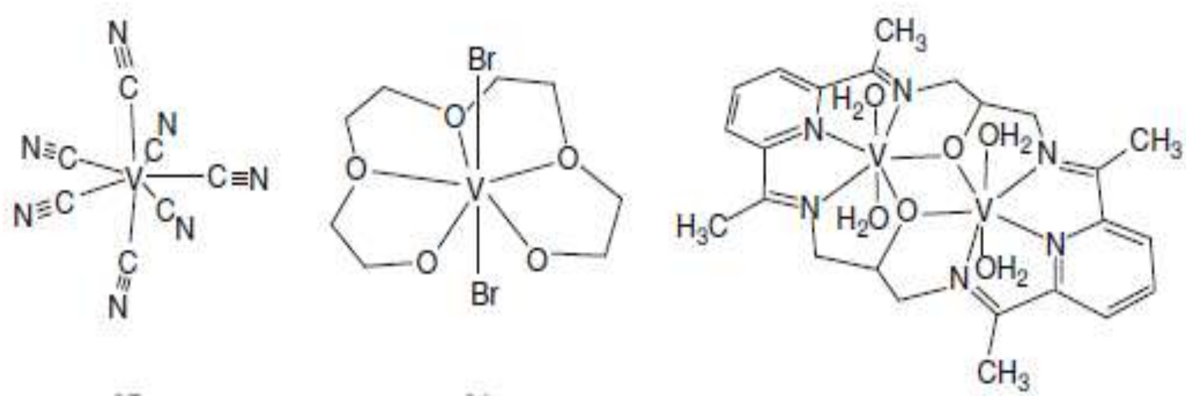

Figure 1.16 Hebtacoordinate pentagonal bipyrmiadal complexes

Although heptacoordinate pentagonal bipyramidal vanadium compounds are still rare with conventional ligands, monoperoxo and diperoxo vanadium(V) complexes with chelate ligand(s) usually adopt this structure, as illustrated in (Fig. 1.13), $[V(V)O(O_2)(oxalate)_2]^{3-}$, $[V(V)O(O_2)$(picolinato)(picolinamide)], and (X=O)

$[V(V)O(O_2)_2(bpy)]^-$. Persulfide, S_2^{2-} ligand also behaves in the same manner as O_2^{2-}, (X=S) $[V(V)O(S_2)_2(bpy)]^-$, and $[V(V)O(S_2)_2$ (terpyridine)$]^-$. The small bite angles of the three-membered chelate ring formed by the side-on coordination of the peroxo or persulfido group (45° and 51°, respectively) would enable the arrangement of five donor atoms in the equatorial plane. Other examples in which ligands giving a small bite angle enable vanadium to form a pentagonal equatorial plane are shown in **Fig. 1.15**. The bidentate coordination of nitrate in, $[V(V)O(NO_3)_3(CH_3CN)]$ and sulfate in, $[V(III)_2(SO_4)_3$(*N,N'*-bis(2-pyridylmethyl)-1,2-ethanediamine$)_2]$ forming four membered chelate rings gives bite angles of ca. 61ı and 66.6ı, respectively. These bite angles can be regarded as small enough to allow five donor atoms to arrange in the equatorial plane. Compound, [V(III)(dipicolinato)(picolinato)$(H_2O)_2$] is a unique example of a heptacoordinate complex that includes neither the three membered chelate ring nor the four-membered chelate ring; instead, the tridentate meridional coordination of dipic is highly distorted from the ideal angle for meridional coordination (180°), giving an O-V-O angle of 142.1°, and thus leaves enough space to accommodate a normal bidentate ligand on the opposite side of the dipicolinate (dipic). Among the three ideal geometries of seven-coordination, the capped octahedron and capped trigonal prism are rare. Nonetheless, these geometries as well as the pentagonal bipyramidal geometry, though distorted to some extent, have been realized for vanadium(III) complexes using aminopolycarboxylates and its analog with a pyridyl functionality **Fig. 1.17**. The geometry of compound, $[V(III)(OH_2)_3$(nta)] (nta=nitrilotriacetate) can best be described as a capped octahedron, with the amino nitrogen occupying the capping position, whereas compound, [V(III)(EDTA)$(H_2O)]^-$has been shown to adopt a capped trigonal prism with the water molecule occupying the capping position. [V(III)(hedtra)$(H_2O)]^-$ (hedtra=*N*-

hydroxyethyl- *N*,*N'*,*N'*-triacetate) and [V(III)(Hedta)(H_2O)], An edta-like hexadentate ligand, H_2bpedda, in which the two acetate groups of edta were substituted by two pyridyl methyl groups, were prepared. This ligand also gives the heptacoordinate vanadium(III) complex, [V(III)(bpedda)(H_2O)]$^+$ of which the structure is different from that of the edta complex and has been described as a distorted pentagonal bipyramid (Kanamori *et al.*, 2001).

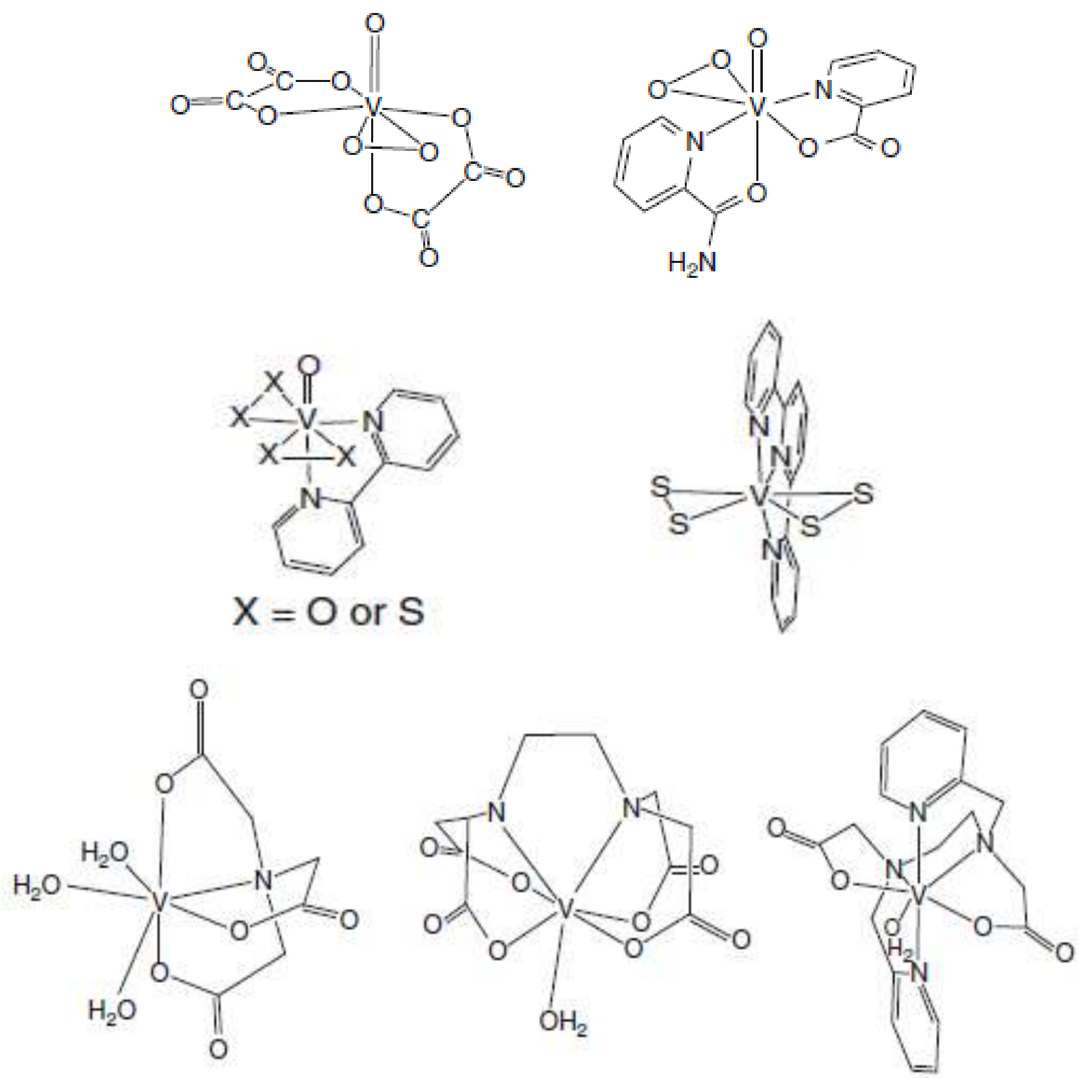

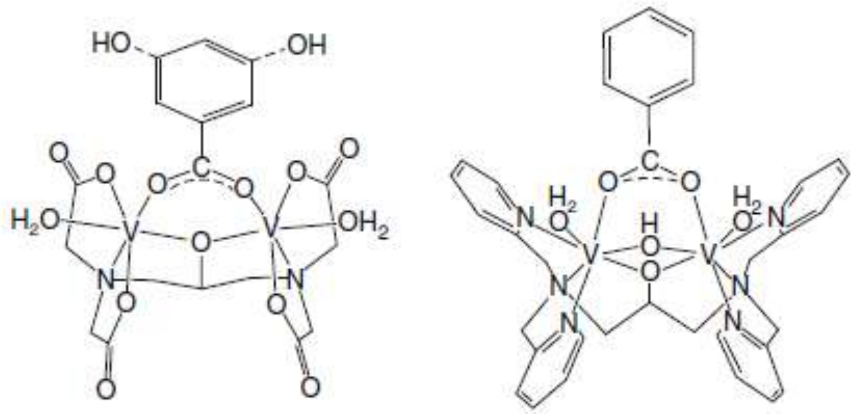

Figure 1.17 Varius structure of hebtacoordinate vanadium complexes with different ligand

The reason why such tetra- and hexadentate ligands afford the heptacoordinate vanadium(III) complexes has been explained; these ligands would be too small to encircle the vanadium(III) ion, leaving an additional coordination site for the seventh ligand.

As shown above, the geometries of vanadium(III) complexes are flexible, depending on the ligand structure and functional groups. This flexibility may be an important property for metal ions in biological systems. An interesting example illustrating the flexibility in coordination mode of vanadium(III) is presented in **Figure 1.17**. Compounds, [V(III)$_2$(dpot)(*m*-hydroxybenzoato)(H$_2$O)] (H$_5$dpot=2-hydroxy-1,3-diaminopropane-*N*,*N*,*N*0,*N*0-tetraacetic acid) and, [V(III)$_2$(benzoate)(OH)(tphpn)(H$_2$O)$_2$]$^{3-}$, (Htphpn=*N*,*N*,*N*',*N*'-tetrakis(2-pyridylmethyl)- 2-hydroxy-propane-1,3-diamine) both contain a heptadentate binucleating ligand with a bridging alkoxo group (dpot or tphpn) and a bridging carboxylate group (*m*-hydroxybenzoate or benzoate).Dinuclear units that contain the carboxylato and oxo (or hydroxo) bridges have been found in iron-containing biomolecules, such as hemerythrin, ribonucleotide reductase (RR), and methane monooxygenase (MMO).That vanadium(III) yields a similar dinuclear complex may indicate a potential role for vanadium(III) in biological systems(Kanamori and Tsuge, 2012).

- ***e: Coordination Number 8***

Ideal geometries for octacoordination are the dodecahedron and square antiprism. Although vanadium complexes with CN 8 are very rare, a natural vanadium(IV) compound isolated from *Amanita muscaria*, named amavadin, has been shown to adopt a unique octacoordinate structure. **Figure 1.18**, illustrates the structure of amavadin (Berry *et al.*, 1999). a fully deprotonated form of *N*-hydroxyimino-2,2'-diisopropionic acid (H_3hidpa) coordinates to a bare vanadium(IV) center as a tetradentate ligand through three O and one N atoms. Although the eight donor atoms coordinate to the vanadium(IV), the geometry of this compound would better be described as a special case of octahedron if the side-on coordination of the NO group is regarded to occupy one coordination site of the octahedron. Themonoanionic vanadium(V) compound with hidpa, $[V(V)(hidpa)_2]^-$ and the model compound with *N*-hydroxyiminodiacetatic acid (H3hida), $[V(IV)(hida)_2]^{2-}$ adopt almost the same structure as amavadin. The structures of these compounds are rare examples of bare vanadium(IV) and –(V) complexes and they contributed very much to determining the structure of amavadin.

The tetraperoxovanadium(V) complex, $[V(V)(O_2)_4]^{3-}$ is the complex with the highest number of peroxides among structurally well-characterized peroxovanadium(V) complexes and it adopts a dodecahedral structure. Dithiocarboxylate yields a dodecahedral vanadium complex, $[V(IV)(dithioacetato)_4]$ Dithiobenzoate and phenyldithioacetate (Dalton *et al.*, 1972).

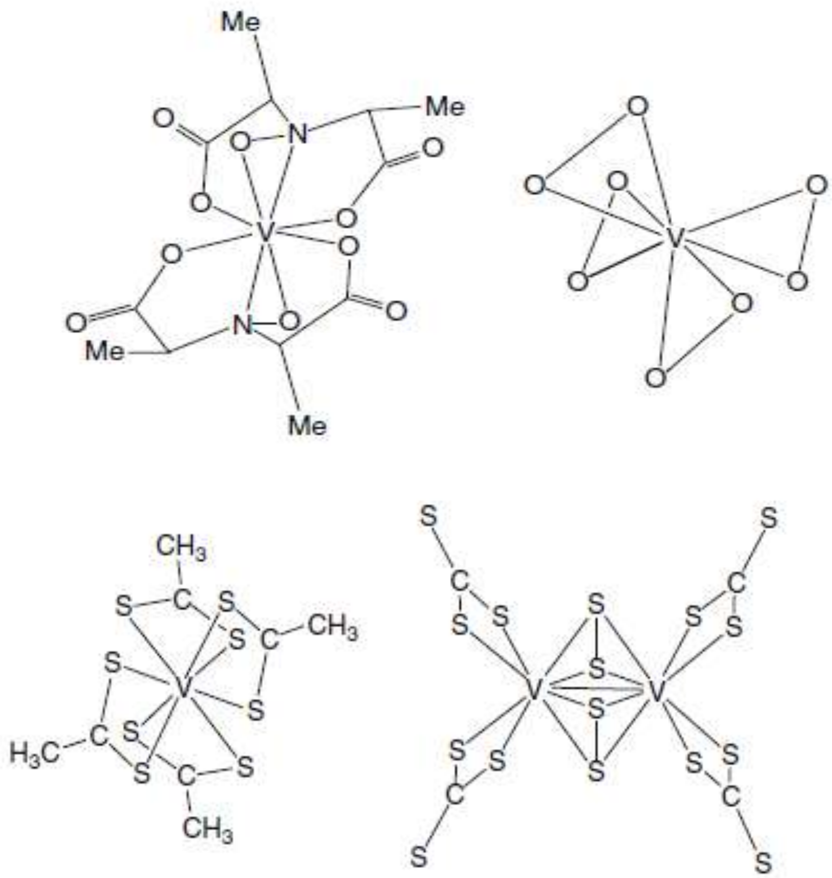

Figure 1.18 Octacoordinate vanadium complexes

If this V-V bond is counted into the coordination number, the vanadium center can be regarded as a nonacoordinate complex and its geometry can be described as a tri capped trigonal prism (Kanamori and Tsuge, 2012).

1.4 The Biology of vanadium

High levels of vanadium are found in the mushroom *Amanita muscaria* and in marine tunicates (sea squirts). In the former organism, a siderophore-like ligand that binds vanadium(IV)

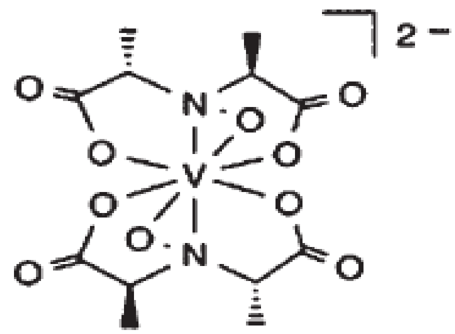

Figure 1.19 Structure of amavadine.

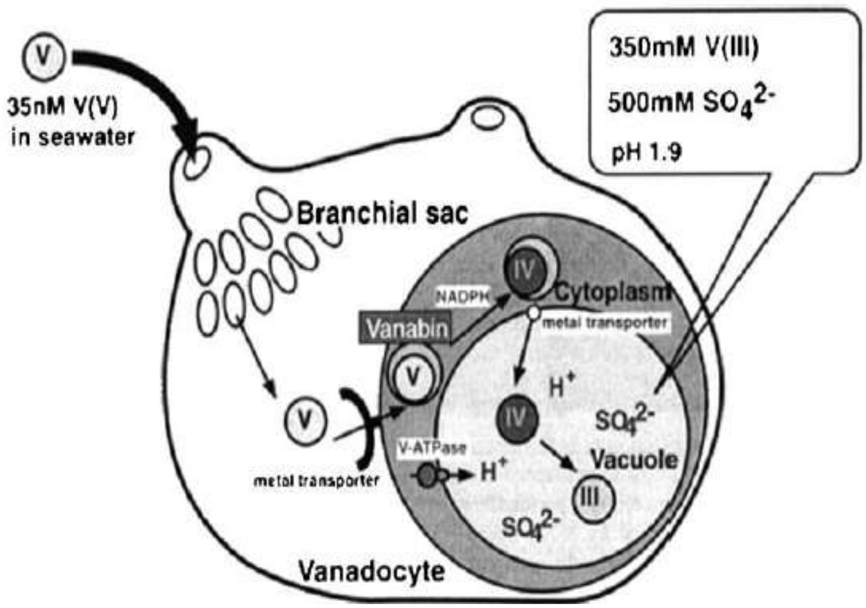

Figure 1.20 Model of the pathway for reduction and accumulation of vanadium in ascidian vanadocytes(Crans *et al.*, 2004)

called amavadine is found. Amavadine is a metal complex containing one equivalent of vanadium and two quivalents of the ligand S^{-2}, S^{-2}, hydroxyiminopropionic acid **Figure 1.19**. The complex is stable to hydrolysis, and has reversible one-electron redox properties, suggestive of a possible role in biology as a one-electron redox mediator.

Vanadium, as $VOSO_4$, has been found to interfere with siderophore-mediated iron transport in bacteria and plants. This seems to imply that vanadium can be transported by siderophores, and a number of studies focussing on applications of hydroxamate V-complexes in biology have been initiated. Tunicates (ascidians or sea-squirts) are invertebrate marine organisms, which can accumulate vanadium at concentrations approaching 350 mM (the concentration of vanadium in sea water is ~10^{-8} M). This vanadium is taken up as V(V) from seawater **Figure 1.20**, reduced to oxidation state III or IV and stored in a soluble form in the blood cells within acidic vacuoles at concentrations a million fold higher than in their external surroundings.

Vanadium seems to be bound in the cytoplasm to vanadium binding proteins (vanabins, of molecular weights 12–16 kDa). However, the precise role of vanadium in these marine organisms remains unknown (Crichton, 2007).

1.4.1 Enzymes containing vanadium

Haloperoxidases are enzymes that catalyse the oxidation of halides to the corresponding hypohalous acids (or to a related two-electron oxidised halogenating intermediate such as OX^-, X^{3-} and X^+) using hydrogen peroxide as the oxidant. In the presence of suitable nucleophilic acceptors, halogenated compounds are formed. The nomenclature of these enzymes is based on the most electronegative halide which can be oxidised by the enzyme. Thus iodoperoxidase merely catalyses the oxidation of iodide, bromoperoxidase catalyses the oxidation of bromide, and iodide, while chloroperoxidase catalyses the oxidation of chloride, bromide and iodide. The function of these haloperoxidases *in vivo* is the generation of a diversity of halogenated organic compounds. These products probably are formed because of the biocidal effects of HOBr and some of the organohalogens. Presumably, these compounds are part of the host defence system, because they may prevent fouling by microorganisms or act as an antifeeding system (Ligtenbarg, 2001).

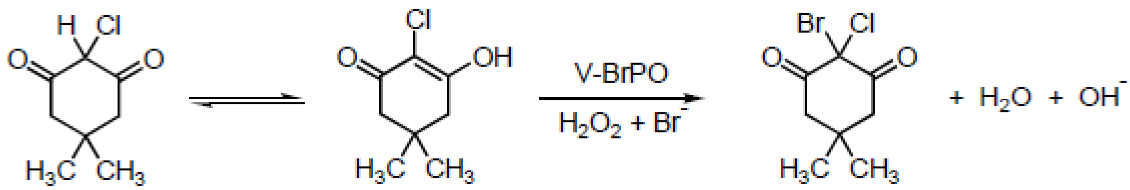

Figure 1.21 Bromination of MCD, the standard substrate in haloperoxidase activity determinations.

Vanadium peroxidases have been shown to catalyse the bromination of various organic substrates including monochlorodimedone (MCD, 2-chloro-5,5-dimethyl-1,3-cyclohexanedione), the standard substrate for the determination of haloperoxidase activity, using H_2O_2 as the oxidant **Figure 1.21** (Blanke, and Hager, 1989) In the absence of a nucleophilic acceptor, however, a second equivalent of hydrogen peroxide reduces the brominating intermediate resulting in the formation of bromide and singlet oxygen. This disproportionation reaction of hydrogen peroxide is a bromide-mediated reaction, *i.e.* V-BrPO does not catalyse the formation of singlet oxygen in the absence of bromide. At pH 6.5, the enzyme functions with a turnover rate of 4.7 x 10^5 mol of brominated product per mol of enzyme per hour (Butler and Carrano, 1991). A common intermediate (Br^+) is likely to exist of which the formation is rate determining and which is responsible for both the generation of singlet dioxygen and brominated products see **Figure 1.22.** Nevertheless, the exact nature of this halogenating intermediate still is a matter of debate.

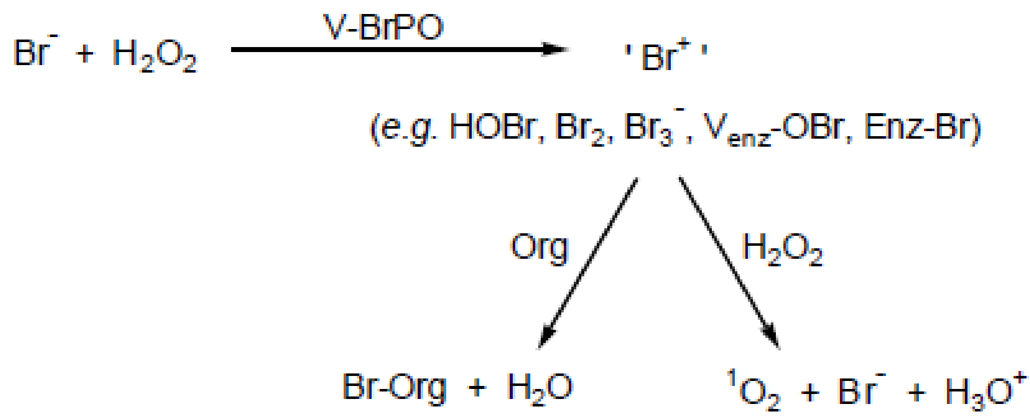

Figure 1.22 Proposed mechanism of bromoperoxidase activity catalysed by V-BrPO.

To get a better understanding of the working mechanism of the enzyme and to determine the role of vanadium, many functional mimics of V-BrPO have been developed. Furthermore, many spectroscopic studies have been carried out in order to reveal the nature of the active site. In 1996, the crystal structure of an azide containing vanadium chloroperoxidase (V-ClPO) isolated from the fungus *Curvularia inaequalis* was determined by (Messerschmidt & Wever, 1997) the X-ray structure of the peroxide form of the chloroperoxidase enzyme was published. In the native state, a five-coordinated trigonal bipyrimidal V(V) moiety is present which is coordinated by three nonprotein oxo groups in the equatorial plane and one histidine and a hydroxy group at the axial positions **Figure 1.23**. The oxygens are hydrogen bonded to several amino acid residues of the protein chain. In the peroxo state, the peroxide ligand is bound in an È2-manner in the equatorial plane. The coordination geometry around the vanadium centre is a distorted tetragonal pyramid with the two peroxo oxygens, one oxygen and the nitrogen in the basal plane and one oxygen in the apical position. A partial amino acid sequence comparison of this chloroperoxidase with a vanadium bromoperoxidase showed a close similarity between the enzymes.

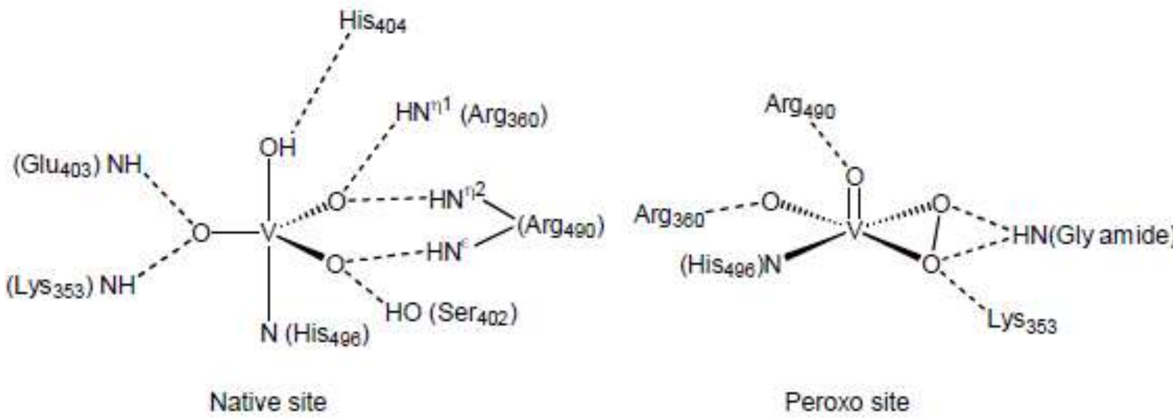

Figure 1.23 The native and peroxo vanadium site in V-ClPO.

A second class of enzymes that contain vanadium are the vanadium nitrogenases. Nitrogenases are multicomponent metalloenzyme complexes that are capable of reducing dinitrogen to ammonia:

$$N_2 + 12\,e^- + 12\,H^+ \longrightarrow 2\,NH_3 + 3\,H_2$$

Many nitrogenases consist of a Fe-S cluster and a molybdenum-dependent component.The first vanadium containing nitrogenase, *i.e.* a VFe-protein **Figure 1.24**, was isolated and purified in 1986 from certain nitrogen-fixing bacteria (Ligtenbarg, 2001).

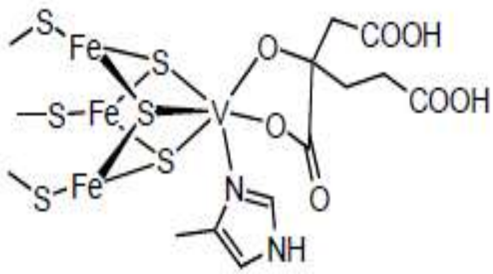

Figure 1.24: Proposed vanadium environment in vanadium nitrogenase.

To gain more insight into the coordination properties of sulfur containing ligands, many thiovanadium complexes have been studied in recent years and their redox activity examined. **Figure 1.25** (Wang *et al.*, 2001)**.**The oxidation state of vanadium in these compounds range from +2 to +5.

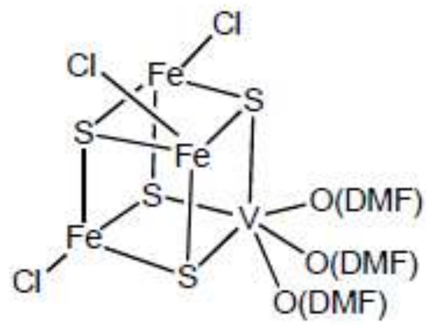

Figure 1.25 Schematic representation of the $[VFe_3S_4Cl_3(DMF)_3]^-$ cluster (Ligtenbarg, 2001)

1.4.2.1Structure and Function of Vanadium Haloperoxidases

Vanadium is the second most abundant metal in seawater at a concentration of about 35 nM,(Butler, 1998) and universally distributed in the soil. The metal oxide is the prosthetic group in the vanadium haloperoxidases from seaweeds and in a group of fungi, the dematiaceous hyphomycetes. (Vilter, 1984) was the first to demonstrate evidence for the involvement of vanadium in the vanadium-dependent haloperoxidase. He showed that the bromoperoxidase isolated from *Ascophyllum nodosum* was inactivated by dialysis at pH 3.8 in phosphate buffer containing EDTA and that the enzyme was reactivated by vanadate in suitable buffers. Subsequently it was demonstrated that vanadate was the prosthetic group in the bromoperoxidase and that since phosphate is a structural and electronic analogue of vanadate it replaces vanadate in the enzyme. (Wever et al, 1985), (Boer, *et al.*, 1986), (Boer, *et al*, 1986) The vanadium chloroperoxidases with similar enzymatic and kinetic properties as the bromoperoxidases were detected a few years later in a family of terrestrial fungi (Schijndel *et al.*, 1993). The oxidation state of the metal in the native form of the haloperoxidases is vanadium V that upon reduction is converted into the catalytically inactive IV state. As a d^1 metal ion, vanadium IV has a single electron that is strongly coupled to the ^{51}V nucleus (I=7/2). This redox state of the metal can easily be detected by EPR since it gives rise to an EPR signal of either 8 or 2 sets of 8 overlapping lines. This technique allows the detection of relatively low concentrations of these enzymes. Unfortunately at this redox state the enzyme is inactive (Gengenbach, 1996). Unlike heme peroxidases the UV-VIS spectra of these vanadium enzymes show only a modest absorption in the optical spectra around 315 nm due to the bound cofactor. Haloperoxidases catalyze the two-electron oxidation of halides (Cl^-, Br^-, I^-) by H_2O_2 to hypohalous acids:

$$H_2O_2 + H^+ + X^- \longrightarrow HOX + H_2O$$

In fact this reaction can be regarded as an oxygen-transfer reaction from the peroxide to the halide ion. These hypohalous acids or related halogenating intermediates, such as OX^-, X^{3-} and X^+ are released from the active site during turnover and they may act nonspecifically on a variety of organic compounds (RH) that are susceptible for electrophilic attack resulting in the production of a diversity of halogenated compounds (RX).

$$HOX + R\text{-}H \longrightarrow RX + H_2O$$

In the absence of a nucleophilic acceptor a reaction may also occur between HOX and H_2O_2 resulting in the formation of singlet oxygen.

$$HOX + H_2O_2 \longrightarrow {}^1O_2 + H_2O + HX$$

The historical nomenclature convention of the vanadium haloperoxidases is based on the most electronegative halide oxidized by these enzymes. Chloroperoxidases catalyze the oxidation of Cl^- and Br^- and I^-, bromoperoxidases catalyze only the oxidation of Br^- and I^- and iodoperoxidases are specific for iodide oxidation. However the distinction between the haloperoxidases is somewhat arbitrary since a bromoperoxidase may also oxidize chloride albeit with a low specificity constant (Wever, 2012).

1.5 The Biochemistry of Vanadium

Vanadium is beneficial and possibly essential for humans. It is certainly essential for a number of organisms. Vanadate (oxidation state V) and its derivatives are phosphate analogues, showing both ground state and transition state analogy (both structural and electronic) with phosphorus compounds. The analogy of five-coordinate vanadium compounds with the transition state of phosphate ester hydrolysis is well documented, and explains why so many vanadium compounds are potent inhibitors of phosphatases, ribonucleases and ATPases. Haloperoxidases represent the first and best-characterized class of vanadium enzymes, capable of catalysing the two-electron oxidation of a halide by hydrogen peroxide. The chloroperoxidases, found in many algae, seaweed, lichens and fungi, can oxidize both Cl^- and Br^-, whereas bromoperoxidases, found in many marine extracts, can only oxidize Br^-. The X-ray structures of a number of vanadate-dependent haloperoxidases have been reported **Figure 1.26**. On the basis of spectroscopic evidence, it is now thought that the oxidation state of the vanadium remains at V throughout catalysis, and that the mechanism for both types of vanadium haloperoxidases are the same, as indicated in **Figure 1.27**. The reaction proceeds by initial binding of H_2O_2 followed by protonation of bound peroxide and addition of the halide. NMR spectroscopy confirms the presence of VO_2–O_2, and there is no evidence for direct binding of halide to the vanadium ion. The rate-limiting step in the catalysis is the nucleophilic attack of the halide on the protonated protein–peroxide complex, generating an 'X^-, species, which reacts directly with organic substrates (RH) to halogenate them (RX). In the absence of RH this step will generate singlet oxygen.

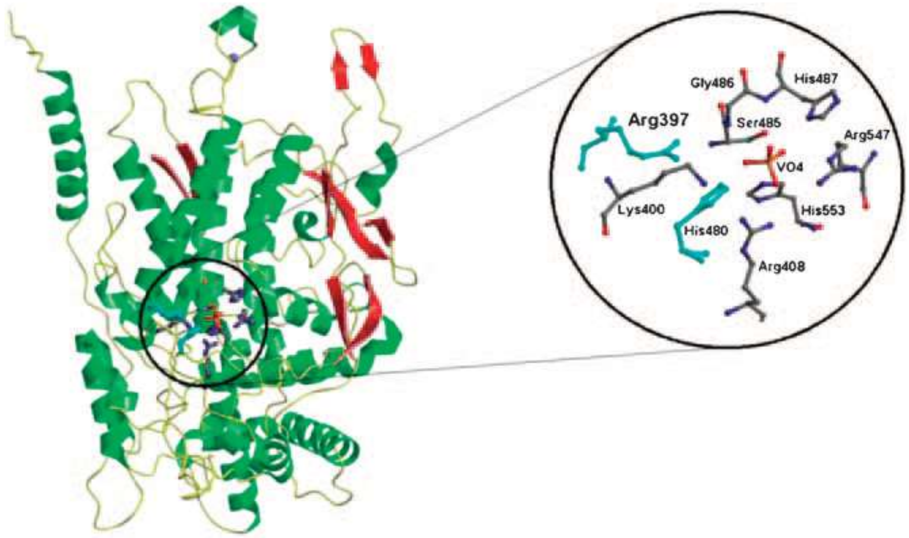

Figure1. 26 The structure and active site of the bromoperoxidase subunit from *C. pilulifera*. Residues conserved in all vanadium bromo- and chloroperoxidases are in grey, those that vary in cyan(Jennifer *et al.*, 2009)

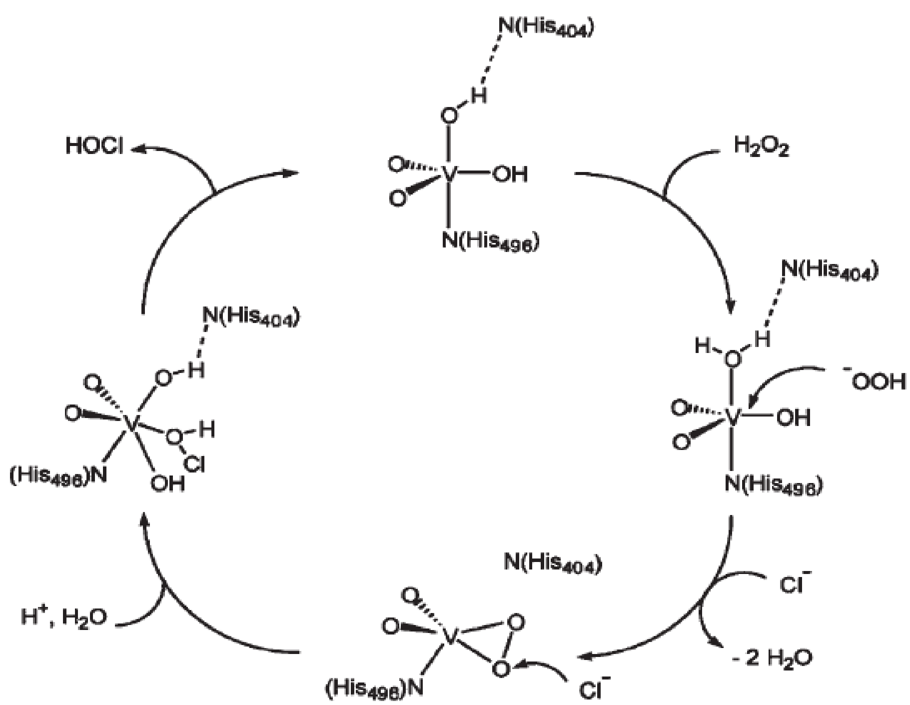

Figure 1.27 Proposed mechanism for the vanadium chloroperoxidase oxidation of chloride by hydrogen peroxide (Xia et al, 2012)

The halide specificity of the vanadium-dependent bromoperoxidase from the marine algae *Corallina pilulifera* **Figure 1.26** has been changed by the single amino acid substitution of Arg379 by either Trp or Phe. Both mutant enzymes R379W and R379F showed significant chloroperoxidase, as well as bromoperoxidase activity, supporting the existence of a specific halogen-binding site within the catalytic cleft of vanadium haloperoxidases. It is also of interest to point out that the amino acid sequence and structure of the active site of vanadium haloperoxidases is conserved within several families of phosphatases, with conservation of the amino acids involved in vanadate binding in one and phosphate binding in the other. Information, particularly structural, concerning vanadium-dependent nitrogenases, is relatively limited. The consensus is that they resemble the molybdenum nitrogenase in most aspects except for the presence of a FeV cofactor (Crichton, 2007).

1.6 Vanadium in medicine

1.6.1 Diabetes mellitus (DM)

Diabetes mellitus (DM) is a disease where the body either does not produce insulin (Type 1diabetese) or the body cannot use insulin (Type 2 diabetese).Insulin is a hormone that signals the cellular uptake of glucose for metabolism. Since 1899, vanadium salts have been used to treat diabetes (Natasha, 2004).

Diabetes mellitus (DM) caused by a dysfunction of glucose homeostasis, affecting one out of 20 people in industrialized nations. DM manifests itself either as type 1 (insulin-dependent DM) or type 2 (non-insulin dependent DM). Type 1 requires daily subcutaneous injections of insulin; consequently, there is considerable interest in the development of orally active alternatives to insulin and other currently used therapeutic agents. Investigations carried out during the last two decades has shown that chromium , manganese, molybdenum, copper, cobalt , zinc, and vanadium ions can exhibit insulin-mimetic or -enhancing properties in vitro and in vivo. Among these metal ions, vanadium seems to be the most promising one, especially when coordinated to organic ligands. Sakurai et al. have reported that bis(pyridine-2-carboxylato)oxovanadium (IV) ($[VO(pic)_2]$) has a higher insulin-mimetic activity than $VOSO_4$, and vanadium complexes such as $[VO_2(dipic)^2]^-$ ($dipic^{2-}$ = 2,6-pyridinedicarboxylate), [VO(5-alkoxycarbonyl-picolinate)$_2$(H_2O)] and $[VO(ma)_2]$ (ma = maltol = 3-hydroxy-2-methyl-4- pyrone) were found to exhibit high insulin-mimetic activities, as do complexes of other metals with picolinates and maltolate, such as $[Zn(ma)_2]$, $[Zn(pic)_2]$ and $[Co(dipic)_2]^{2-}$. Recently, (Nakai *et al.*, 2005) have reported that [VO(Hhpic-O,O)(Hhpic-O,N)(H_2O)] (H_2hpic = 3-hydroxypyridine- 2-carboxylic acid) exhibits high insulin-mimetic activity. Based on these promising results, we report here the structure and insulin-mimetic activities of the complexes $[Co(Hhpic)_2(H_2O)_2]$, $[Fe(Hhpic)_2(H_2O)_2]$, $[Zn(Hhpic)_2(H_2O)_2]$, $[Mn(Hhpic)_2(H_2O)_2]$, and $[Cu(Hhpic)_2]$. Complexes 3, 4 and 5 have been previously synthesized and structurally characterized by using a hydrothermal method. However, they have presented a less intricate method for the synthesis of these complexes.

1.6.2 Sites of insulin and vanadate action

The insulin receptor is an insulin-activated protein-tyrosine- kinase *(*InsRTK*)*. Following insulin binding, the receptor undergoes activation by autophosphorylation and subsequently phosphorylates several endogenous proteins on tyrosine moieties. Tyrosyl phosphorylation is linked to a serine/threonine phosphorylation state of key enzymatic systems controlling glucose and fat metabolism. When insulin is removed, termination occurs at several levels, one of which is dephosphorylation of tyrosyl residues by endogenous protein phosphotyrosine phosphatases *(*PTPases*)*. Since vanadate is an inhibitor of PTPases, it was initially believed that the ion acts intracellularly by blocking the PTPase, acting at the insulin receptor and therefore activates it in an insulin-ndependent manner. This, however, turned out not to be the case. Numerous groups have reported no significant increase in the phosphotyrosine content of the insulin receptor in vanadate-pretreated cells or tissues. This issue was further substantiated when quercetin was found to inhibit InsRTK-catalyzed phosphorylation of exogenous substrates *(*ID50s2"0.2 mM; and the stimulatory effect of insulin in intact rat adipocytes. The same biological effects when triggered by vanadate were not inhibited by quercetin. This left us with two alternative working hypotheses for vanadate signaling: *(*a*)* vanadate bypasses the tyrosine phosphorylation step, or *(*b*)* vanadate effects can be signaled through additional non-insulin receptor protein-tyrosine-kinase*(*s*)* (Goldwaser *et al.*, 2000).

1.6.3 Oxovanadium(IV) insulin enhancing agents

Before the discovery of insulin and its clinical trials for treating diabetes mellitus (DM), inorganic salts of vanadium have long been known to act as orally viable mimics or enhancing agents for increased activity of insulin *in vitro* and *in vivo*.

The first report of vanadium salts being used as a metallotherapeutic agent appeared in 1899 (Thomas, et al, 2016). Consistent with medical trials of that era, Lyonnet and his colleagues first tried the proposed drug on themselves, then on 60 of their patients (three of whom were diabetic) over a period of some months. They described what might be considered today a “Phase 0” clinical trial in somewhat vague terms: 4-5 mg sodium metavanadate (before meals) every 24 h, three times per week, with 19 resulting two out of the three diabetic patients said to have obtained a slight, transient, lowering of sugar levels. No ill effects were noted in any of their patients. This result remained relatively unnoticed until much later in 1979 by (Tolman, et al, 1979), who demonstrated that a millimolar administration of sodium metavanadate to fat cells stimulated glucose uptake and inhibited lipid breakdown in a tissue-specific manner, similar to insulin. Although inorganic salts have been successful at enhancing the activity of insulin, the poor *in vivo* absorption and high dose requirement resulted in increased toxicity. Since insulin is not orally active, great effort has therefore been made to synthesize oxovanadium(IV) complexes of organic ligands of high biological activity (hydro/lipophilicity) and low toxicity which are readily absorbed.(Winfried, 1997) Potent complexes with various coordination modes $VO(O_4)$, $VO(N_2O_2)$, $VO(N_2S_2)$, $VO(S_4)$, $VO(S_2O_2)$, and $VO(N_4)$, and the relationship between their structures and insulin-mimetic activities has been examined by evaluating both *in vivo* and *in vitro* results (NEJO, 2009).

1.6.4 Organo-vanadium complexes

Vanadium salts are seriously considered as a possible treatment for diabetes. Because of their toxicity, only a low dose of vanadium *(*2 mg*/*kg*/*day*)* was used in clinical studies.

Although this was about 20-fold lower than doses used in most animal studies, several beneficial effects were observed and documented. Any manipulation to elevate the insulinomimetic efficacy of vanadium without increasing its toxicity is of major clinical interest for the future care of diabetes in humans.

Several organically chelated vanadium compounds, such as vanadium-acetylacetonate and vanadium RL-252 $[(CH_2)_2\text{-C-}\{CH_2O\text{-}(CH_2)_2\text{-CO-NHCH }(iBu)\ CONOHCH_2\}_2]$, are more potent than free vanadium in facilitating insulin-like effects in rat adipocytes, Similarly, chelated vanadium compounds, such as bis*(*maltolato*)*oxovanadium and bis*(*picolinato*)*oxovanadium, are more effective than free vanadium in reducing circulating glucose levels in hyperglycemic STZ-treated rats (Goldwaser *et al.*, 2000).

Objectives:

The objectives of this research work are:

- Mainly the synthesis and analysis of organic vanadium complexes that are biological importance

-Synthesizes and analysis of some vanadium complexes that do not have side effects for animals.

-Study of the anti-diabetic effects of vanadium compounds on animal models of insulin mimics.

- Investigation of the efficacy and effects of small doses of vanadium complexes in diabetic rats.

Chapter two

2.Meterials and Methods

2. 1Materials

2.1.1Chemicals

Table 2.1Shows Names,molecular formula and details of materials

Name	Molecular Formula	Details
Vanadium sulfate hydrate	$VOSO_4.H_2O$	Aldrich-233706-25g-USA
Vanadium acetyle acetone	$VO(acac)_2$	Alfa Aesar-61100162-10g-Germany
Vanadium penta oxide	V_2O_5	Alfa Aesar-111093-250g-Germany
Glycine	$C_2H_5NO_2$	MERCK-0053747-100G-Germany
L-Tyrosine	$C_9H_{11}NO_3$	Cambrain chemicals-2012580303-Canada
L-Cysteine	$C_3H_7NO_2S$	Aldrich 168149-25g-USA
L-Homoserine	$C_4H_9NO_3$	Aldrich-672151-5g- Germany
Tartaric acid	$C_4H_6O_6$	HQPK-841000-100g-England
2-picolinic acid	$C_6H_5NO_2$	Aldrich-p42800-100g-USA
Sodium succinate hexa hydrate	$C_4H_4NaO_4.6H_2O$	Loba chemic-6106214-250g-India
2.6pyridine carboxalic acid	$C_7H_3NO_4$	Aldrich-p63808-100g-USA
1.10phenanthroline	$C_{12}H_8N_2$	MERCK-K-13601225-5g-Germany
1.10 Phenanthrolinum chloride monohydrate	$C_{12}H_8N_2.HCl$	MERCK-L-801223-5g-Germany
Sodium bicarbonate	$NaHCO_3$	Elgomhouria-697-Kg-Egypt
Salicylsaldehyde thiosemicarbazone	$C_8H_9N_3SO$	Sigma-Aldirch-658774-1g-USA
2Chlorobenzaldehyde thiosemicarbazone	$C_8H_8Cl\ N_3S$	Alfa Aesar-E9773B-5g-Germany

3-Amino pyridine Thiosemicarbazone	$C_7H_9N_5S$	Sigma-Aldirch-62315-0.5g-USA
Salicysaldehyde	C_7H_9O	Loba chemic-0563400250-250ml-India
3-Hydroxypyridine	C_5H_5NO	Alfa Aesar-A13910-50g-Germany
N. N Dimethylethelynediamine	$C_4H_{12}N_2$	Sigma-Aldrich-D158003-25g-Germany
1.2 Diamine propane	$C_3H_{10}N_2$	Aldrich-239585-50g- Germany
2-Picolylamine	$C_6H_8N_2$	Aldrich-239585-50g- Germany
Potasium dichromate	$K_2Cr_2O_7$	APOLDA-35473-100g-Germany
Sulfuric acid	H_2SO_4	ADWIC-5221F-L-Egypt
Hydrochloric acid	HCl	Scharlau – AC0741 –Spain
Ethanol	C_2H_5OH	ADWIC-110404L-Egypt
Methanol	CH_3OH	ADWIC-67561-L-Egypt
Diethyl ether	$C_2H_{10}O$	Laboratory Rasyan -0011202077-India
Argon gas	Ar	CULF-Cryo-124239- Egypt
Streptozotocin –STZ	$C_8H_{15}N_3O_7$	Sigma-Aldirch-
Sodium citrate Buffer		Bio diagnestic and research reagent –L- Egypt

2.1.2General Instruments

- Hot plate with magnetic stirrer model - VELP -Europe.
- Magnetic stirrer model Torreypines- 220 v - USA.
- Sensitive balance model Sartorius - BI2105-Canada.
- Water path.
- Bran sonic- ultra sonic cleaner –Branson 2510- USA.
- Rotary evaporator – Heidolph – Germany.
- Determination of Melting Points

The melting points of complexes were determined by Fisher-Johns melting point apparatus in ˚C – Fisher Scientific Company - USA model 6200.

- Magnetic Susceptibility

  The magnetic Susceptibilities of complexes were measured on Sherwood scientific-England.

- Conductivity meter

  Molar conductivities were measured on conductivity meter model-JENCO-3173R-USA.

2.1.3 Spectroscopic Instruments

Infrared spectra were recorded on a 8001-PC FT-IR- Schimadzu spectrophotometer using KBr pellets in the mid-infrared region 4000-400 Cm^{-1}., Ultra violet-vis spectra were recorded on UV.3101PC-Schimadzu Japan, the ^{1}H-^{13}CNMR spectra were recorded on a Varian Mercury VX-300 NMR Spectrometer. ^{1}H spectra were run at 75.46 MH_Z and ^{13}C spectra were run at 300 MH_Z in DMSO-d_6/$CDC1_3$/D_2O as a solvent and TMS as an internal standard.

2.1.4 Thermal measurements

Thermogravimetric Analysis studies (TGA), was carried out on a Thermo Gravimetric Analyzer, TGA- Q500 –TA instruments.

2.2Methods

2.2.1Synthesis of complexes C1-C15

* Four groups of oxo and dioxo vanadium complexes were synthesized (scheme2.1)

- **Group one:** Vanadium salt was dissolved and mixed with amino acids ligands L1-L5 and 1,10phenantheoline L2 on ethanolic solution obtained oxovanadium complexes C1-C4.

- **Group two:** Vanadium salt was dissolved and mixed with carboxylic acids, L6-L9 and 1,10phenantheoline L2 on ethanolic solution obtained oxovanadium complexes C5-C8.

-**Group three:** Vanadium salt was dissolved and mixed with thiosemicarbazone ligands L10-L13 on ethanolic solution and an under argon atmosphere, obtained oxovanadium complexes C9-C12.

- **Group four:** Schiff-base ligands L14-L16 were prepared; Vanadium oxide dissolved and mixed on ethanolic solution under argon atmosphere, obtained dioxovanadium complexesC13-C15.

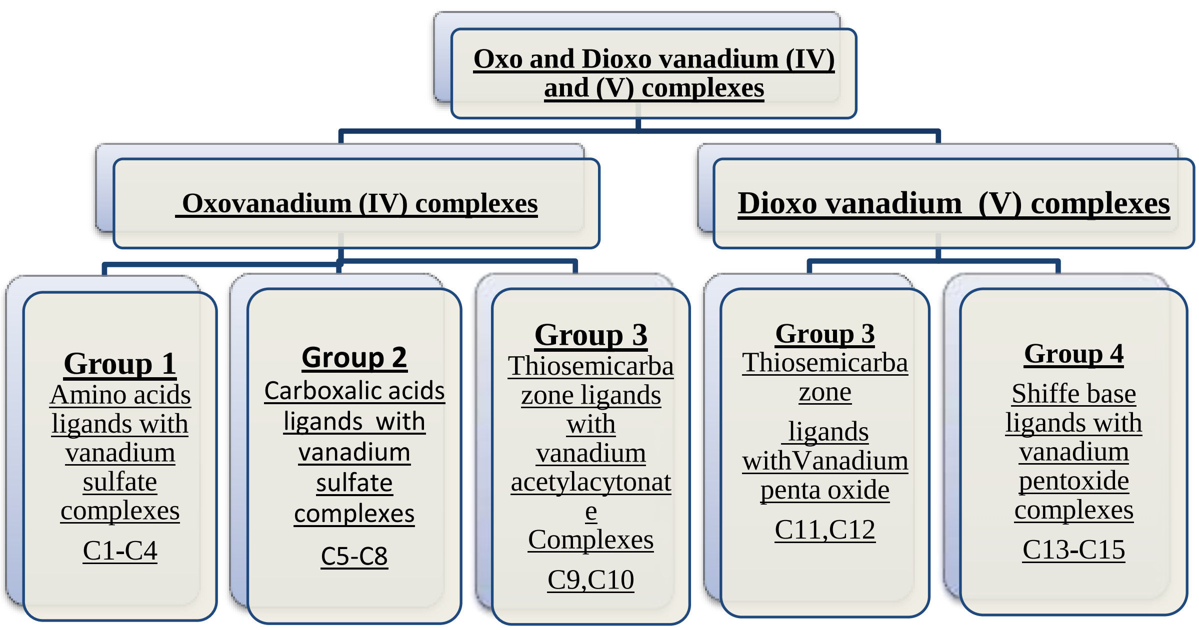

- ***Scheme 2-1To illustrate groups of synthsis of Oxo and Dioxo vanadium (IV)\ (V) complexes (C1-C15)***

2.2.2Charactraization of complexes C1-C15

Complexes from C1-C15 were characterized, and identified by physiochemical analysis, spectroscopic techniques, and thermal analysis.

-Conductivities of complexes:

The molar conductivity values, of the complexes measured in DMF solution ($c = 1.0\times10^{-3}$ Mol/cm^{-3}).

- Magnetic susceptibility measurements of complexes

The magnetic moment is calculated from the magnetic susceptibility, since the magnetic moment is not measured directly.

- Infrared Spectrophotometer (IR)

Infrared spectra were recorded using KBr pellets in the mid-infrared region 4000-400 Cm^{-1}.

- Ultra Violet Spectrophotometer (UV)

Complexes solutions ($c = 1.0\times10^{-3}$mol /cm^{-3}) were prepared to recorded Ultra violet-vis spectra.

-Nuclear Magnetic Resonance Spectrophotometer (NMR)

Complexes were identified by the ^{1}H NMR and ^{13}C NMR spectra, Chemical shifts (δ) are reported in ppm. Splitting patterns are designed as follows: s- singlet, d- doublet, t- triplet, q- quartet and m- multiplet.

-Thermogravimetric studies (TGA)

Thermo gravimetric studies TGA for the complexes C1-C15 were carried out within the temperature range from room temperature up to 1000 ºC with a heating rate of 10 degree/min.

-Theoretical DFT calculations

The density functional theory was applied to calculate the optimized geometries using the Gaussian09 program. The DFT/B3LYP method was used for the geometry optimization. Full geometry optimization was performed using B3LYP/LANL2DZ as a basis set to generate the optimized structure for ligands and complexes.

2.2.3 Computer programms

- MDL isis drow 2.5

MDL isis drow 2.5 program was used to draw structures of compounds (C1-C15).

- Chemcraft version 1.8

Chemcraft version 1.8 program was used to render 3-dimensional pictures of molecules by atomic coordinates with the possibility to examine or modify any geometrical parameter in the molecule (distance, angle), and provide very detailed structured visualization of output files of complexes (C1-C15).

- Gaussian09 program

Gaussian09 program was used to calculate the optimized geometries and performed minimize the energy of a molecule by modifying its structure, provides the energetically-preferred structures of a complexes (C1-C15).

- Statistical Package for the Social Sciences (SPSS)

SPSS Statistics is a software package used for logical batched and non-batched statistical analysis, which included in the base software Analysis of variance (ANOVA) is a collection of statistical models used to analyze the differences among group means and their associated procedures developed by statistician and evolutionary biologist Ronald Fisher. In the ANOVA setting, the observed variance in a particular variable is partitioned into components attributable to different sources of variation. In its simplest form, ANOVA provides a statistical test of whether or not the means of several groups are equal, and therefore generalizes the *t*-test to more than two groups. ANOVAs are useful for comparing (testing) three or more means (groups or variables) for statistical significance (Bryman, Cramer, 2011).

Chapter Three

3.Experimental and Results

3.1 Experimental

3.1.1 Synthesis of Oxovanadium (IV) complexes

3.1.1.1 Synthesis of Amino acids and vanadium sulfate complexes (group1)

- Complex 1(C1) Cystinato 1,10 phenanthroline oxovanadium (IV)

- Chemical formula [VO(cys)(phen)] [$C_{15}H_{13}N_3O_3SV$]

- Synthesis of complex

(0.163g, 1mmol) of vanadyl sulfate was dissolved in 20 cm^3 water, (0.121g, 1mmol) of cysteine dissolved in 20ml ethanol and mixed with (0.234g, 1mmol) of 1,10 phenanthroline chloride monohydrate dissolved in 20 cm^3 ethanol , added (0.168g, 1mmol) of sodium bicarbonate mixture was stirred and refluxed for 6h at 72°C green ppt was formed ,which was filterd and washed with ethanol.

$$VOSO_4 + C_{12}H_8N_2\text{-}HCl + C_3H_7NO_2S \xrightarrow[Na_2CO_3/72^0C]{\text{ethanol}} [C_{15}H_{13}N_3O_2SV]$$

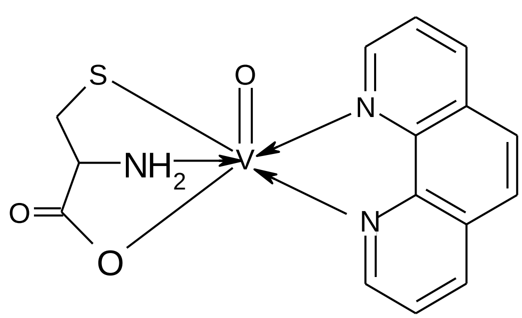

- Complex 2 (C2) Chloro Glycinato 1,10 phenanthroline oxovanadium(IV)

- Chemical formula [VO(Cl) (gly)(phen)] - [$C_{14}H_{12}Cl\ N_3O_3V$].H_2O

- Synthesis of complex

(0.163g, 1mmol) of vanadyl sulfate was dissolved in 20 cm^3 water and added to (0.075g, 1mmol) of glycine which was dissolved in 20 ml ethanol and mixed with (0.234g, 1mmol) of 1,10 phenanthroline chloride monohydrate dissolved in 20 cm^3 ethanol, after adding (0.168g, 1mmol) of sodium bicarbonate mixture was stirred and refluxed for 6h at 72°C a dark green ppt was formed ,solid was filterd and washed with ethanol.

$$VOSO_4 + C_{12}H_8N_2\text{-}HCl + C_2H_5NO_2 \xrightarrow[Na_2CO_3\,/\,72^0C]{\text{ethanol}} [C_{14}H_{12}ClN_3O_3SV]$$

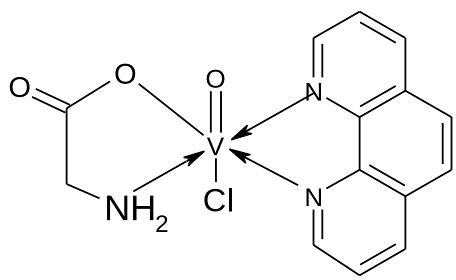

- Complex 3 (C3) Chloro tyrosinato 1, 10 phenanthroline oxovanadium (IV)

- Chemical formula [VO (Cl) (tyro)(phen)] - [$C_{21}H_{18}\ Cl\ N_3O_4V$].$H_2O$

- Synthesis of complex

(0.163g, 1mmol) of vanadyl sulfate was dissolved in 20cm^3 water and added to (0.181g, 1mmol) of tyrosine dissolved in 20cm^3 ethanol and mixed with (0.234g, 1mmol) of 1.10phenanthroline chloride monohydrate dissolved in 20cm^3 ethanol, added (0.168g, 1mmol) of sodium bicarbonate mixture was stirred and refluxed for 6h at 72°C a dark green ppt was obtained, which was filterd and washed with ethanol.

$$VOSO_4 + C_{12}H_8N_2\text{-}HCl + C_9H_{11}NO_3 \xrightarrow[Na_2CO_3/72^0C]{ethanol} [C_{21}H_{18}ClN_3O_4V]$$

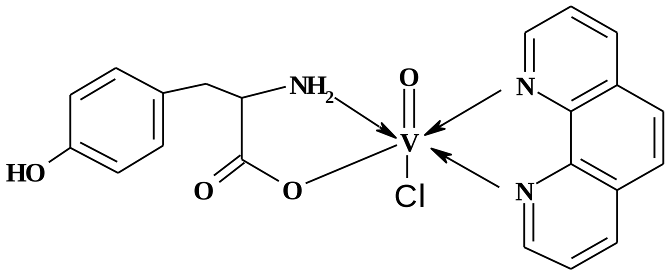

- Complex 4 (C4) Homoserinato 1,10 phenanthroline oxovanadium (IV)

-Chemical formula [VO(homo)(phen)] $[C_{16}H_{15}N_3O_4V]$

-Synthesis of complex

(0.163g, 1mmol) of vanadyl sulfate was dissolved in 20 cm^3 water and added to (0.119g, 1mmol) of homoserine which was dissolved in 20 cm^3 ethanol and mixed with (0.234g, 1mmol) of 1,10 phenanthrolin chloride monohydrate dissolved in 20 cm^3 ethanol, after adding (0.168g, 1mmol) of sodium bicarbonate mixture was stirred and refluxed for 6h at 72°C a dark green ppt was obtained, which was filtterd and washed with ethanol.

$$VOSO_4 + C_{12}H_8N_2\text{-}HCl + C_4H_9NO_3 \xrightarrow[Na_2CO_3\ 72^0C]{ethanol} [C_{16}H_{15}N_3O_4V]$$

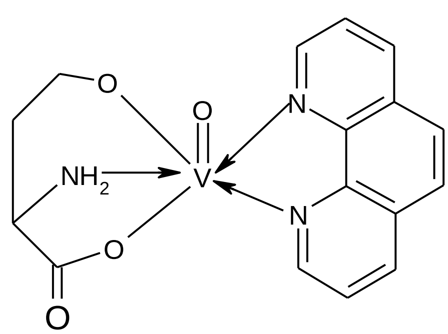

3.1.1.2 Synthesis of Carboxalic acids and vanadium sulfate complexes (group 2)

- Complex 5 (C5) Bis1, 10 phenanthroline tartarato dioxovanadium(IV)

-Chemical formula [$(VO)_2$(tartar)$(phen)_2$] [$C_{28}H_{18}N_4O_8V_2$]

-Synthesis of complex

(0.326g, 2mmol) of vanadyl sulfate was dissolved in 20 ml water and added to (0.1g, 10ml) (Sakurai, et al, 2005) of tartaric acid dissolved in 10 cm^3 water and mixed with (0.360g, 2mmol) of 1.10phenanthroline dissolved in 20 cm^3 ethanol , mixture was stirred and refluxed for 6h at 72°C a dark green ppt was obtained, was filterd and washed with ethanol.

$$2VOSO_4 + 2C_{12}H_8N_2 + C_4H_6O_8 \xrightarrow[72^0C]{\text{ethanol}} [C_{28}H_{18}N_4O_8V_2]$$

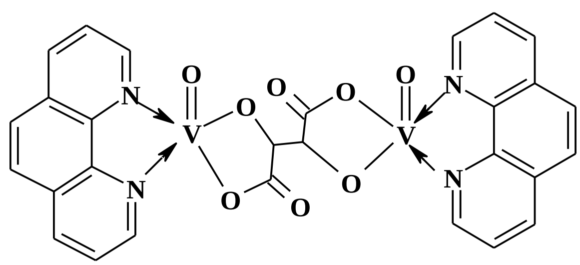

- Complex 6 (C6) 1, 10 phenanthroline 2.6pyridin oxovanadium (IV)

- Chemical formula [VO(2.6pyr)(phen)] [$C_{19}H_{11}N_3O_5V$]

-Synthesis of complex

(0.163g, 1mmol) of vanadyl sulfate was dissolved in 20 cm^3 water and added to (0.167g, 1mmol) of 2, 6 pyridine carboxalic acid dissolved in 20 cm^3 water and mixed with (0.180g, 1mmol) of 1,10 phenanthroline dissolved in 20 cm^3 ethanol, mixture was stirred and refluxed for 6h at 72°C a brown ppt was obtained, which was filterd and washed with ethanol.

$$VOSO_4 + C_{12}H_8N_2 + C_7H_5NO_4 \xrightarrow[72^0C]{\text{ethanol}} [C_{19}H_{11}N_3O_5V]$$

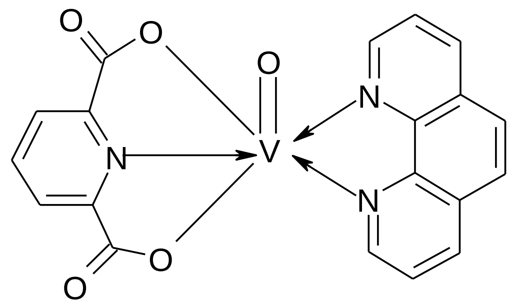

-Complex 7(C7) 1, 10 phenanthroline Succinato oxovanadium (IV)

-Chemical formula [VO(succ)(phen)] $[C_{16}H_{12}N_2O_5V]$

-Synthesis of complex

(0.163g, 1mmol) of vanadyl sulfate was dissolved in $20cm^3$ water and added to (0.162g, 1mmol) of sodium succinate dissolved in $20cm^3$ water and mixed with (0.180g, 1mmol) of 1,10 phenanthroline was dissolved in 20 cm^3 ethanol, mixture was stirred and refluxed for 6h at $72^{\circ}C$ a brown ppt was obtained,which was filterd and washed with ethanol.

$$VOSO_4 + C_{12}H_8N_2 + C_4H_4Na_2O_4 \xrightarrow[72^0C]{\text{ethanol}} [C_{16}H_{12}N_2O_5V] + Na_2SO_4$$

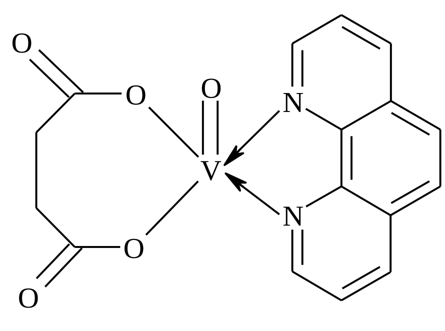

- Complex 8 (C8) glycinato 2-picolonito oxovanadium (IV)

- Chemical formula [VO (gly)(2-Pico)] - [$C_8H_8N_2O_5V$]

- Synthesis of complex

(0.163g, 1mmol) of vanadyl sulfate was dissolved in 20cm^3 water and was added to (0.075g, 1mmol) of glycine dissolved in 20cm^3 ethanol and mixed with (0.123g, 1mmol) of 2-picolinic acid was dissolved in 20cm^3 water, mixture was stirred and refluxed 6h at 72°C a dark green ppt was obtained, which was filterd and washed with ethanol.

$$VOSO_4 + C_2H_5NO_2 + C_6H_5NO_2 \xrightarrow[72^0C]{ethanol} [C_8H_8N_2O_5V]$$

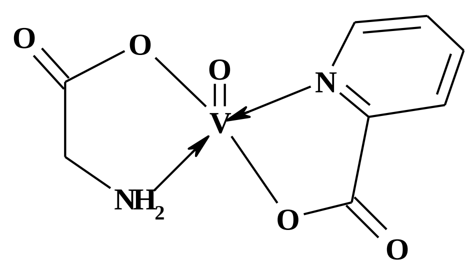

3.1.1.3 Thiosemicarbazone ligands and vanadium acetylacytonate Complexes (group 3)

-Complex 9(C9) 2-chlorobenzaldehyde thiosmicarbazone 1, 10 phenanthroline oxovanadium (IV) Chloride

-Chemical formula [VO(ClBTSC)(phen)] Cl - [$C_{20}H_{15}ClN_5OSV$]Cl

-Synthesis of complex

(0.213g, 1mmol) of 2-Chlorobenzaldehyde thiosemicarbazone was dissolved in 20 ml ethanol, (0.234g, 1mmol) of 1,10 phenanthroline chloride monohydrate was dissolved in 20 cm^3 ethanol, solutions were mixed and stirred for 30min at 72◦C ,(0.265g, 1mmol) of vanadium acetyl acytone was dissolved in 20 cm^3 ethanol and added to above solution ,mixture was stirred and refluxed under argon atmosphere for 8h at 72◦C a brown ppt was obtained, solid was filterd and washed with ethanol.

$$VO(acac)_2 + C_{12}H_8N_2\text{-}HCl + C_8H_8ClN_3S \xrightarrow[72^0C\backslash Ar]{ethanol} [C_{20}H_{14}ClN_5SOV]Cl$$

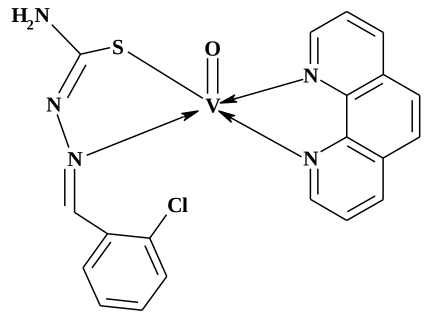

-Complex 10(C10) bis 2-chlorobenzaldehydethiosmicarbazone di 3-hydroxy pyridine oxo vanadium (IV)

-Chemical formula [VO(ClBTSC)(3-HPy)$_2$] - [$C_{18}H_{16}ClN_5O_3SV$]

-Synthesis of complex

(0.213g, 1mmol) of Chlorobenzaldehyde thiosemicarbazone was dissolved in 20 cm^3 ethanol, (0.190g, 2mmol) of 3-hydroxypyridine was dissolved in 20 cm^3 ethanol, solutions were mixed and stirred for 30min at 72◦C, (0.265g, 1mmol) of vanadium acetyl acytone was dissolved in 20 cm^3 ethanol and added to above solution, mixture was stirred and refluxed under argon atmosphere for 8h at 72◦C a dark gray ppt was obtained, which was filterd and washed with ethanol.

$$VO(acac)_2 + 2C_5H_5NO + C_8H_8ClN_3S \xrightarrow[72'C\backslash Ar]{ethanol} [C_{18}H_{16}ClN_5O_3SV]$$

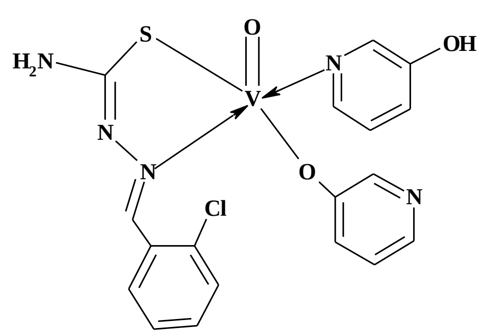

3.1.2 Dioxovanadium (V) complexes

3.1.2.1 Synthesis of Thiosemicarbazone ligands and Vanadium penta oxide (group3)

-Complex11(C11) Sodium 3 – hydroxypyridine Salicylsaldehyde thiosemicarbazone dioxovanadate (V)

-Chemical formula $Na[VO_2(SALTSC)(3\text{-}Hpy)]$ - $Na[C_{13}H_{12}N_4O_4SV]$

-Synthesis of complex

(0.195g, 1mmol) of salicyaldehyde thiosemicarbazone (SALTSC) was dissolved in 20cm^3 ethanol, (0.095g, 1mmol) of 3-Hydroxypyridine was dissolved in 20cm^3 ethanol too and was added in (SALTSC) solution , solutions were mixed and stirred for 30min at 72°C, (0.181g, 1mmol) of vanadium pentaoxide was dissolved in aqueous solution of (0.168g, 1mmol) Sodium bicarbonate stirred for 10min and added to above solution ,mixture was stirred and refluxed under argon atmosphere for 8h at 72◦C a yellow ppt was obtained and filterd off and washed with ethanol.

$$V_2O_5 + C_8H_9N_3OS + C_5H_5NO + Na_2CO_3 \xrightarrow[Ar_{atm}]{\text{ethanol } 72^0C} Na[C_{13}H_{12}N_3O_4SV]$$

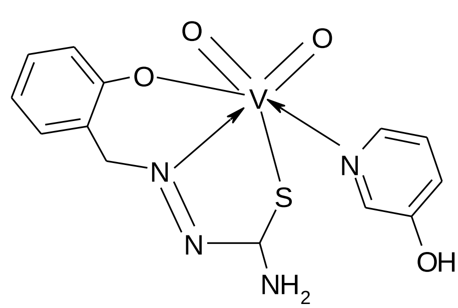

- Complex12(C12) Sodium 3-Aminopyridine2-arbaldehydethiosemicarbazone glycinato dioxovanadate (V)

-Chemical formula $Na[VO_2(3\text{-}AP)(gly)]$ - $Na[C_9H_{12}N_6O_4SV]$

- Synthesis of complex

(5mg, 0.0256mmol) of 3- Aminopyridine 2-Carboxaldehydethiosemicarba zone carbazone was dissolved in $10cm^3$ ethanol, (1.9mg, 0.0256mmol) of glycine was dissolved in $10cm^3$ ethanol too, (4.65mg, 0.0256mmol) of vanadium pentaoxide was dissolved in aqueous solution of (4.3mg, 0.0512mmol) Sodium bicarbonate and mixed with above solutions, mixture was stirred and refluxed under argon atmosphere for 48h at 72◦C a yellow greenwish ppt was obtained, filterd off and washed with ethanol.

$$V_2O_5 + C_7H_9N_5S + C_2H_5NO_2 + Na_2CO_3 \xrightarrow[Ar_{atm}]{\text{ethanol } 72^{\circ}C} Na[C_9H_{12}N_6O_4SV]$$

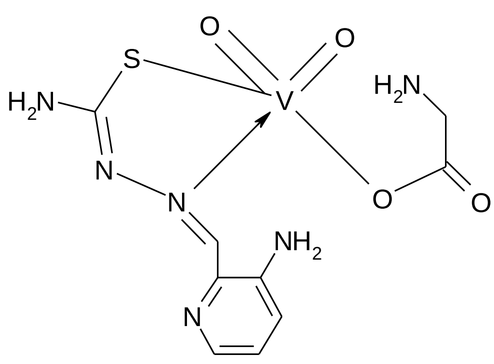

3.1.2.2 Shiffe base ligands and vanadium pentoxide complexes(group4)

-Complex 13: 2-NSalicylidene N, Ndimethylaminoethylamino dioxovanadate (V)

-Chemical formula $[VO_2(Sal\text{-} DMEDA]$ - $[C_{11}H_{15}N_4O_3V]$

- Synthesis of ligand and complex

Schiff base ligand by mixing (2.42g, 20mmol) of salicyldehyde with (1.77g, 20mmol) of N,N-Dimethylethelynediamine, in $20cm^3$ ethanol with continuous stirring and reflux for 3.5h at 72 °C a yellow solid formed and was filterd ,washed , dried and weighted. m.p;130 ◦C (2.1g, 83.0%) .

$$C_4H_{12}N_2 + C_7H_6O_2 . \xrightarrow[\text{refluxed}]{\text{stirred}} [C_{11}H_{16}N_2O] + H_2O$$

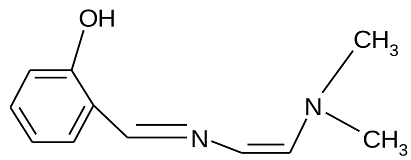

(1.81g, 10 mmol) of vanadium pentaoxide was dissolved in aqueous solution (1.68g, 20 mmol) of Sodium bicarbonate, solution was stirred for 15 min, (1.92g, 10mmol) of ligand was dissolved in 30cm^3 ethanol and was added to above solution, mixture was stirred and refluxed under argon atmosphere for 6h at 72 ^{o}C a yellow ppt was formed, filterd off and washed with ethanol.

$$V_2O_5 + C_{11}H_{16}N_2O + NaHCO_3 \xrightarrow[Ar_{atm}]{\text{ethanol } 72^oC} [C_{11}H_{15}N_2O_3V]$$

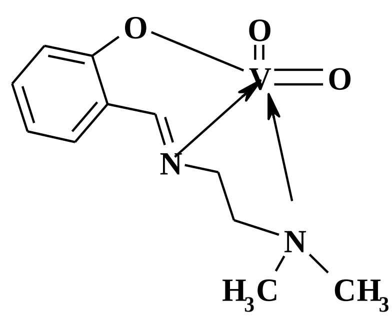

-Complex 14(C14) 2-N Salicylidene1.2diaminopropionate dioxovanadate (V)

- Chemical formula [VO_2(SaL- DAP)] - [$C_{17}H_{16}N_2O_4V$]

-Synthesis of ligand and complex

Schiff base ligand was prepared by mixing (2.42g, 20 mmol) of salicyldehyde with (0.74g, 10mmol) of 1,2-diaminopropane in 20cm^3 ethanol with continuous stirring and reflux for 3.5h at 72 °C, a yellow solid was formed and filterd, washed and dried. m.p; 140 °C (4.2g- 75%).

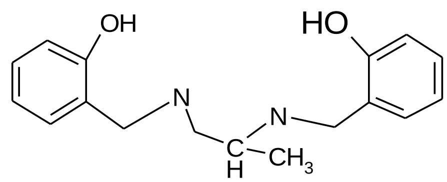

(1.81g, 10 mmol) of vanadium pentaoxide was dissolved in aquoes solution (1.68g, 20 mmol) of Sodium bicarbonate and solutoin was stirred for 15 min, (2.82g, 10 mmol) of ligand was dissolved in 30ml ethanol and added to the above solution, the mixture was stirred and refluxed under argon atmosphere for 6h at 72°C, Yellow ppt was formed, filtterd off and washed with ethanol.

$$V_2O_5 \quad + \quad C_{17}H_{18}N_2O_2 \xrightarrow[Ar_{atm}]{ethanol/72^{\circ}C} [C_{17}H_{16}N_2O_4V]$$

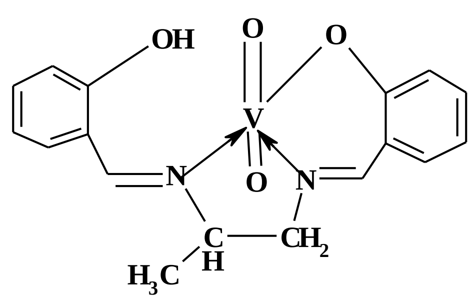

-Complex 15(C15) 2-N Salicylidene2-picoloamino dioxovanadium(V)

-Chemical formula $[VO_2(SaL\text{-}2PA)]$ $[C_{13}H_{11}N_2O_3V]$

-Synthesis of ligand and complex

Schiff base ligand was prepared by mixing (2.42g, 20 mmol) of salicyldehyde with (2.16g, 20 mmol) of 2-picolyamine in 20 cm^3 ethanol with continuous stirring and reflux for 3.5h at 72 °C, a brown oily solid was formed and kept in referigerator for two weeks, a bright yellow solid was formed, filterd, washed and dried. m.p 130°C (2.9g , 69%).

$$C_6H_8N_2 + C_7H_6O_2 \xrightarrow[\text{refluxed}]{\text{stirred}} [C_{13}H_{12}N_2O] + H_2O$$

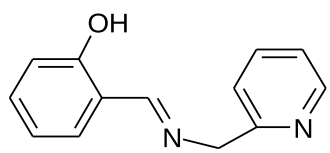

(1.81g, 10 mmol) of vanadium pentaoxide dissolved in aquoes solution (1.68g, 20 mmol) of sodium bicarbonate and solutoin was stirred for 15 min, (2.12g, 10 mmol) of ligand was dissolved in 30cm^3 ethanol and added to the above solution, the mixture was stirred and refluxed under argon atmosphere for 48h at 72°C, a greenish yellow ppt was formed, filterd off, washed and dried.

$$V_2O_5 + C_{13}H_{12}N_2O \xrightarrow[Ar_{atm}]{\text{ethanol } 72'C} [C_{13}H_{11}N_2O_3V]$$

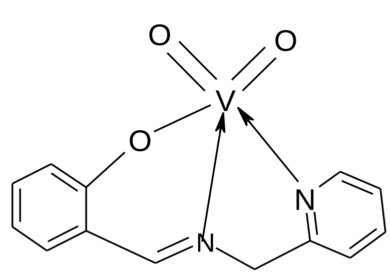

Table 3.1 shows scientific names of synthesized complexes (C1-C15)

Code	Name of complexes
	GROUP I
C1	Cystinato 1.10 phenanthroline oxovanadium (IV)
C2	Chloro Glycinato 1.10 phenanthroline oxovanadium(IV)
C3	Chloro tyrosinato 1.10 phenanthroline oxovanadium (IV)
C4	Homoserinato 1.10 phenanthroline oxovanadium (IV)
	GROUP II
C5	Bis1.10-phenanthroline tartarato dioxovanadium (IV)
C6	1.10-phenanthroline 2.6 pyridin oxovanadium (IV)
C7	1.10-phenanthroline Succinato oxovanadium (IV)
C8	glycinato 2- picolonito oxovanadium (IV)
	GROUPIII
C9	2-chlorobenzaldehyde thiosmicarbazone 1.10 phenanthroline oxovanadium (IV) Chloride
C10	Bis 2-chlorobenzaldehyde thiosmicarbazone 3-hydroxypyridine oxovanadium (IV)
C11	Sodium 3-hydroxypyridine Salicylsaldehyde thiosemicarbazone dioxovanadate (V)
C12	Sodium 3-Aminopyridine 2-Carbaldehyde thiosemicarbazone glycinato dioxovanadate (V)
	GROUP(IV)
C13	2-N Salicylidene N^1,N^1 dimethylamino dioxovanadium (V)
C14	2-N diSalicylidene 1.2 diamino propionate dioxovanadium(V)
C15	2-N Salicylidene2-picoloamino dioxovanadium (V)

Table 3.2 Structures of synthesized complexes (C1-C15)

Code	Type	Formula	Abbreviation in article
		GROUP I	
C1	Neutral	$[C_{15}H_{13}N_3O_3SV]$	[VO(cys)(phen)]
C2	Neutral	$[C_{14}H_{12}ClN_3O_3V].H_2O$	[VO(Cl) (gly)(phen)]
C3	Neutral	$[C_{21}H_{18}ClN_3O_4V].H_2O$	[VO(Cl)(tyro)(phen)]
C4	Neutral	$[C_{16}H_{15}N_3O_4V]$	[VO(homo)(phen)]
		GROUP II	
C5	Neutral	$[C_{28}H_{18}N_4O_8V_2]$	[VO(tart)(phen)]
C6	Neutral	$[C_{19}H_{11}N_3O_5V]$	[VO(2.6py)(phen)]
C7	Neutral	$[C_{16}H_{12}N_2O_5V]$	[VO(succ)(phen)]
C8	Neutral	$[C_8H_8N_2O_5V]$	[VO(2-pA)(gly)]
		GROUP III	
C9	cationic	$[C_{20}H_{15}ClN_5OSV]$ Cl	[VO(ClBTSC)(phen)]Cl
C10	Neutral	$[C_{18}H_{17}ClN_5O_3SV]$	[VO (ClBTSC) (3.Hpy)$_2$]
C11	Anionic	$Na[C_{13}H_{12}N_4O_4SV]$	Na[VO$_2$(SALTSC)(3.HPy)]
C12	Anionic	$Na[C_9H_{12}N_6O_4SV]$	Na[VO$_2$(gly)(3-AP)]
		GROUP IV	
C13	Neutral	$[C_{11}H_{15}N_2O_2V]$	[VO$_2$(SaL- DMEDA)]
C14	Neutral	$[C_{17}H_{17}N_2O_4V]$	[VO$_2$(SaL-DAP)]
C15	Neutral	$[C_{13}H_{11}N_2O_3V]$	[VO$_2$(SaL-2.PA)]

Table 3.3 Physiochemical data of synthesized complexes (C1-C15)

No	Color	Molecular formula	M.W	Yield %	M.P °C	Conductivity $mScm^2mol^{-1}$
		GROUPI				
C1	Green	$[C_{15}H_{13}N_3O_3SV]$	366.2	68.6	340	22.1
C2	Dark green	$[C_{14}H_{12}ClN_3O_3V].H_2O$	356.7	56.2	240	25.9
C3	Dark green	$[C_{21}H_{18}ClN_3O_4V].H_2O$	462.8	43.5	360	29.3
C4	Green	$[C_{16}H_{15}N_3O_4V]$	364.2	44.4	240	18.4
		GROUP II				
C5	Green	$[C_{28}H_{18}N_4O_8V_2]$	640.4	46.8	320	30.1
C6	Brown	$[C_{19}H_{11}N_3O_5V]$	412.2	63.4	336	21.6
C7	Dark brown	$[C_{16}H_{12}N_2O_5V]$	363.2	72.2	290	26.7
C8	Dark green	$[C_8H_8N_2O_5V]$	263.1	92.3	300	20.9
		GROUP III				
C9	Brown	$[C_{20}H_{15}\ ClN_5OSV]\ Cl$	496.2	48.9	>300	64
C10	Dark gray	$[C_{18}H_{17}ClN_5O_3SV]$	468.1	21.3	280	24.1
C11	Yellow	$Na[C_{13}H_{12}\ N_4O_4SV]$	394.3	96.3	>300	37.8
C12	Yellow	$Na[C_9H_{12}\ N_6O_4SV]$	374.2	62.5	280	35
		GROUP IV				
C13	Yellow	$[C_{22}H_{30}\ N_4O_4V]$	247.2	88.8	290	24.2
C14	Yellow	$[C_{17}H_{17}\ N_2O_4V]$	364.2	28.5	280	23.5
C15	Greenish-yellow	$[C_{13}H_{11}\ N_2O_3V]$	294.2	51	255	24.3

3.2 Results

3.2.1 Conductivities of complexes (C1-C15):

(Table 3-3) gives the electrical conductivity of aqueous solutions of complexes, a function of concentration. All values refer to room temperature 25 °C. The molar conductivity Λ is related to this by Λ = κ\c, C is the amount of substance concentration of the electrolyte .Thus if κ has units of millisiemens per centimeter (mS /cm), as in the (Table 3-3), and c is expressed in mol / L (Boca Raton, 1989) (Wolf, A. V, 1966).

3.2.2 Magnetic susceptibility measurements of complexes (C1-C15)

Measurements of magnetic properties have been used to characterize a wide range of systems from oxygen, metallic alloys, solid state materials, and coordination complexes containing metals.

The number of unpaired electrons provides information about the oxidation state and electron configuration. The magnetic moment is calculated from the magnetic susceptibility, since the magnetic moment is not measured directly.

The mass magnetic susceptibility $\chi g = [LC(R-R0)]/(m-m_0 \times 10^9)$

The molar susceptibility $\chi_m = \chi_g$ (M.W. in g mol) $^{-1}$

:

L = sample height in centimeters

m = sample mass in grams

$m_{0=}$ tube mass in grams

C = balance calibration constant (printed on back of balance) = 2.086

R = reading from the digital display (sample and tube)

R_0 = reading from the digital display (empty tube)

-Measured magnetic moments, *d*-configuration, and number of unpaired electrons For Vanadium (V^{+5}, V^{+4}) ions with an octahedral and tetrahedral geometry (Housecroft & Sharpe, 2008)(Figgis, et al, 1960).

Metal	d-configuration	Number of Unpaired Electrons	Magnetic moment
V^{+5}	d^0	0	0
V^{+4}	d^1	1	1.7-1.8

Table 3.4 Measured magnetic moments of synthesized complexes (C1-C15)

No	L	R	Ro	m	mo	xg	M.W	Xm	μ_s
C1	1	50	-30	0.87	0.81	2.78	366.2	0.0010	1.56
C2	0.7	83	-30	0.84	0.81	4.13	356.7	0.0013	1.87
C3	1	20	-30	0.84	0.81	3.48	462.8	0.0014	1.83
C4	0.7	22	-30	0.83	0.81	3.8	364.2	0.0013	1.81
C5	1	95	-30	0.85	0.81	6.52	640.3	0.0042	3.16
C6	0.7	30	-30	0.84	0.81	2.92	412.2	0.0012	1.69
C7	1	-20	-30	0.82	0.81	2.09	363.2	0.0007	1.34
C8	1	54	-30	0.87	0.81	2.92	263.1	0.0009	1.51
C9	0.8	-8	-30	0.83	0.81	1.84	496.2	0.0006	1.47
C10	1	-2	-30	0.83	0.81	2.09	468.1	0.0013	1.80
C11	1	-26	-30	0.87	0.81	1.4	394.3	5.482	0.36
C12	0.7	-32	-30	0.84	0.81	-9.7	374.2	-3.642	0
C13	1	-32	-30	0.84	0.81	-9.7	274.2	-5.719	0
C14	0.7	-28	-30	0.83	0.81	1.4	364.2	5.318	0.35
C15	0.7	-28	-30	0.84	0.81	9.73	294.1	2.8637	0.26

3.2.3 Ultra Violet Spectra (UV) of synthesized complexes

Ultra violet-vis spectra in complexes solutions C1-C15 ($c = 1.0\times10^{-3}$mol dm^{-3}) were recorded on UV.3101PC-Schimadzu Japan.

Table 3.5 Ultra violet spectrum bands (λ) nm of synthesized complexesC1-C8 and Vanadium sulfate

No	Ultra violet spectrum bands (λ) nm	$(\lambda)_{max}$
	Vanadium sulfate (λ) 242nm	
C1	270 - 291sh	270 nm
C2	201-222-292sh-270	270 nm
C3	202 - 222 – 270 – 292sh	270 nm
C4	223 - 263	263 nm
C5	220 – 270	270nm
C6	222 – 264 – 282sh	264nm
C7	203 - 223 - 270 - 289sh	270nm
C8	205 – 261	261nm

Table 3.6 Ultra violet spectrum of synthesized complexesC9-C10 and Vanadium acetyl acetone

No	Ultra violet spectrum bands (λ) nm	$(\lambda)_{max}$
	Vanadium acetyl acetone(λ) 304 nm	
C9	267 - 303 - 310	310nm
C10	267 - 306	306nm

Table 3.7 Ultra violet spectrum of synthesized complexesC11-C15 and Vanadium penta oxide

No	Ultra violet spectrum bands (λ) nm	$(\lambda)_{max}$
	Vanadium penta oxide (λ) 264 nm	
C11	222 - 267	267nm
C12	207 - 255	255nm
C13	209 – 254 – 319	319nm
C14	211- 258 - 264	264nm
C15	210 – 260	260nm

3.2.4 IR spectrum bands (KBr) cm^{-1} of synthesized complexes

C1-C15

Infrared spectra were recorded on a 8001-PC FT-IR- Schimadzu spectrophotometer using KBr pellets in the mid-infrared region 4000-400 Cm^{-1}

Table 3.8 IR spectrum bands (KBr) cm^{-1} of synthesized complexes

No	V = O	V ─ O	V ─ N	V ─S	C =N	C =O	Ar	N ─H_2
GROUB I								
C1	975	602	541	723	1588	1646	1416-1655	3388
C2	972	682	548	-	1604	1752	1419-1662	3338
C3	851	686	541	-	1588	1630	1460-1592	3398
C4	966	613	550	-	1592	1636	1419-1619	3426
GROUBII								
No	**V = O**	**V ─ O**	**V ─ N**	**-**	**C =N**	**C =O**	**Ar**	**N ─H_2**
C5	962	652	548	-	1588	1675	1423-1648	-
C6	918	686	568	-	1578	1682	1423-1648	-
C7	969	643	560	-	1588	1682	1416-1635	-
C8	953	626	517	-	1583	1635	1477-1619	3421
GROUBIII								
No	**V =O**	**V─O**	**V ─N**	**-**	**C =N**	**C─ S**	**Ar**	**N ─H_2**
C9	975	-	541	-	1584	726	1416-1648	3415
C10	968	674	505	-	1523	723	1471-1610	3419
C11	891-945	602	538	-	1604	753	1448-1616	3327
C12	956-869	692	507	-	1608	709	1453-1638	3170
GROUBIV								
No	**V =O**	**V =O**	**V─O**	**V ─N**	**-**	**C=N**	**Ar**	**C─ S**
C13	908-958	948	618	528	-	1601	1456-1675	-
C14	884-925	921	618	544	-	1604	1443-1672	-
C15	844-1012	1004	602	544	-	1625	1406-1672	-

Table 3.9 IR spectrum bands (KBr) cm^{-1} of Ligands

No	O─H	C = S	C =N	C =O	N-H	Ar	N ─ H_2
L1	3427	898	-	1604	-	-	3166
L2	-	-	1537	-	-	1416-1645	-
L3	3381	-	-	1742	-	-	3035
L4	3425	-	-	1608	-	1514-1600	3206
L5	3415	-		1657	-	-	3250
L6	3361	-	-	1742	-	-	-
L7	3411	-	1567	170 2	-	1413-1678	-
L8	3485	-	-	1682	-	-	-
L9	3438	-	1574	1715	-	1446-1655	-
L10	-	864	1604	-	3247	1433-1651	3411
L11	2910	-	1571	-	-	1480-1614	-
L12	-	888	1591	-	3432	1443-1648	-
L13	-	884	1544	-	-	1406-1665	3432
L14	3432	-	1588	-	-	1460-1665	-
L15	3068	-	1581	-	-	1456-1635	-
L16	3310	-	1594	-	-	1430-1679	-

3.2.5 ^{1}HNMR and ^{13}CNMRdata for synthesized complexes (C1-C15)

The NMR spectra were recorded on a Varian Mercury VX-300 NMR Spectrometer.^{1}H NMR spectra were run at 75.46 MH_Z and ^{13}C NMR spectra were run at 300 MH_Z and 500 MH_Z in DMSO-d_6\ $CDC1_3$ as a solvent and TMS as an internal standard. Chemical shifts (δ) are reported in ppm. Splitting patterns are designed as follows: s- singlet, d- doublet, t- triplet, q- quartet and m- multiplet.

Table 3.10 ^{1}HNMR and ^{13}CNMRdata for synthesized complexes (C1-C15)

Complexes	^{1}H NMR DMSO-d_6,ppm	^{13}CNMR DMSO-d_6, ppm)
[$C_{15}H_{13}N_3O_3SV$]	3.12 (d, 2H- CH_2) 4.16 (s, 1H- CH) 7.8 - 8.5 (m, 8H- arom) 9.11 (s, 2H- NH_2)	55.00 (1C, CH_2) 63.50 (1C, CH) 124.3-137.6 (10C, phen) 144.8 (2C, phen, C=N) 150.1 (1C, C─O─V)
[$C_{14}H_{12}ClN_3O_3V$].H_2O	4.50 (d, 2H- CH_2) 7.77 - 8.49 (m, 8H- arom) 9.06 (s, 2H- NH_2),	40.80 (1C, CH_2) 123.7 - 136.6 (10C, phen) 146.1 (2C, phen, C=N) 150.3 (1C, C─O─V)
[$C_{21}H_{18}ClN_3O_4V$].H_2O	3.45 (m, 2H- CH_2), 4.10 (m, 1H- CH), 6.50 - 6.96 (m, 4H, arom (tyro) 7.76 - 8.48 (m, 8H, phen), 9.10 (s, 2H- NH_2), 9.80 (s, 1H- OH)	40.04 (1C, CH_2) 60.60 (1C, CH) 115.3-128.4(5C,arom(tyro), 129.5 - 149.8 (10C, phen) 155.9 (2C, phen, C=N), 164.4 (1C, C─O─V) 174.7 (1C, C=O).
[$C_{16}H_{15}N_3O_4V$]	2.50 (m, 4H- 2CH_2), 3.50 (m, 1H- CH), 7.7 - 8.8 (m, 8H- phen), 9.10 (s, 2H- NH_2)	36.22 (2C, CH_2) 40.80 (1C, CH) 123.7-136.5 (10C, phen, CH and C), 146.1 (2C, phen C=N), 150.3 (1C, C─O─V)
[$C_{28}H_{18}N_4O_8V_2$]	4.30 (s, 1H- CH), 5.10 (s, 1H- CH), 7.7 - 8.6 (m, 12H-phen), 9.14 (m, 4H- HC=N)	64.80 (1C, CH) 71.30 (1C, CH) 120.4 - 141.9 (10C, phen) 148.8 (2C, phen, C=N) 173.0 (2C, C─O─V)
[$C_{19}H_{11}N_3O_5V$]	8.20 – 9.73 (m, 11H arom)	113.1 – 147.8(13C, arom) 158.1 (2C, C=N, arom) 158.6 (2C, C=N, arom) 165.1 (2C, C─O─V)
[$C_{16}H_{12}N_2O_5V$]	2.3 (s, 4H- 2CH_2) 7.7- 8.5 (m, 6H- phen) 9.02 (m, 2H- HC=N)	30.80 (1C, CH_2) 38.62 (1C, CH_2) 120.4 - 145.1 (10 C, phen) 150.0 (2C, phen, C=N) 174.7 (2C, C─O─V)
[$C_8H_8N_2O_5V$]	5.00 (m, 2H- 2CH_2)	76.93 (1C, CH_2)

	7.5- 8.5 (m, 4H- PA) 8.90 (s, 2H- NH_2)	113.9 – 124.9 (4C, PA) 158.4 (1C, PA, C=N) 158.9, 169.0 (2C, C─O─V)
[$C_{20}H_{15}$ ClN_5OSV] Cl	7.31 - 8.85(m, 10H,arom) 9.25(m, 2H- HC=N) 11.06 (m, 1H- HC=N) 11.57 (2H, NH_2)	113.2 – 147.4 (16C, arom) 157.7 (2C, phen, C=N) 168.2 (1C, CLBTSC, C=N) 178.3 (1C, C─O─V
[$C_{18}H_{17}ClN_5O_3SV$]	7.18 - 7.99(m, 10H,arom) 8.08 - 8.26 - 8.47 (3H, arom CH=N), 9.86 (2H, NH_2) 11.59	120.4 – 138.1 (15C, arom) 177.0 (1C, arom, C=N) 178.2 (2C, C─O─V)
Na[$C_{13}H_{12}$ N_4O_4SV]	6.40 – 7.43 (m, 7H, arom) 8.01(m, 1H- HC=N) 8.12 (m, 1H- HC=N) 8.52 (2H, NH_2) 9.96 (1H, OH)	122.5 – 138.4 (8C, arom) 140.6 (3C, arom, C=N) 154.2 (2C, C─O─V)
[$C_{22}H_{30}$ N_4O_4V]	2.50 (s, 3H- CH_3) 2.51 (s, 3H- CH_3) 3.34 (t, 2H- CH_2) 4.14 (t, 2H- CH_2) 6.79 –7.60 (m, 4H-arom) 8.98 (s, 1H- HC=N)	45.72, 51.46 (2C- CH_3) 55.64, 58.59 (2C- CH_2) 117.0 –136.4(5C- arom) 165.1 (1C- CH=N) 171.0 (1C- C─O─V)
[$C_{17}H_{17}$ N_2O_4V]	1.33 (d, 3H- CH_3) 4.00 (d, 2H-CH_2) 4.92, 5.31 (dd, 1H- CH) 6.78–7.55 (m, 8H-ph) 8.56 (s, 1H, H─C=N) 8.87 (s, 1H, H─C=N) 13.40 (s, 1H, H─CO)	20.70 (1C- CH_3) 65.50 (1C- CH_2) 65.00 (1C- CH) 116.94–163(12C-ph) 165.70 (2C-C=N)
[$C_{13}H_{11}$ N_2O_3V]	4.00 (s, 2H- CH_2) 6.96–8.71 (m, 7H- ph) 10.25 (s, 1H-H-C=N ph) 10.98 (s, 1H-H─C=N)	47.91(1C- CH_2) 121.5–160.4(10C-ph) 162.7 (1C- C=N ph) 163.0 (1C- C=N)

3.2.6 Thermal measurements

Thermo gravimetric studies TGA for the complexes C1-C15 were carried out within the temperature range from room temperature up to 1000 ºC with a heating rate of 10 degree/min on a Thermo Gravimetric Analyzer TGA - Q500.

Table 3.11 Thermo gravimetric studies TGA for the complexes C1-C15

No	Assignment loss	TGA °C	%Wt Loss	
			Found	(Calcd)
C1	VO_2 – remaining	847	22.47	22.64
C2	H_2O	95.1	4.90	5.04
	VO_2 – remaining	918	22.90	23.25
C3	H_2O	100	3.50	3.88
	VO_2 – remaining	826	17.55	17.92
C4	VO_2 – remaining	960	22.90	22.77
C5	VO_2 – remaining	900	26.25	25.90
C6	VO_2 – remaining	898	20.13	20.11
C7	VO_2 – remaining	880	22.83	22.83
C8	VO_2 – remaining	866	31.24	31.52
C9	VO_2 – remaining	910	16.78	16.74
C10	VO_2 – remaining	675	17.58	17.69
C11	$NaVO_3$ – remaining	837	30.7	30.9
C13	V_2O_5 – remaining	790	33.03	33.16
C14	V_2O_5 – remaining	890	24.43	24.96
C15	V_2O_5 – remaining	880	30.60	30.91

The TGA curve shows many steps .The first steps shows the loss of ligands and the residue of range (16%-33%) corresponding to VO_2, $NaVO_3$ and V_2O_5.

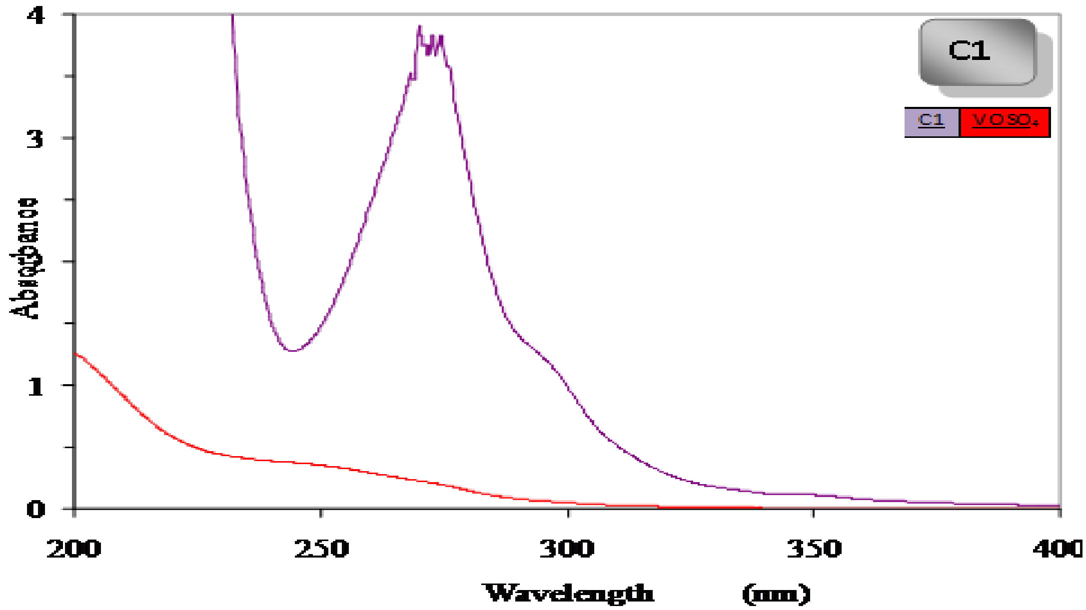

Figure 3.1: Ultra violet spectrum of C 1

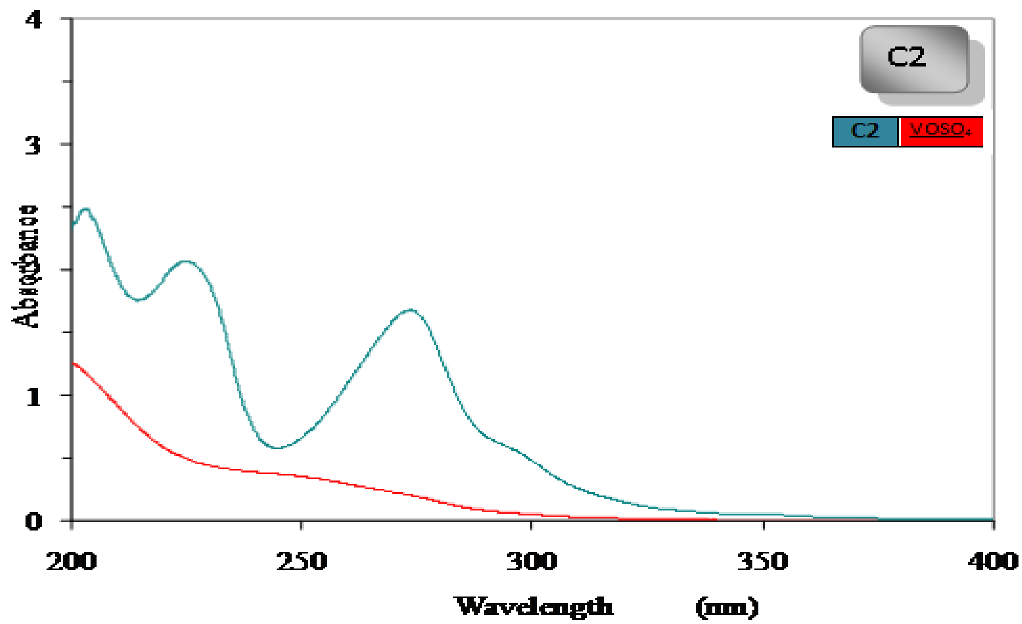

Figure 3.2: Ultra violet spectrum bands (λ) nm of C 2

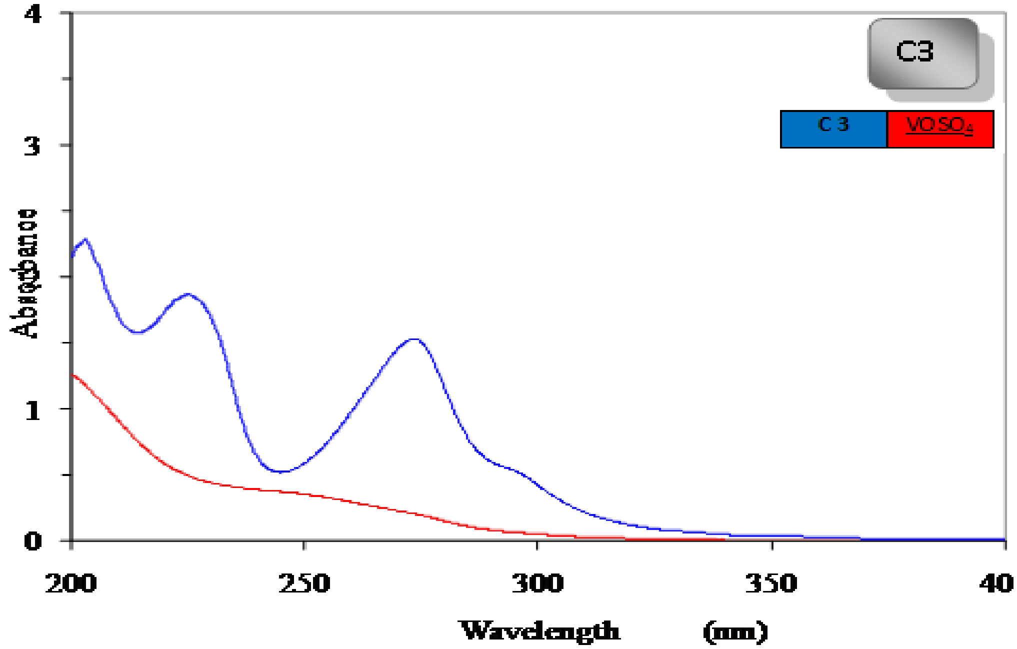

Figure 3.3: Ultra violet spectrum of C 3

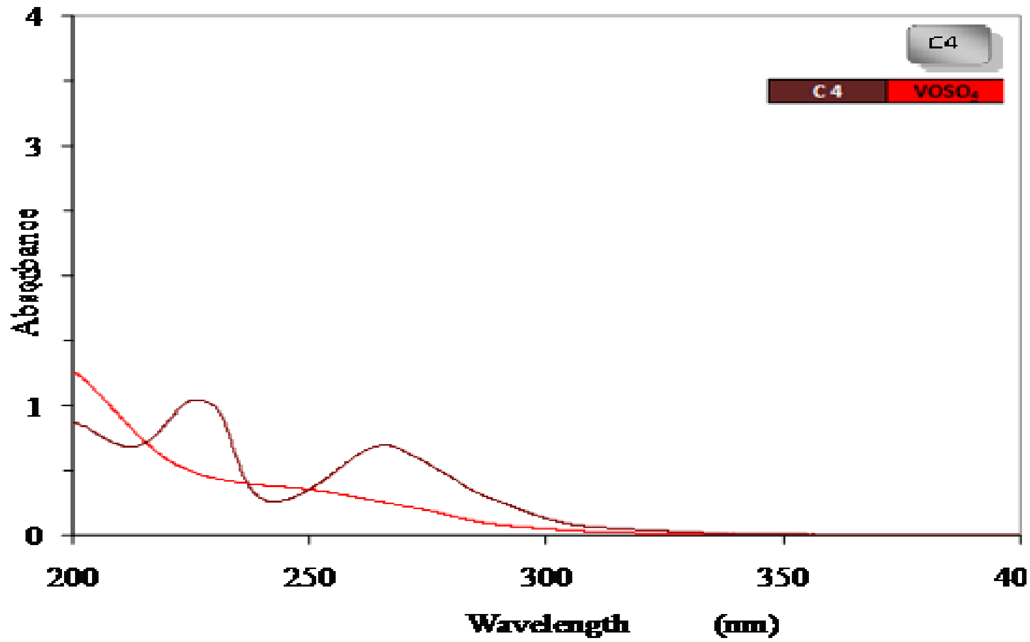

Figure 3.4: Ultra violet spectru of C 4

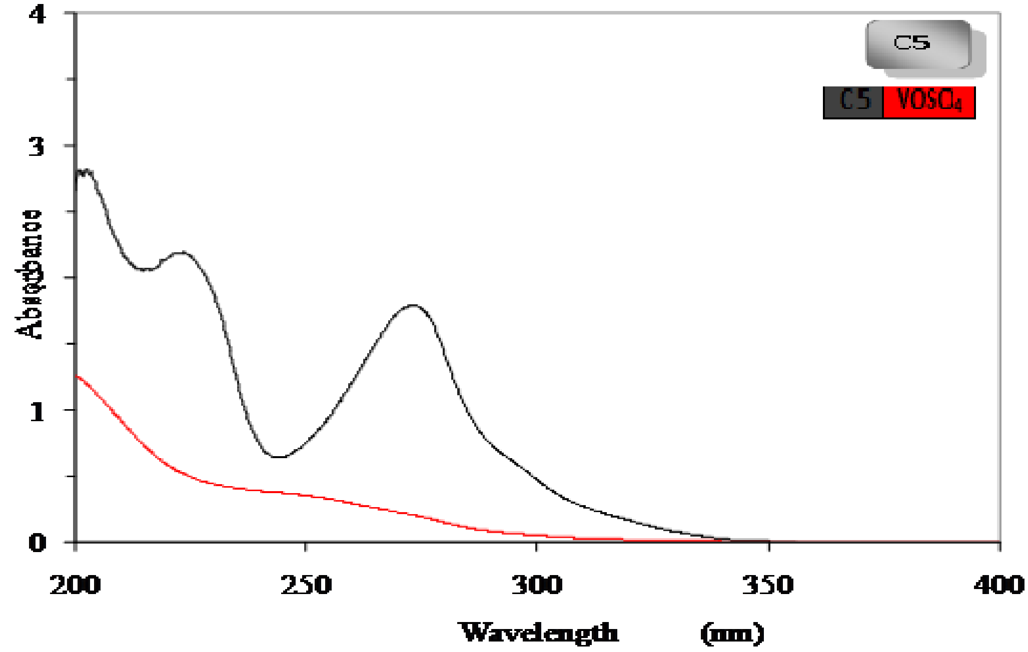

Figure 3.5: Ultra violet spectrum of C5

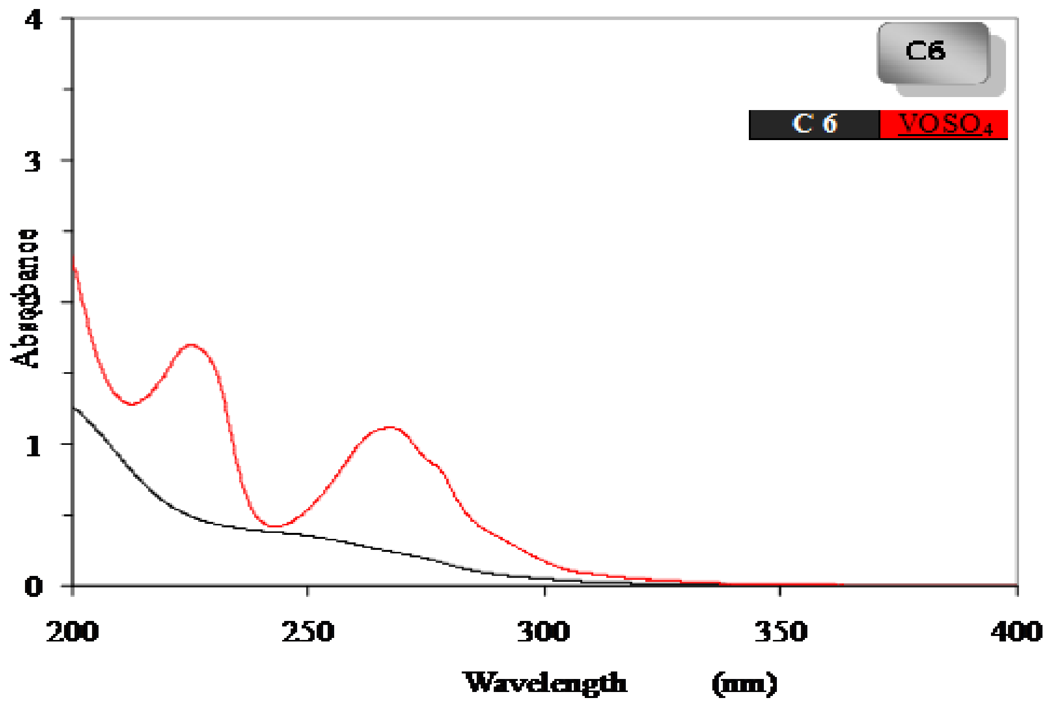

Figure 3.6: Ultra violet spectrum of C 6

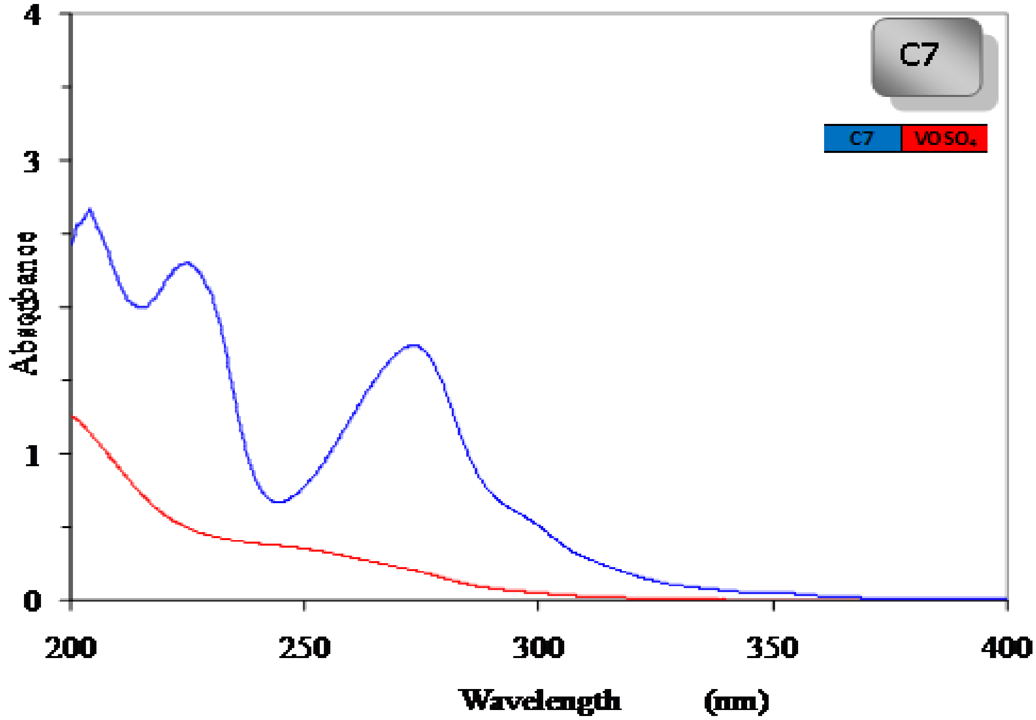

Figure 3.7: Ultra violet spectrum of C7

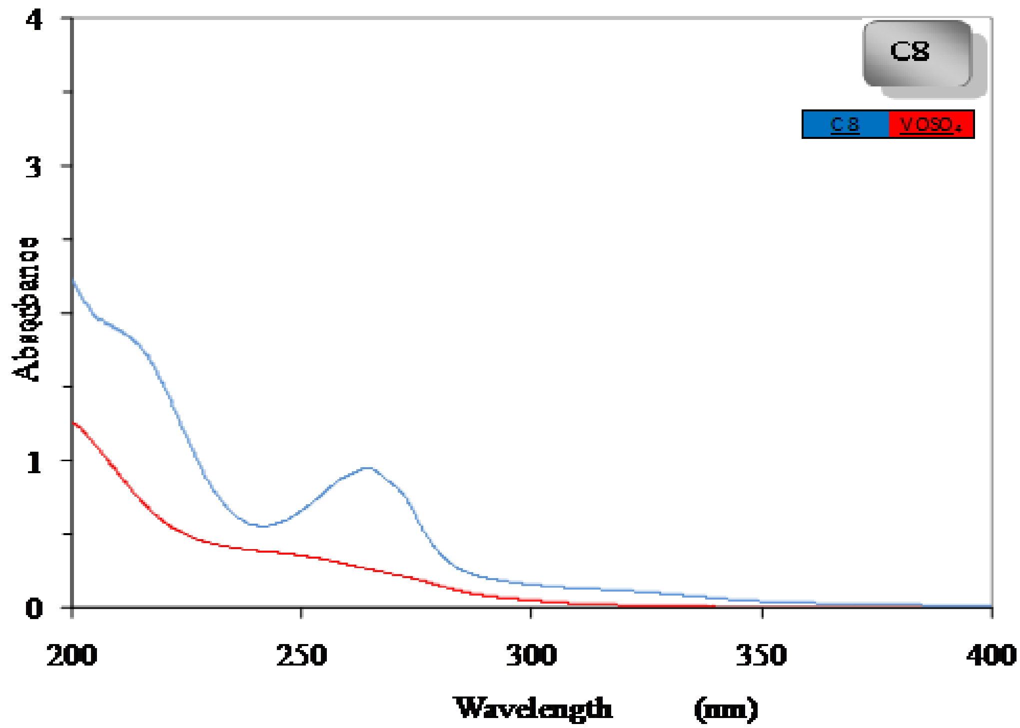

Figure 3.8: Ultra violet spectrum of C 8

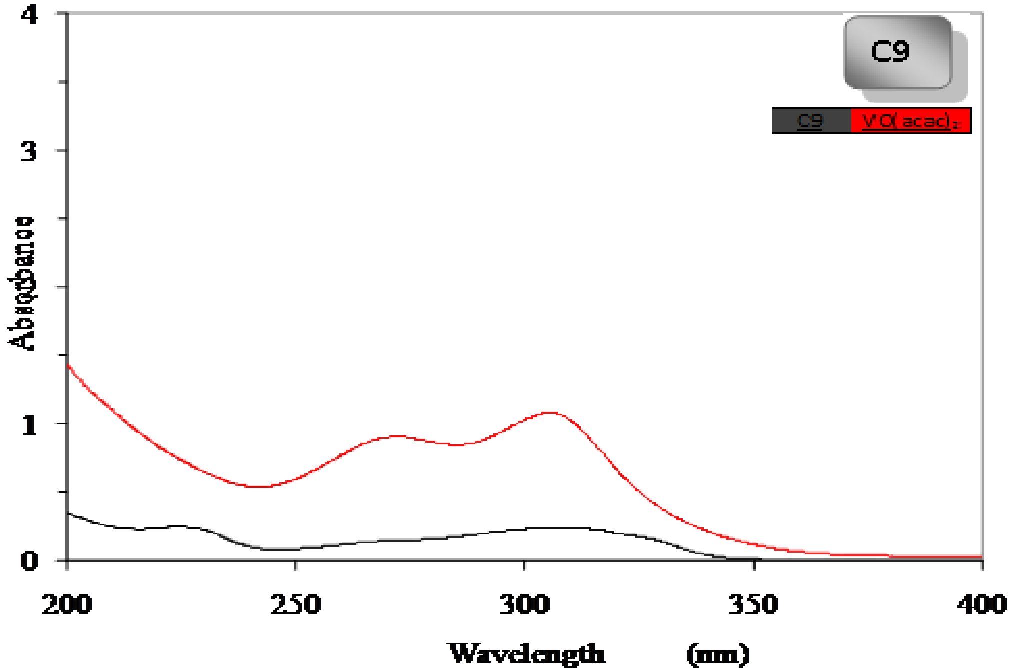

Figure 3.9: Ultra violet spectrum of complex 9

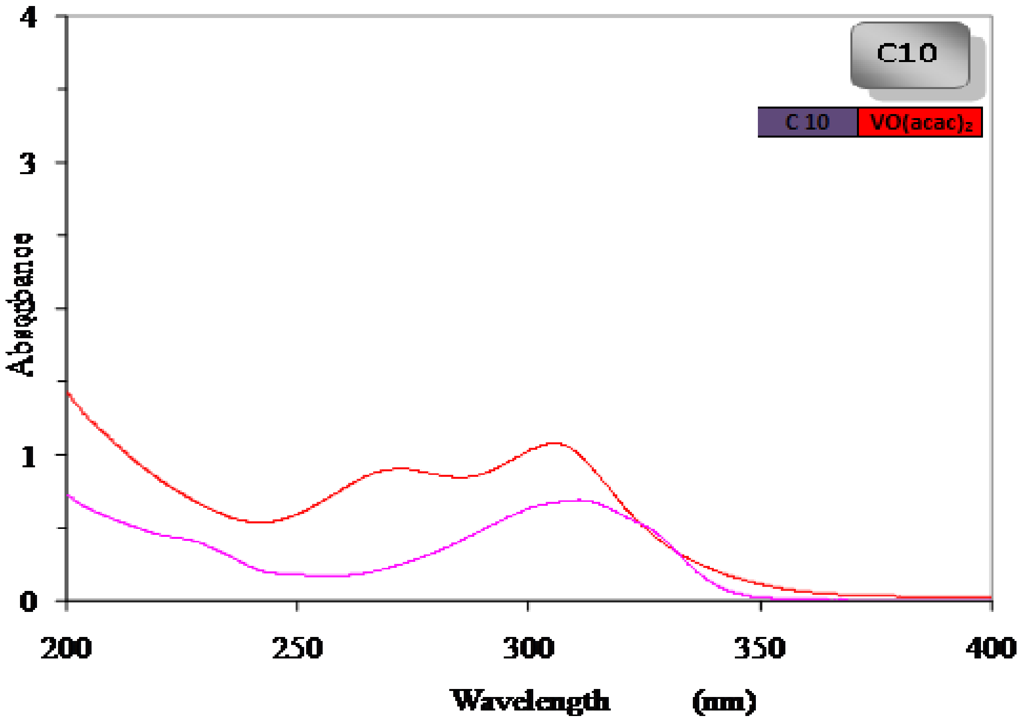

Figure 3.10: Ultra violet spectrum of C 10

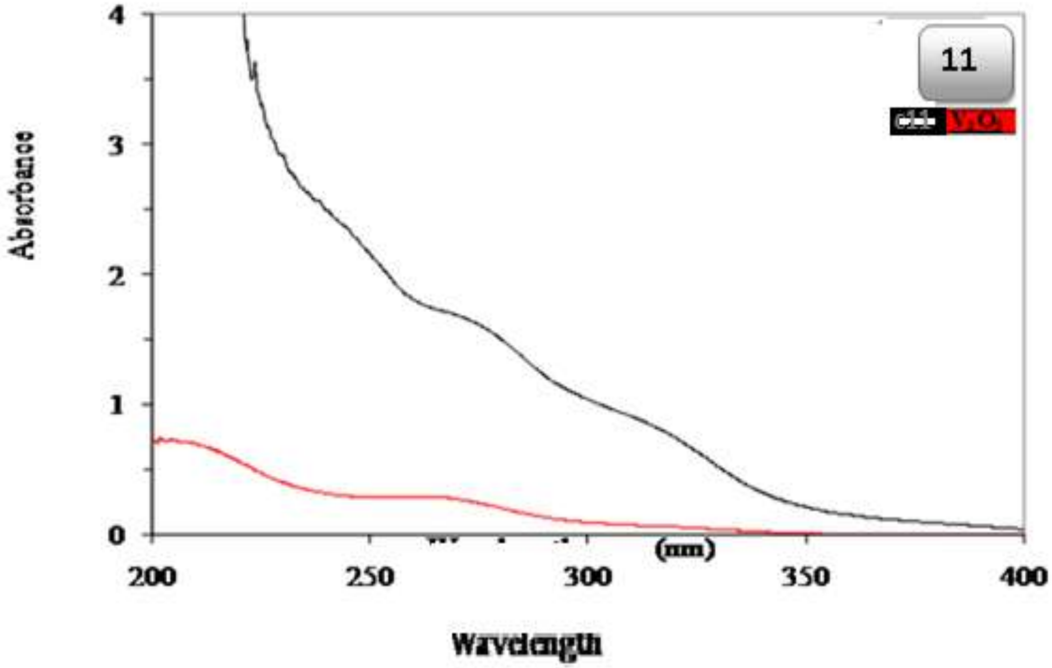

Figure 3.11: Ultra violet spectrum of C 11

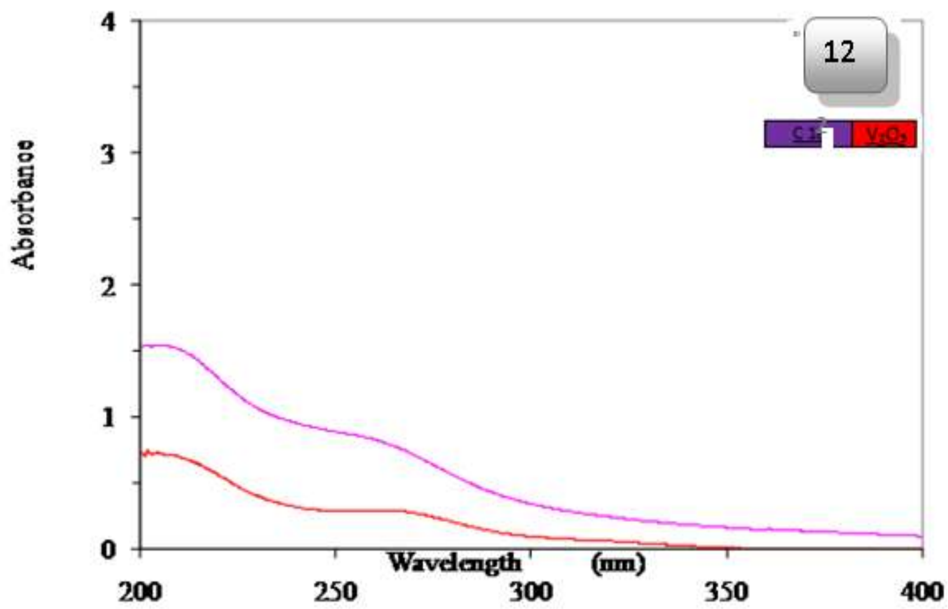

Figure 3.12: Ultra violet spectrum of C12

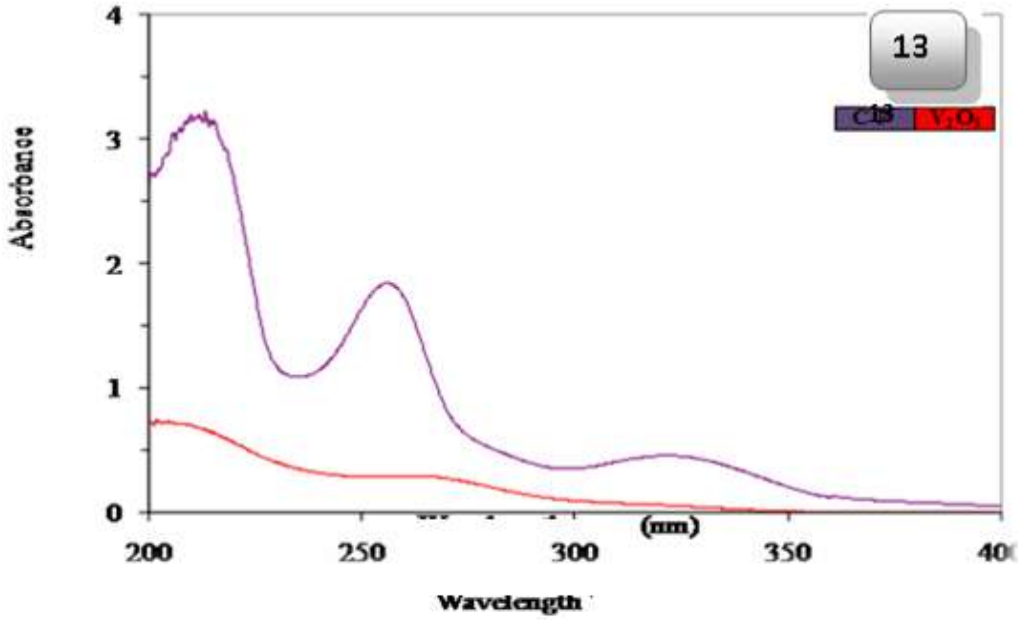

Figure 3.13: Ultra violet spectrum of C13

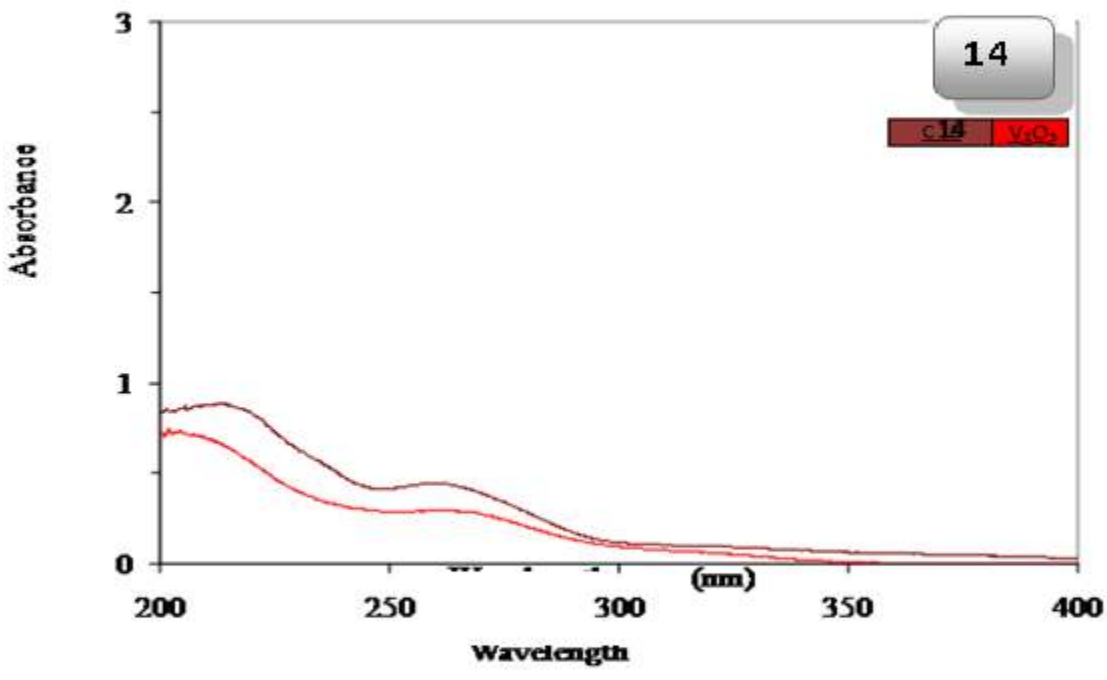

Figure 3.14: Ultra violet spectrum of C 14

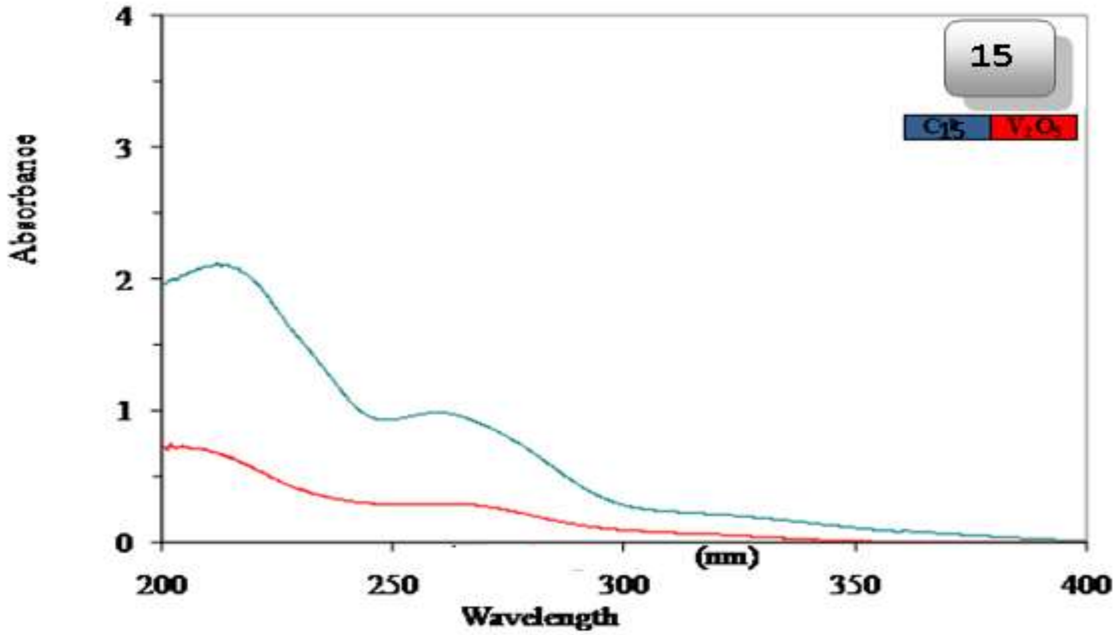

Figure 3.15: Ultra violet spectrum of C 15

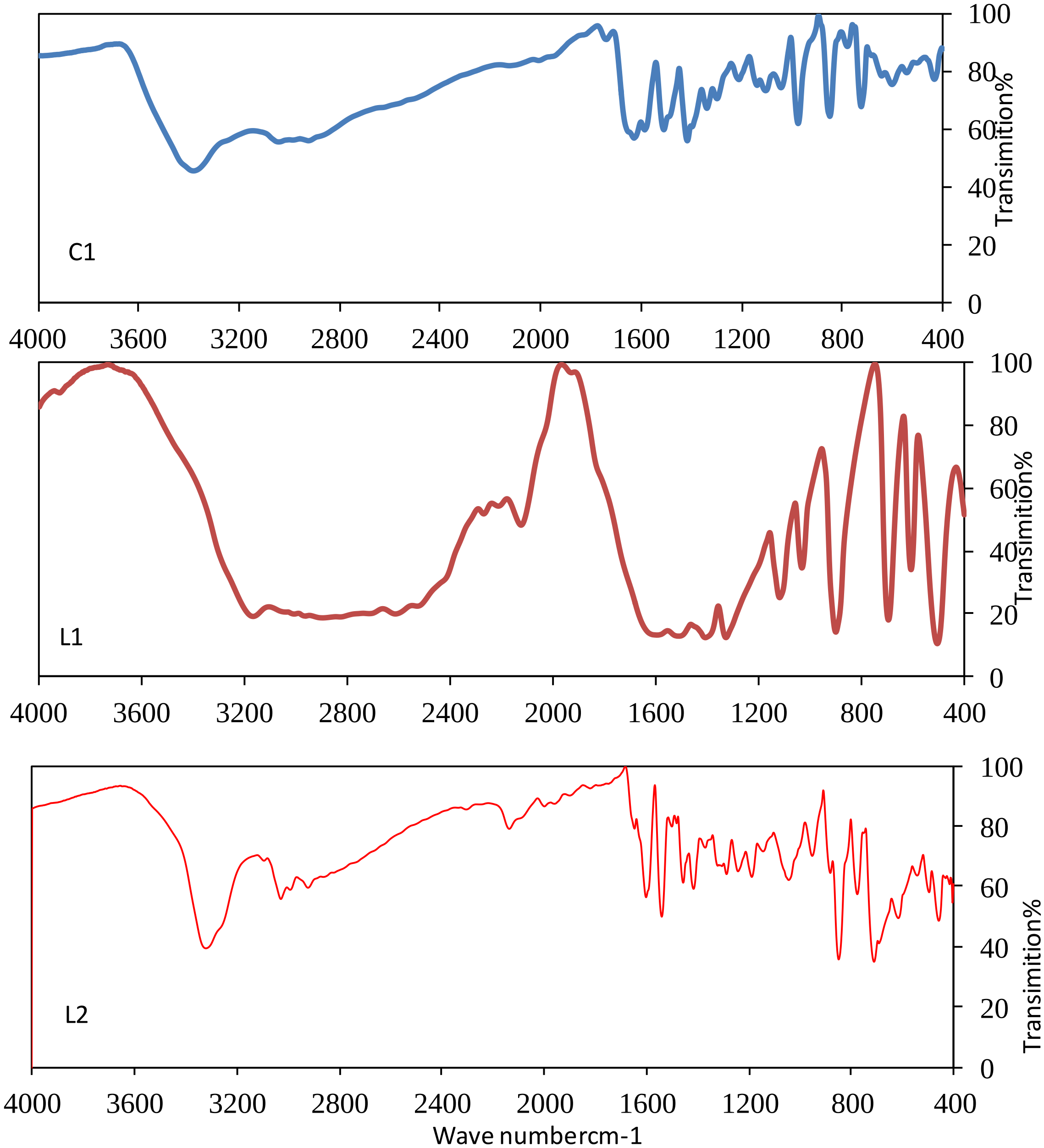

Figure 3.16 Infra red spectrum of C1 [VO (cys) (phen)]

*all the L2 refer to 1,10 phenanthrolin

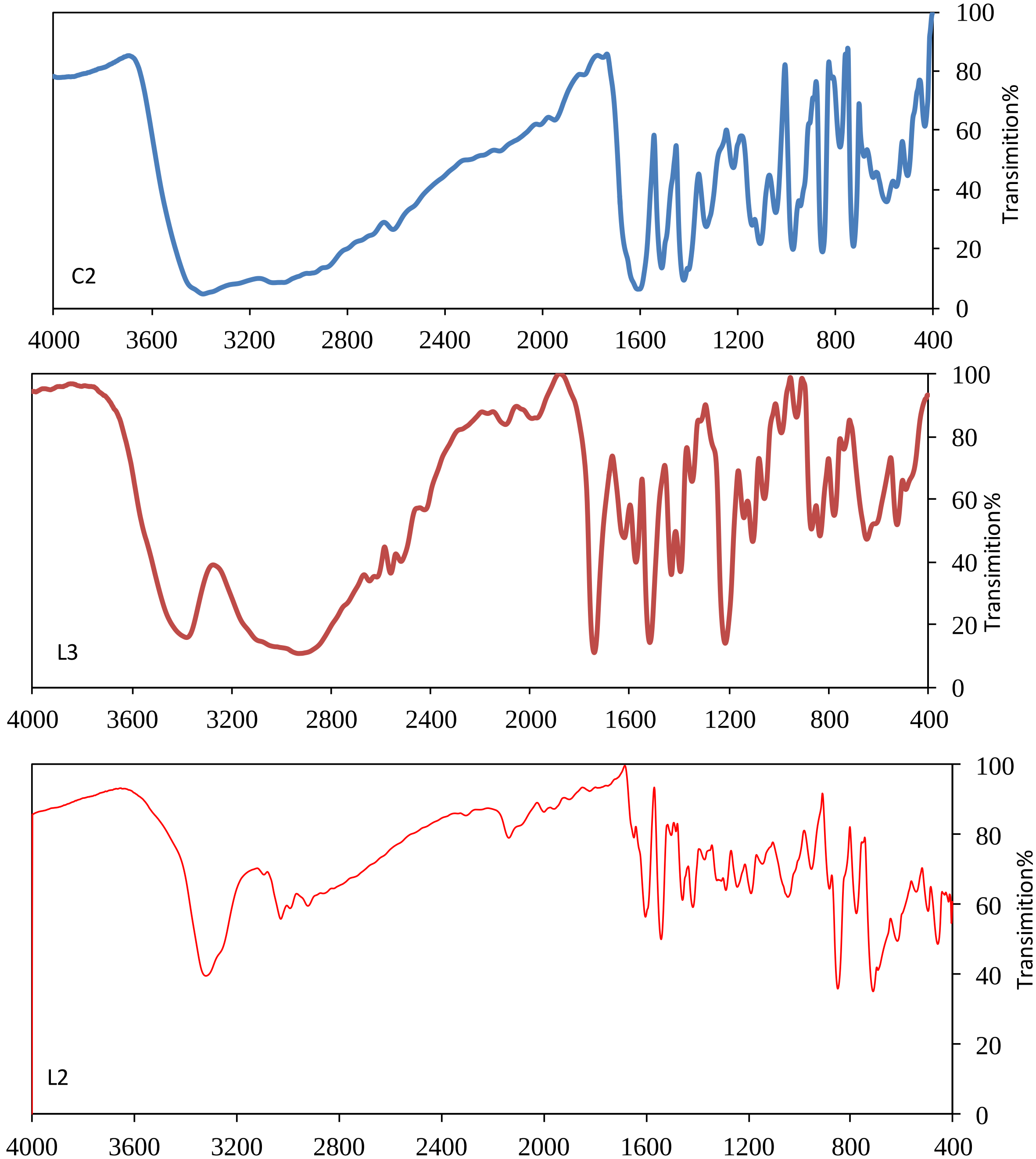

Figure 3.17 Infra red spectrum of C2 [VO (Cl) (gly) (phen)] and L1, L2

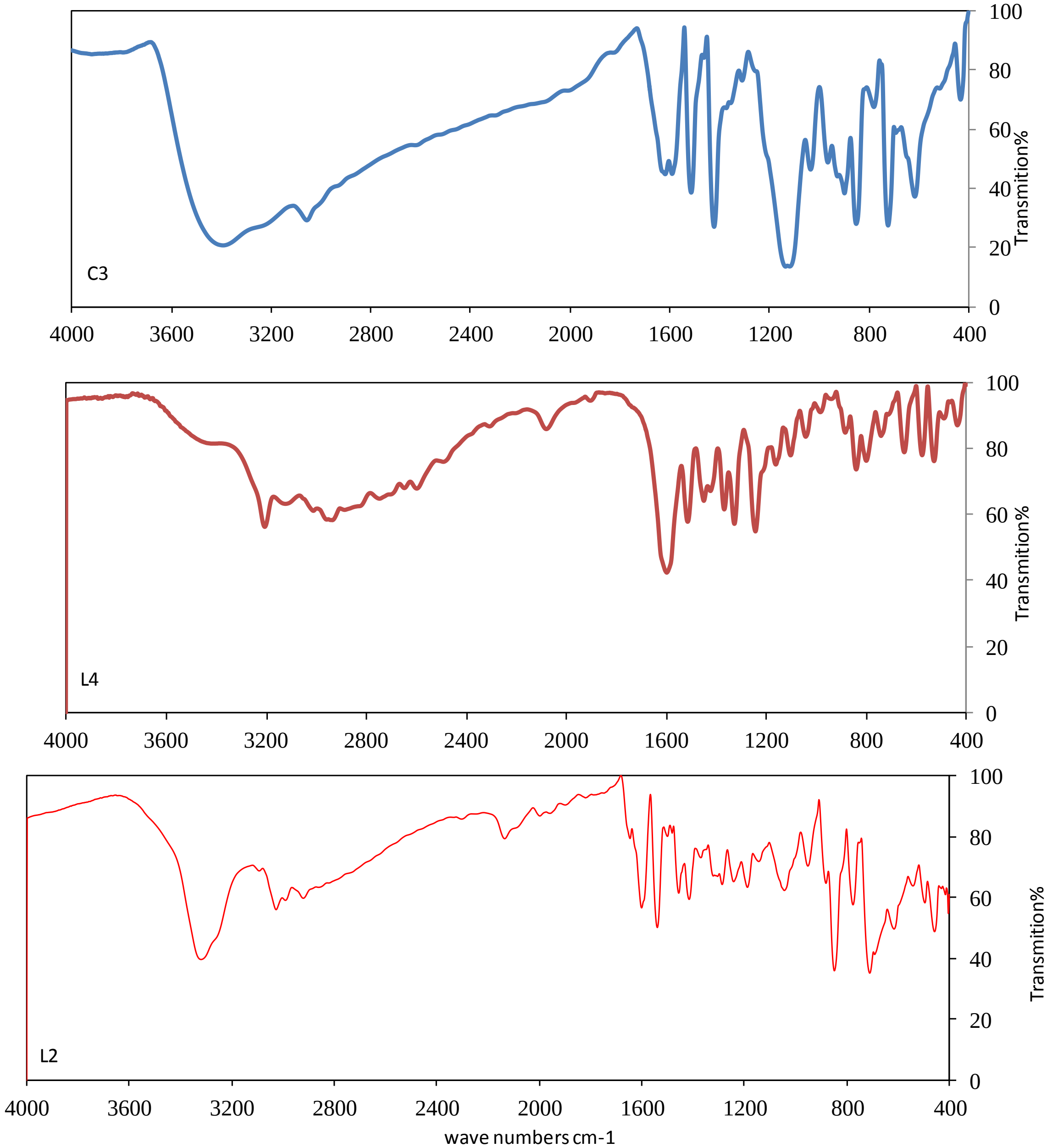

Figure 3.18 Infra red spectrum of C3 [VO(Cl) (tyro)(phen)] and L4, L2

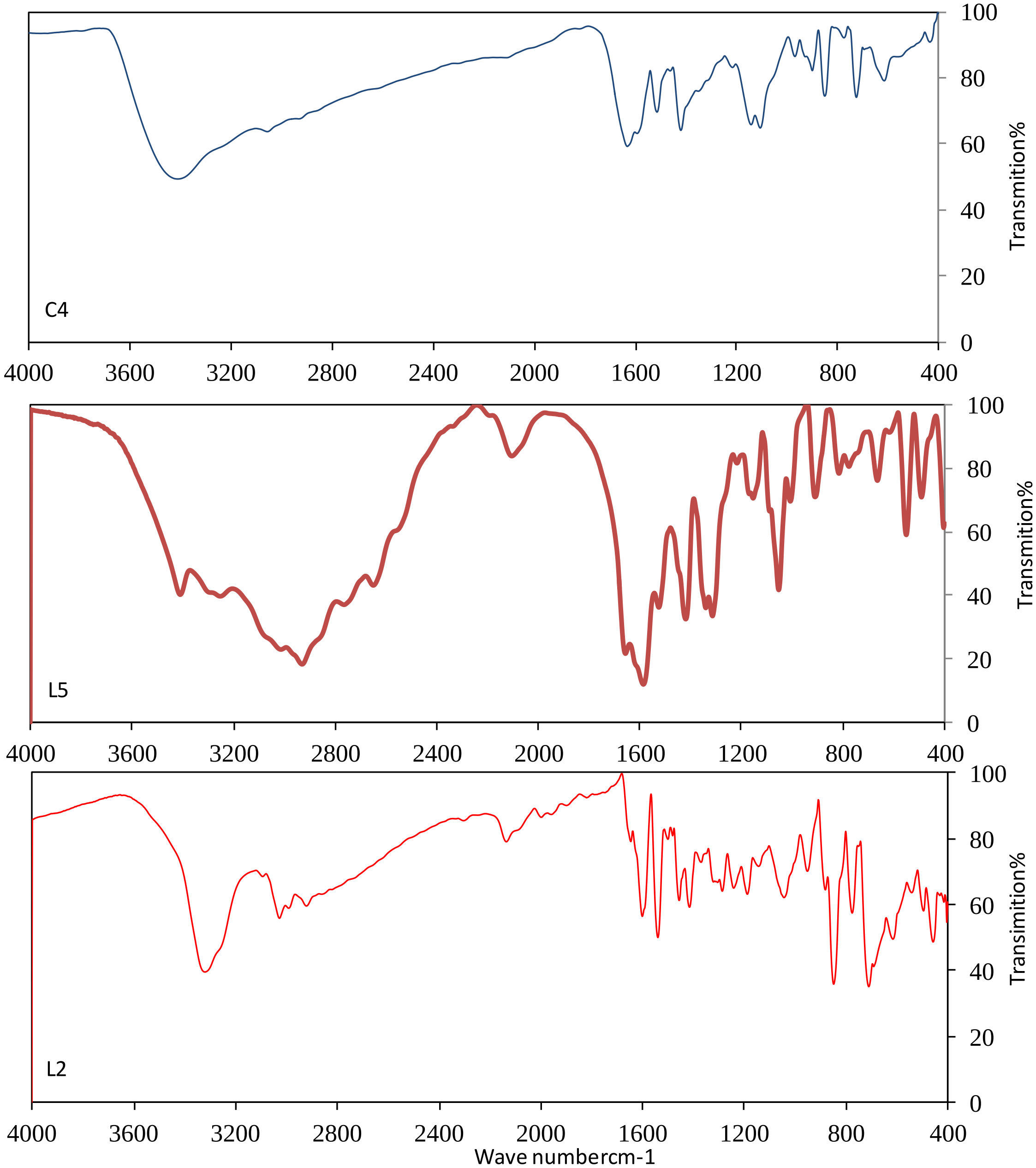

Figure 3.19 infra red spectrum of C4 [VO (homo)(phen)] and L5, L2

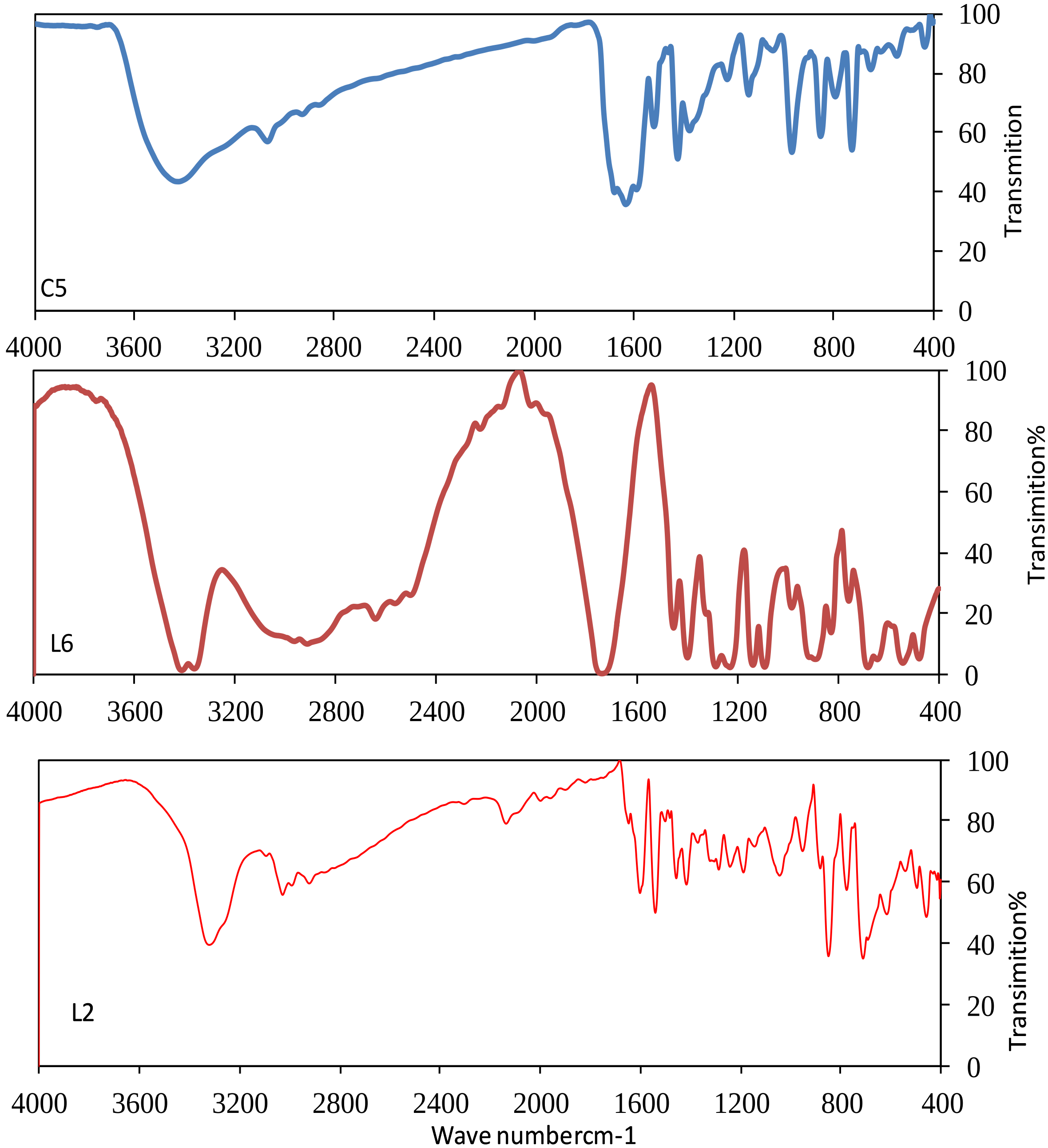

Figure 3.20 Infra red spectrum bands of C5 [VO (tart) (phen)] and L6, L2

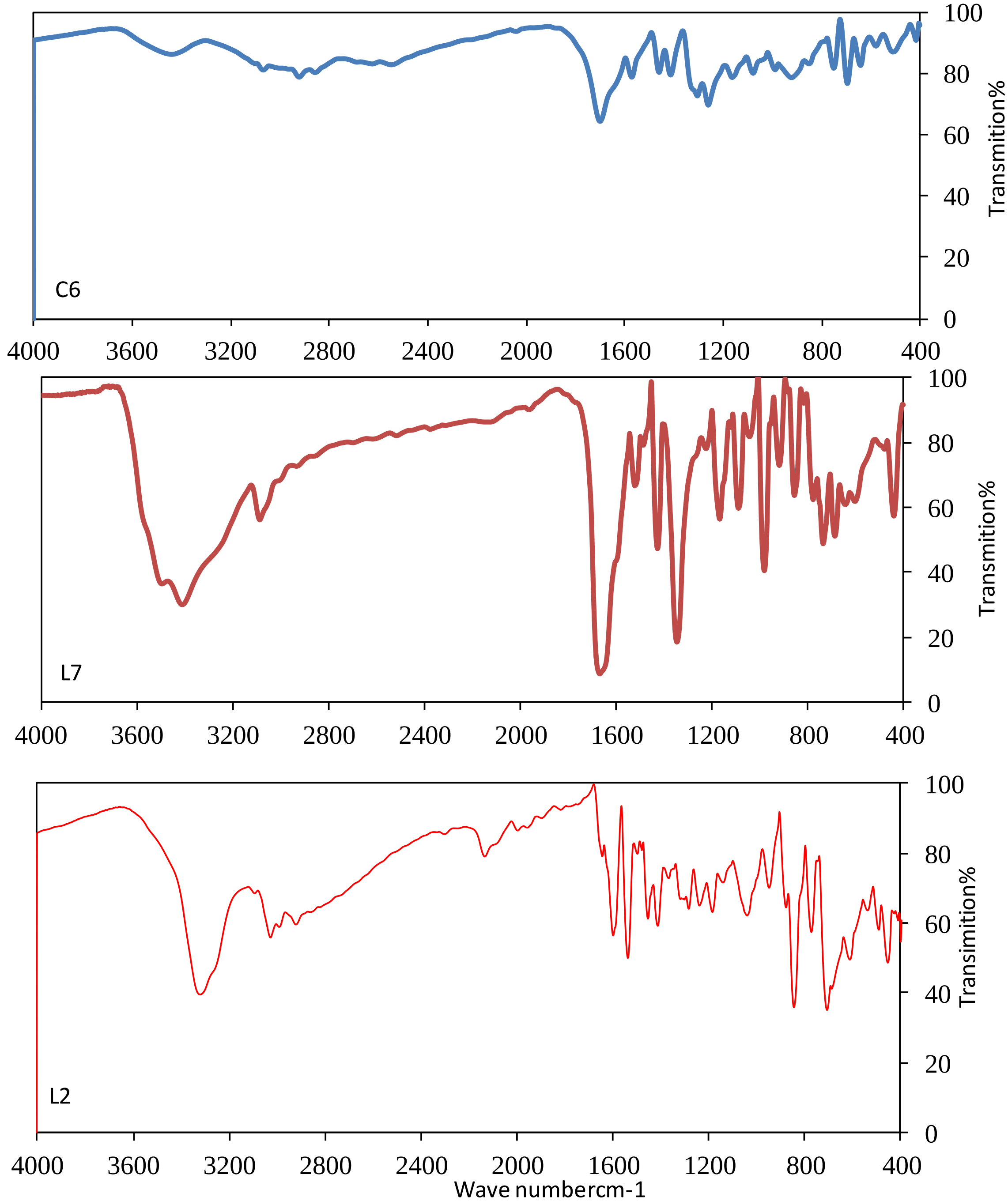

Figure 3.21 Infra red spectrum of C6 [VO (2, 6 Py) (phen)] and L7, L2

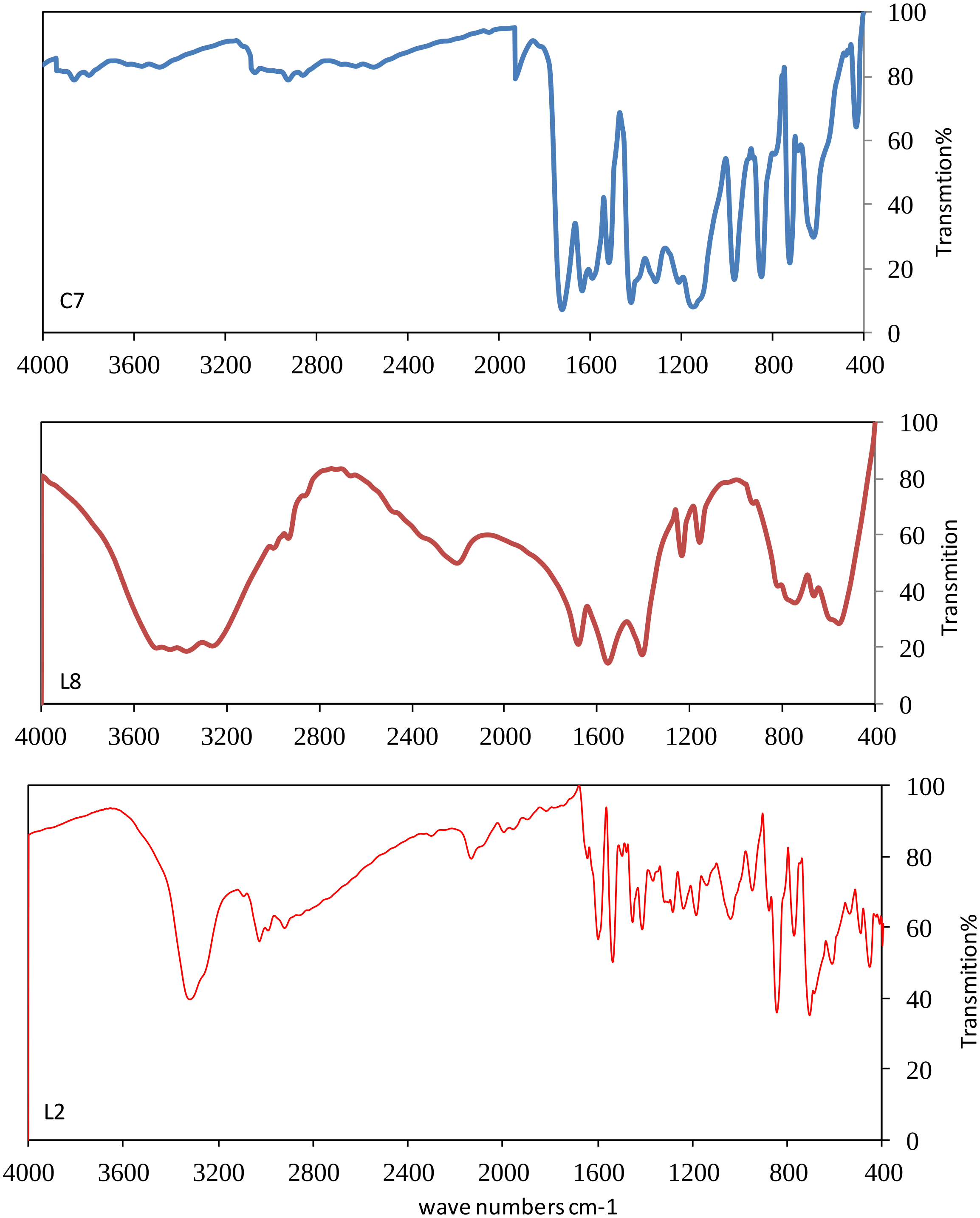

Figure 3.22 Infra red spectrum of C7 [VO (succ) (phen)] and L8, L2

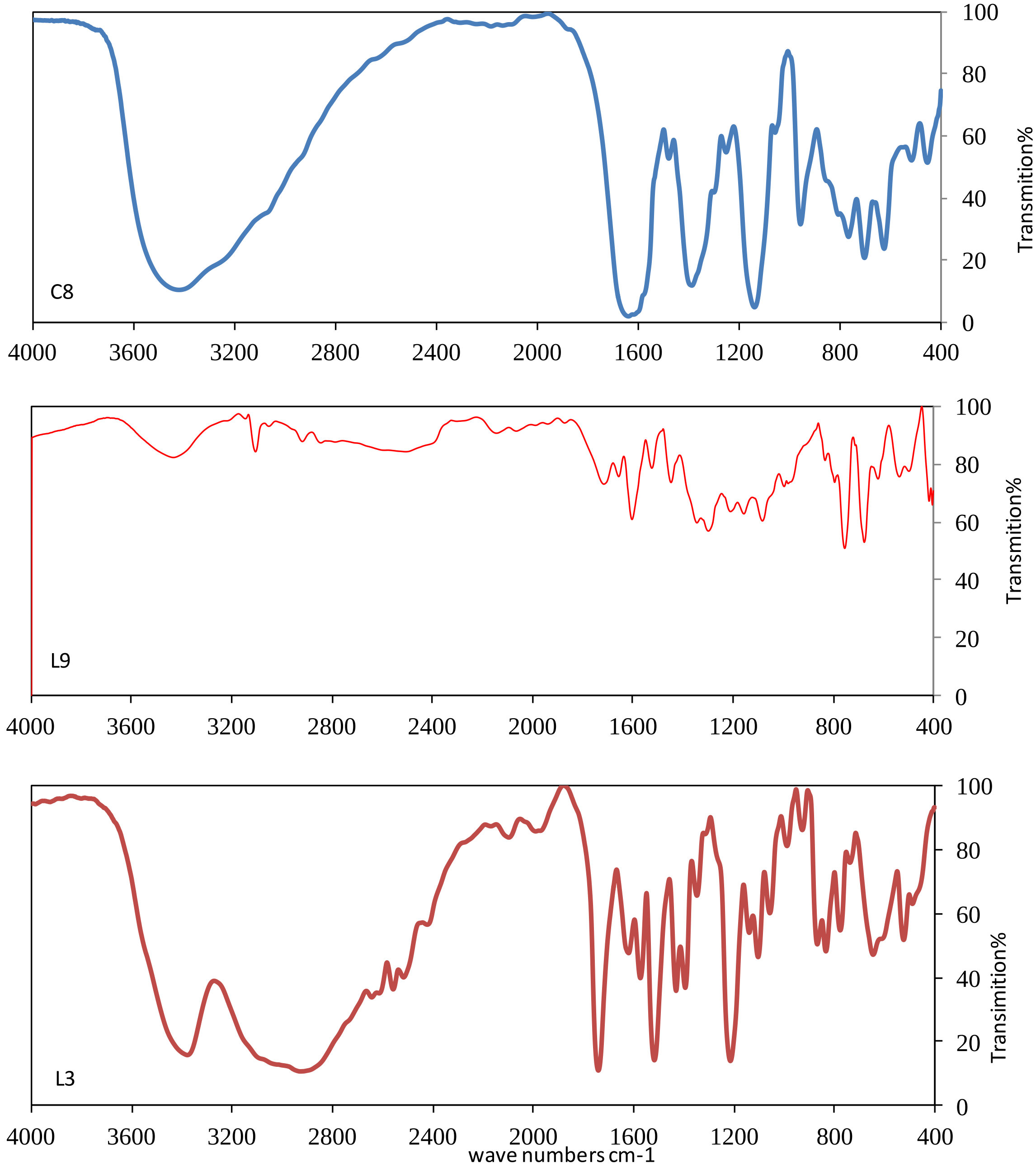

Figure 3.23 Infra red spectrum of C 8[VO (gly) (2-Pico)] and L9, L2

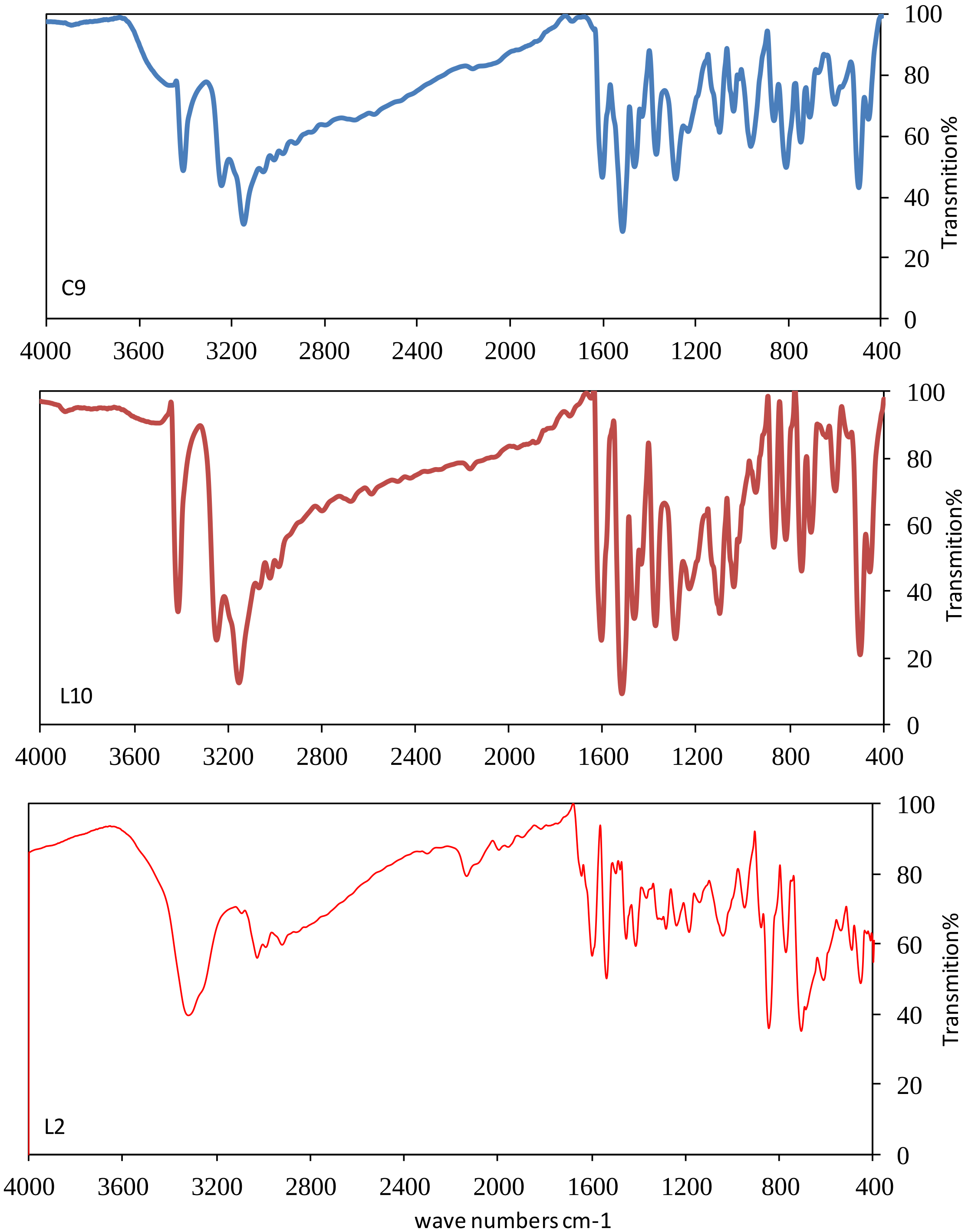

Figure 3.24 Infra red spectrum of C9 [VO (CLBTSC) (phen)] and L10, L2

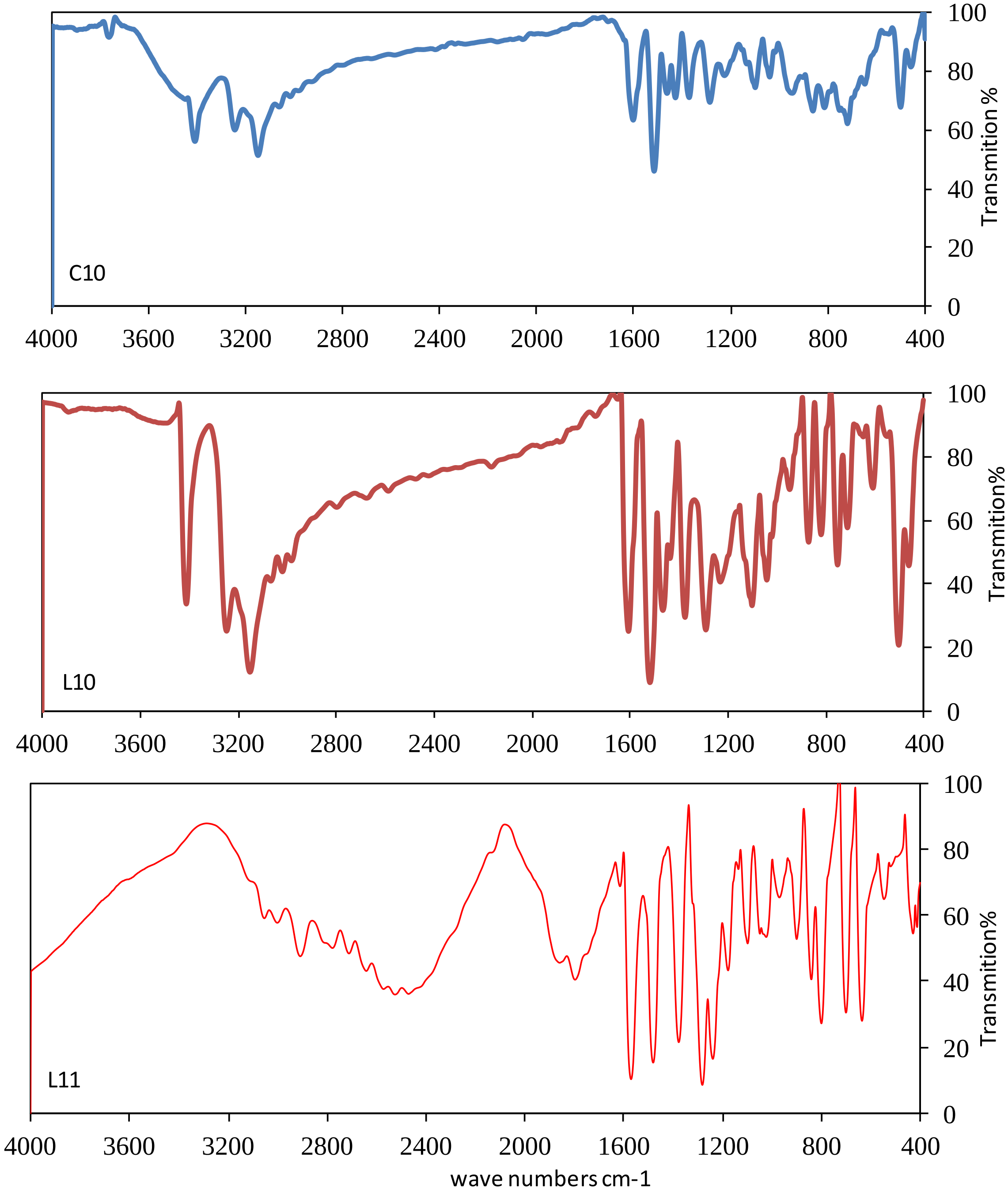

Figure 3.25 Infra red spectrum of C10 [VO (CLBTSC) (3-Hyp)$_2$] and L10, L11

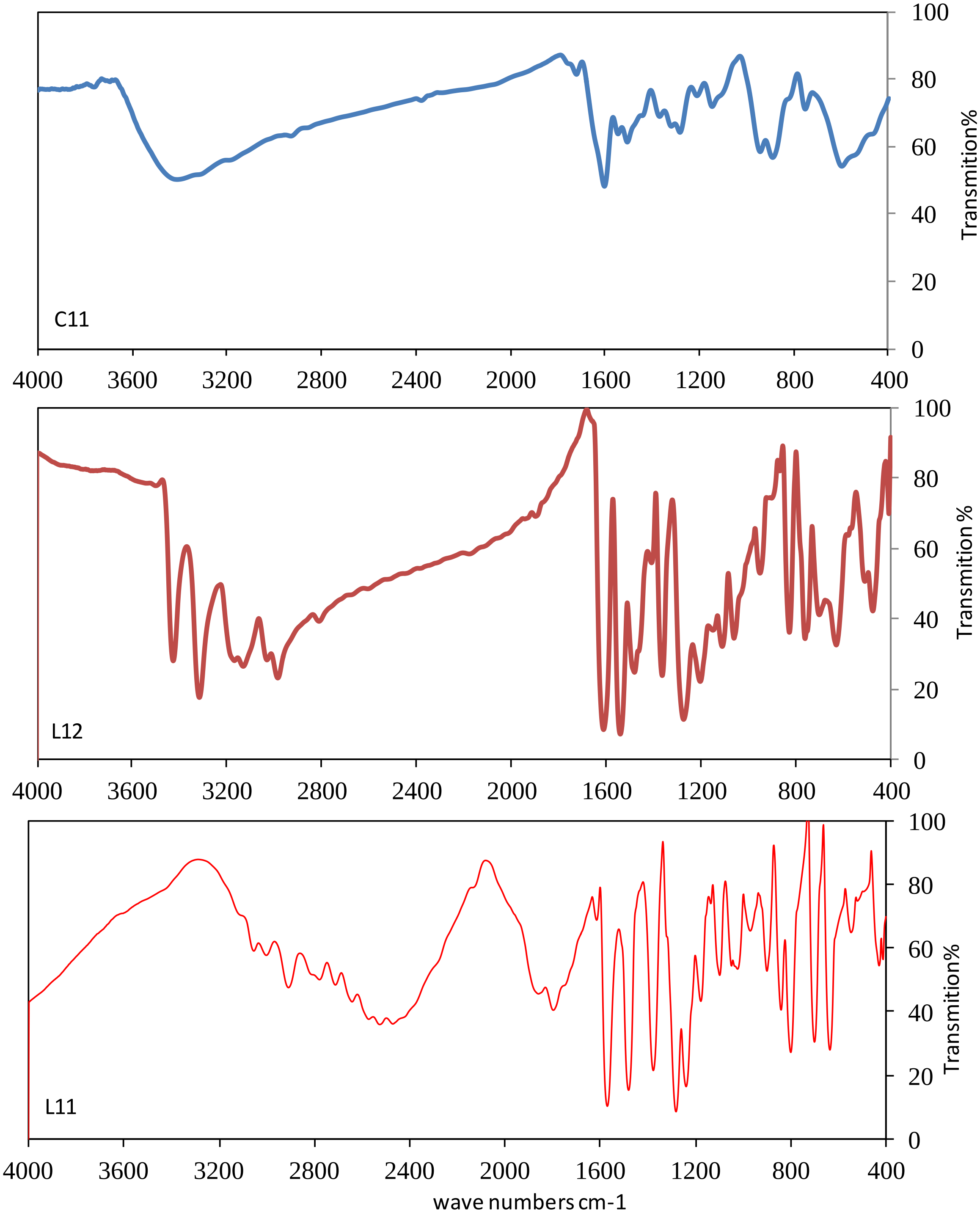

Figure 3.26 Infra red spectrum of C11 [VO_2 (SALTSC)(3-Hpy)] and L12, L11

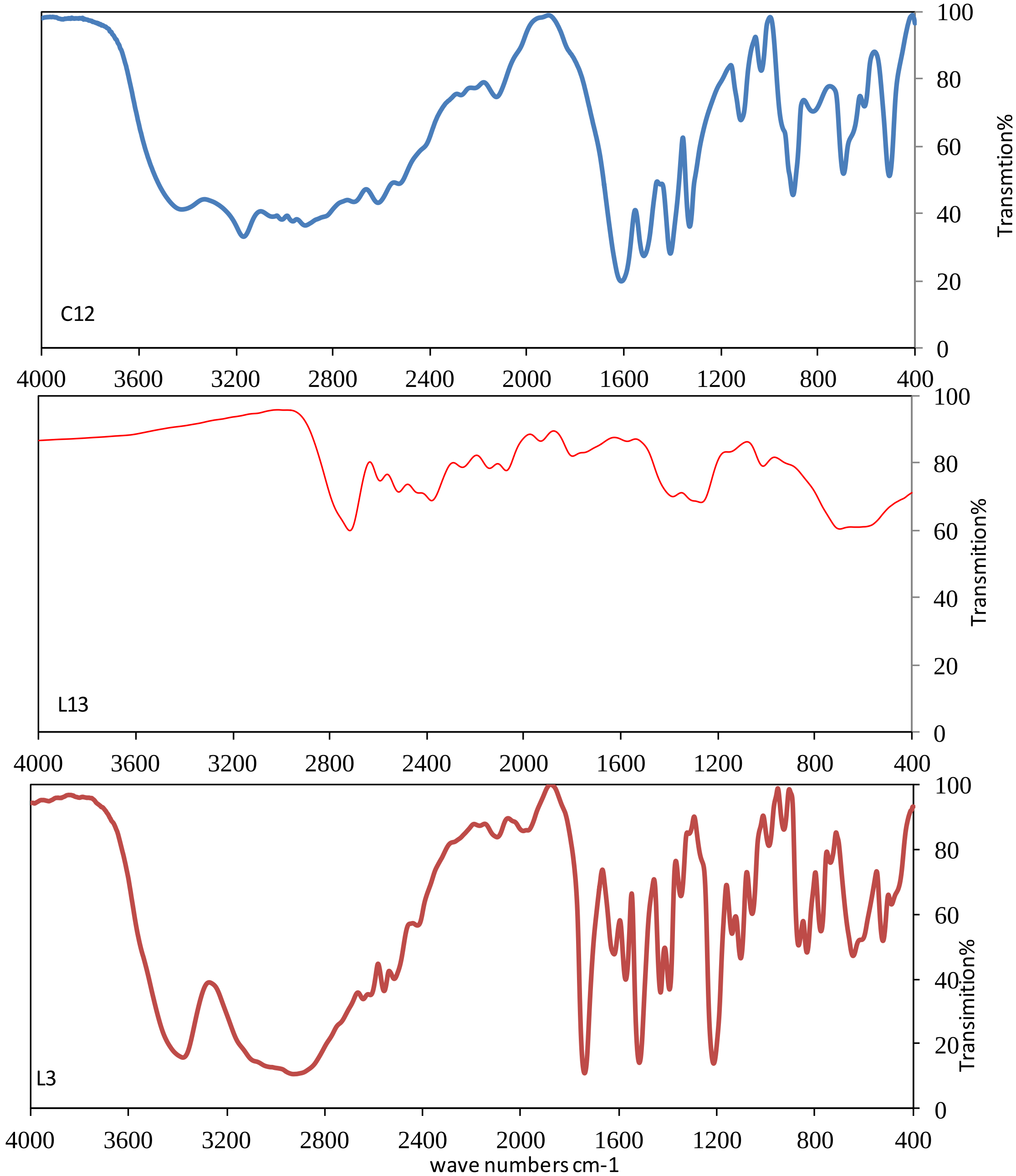

Figure 3.27 Infra red spectrum of C12 [VO_2 (3-APTSC) (gly)] and L13, L3

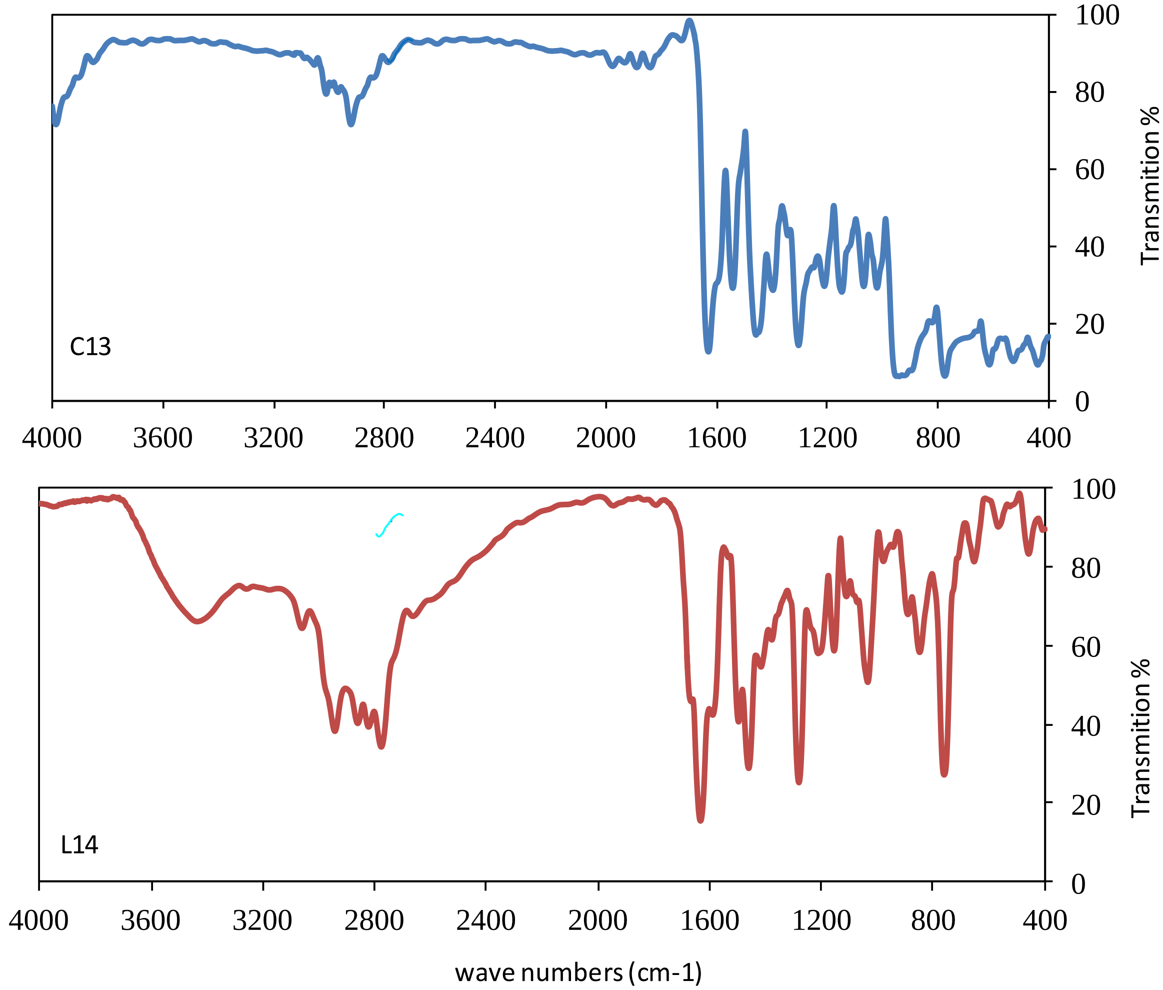

Figure 3.28 infra red spectrum of C13 [VO_2 (Sal-DMEDA)] and L14

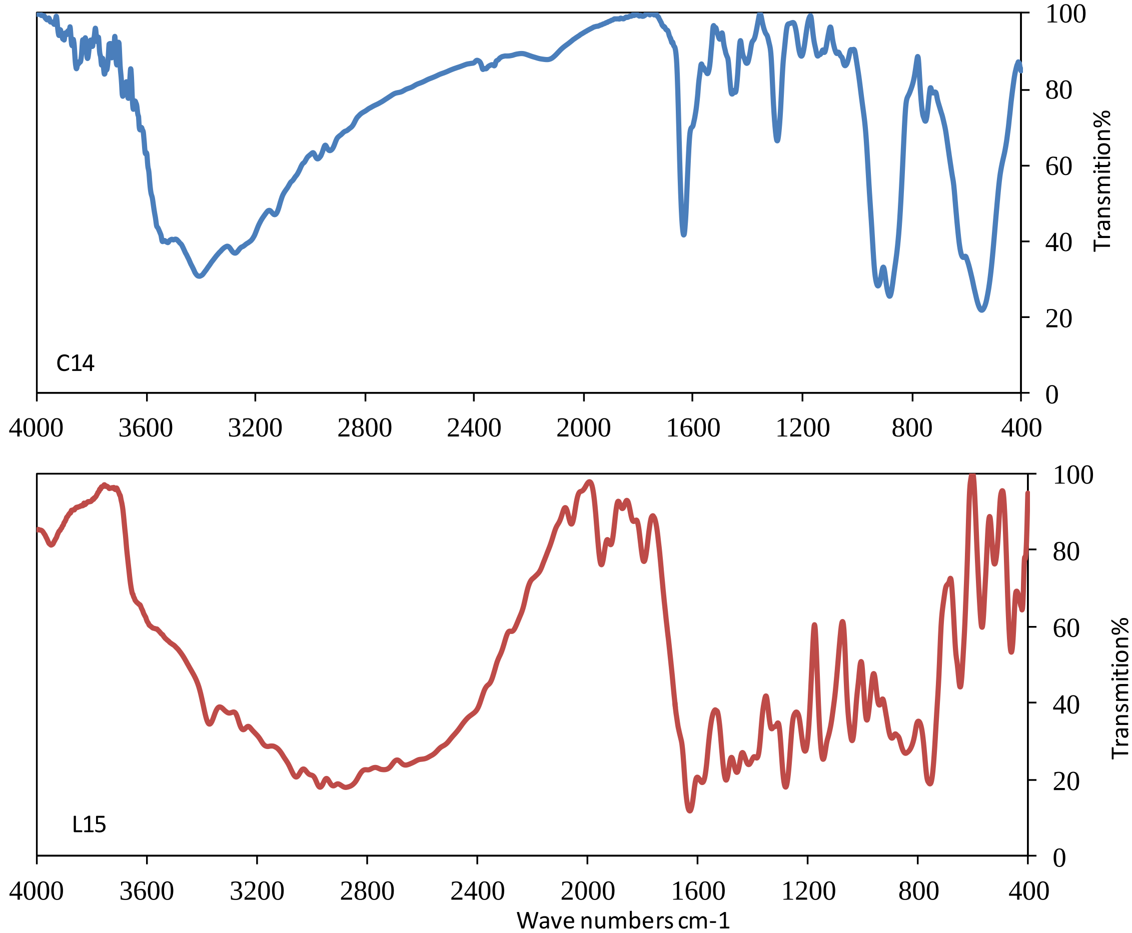

Figure 3.29 infra red spectrum of C14 [VO_2 (Sal-DAP)] and L15

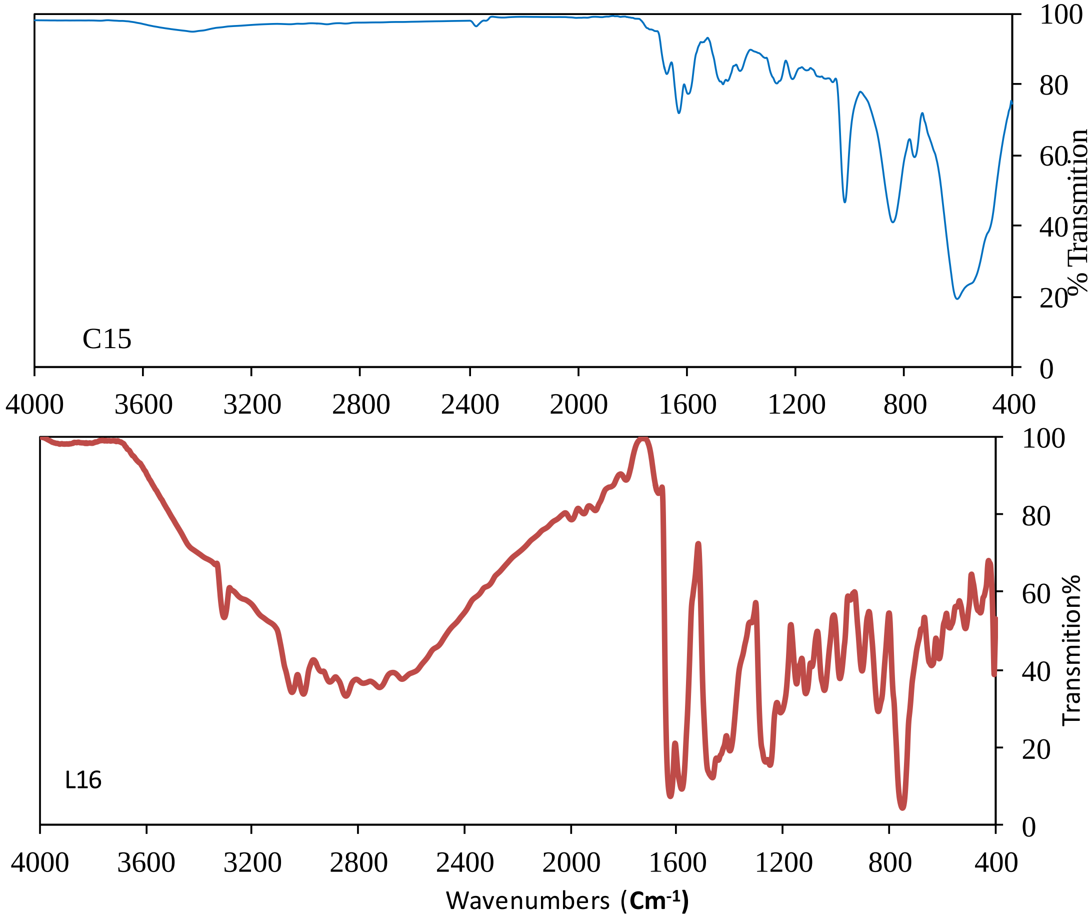

Figure 3.30 Infra red spectrum of C15 [VO_2 (Sal-2-PiA)] and L16

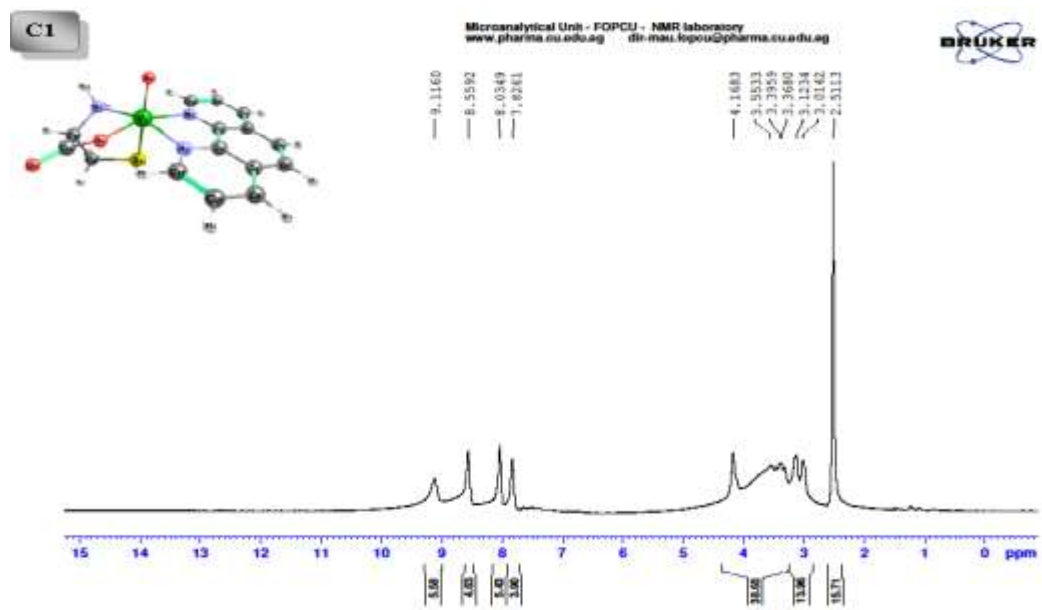

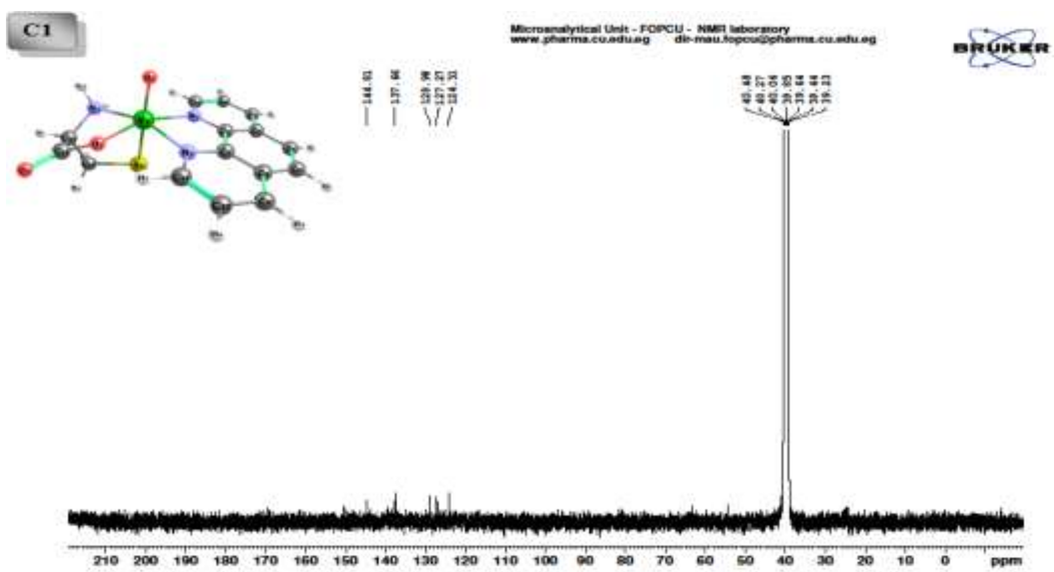

Figure 3.31 ^{1}HNMR and ^{13}C NMR of C1

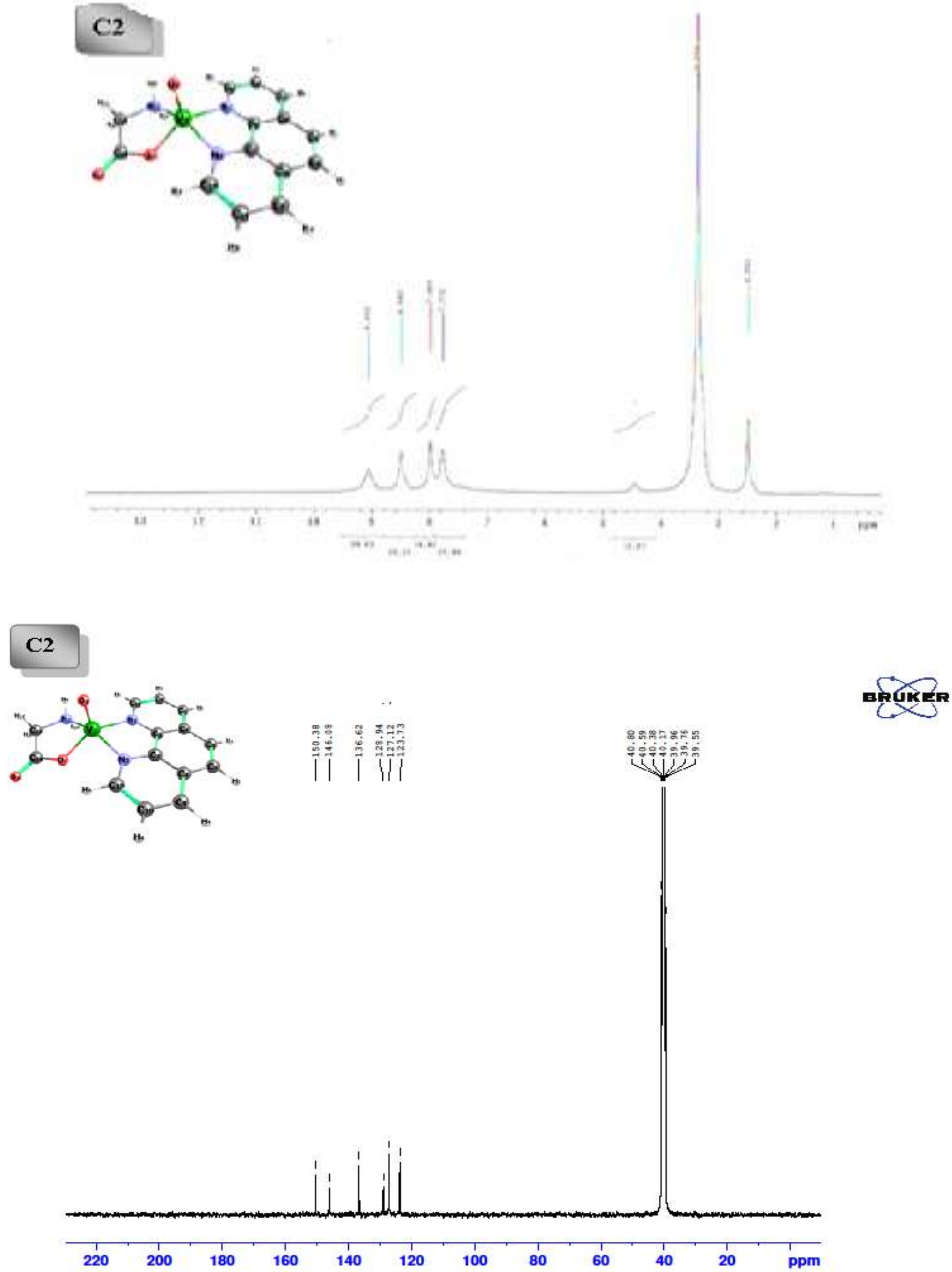

Figure 3.32 ^{1}HNMR and ^{13}C NMR of C2

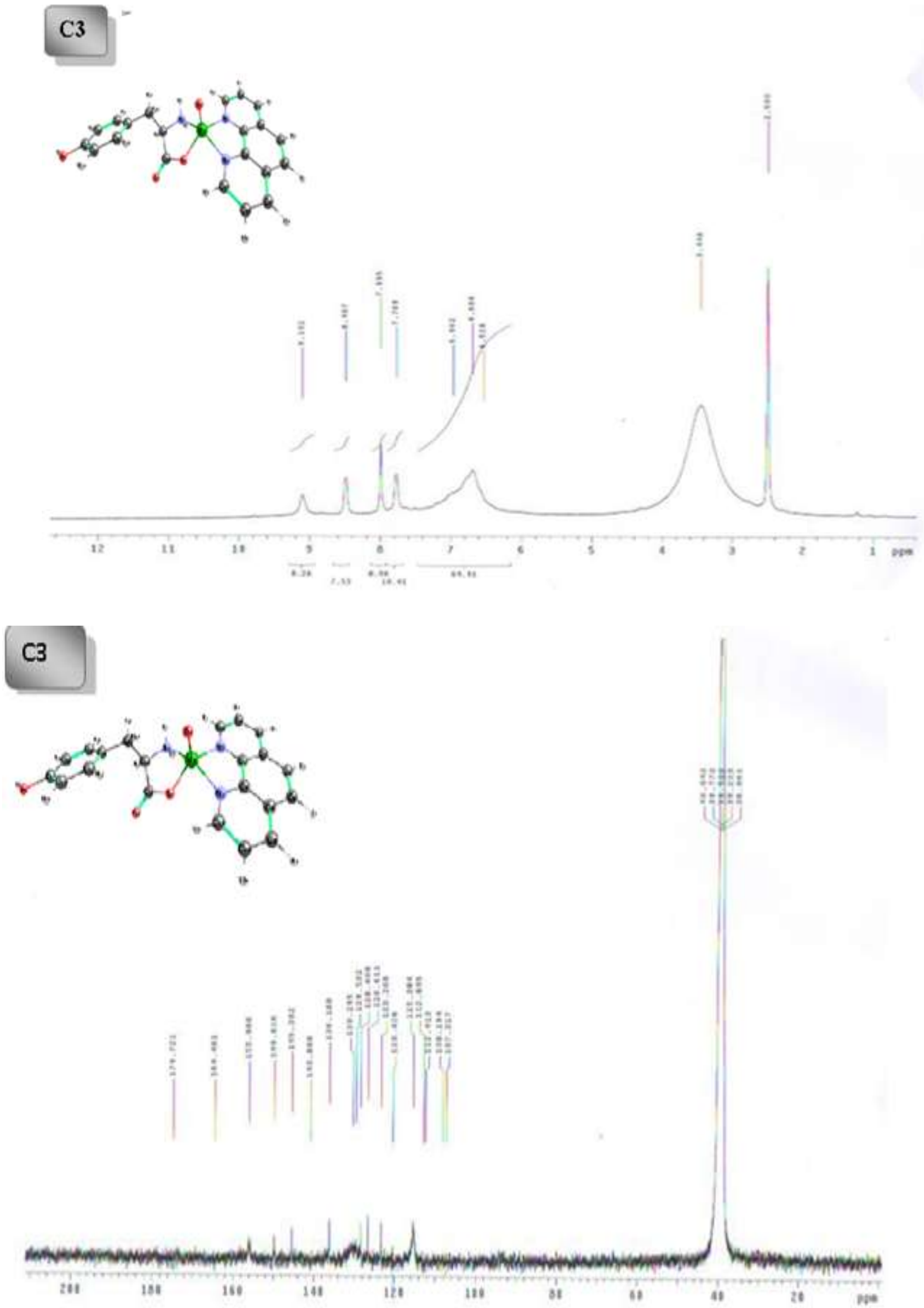

Figure 3.33 ^{1}HNMR and ^{13}C NMR of C3

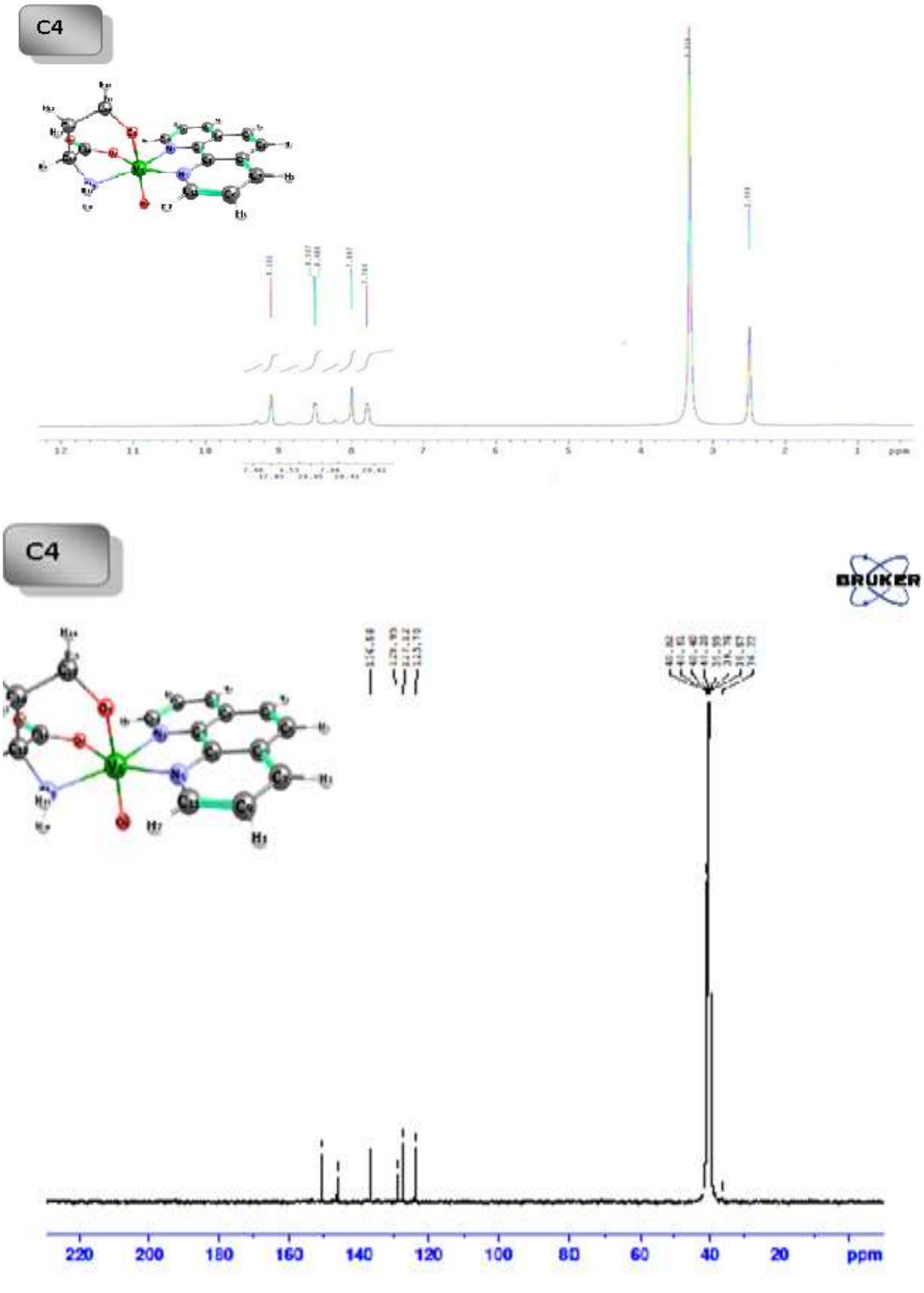

Figure 3.34 ^{1}HNMR and ^{13}C NMR of C4

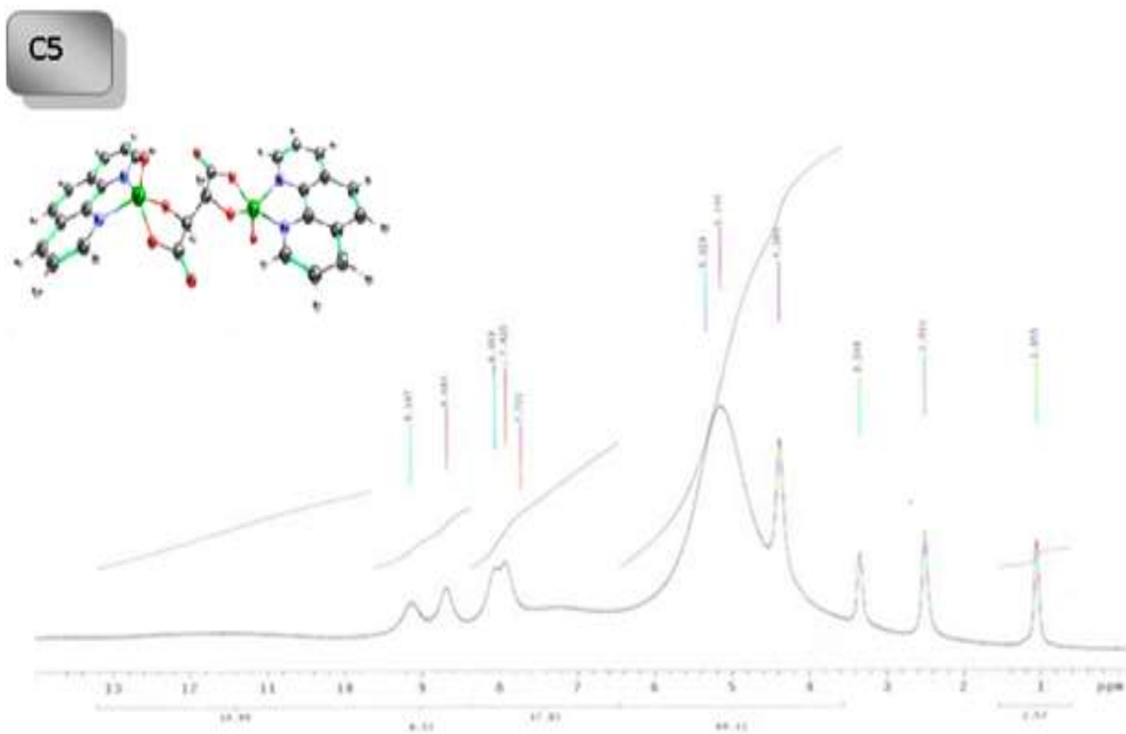

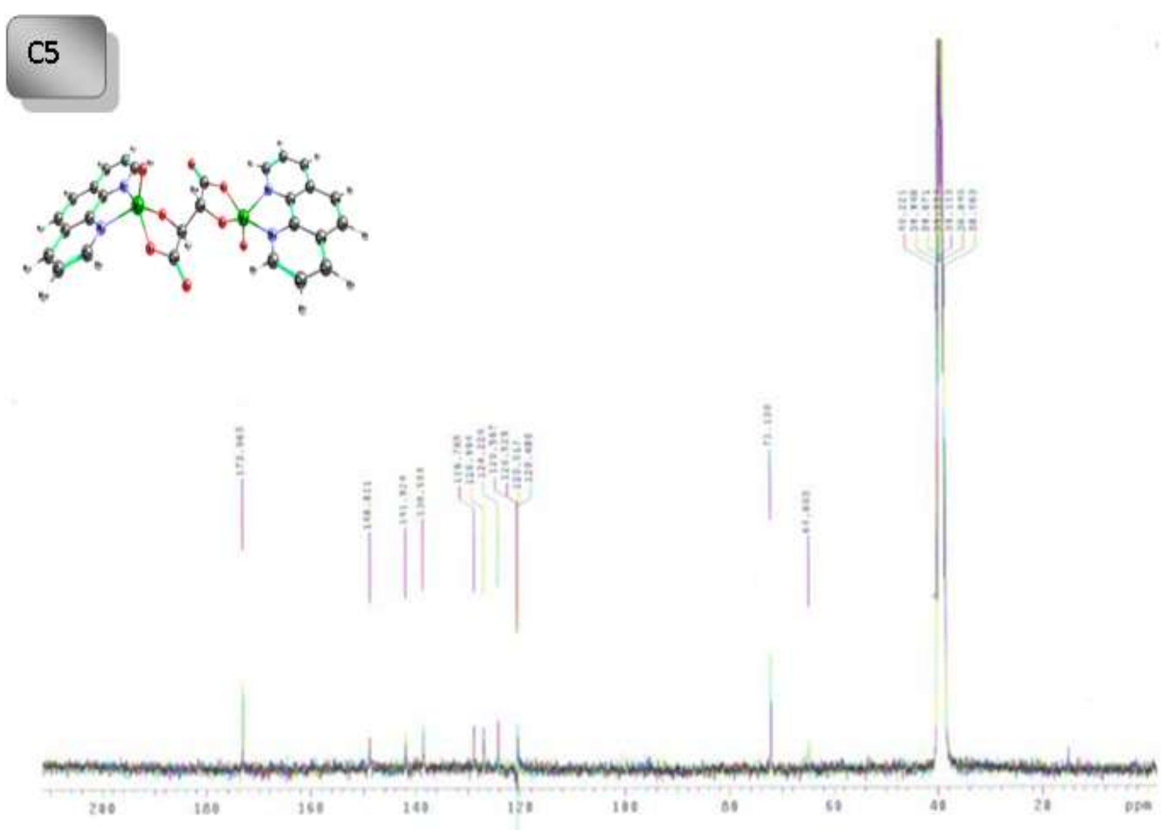

Figure 3-35 ^{1}HNMR and ^{13}C NMR of C5

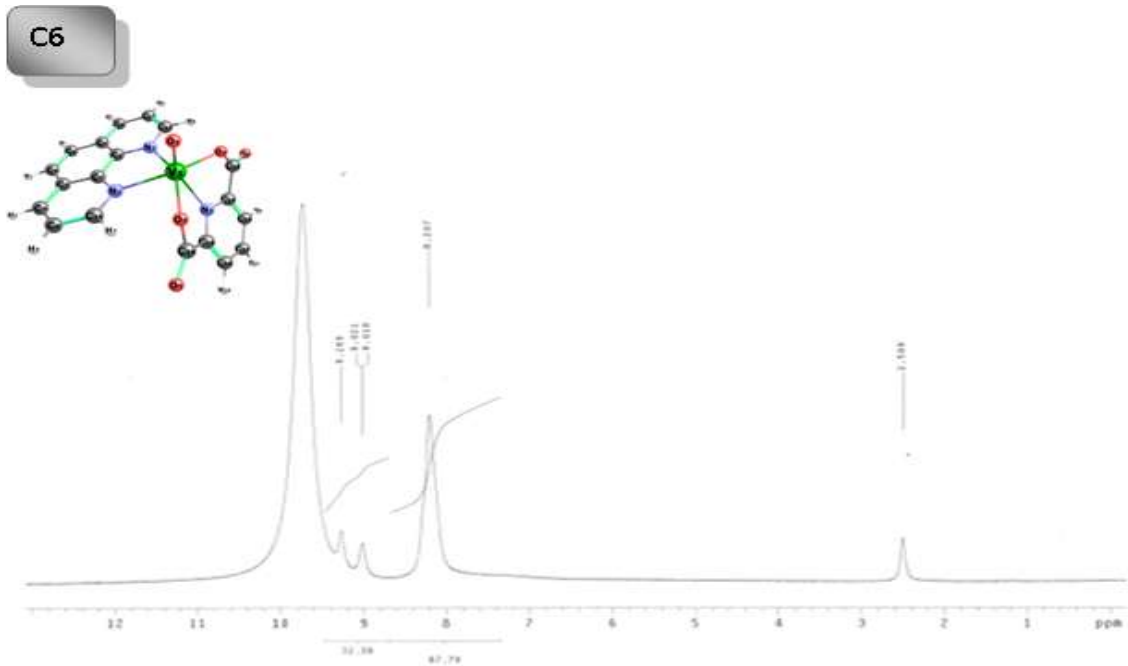

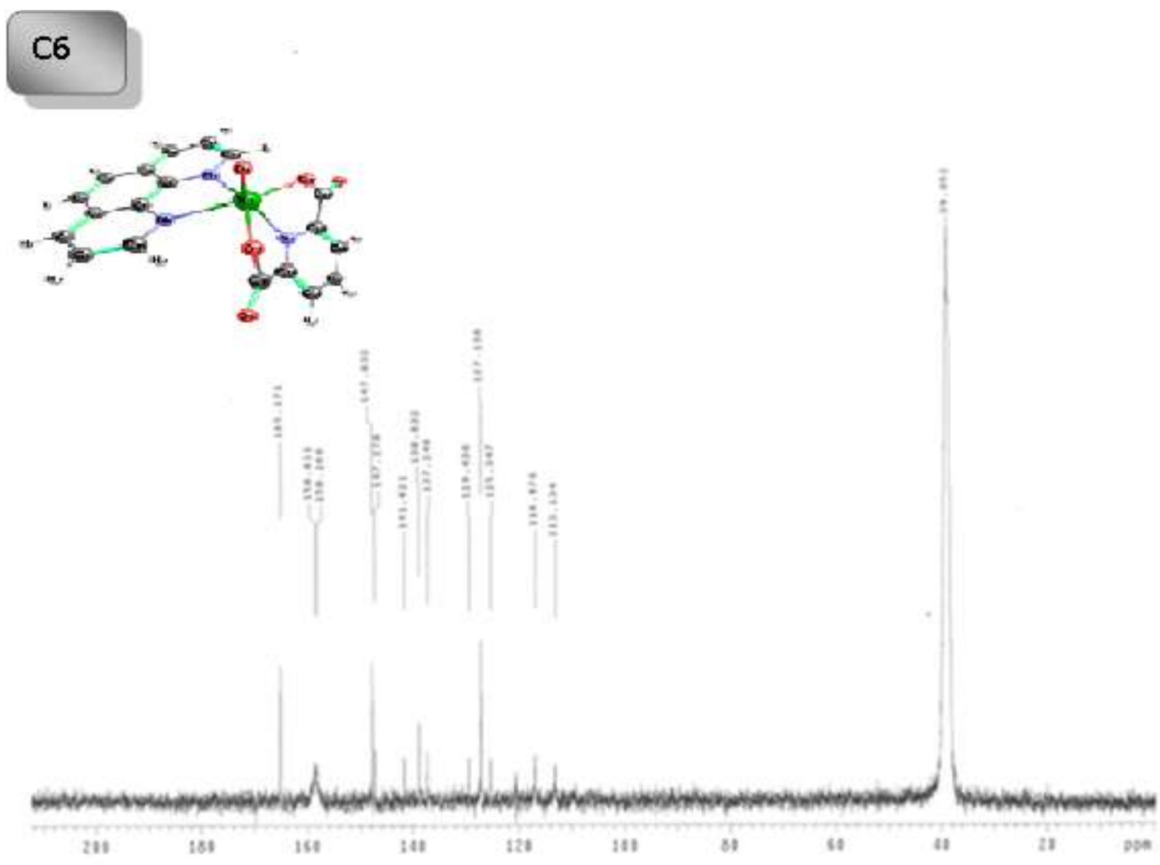

Figure 3.36 ^{1}HNMR and ^{13}C NMR of C6

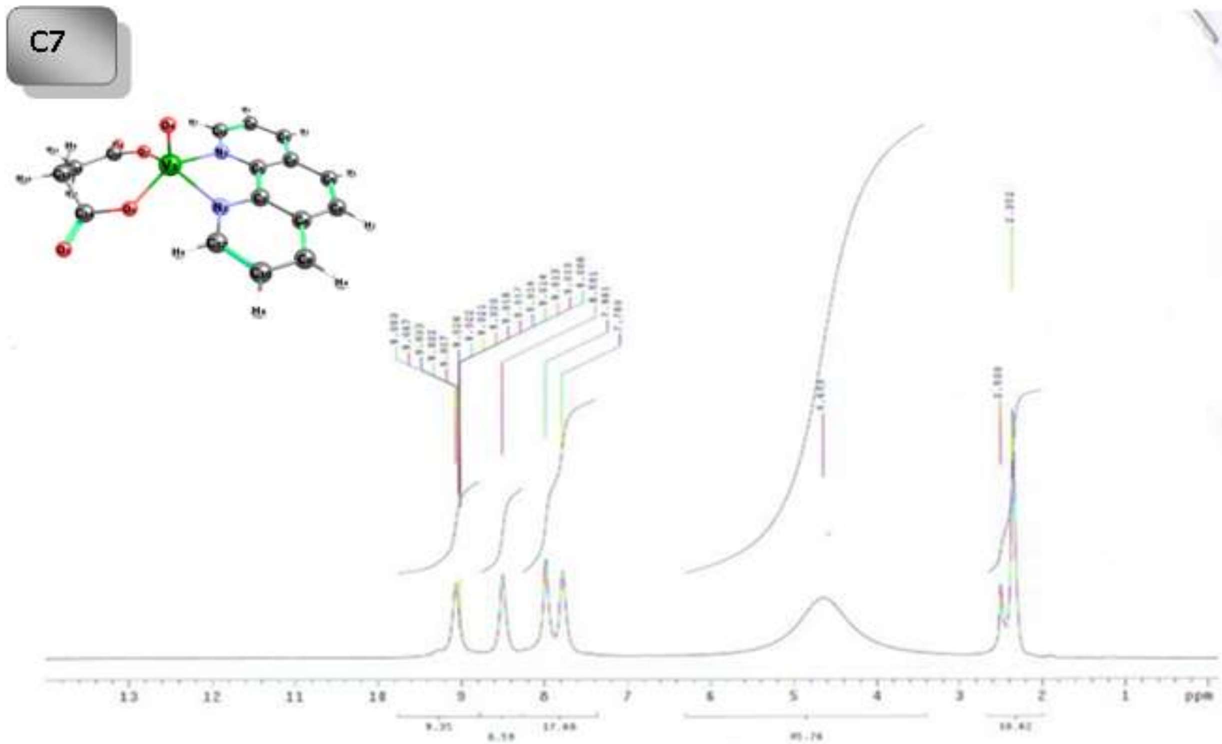

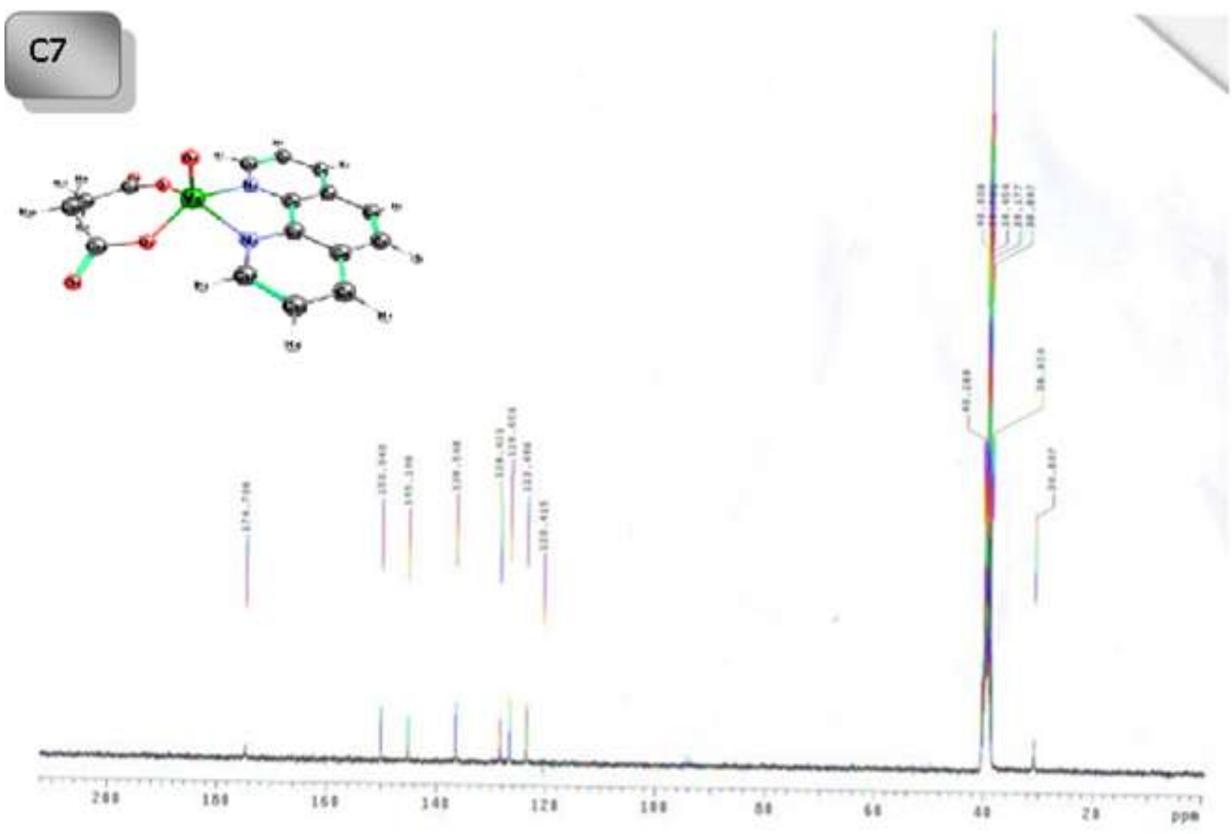

Figure 3.37 ^{1}HNMR and ^{13}C NMR of C7

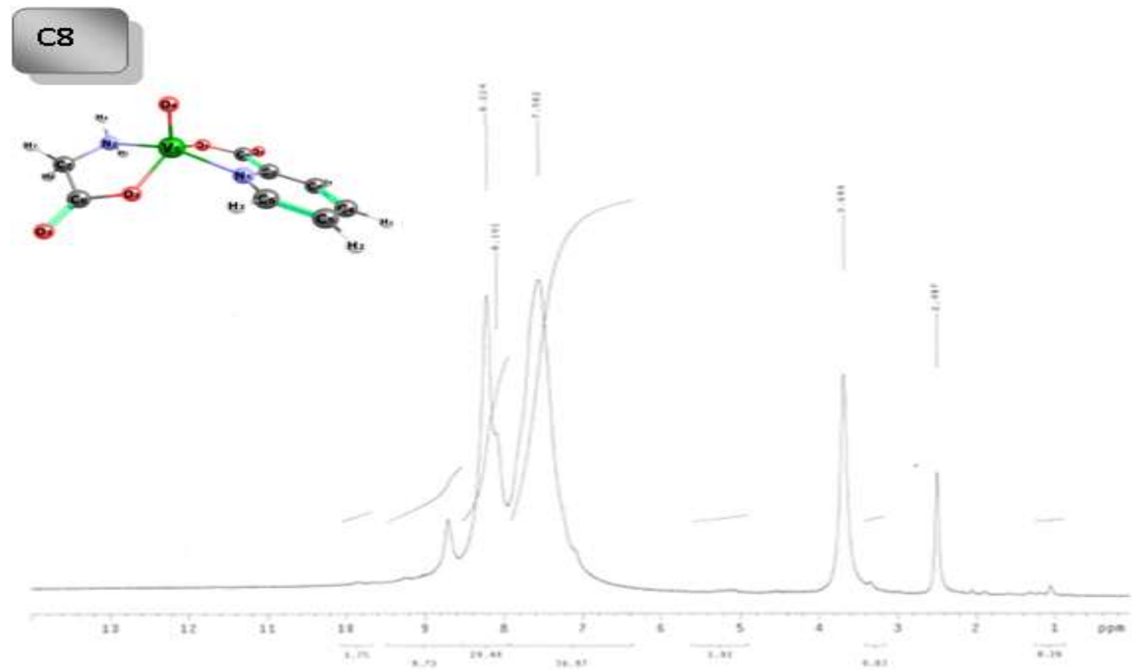

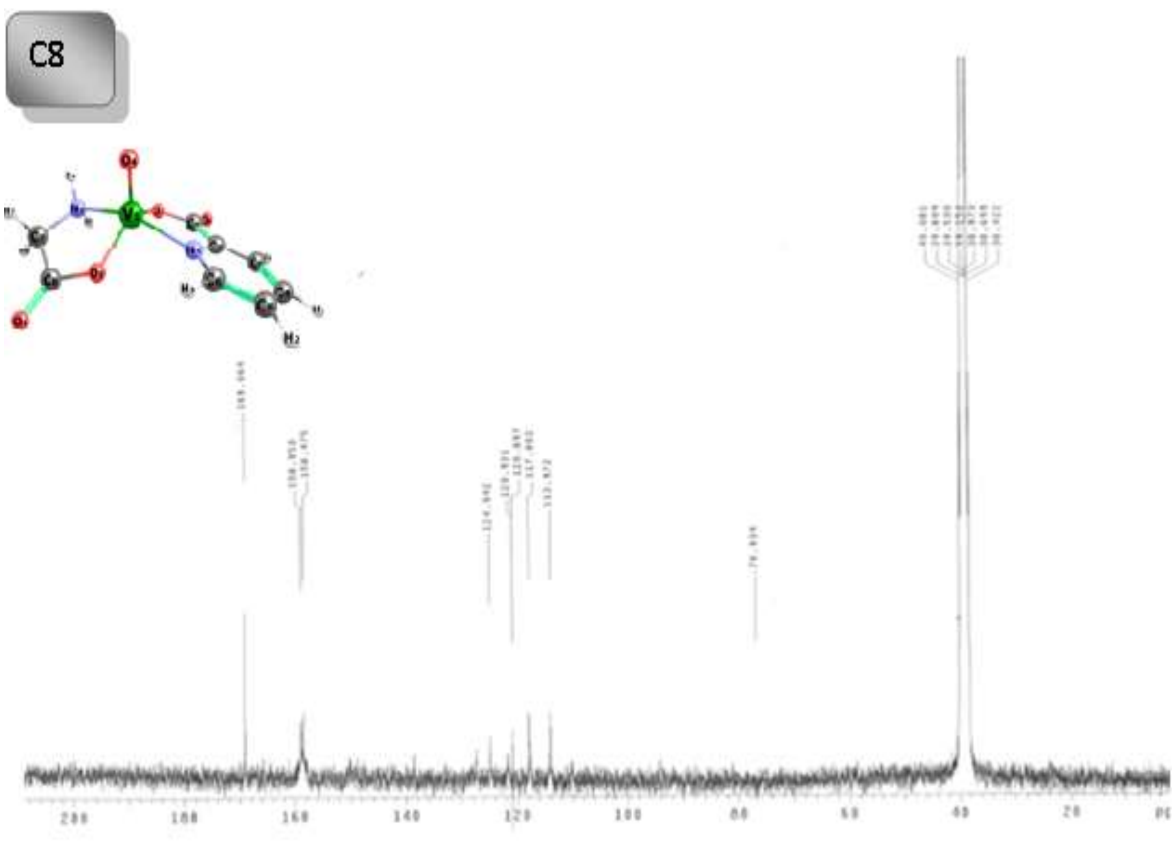

Figure 3.38 ^{1}HNMR and ^{13}C NMR of C8

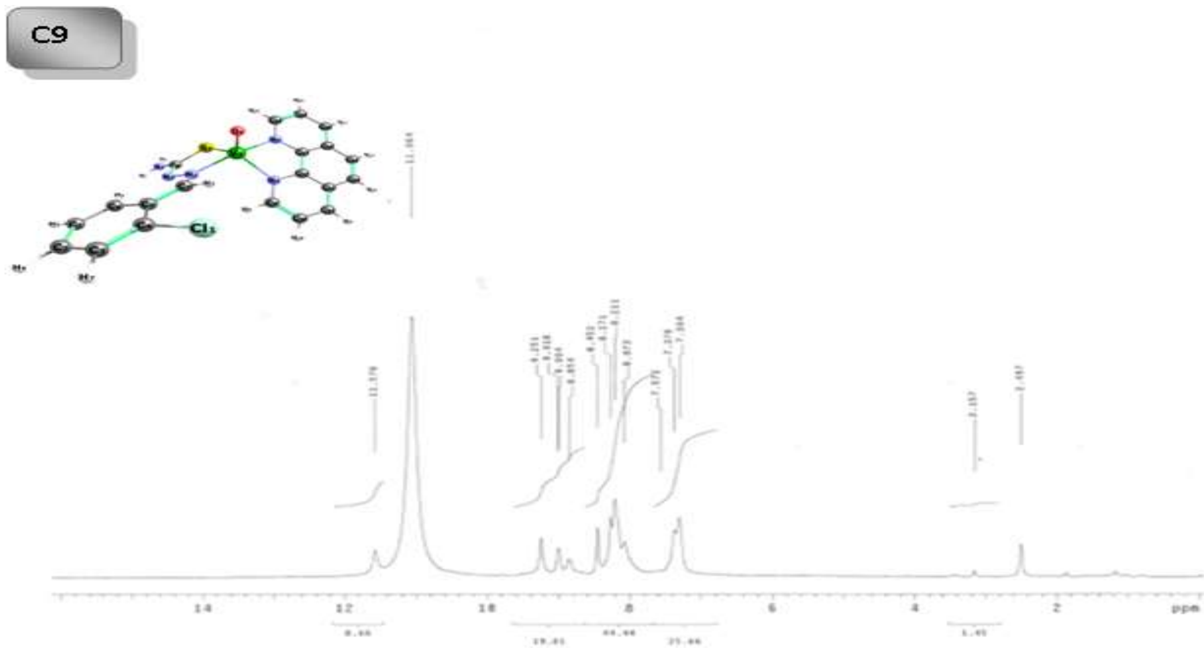

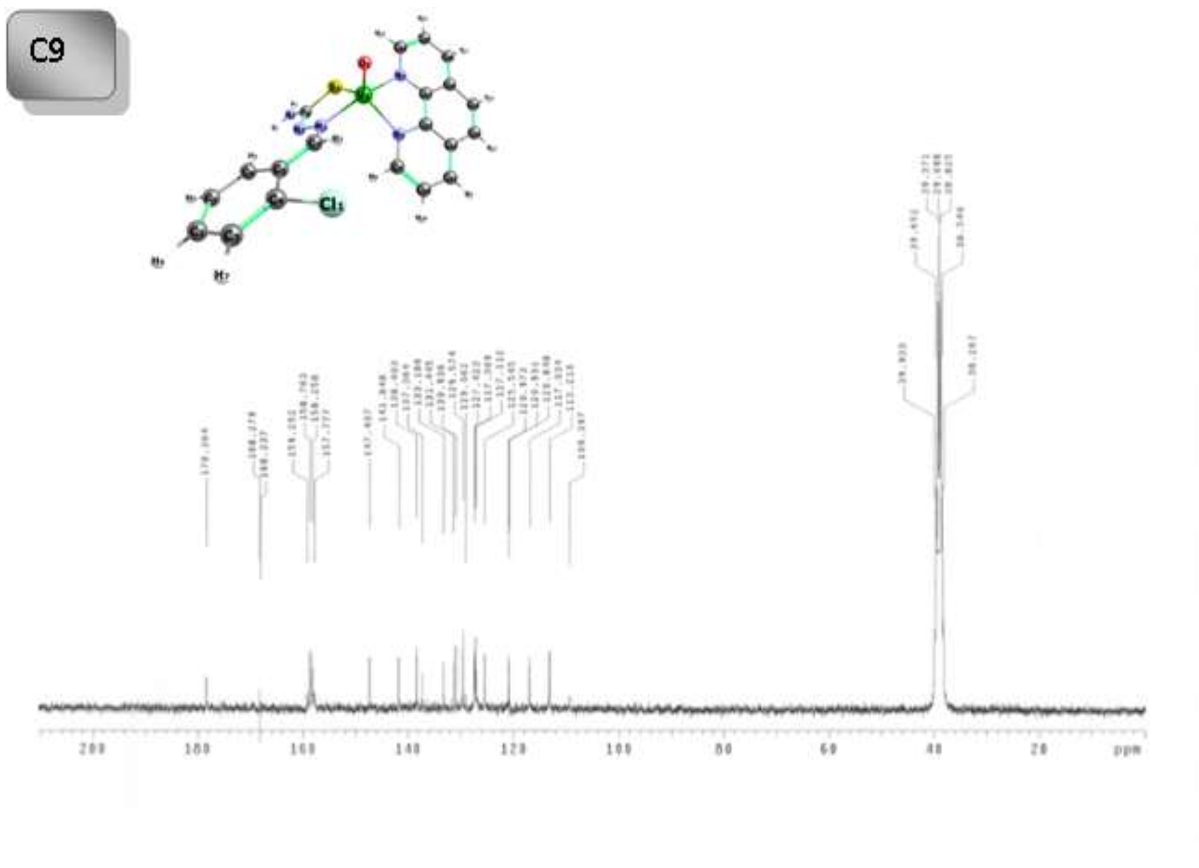

Figure 3.39 ^{1}HNMR and ^{13}C NMR of C9

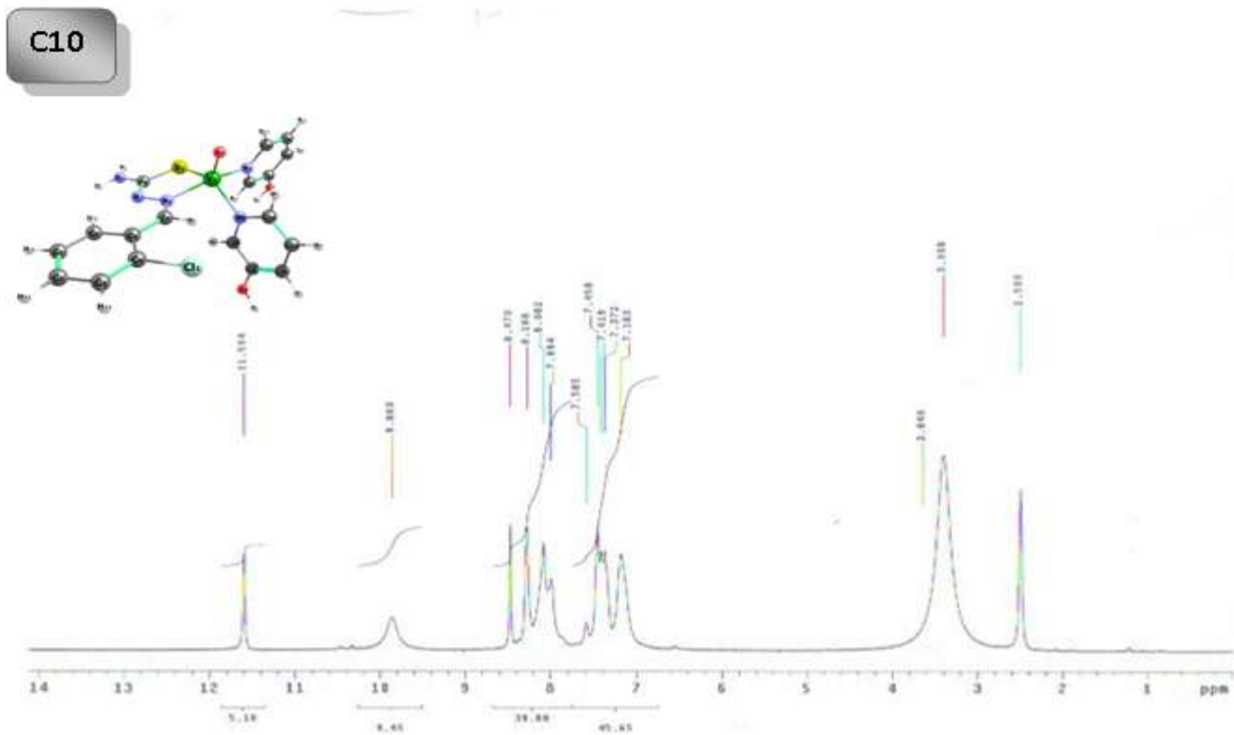

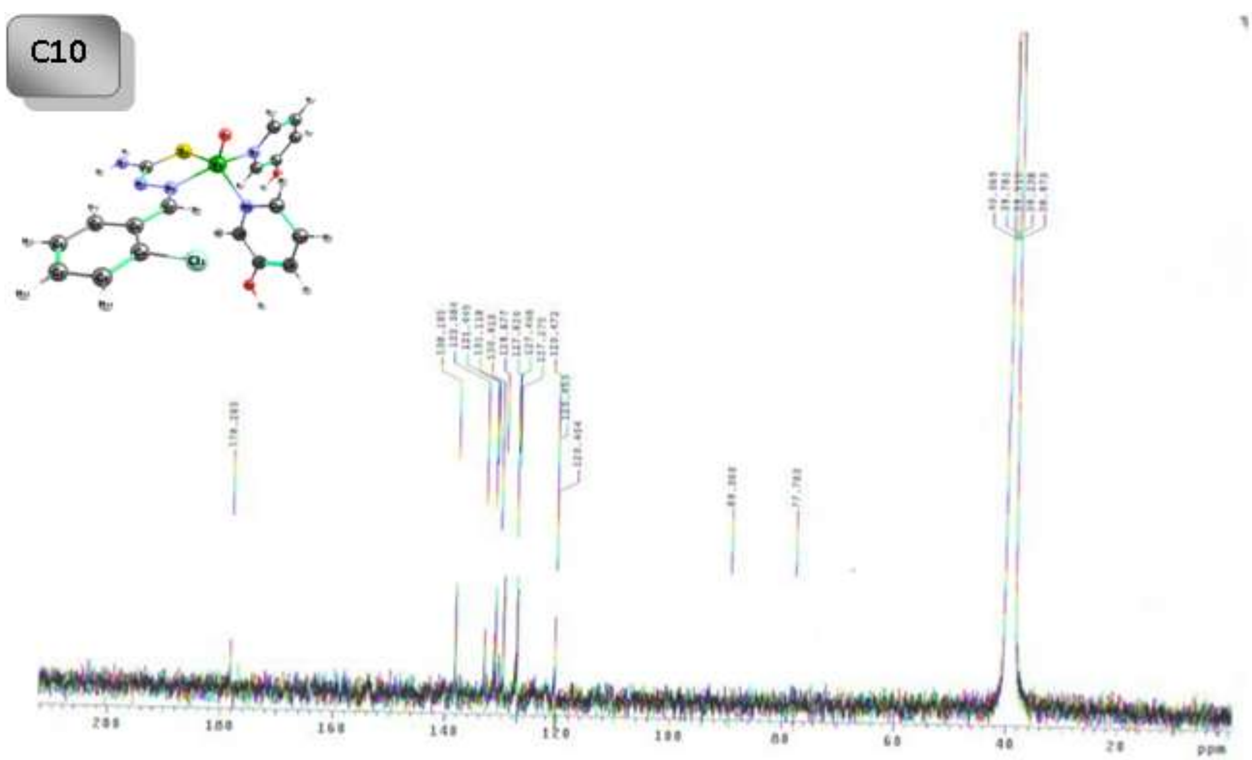

Figure 3.40 ^{1}HNMR and ^{13}C NMR of C10

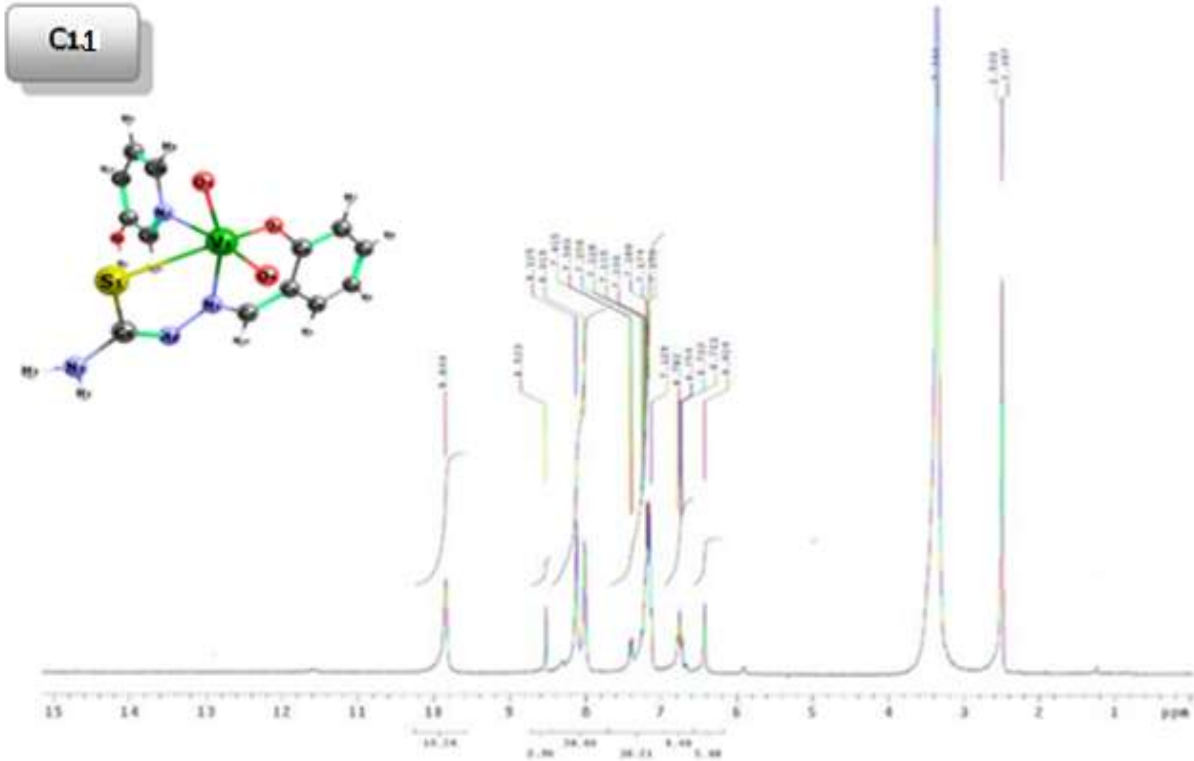

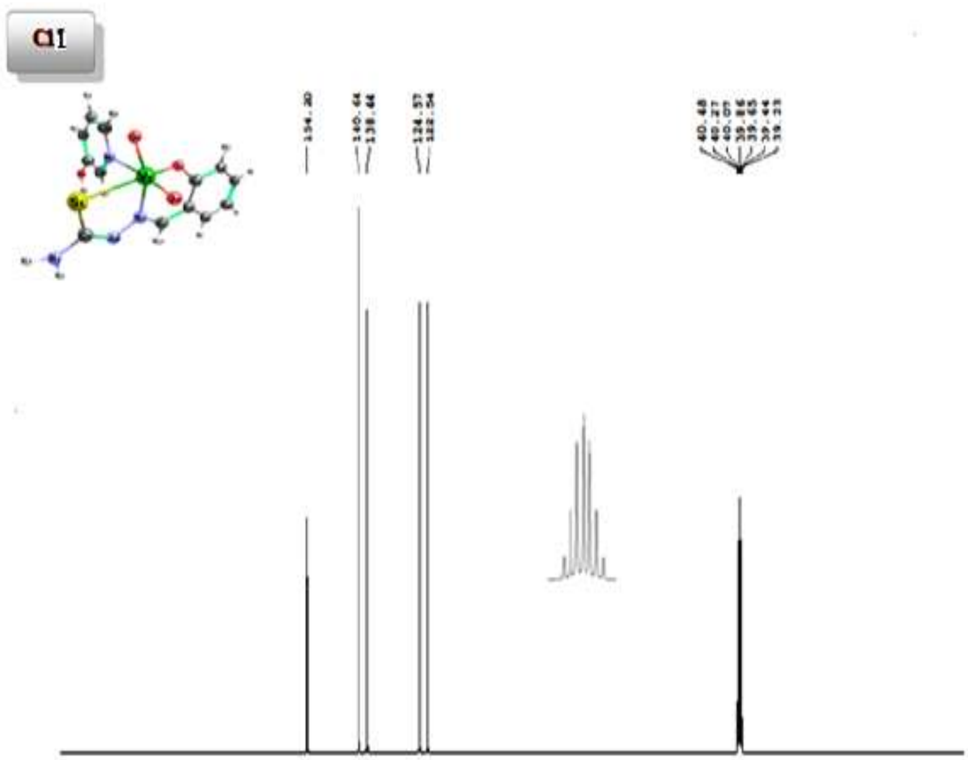

Figure 3.41 ^{1}HNMR and ^{13}C NMR of C11

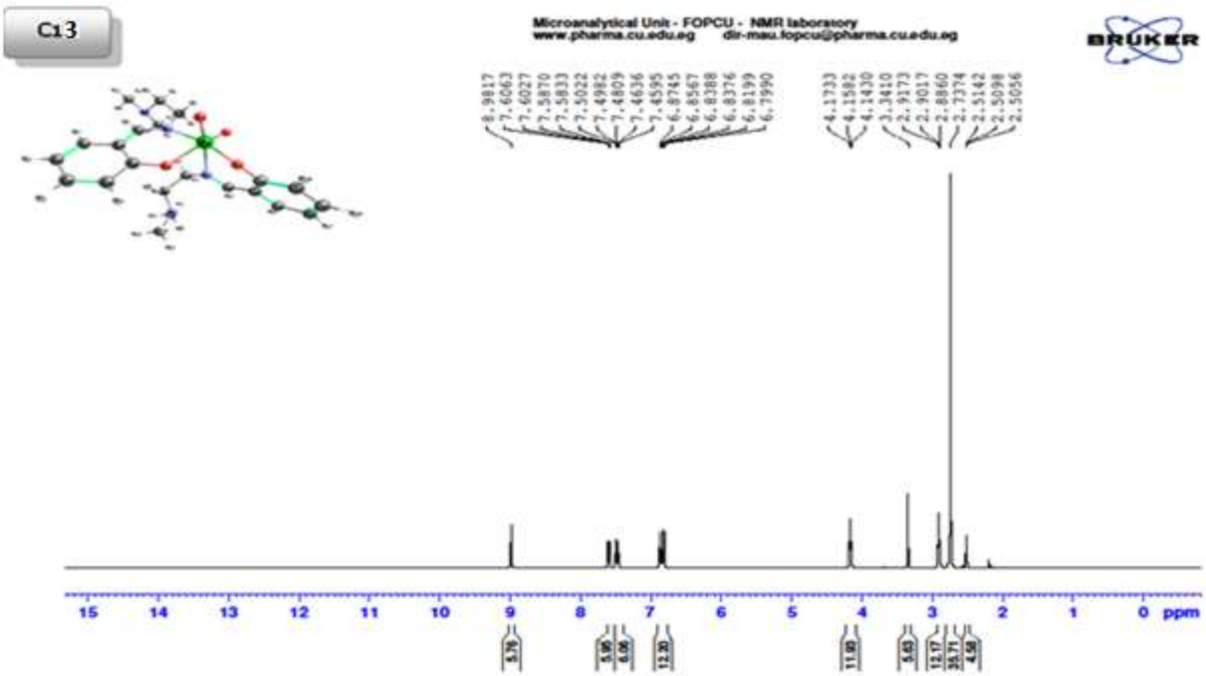

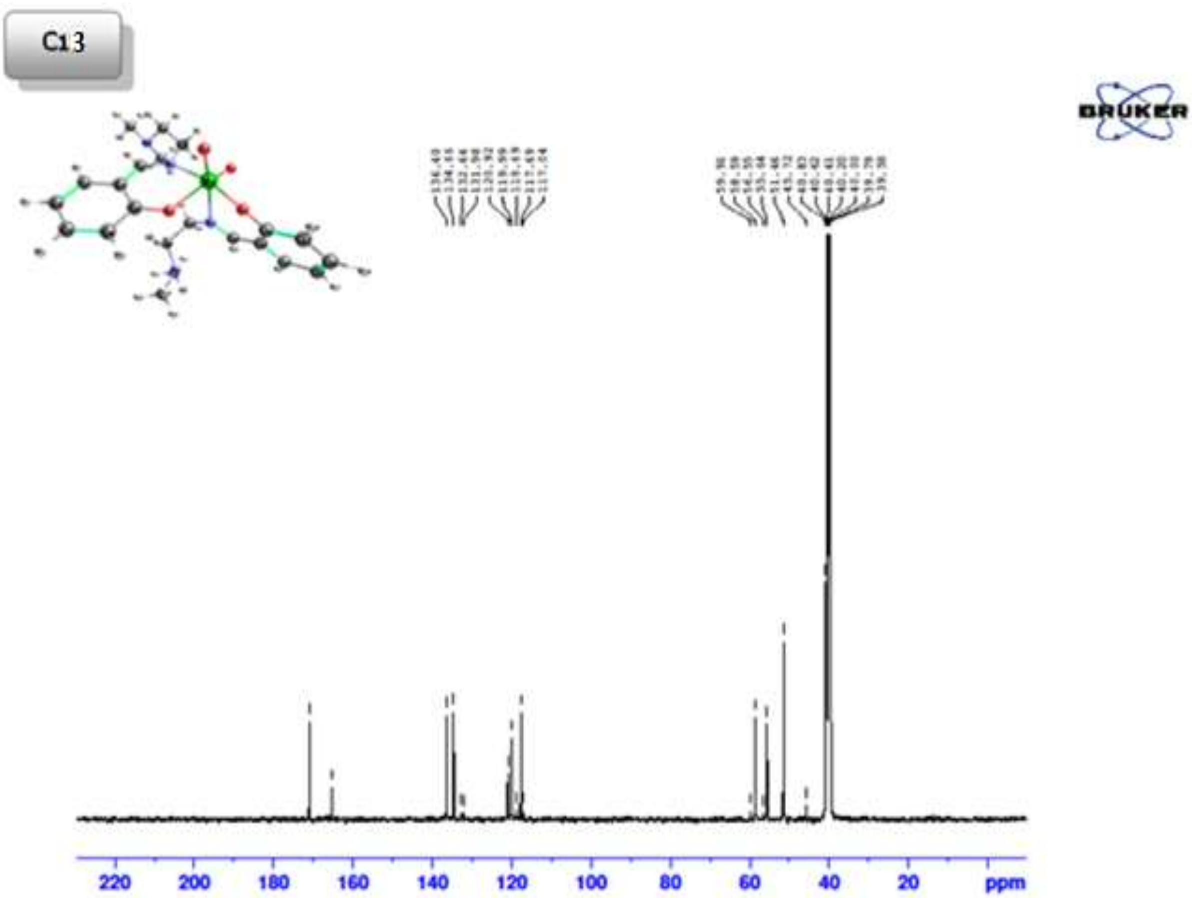

Figure 3.42 ^{1}HNMR and ^{13}C NMR of C13

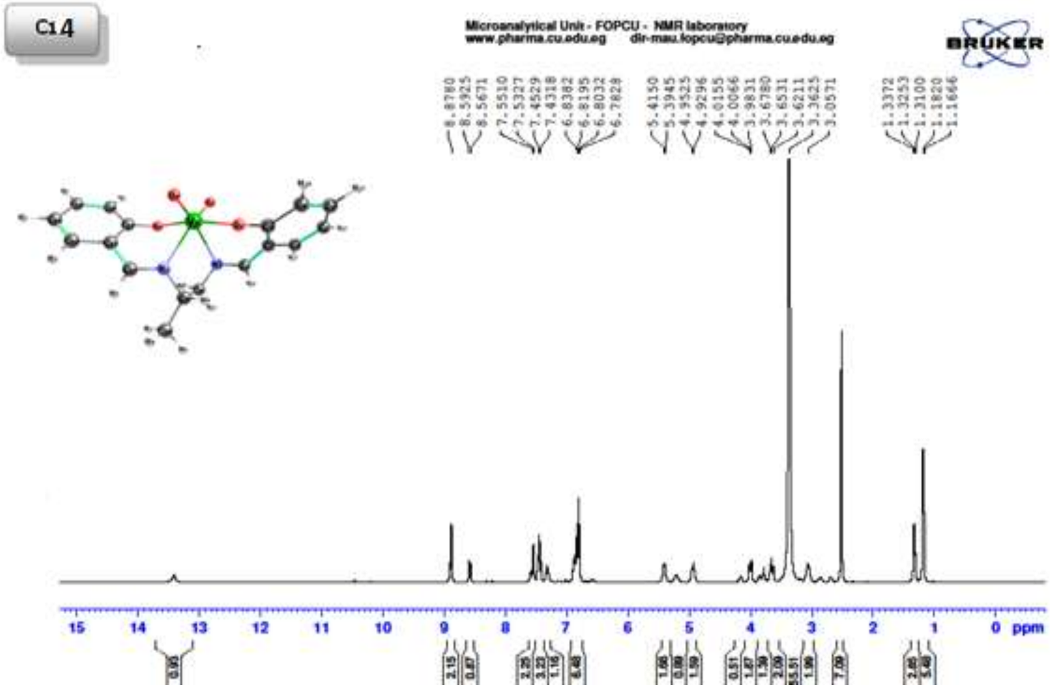

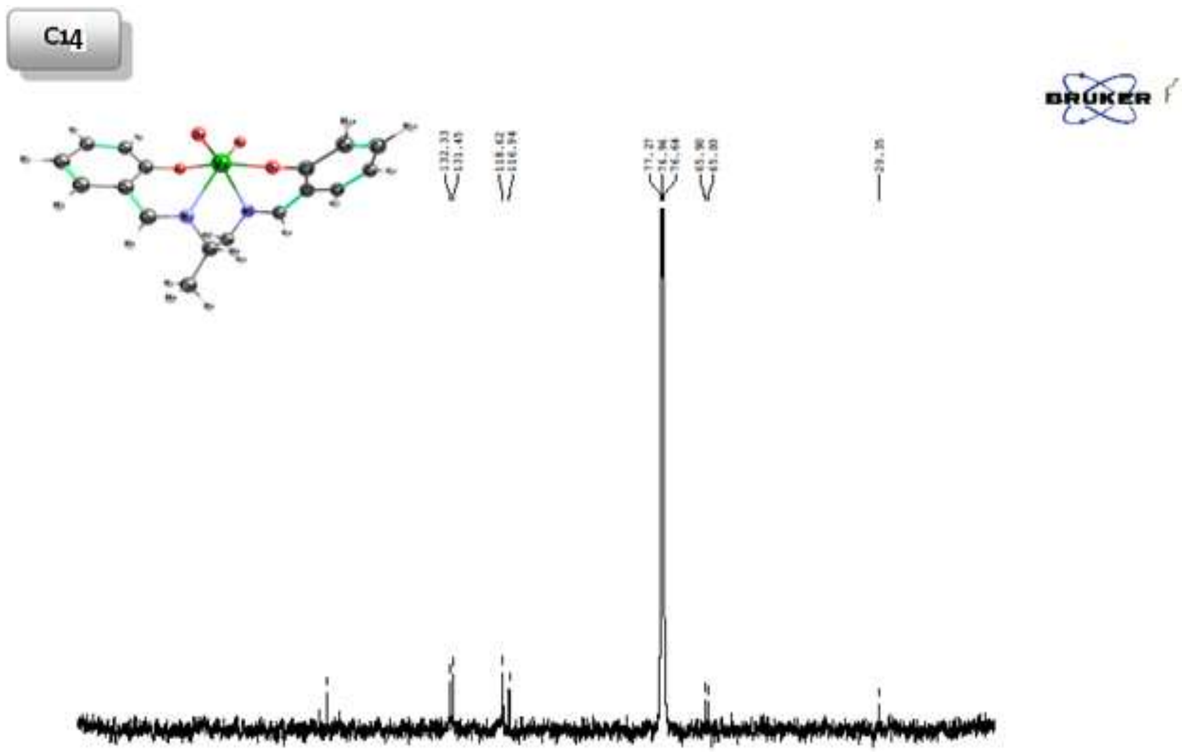

Figure 3.43 ^{1}HNMR and ^{13}C NMR of C14

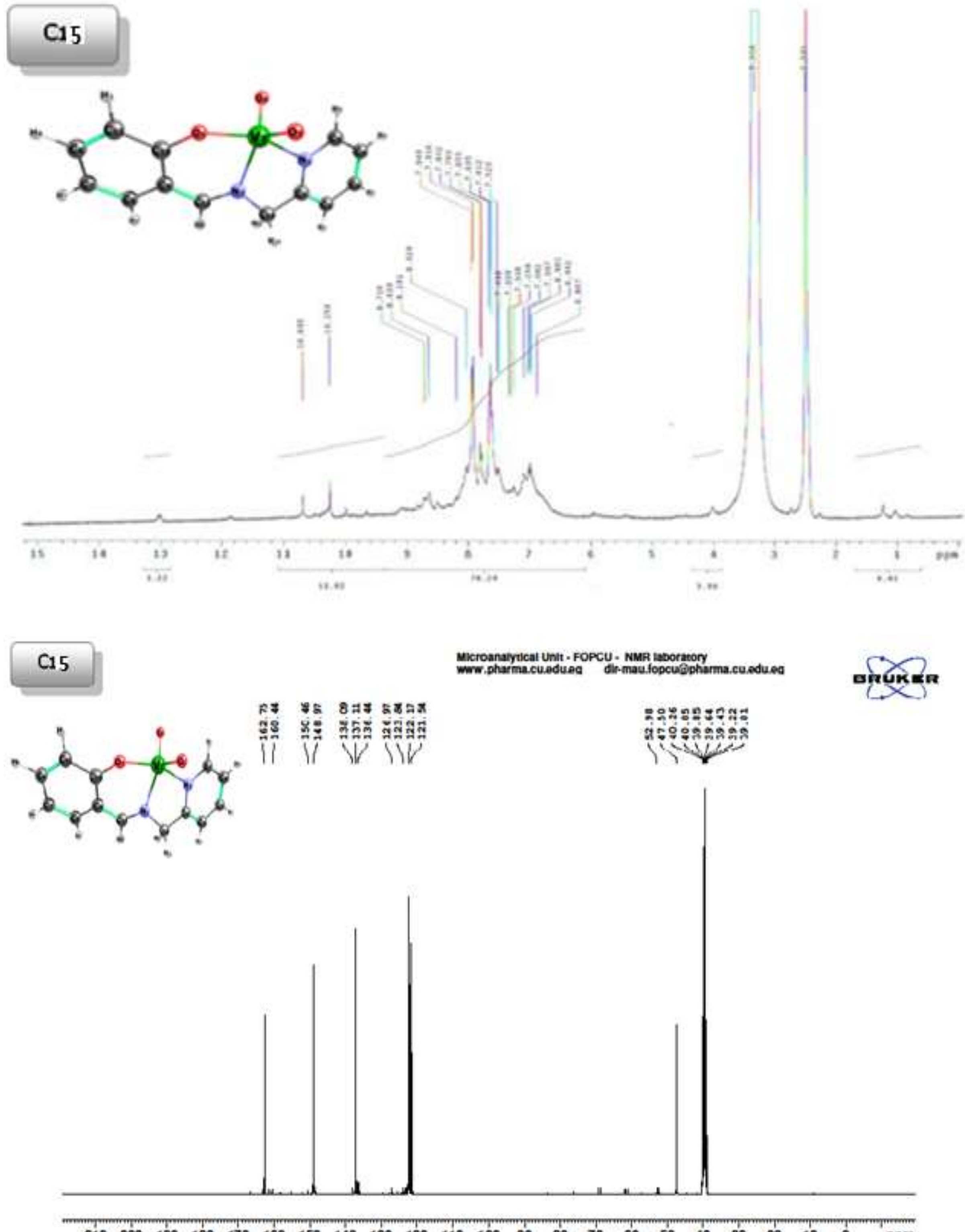

Figure 3.44 ^{1}HNMR and ^{13}C NMR of C15

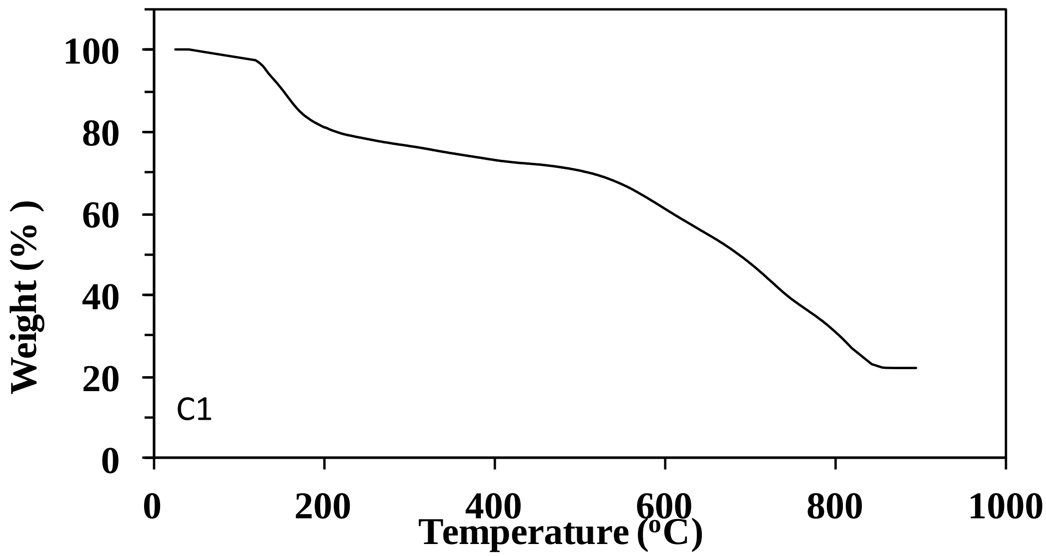

Figure 3.45 TGA curve of C1

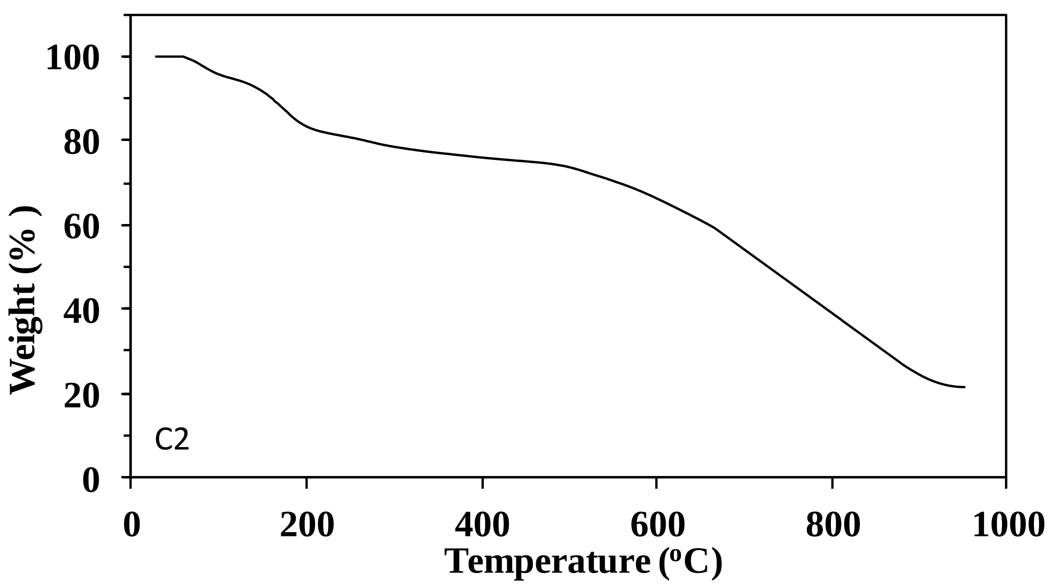

Figure 3.46 TGA curve of C2

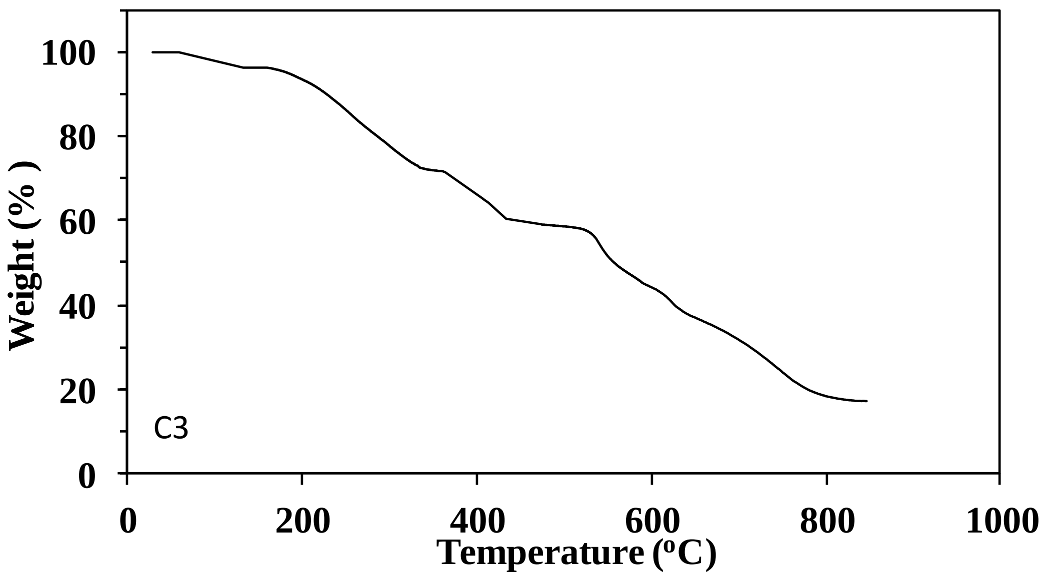

Figure 3.47 TGA curve of C3

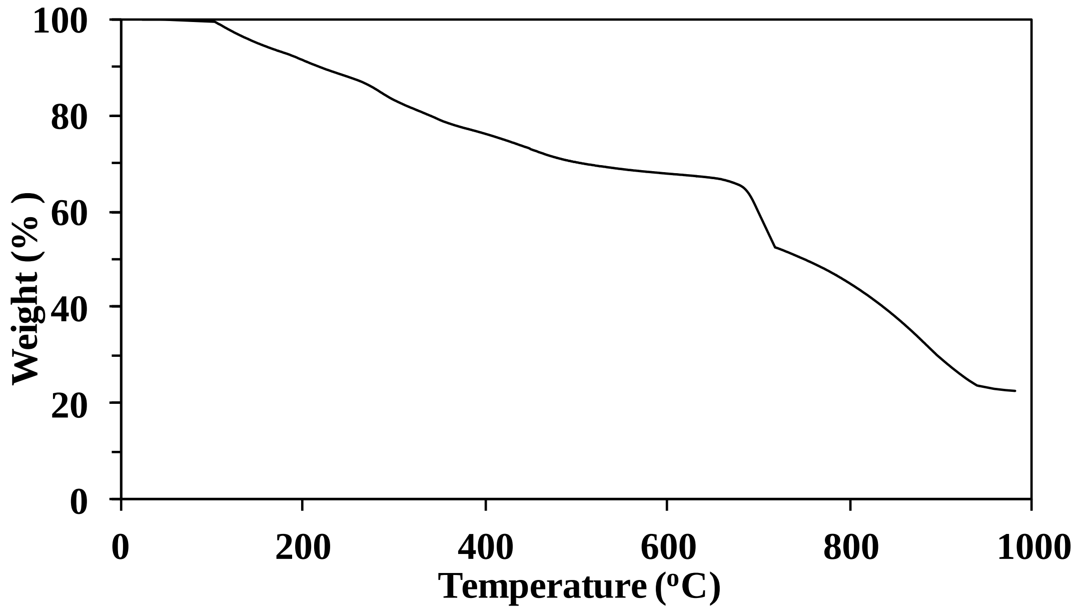

Figure 3.48 TGA curve of C4

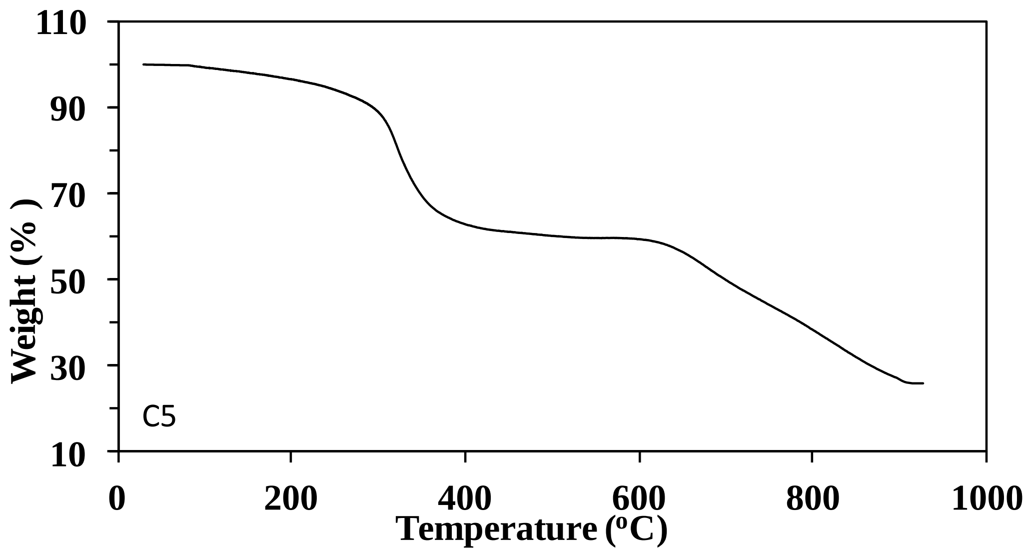

Figure 3.49 TGA curve of C5

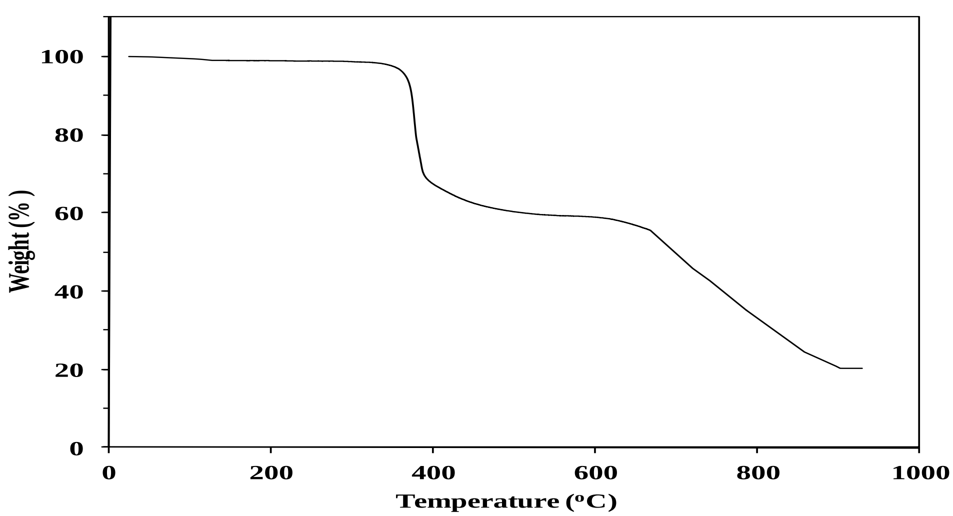

Figure 3.50 TGA curve of C6

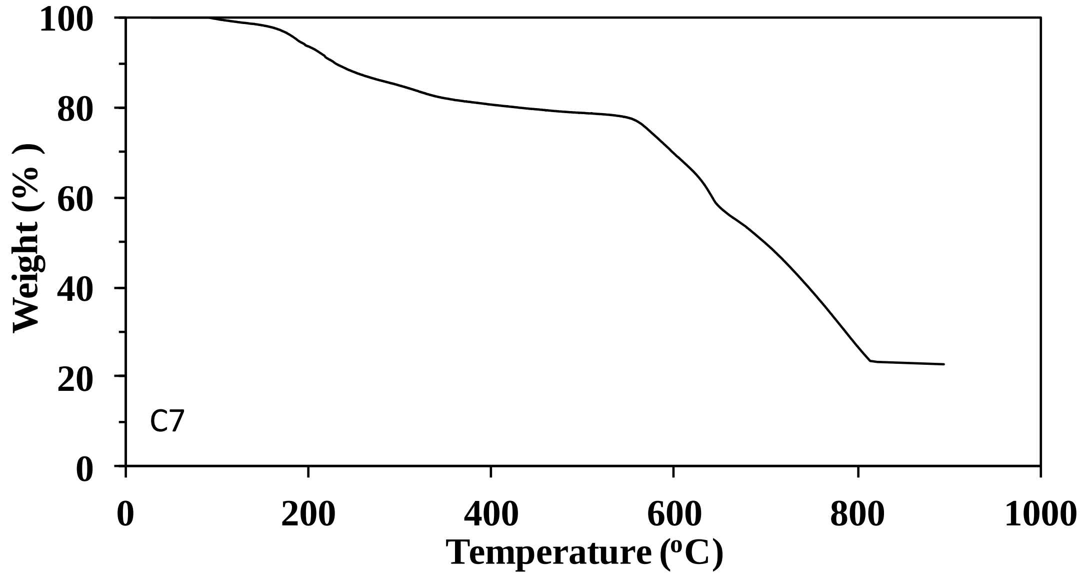

Figure 3.51 TGA curve of C7

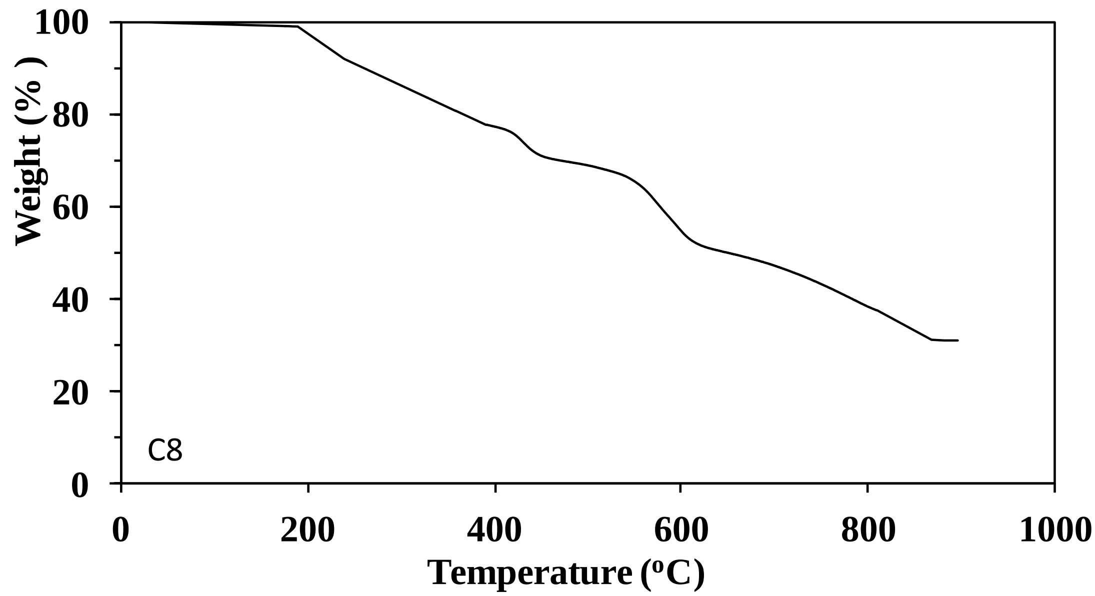

Figure 3.52 TGA curve of C8

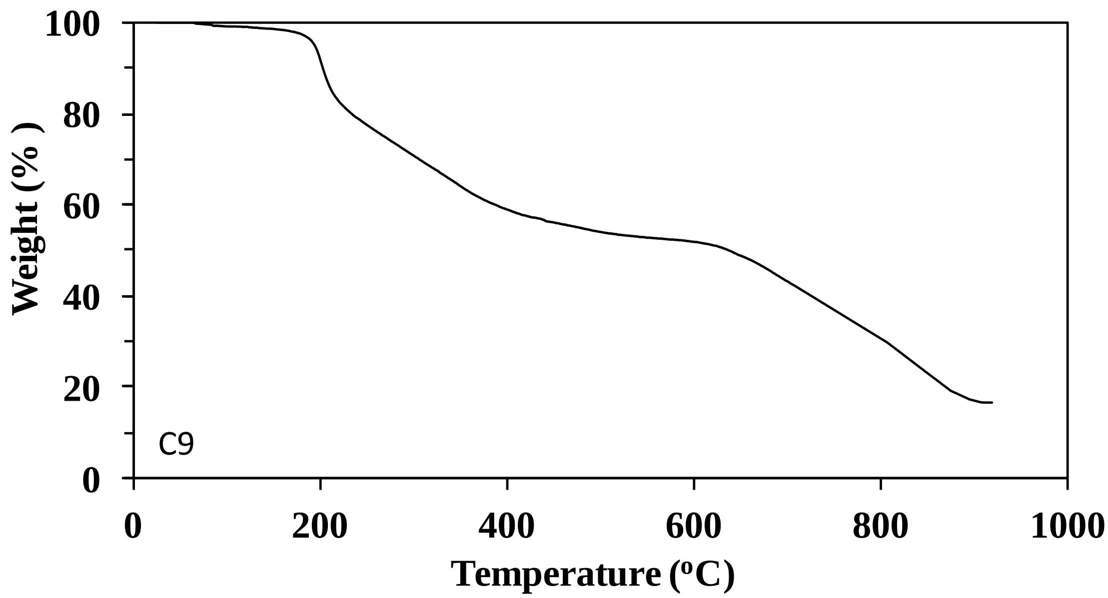

Figure 3.53 TGA curve of C9

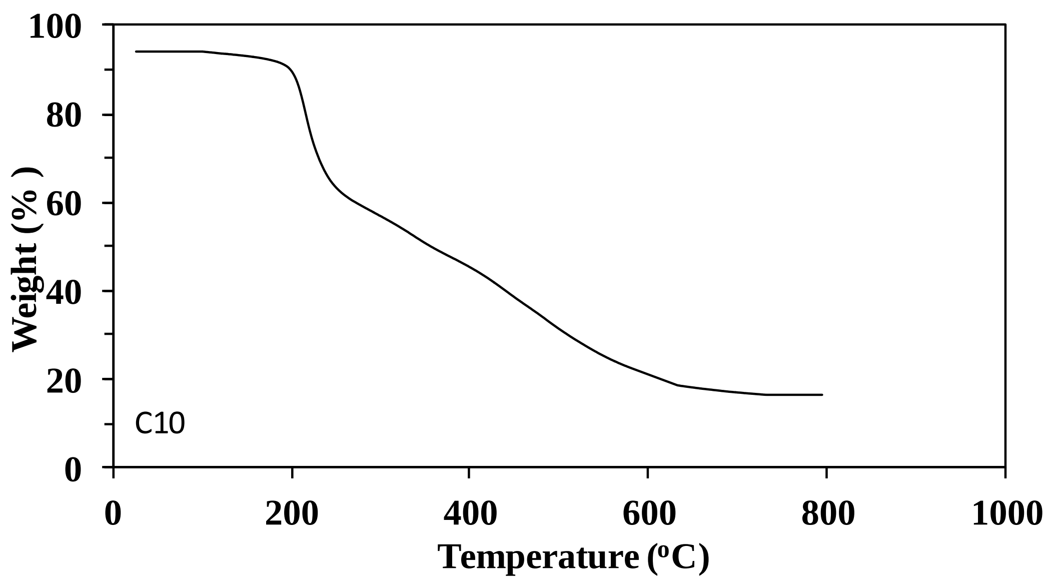

Figure 3.54TGA curve of C10

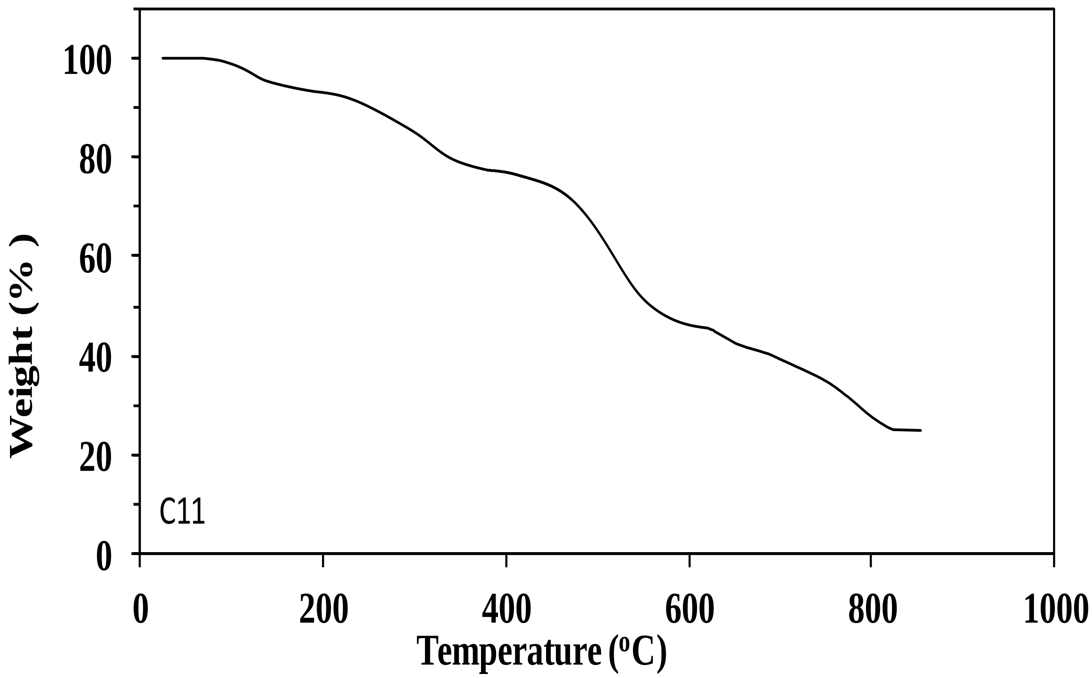

Figure 3.55 TGA curve of C11

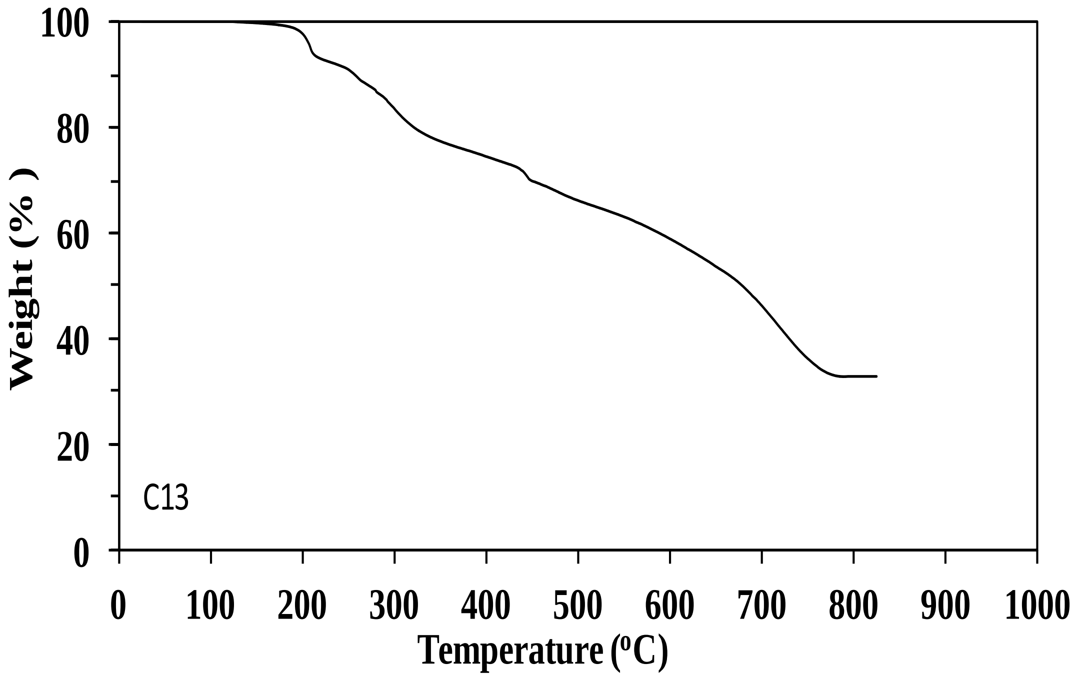

Figure 3.56 TGA curve of C13

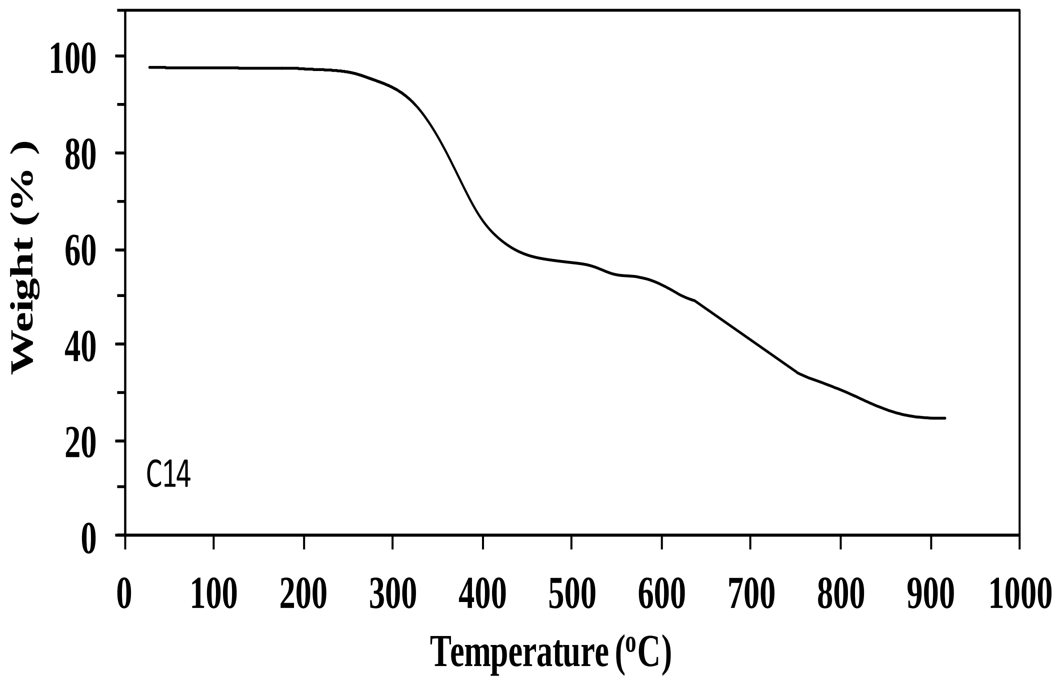

Figure 3.57 TGA curve of C14

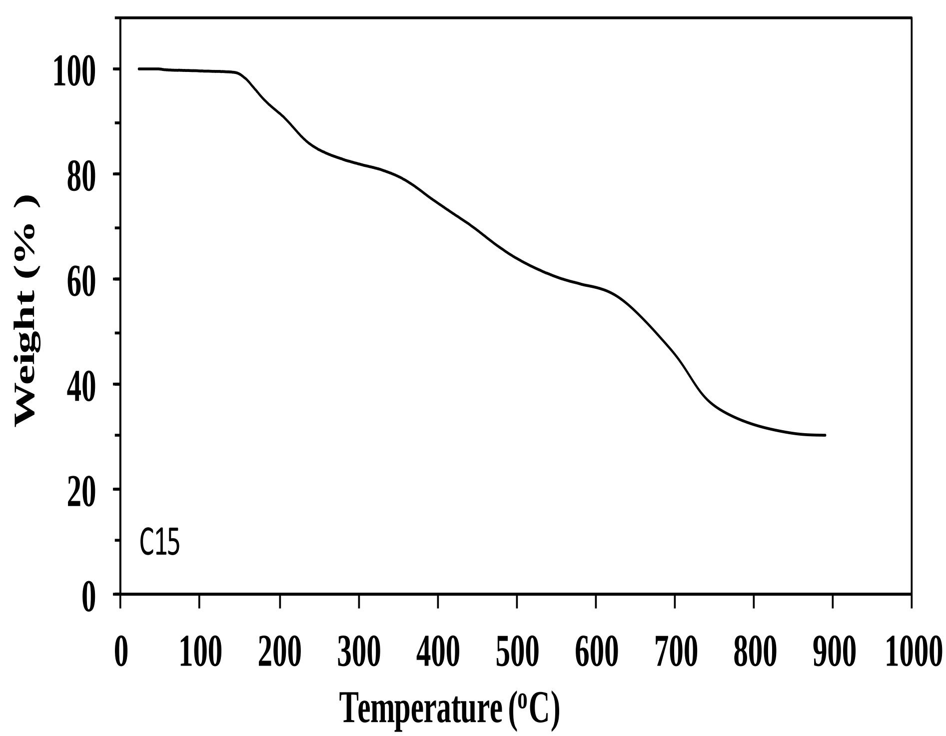

Figure 3.58 TGA curve of C15

3.3 Theoretical DFT calculations

The density function theory was applied to calculate the optimized geometries using the Gaussian09 program. The DFT/B3LYP method was used for the geometry optimization. Full geometry optimization was performed using B3LYP/LANL2DZ as a basis set to generate the optimized structure for ligands and complexes.

3.3.1 The Molecular modeling of ligand L1, L2 and complex C1:

(Figure 3.59) shows the optimized structures of ligand (L1), (L2) and their complex (C1) as the most stable configuration. The vanadium atom is six-coordinate in a distorted octahedral geometry, the bond angles ranging from 74.81 to 159.7°, (Table3.12).

The distance between donor atoms involved in coordination N1- - - - -N2 decreased upon complex formation from 2.735Å (in free ligand) to 2.681 Å (in the complex). The distance between N3- - - - -O1, S1- - - - -O1 are also decreased from 4.633 and 2.756Å (in free ligand) to 3.292 and 2.599Å respectively (in the complex).The bond length of V-O1 is 1.904Å longer than V=O3 1.618.

The atoms N1, N2, N3 and O1 are almost in one plane deviated by 0.87°. The axial bond angles of N1-V-O1 and N1-V-N3, 159.1° and 159.7° is deviated from linearity due to coordination to vanadium. The bite angle N1-V-N2 , O1-V-N2 and N3-V-O1 are 77.12°, 86.43°, and 78.36 respectively lower than 90° due to coordination, and The bite angles N2-V-NS1 and N3-V-N1 are also 92.23°, 113.9° more than 90° due to coordination.

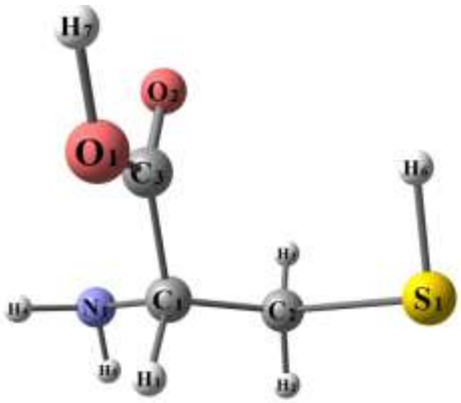

L1 Cystine

L2 1,10 Phenanthorline

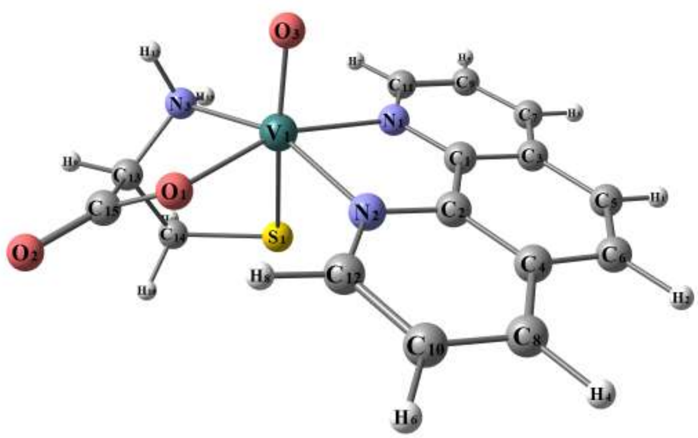

C1 [VO (cys) (phen)]

Figure 3.59 *Optimized structure of **C1** by density function theory B3LYP/LANL2DZ, ligands in upper and complex in lower.*

Table 3.12 *Calculated energies, Optimized bond lengths and angles of C1*

Ligand	E^a	$HOMO^b$	$LUMO^c$	ΔE^d	Dipole moment[d]
Cystine	-333.768	-0.2467	-0.0312	0.2155	2.722
1,10 phenanthroline	-571.488	-0.2310	-0.0654	0.1656	4.096
[VO(Cys)(1.10ph)]	-1050.869	-0.1772	-0.1035	0.0737	10.255

Type of Angle	Angle (°)	Type of Angle	Angle (°)	Type of bond	Bond length(Å)
	C1		C1		C1
O1-V1-N3	78.364	N1-V-O3	89.062	V - O3	1.618
O1-V1-O3	107.609	N2-V-N3	159.719	V - O1	1.940
O1-V1-N1	159.066	N2-V-O3	103.882	V - N1	2.182
O1-V1-N2	86.426	N2-V-S1	92.225	V - N2	2.112
O1-V1-S1	90.757	S1-V-N3	74.817	V - N3	2.166
N1-V-N2	77.122	S1-V-O3	156.045	V - S1	2.634
N1-V-N3	113.987	N3-V-O3	93.548		
N1-V-S1	77.216				

3.3.2 The Molecular modeling of ligand L3, L2 and complex C2:

(Figure 3.60) shows the optimized structures of ligand (L2), (L3) and their complex (C2) as the most stable configuration. The vanadium atom is six-coordinate in a distorted octahedral geometry, the bond angles ranging from 77.57 to 162.3°, (Table 3.13).

The distance between donor atoms involved in coordination N1- - - - -N2 decreased upon complex formation from 2.735Å (in free ligand) to 2.695 Å (in the complex). But the distance between N1- - - - -O1, is slightly increased from 2.588 (in free ligand) to 2.625Å (in the complex) this is probably due to the formation of hydrogen bonding between N1---HO1 in L3. The bond length of V-O1 is 1.925Å longer than V=O3 1.610.

The atoms N1, N2, N3 and O1 are almost in one plane deviated by 3.98°. The axial bond angles of N1-V-O1 and N1-V-N3, are 162.3° and 160.0° deviated from linearity due to coordination to vanadium. The bite angles N1-V-N2, O1-V-N2 and N3-V-O1 are 77.57°, 87.25°, and 79.84 lower than 90° due to coordination, and The bite angle N3-V-N1 is also 112.0° more than 90° due to coordination .

L2 1,10 Phenanthorline

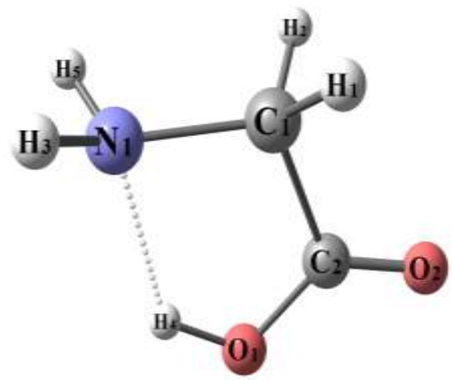

L3 Glycine

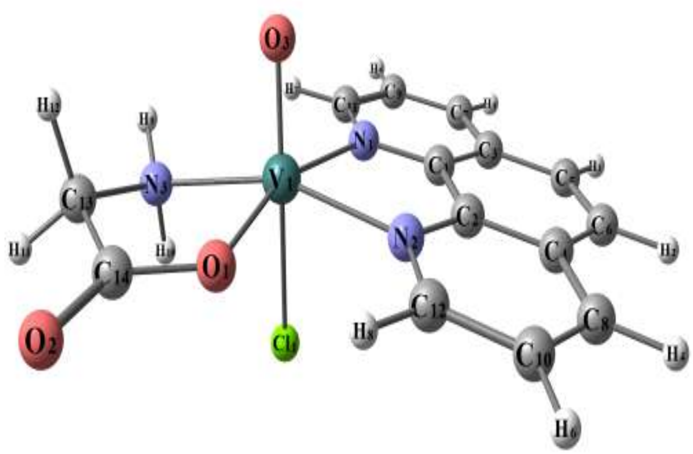

C2 [VO (Cl) (gly) (phen)] .H_2O

Figure 3.60 *Optimized structure of **C2** by density function theory B3LYP/LANL2DZ, ligands in upper and complex in lower.*

Table 3.13 *Calculated energies-Optimized bond lengths and angles of C2*

Ligand	E^a	$HOMO^b$	$LUMO^c$	ΔE^d	Dipole moment ^{d}
Glycine	-284.382	-0.2405	-0.0206	0.2199	1.803
1,10 phenanthroline	-571.488	-0.2310	-0.0654	0.1656	4.096
[VO(gly) (phen)]	-1017.053	-0.2274	-0.1043	0.1231	10.873

Type of Angle	Angle (°) C2	Type of Angle	Angle (°) C2	Type of Bond	Bond length(Å)
O1-V1-N1	160.0	N1-V-N2	77.57	V-O1	1.925
O1-V1-N2	87.25	N1-V-N3	112.0	V-O3	1.610
O1-V1-N3	79.84	N2-V-N3	162.3	V-N1	2.198
O1-V1-O3	104.7	O1-V-Cl	93.31	V-N2	2.101
O3-V-N1	87.95	O3-V-Cl	159.2	V-N3	2.156
O3-V-N2	103.7	N2-V-Cl	87.21	V- Cl	2.588
O3-V-N3	94.40	N3-V-Cl	78.45	V-O1	1.924

3.3.3 The Molecular modeling of ligand L4, L2 and complex C3:

(Figure 3.61) shows the optimized structures of ligand (L2), (L4) and their complex (C3) as the most stable configurations. The vanadium atom is six-coordinate in a distorted octahedral geometry, the bond angles ranging from 78.27 to 162.5°, (Table 3.14).

The distance between donor atoms involved in coordination N1- - - - -N2 decreased upon complex formation from 2.735Å (in free ligand) to 2.695 Å (in the complex). The distance between N3- - - - -O1, is also decreased from 3.535Å (in free ligand) to 2.611 Å (in the complex).The bond length of V-O1 is 1.920Å longer than V=O3 1.611 Å.

The atoms N1, N2, N3 and O1 are almost in one plane deviated by 6.28°. The axial bond angles of N1-V-O1 and N2-V-N3, 162.5° and 159.1° were deviated from linearity due to coordination to vanadium. The bite angles N1-V-N2, O1-V-N2 and N3-V-O1 are 77.54°, 87.39°, and 79.39° respectively are, lower than 90° due to coordination, and the bite angle and N3-V-N1 are also 112.2° more than 90° due to coordination.

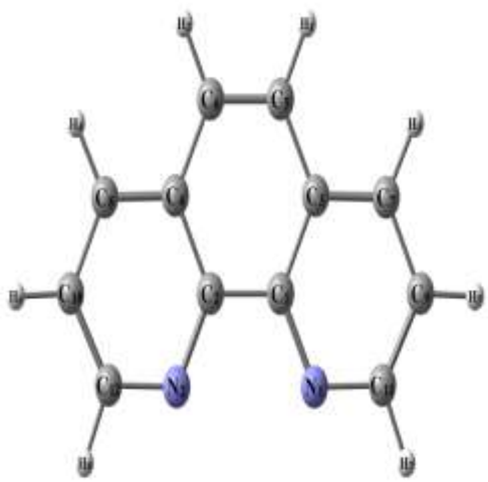

L2 1,10 Phenanthorline

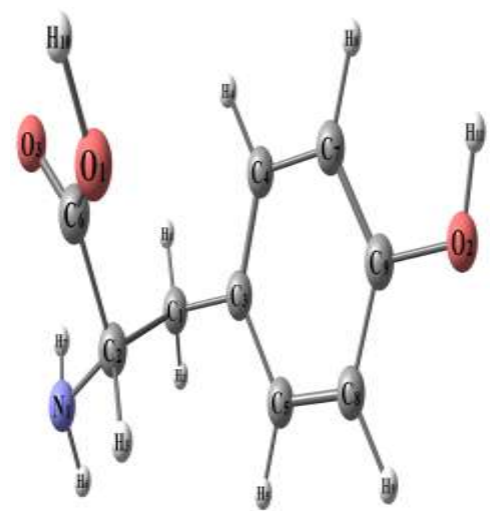

L4 Tyrosine

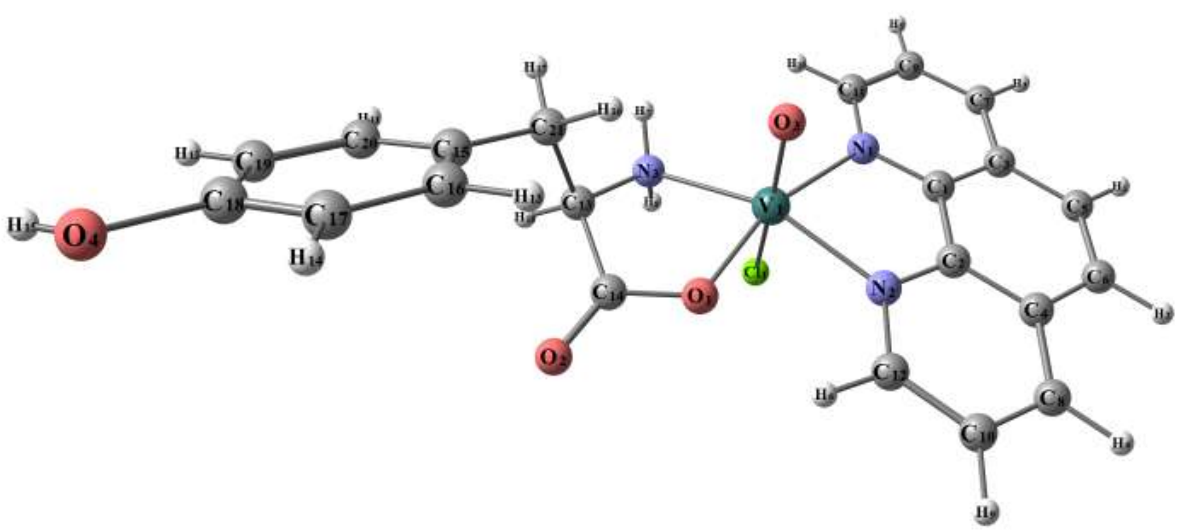

C3 [VO (Cl) (tyro) (phen)].H_2O

Figure 3-61 *Optimized structure of **C3** by density function theory B3LYP/LANL2DZ, ligands in upper and complex in lower.*

Table 3.14 Calculated energies -Optimized bond lengths and angles of C3

Ligand	E^a	$HOMO^b$	$LUMO^c$	ΔE^d	Dipole moment^d
Tyrosine	-629.904	-0.2233	-0.0188	0.2045	2.206
1,10 phenanthroline	-571.488	-0.2310	-0.0654	0.1656	4.096
[VO(Tyro)(1,10ph)]	-1362.585	-0.2152	-0.1035	0.1117	10.297

Type of Angle	Angle (°)	Type of Angle	Angle (°)	Type of	Bond length(Å)
	C3		C3	bond	C3
O1-V1-N3	79.39	N2-V-N3	159.1	V - O1	1.920
O1-V1-O3	104.8	N2-V-O3	106.7	V - O3	1.611
O1-V1-N1	162.5	O3-V-N3	103.4	V - N1	2.201
O1-V1-N2	87.39	O1-V-Cl	93.49	V - N2	2.101
N1-V-O3	87.61	O3-V-Cl	159.5	V - N3	2.157
N1-V-N2	77.55	N2-V-Cl	86.39	V - Cl	2.594
N1-V-N3	112.2	N3-V-Cl	78.27	V - O1	1.920

3.3.4 The Molecular modeling of ligand L5, L2 and complex C4:

(Figure 3.62) show the optimized structures of ligand (L2), (L5) and their complex (C4) as the most stable configurations. The vanadium atom is six-coordinate in a distorted octahedral geometry, the bond angles ranging from 77.85 to 164.3°, (Table 3.15). The distance between donor atoms involved in coordination N1- - - - -N2 decreased upon complex formation from 2.735Å (in free ligand) to 2.696 Å (in the complex). The distance between N3- - - - -O1, N3- - - - -O2 are also decreased from 4.350 and 3.620Å (in free ligand) to 2.689 and 2.630Å (in the complex).The bond length of V-O1, V-O2 is 1.963, 1.940Å longer than V=O4 1.636.

The atoms N1, N2, N3 and O2 are almost in one plane deviated by 5.25°. The axial bond angles of N1-V-O2 and N1-V-N3, 160.3° and 164.3° is deviated from linearity due to coordination to vanadium. The bite angle N1-V-N2 , O2-V-N2 and N3-V-O2 are 76.55°, 86.99°, and 77.85 lower than 90° due to coordination, and The bite angle N3-V-N1 of 117.4° is also more than 90° due to coordination.

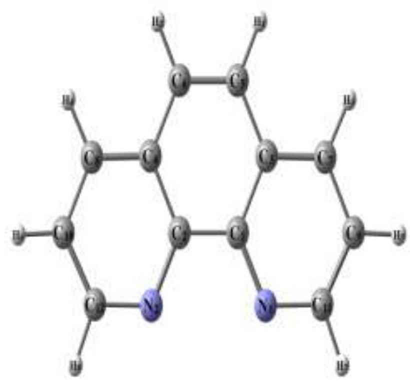

L2 1,10 Phenanthorline

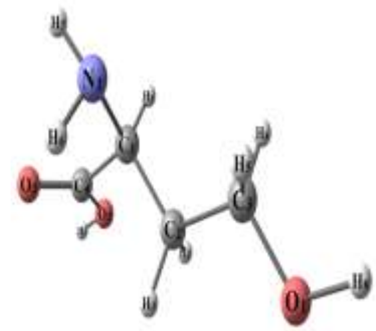

L5 Homoserine

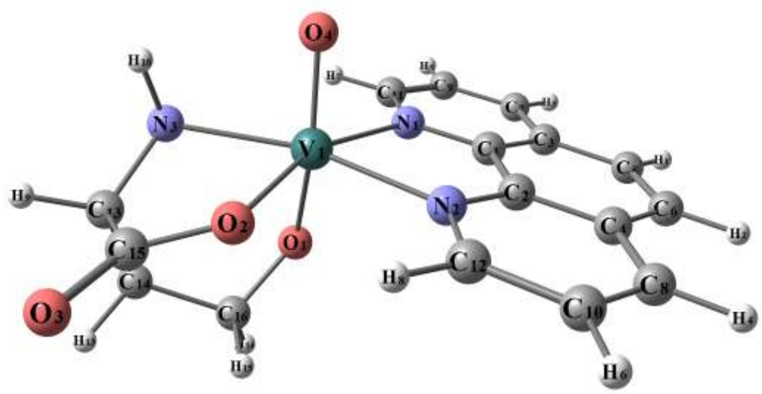

C4: [VO (homo) (phen)]

Figure 3.62 *Optimized structure of **C4** by density function theory B3LYP/LANL2DZ, ligands in upper and complex in lower.*

Table 3.15*Calculated energies-Optimized bond lengths and angles of C4*

Ligand	E^a	$HOMO^b$	$LUMO^c$	ΔE^d	Dipole moment ^{d}
Homoserine	-438.199	-0.2419	-0.0221	0.2198	1.364
1,10 phenanthroline	-571.488	-0.2310	-0.0654	0.1656	4.096
[VO(homo)(phen)]	-1155.287	-0.2122	-0.0957	0.1165	10.359

Type of Angle	Angle (°) C4	Type of Angle	Angle (°) C4	Type of bond	Bond length(Å) C4
O1-V1-O2	93.31	O2-V-N3	77.85	V-O1	1.939
O1-V1-O4	154.3	N1-V-O4	87.43	V-O2	1.962
O1-V1-N1	78.15	N1-V-N2	76.55	V-O41	1.635
O1-V1-N2	96.46	N1-V-N3	117.4	V-N1	2.226
O1-V1-N3	80.44	N2-V-N3	164.3	V-N2	2.125
O2-V-O4	106.5	N2-V-O4	100.7	V-N3	2.212
O2-V-N1	160.3	O4-V-N3	87.77		
O2-V-N2	86.99				

3.3.5 The Molecular modeling of ligand L6, L2 and complex C5:

(Figure 63) shows the optimized structures of ligand (L2), (L5) and their complex (C5) as the most stable configurations. The vanadium atom is five-coordinate in a distorted square pyramidal geometry, the bond angles ranging from 78.18° to 150.4°, (Table 3.16).

The distance between donor atoms involved in coordination N1- - - - -N2, N3- - - - -N4 decreased upon complex formation from 2.735Å (in free ligand) to 2.628 and 2.661Å (in the complex). The distance between O2- - - - -O4, O3- - - - -O7 are also decreased from 3.634 and 3.590Å (in free ligand) to 2.466 and 2.446Å (in the complex).The bond length of V1- O2, V1- O4 is 1.918, 1.827Å longer than V1=O5 1.601 Å. The bond length V2- O3, V1- O7 are also 1.822, 1.906Å longer than V1=O8 1.603 Å.

The atoms N1, N2, O2 and O4 are almost in one plane deviated by 12.84°. N3, N4, O3 and O7 are almost in one plane deviated by 5.19° too. The axial bond angles of N1-V1-O4, N2-V1-O2, N3-V2-O3 and N4-V2-O7, are 132.4° and 150.4°, 141.9° and 149.8° respectively are deviated from linearity due to coordination to vanadium. The bite angles N1-V1-N2, O2-V1-O4, N2-V-O4 and N1-V1-O2 are 78.19°, 82.33°, 86.43° and 89.34° lower than 90° due to coordination, The bite angles N3-V2-N4, O3-V2-O7 and N3-V2-O7 are 78.89°, 81.95° and 89.20°, lower than 90° due to coordination, and the bite angle N4-V2-O3 of 90.36° is also more than 90° due to coordination.

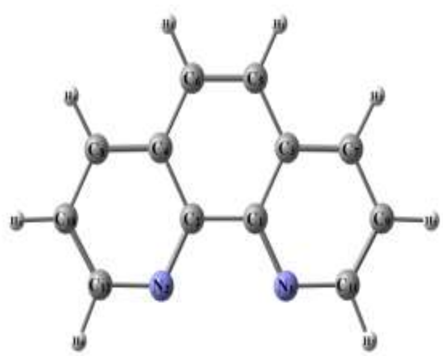

L2 1,10 Phenanthorline

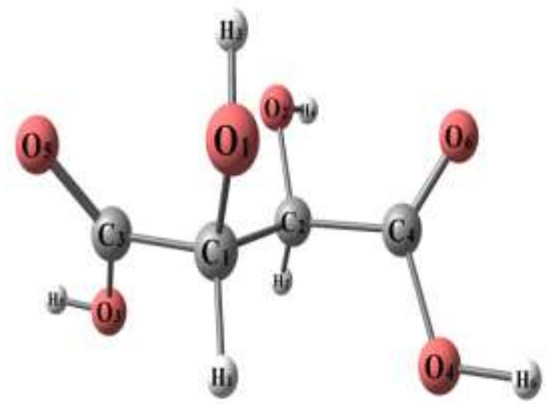

L6 Tartaric acid

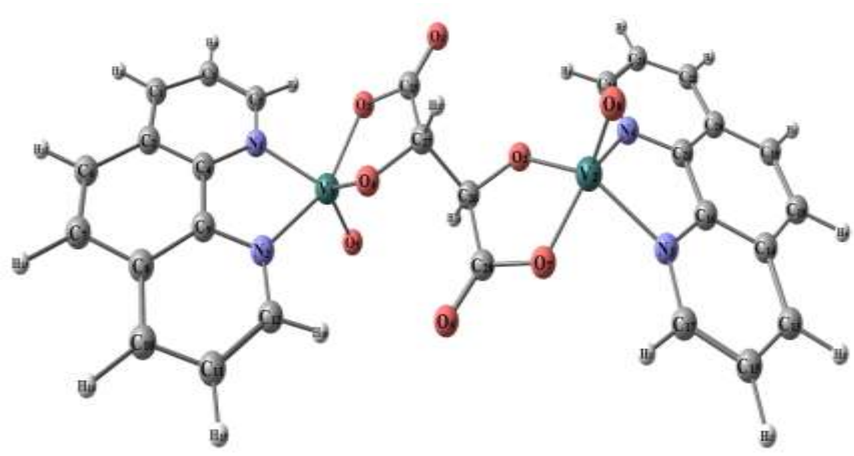

C5 [VO_2 (tart) $(phen)_2$]

Figure 3.63*Optimized structure of* ***C5****by density function theory B3LYP/LANL2DZ, ligands in upper and complex in lower.*

Table3.16 Calculated energies- Optimized Bond Lengths and angles of C5

Ligand	E^a	$HOMO^b$	$LUMO^c$	ΔE^d	Dipole moment[d]
Tartaric acid	-607.299	-0.2938	-0.0438	0.25	4.718
1,10 phenanthrolin	-571.488	-0.2310	-0.0654	0.1656	4.096
[VO(tart)(phen)]	-2041.393	-0.1347	-0.1171	0.0176	2.3268
Type of Angle	**Angle (°) C5**	**Type of angle**	**Angle(°)**	**Type of bond**	**Bond length(Å) C5**
N1-V1-N2	78.189	N3-V2-O7	89.202	V1 - O2	1.918
N1-V1-O2	89.344	N3-V2-O8	102.72	V1 - O4	1.827
N1-V1-O4	132.362	O3-V2-O7	81.949	V1 - O5	1.601
N1-V1-O5	115.141	N4-V2-O7	149.98	V1 - N1	2.095
N2-V1-O2	150.4	N4-V2-O8	98.476	V1 - N2	2.071
N2-V1-O4	86.432	N3-V2-O3	141.89	V2 - O3	1.822
N4-V2-O7	149.98	N3-V2-O7	89.202	V2 - O7	1.906
N4-V2-O8	98.476	N3-V2-O8	102.72	V2 - O8	1.603
N3-V2-O3	141.89	O3-V2-O7	81.949	V2 - N3	2.095
O7-V2-O8	111.39	O3-V2-O8	115.05	V2 - N4	2.093

3.3.6 The Molecular modeling of ligand L7, L2 and complex C6:

(Figure 3.64) shows the optimized structures of ligands L2, L7 and the complex (C6) as the most stable configurations. The vanadium atom is six-coordinate in a distorted octahedral geometry, the bond angles ranging from 70.12° to 150.1°, (Table 3.17).

The distance between donor atoms involved in coordination N1- - - - -N2 decreased upon complex formation from 2.735Å (in free ligand) to 2.674 Å (in the complex). The distance between N3- - - - -O3, N3- - - - -O1 are also decreased from 2.683 and 2.756Å (in free ligand) to 2.477 and 2.477Å (in the complex). The bond length of V=O1 is 1.592 Å shorter than those of V-O2 and V-O3, 2.063 and 2.063 Å, respectively.

The atoms N1, N2, o2 and O3 are almost in one plane deviated by 0.05°. The axial bond angles of N1-V-O2 and N2-V-O3, 150.1°and 150.1° were deviated from linearity due to coordination to vanadium. The bite angles N1-V-N2 , O2-V-N2 and N1-V-O3 are 75.10°, 78.19°, and 78.20 lower than 90° due to coordination, The bite angles of N3-V-N1 were also 123.1° more than 90° due to coordination.

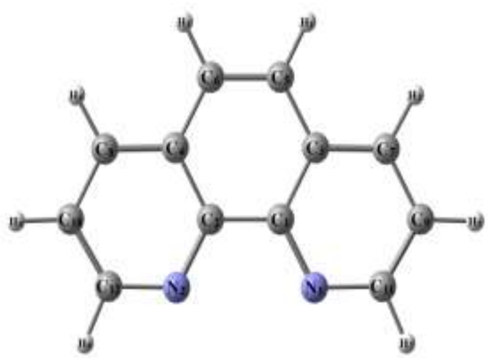

L2 1,10Phenanthorline

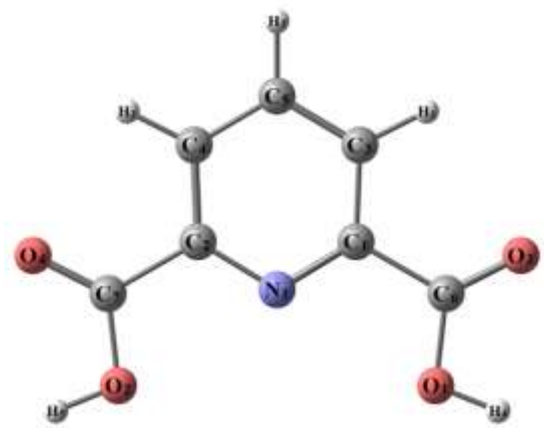

L7 2.6pyridine carboxylic acid

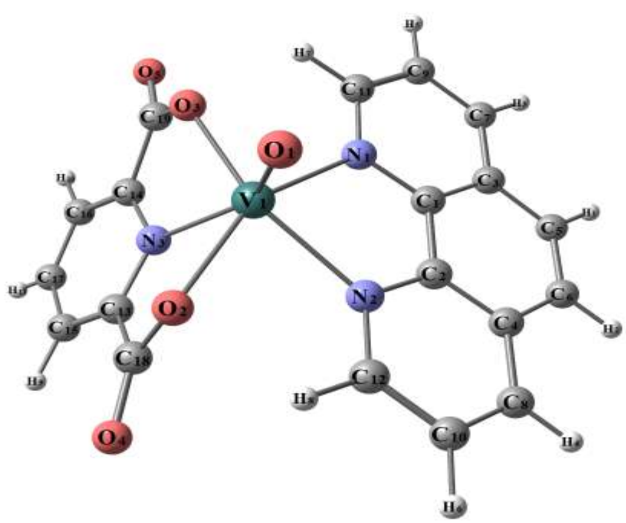

C6 [VO (2.6Pyr) (phen)]

Figure 3.64 *Optimized structure of **C6** by density function theory B3LYP/LANL2DZ, ligands in upper and complex in lower.*

***Table 3*.17** Calculated energies- Optimized Bond Lengths and angles of C6

Ligand	**E**[a]	**HOMO**[b]	**LUMO**[c]	**ΔE**[d]	**Dipole moment** [d]
2,6Pyridine	-625.311	-0.2729	-0.093	0.1798	1.346
1,10 phenanthroline	-571.488	-0.2310	-0.0654	0.1656	4.096
[VO(2,6Py)(1.10ph)]	-1342.395	-0.2489	-0.1170	0.1319	13.059

Type of Angle	**Angle (°)**	**Type of Angle**	**Angle (°)**	**Type of bond**	**Bond length(Å)**
	C6		**C6**		**C6**
O1-V-O2	101.221	O2-V-N3	70.142	V-O1	1.591
O1-V-O3	101.235	N1-V-O3	78.196	V-O2	2.062
O1-V-N1	148.978	N1-V-N2	75.070	V-O3	2.063
O1-V-N2	96.907	N1-V-N3	103.224	V-N1	2.194
O1-V-N3	96.797	N2-V-N3	103.288	V-N2	2.194
O2-V-O3	123.134	N2-V-O3	150.120	V-N3	2.241
O2-V-N1	150.070	O3-V-N3	70.129		
O2-V-N2	78.186				

3.3.7 The Molecular modeling of ligand L8, L2 and complex C7:

(Figure 3.65) shows the optimized structures of ligand (L2), (L8) and their complex (C7) as the most stable configurations. The vanadium atom is five-coordinate in a distorted square pyramidal geometry, the bond angles ranging from 76.54 to 145.2°, (Table 3.18)

The distance between donor atoms involved in coordination N1- - - - -N2 decreased upon complex formation from 2.735Å (in free ligand) to 2.659 Å (in the complex). The distance between O1- - - - -O2, is also decreased from 6.054 Å (in free ligand) to 2.781Å (in the complex). The bond length of V-O1, V-O2 are 1.892, 1.888 Å longer than V=O4 1.599 Å.

The atoms N1, N2, N3 and O1 are almost in one plane deviated by 0.35°. The axial bond angles of N1-V-O1, N2-V-O2 are 144.9° and 145.2° are deviated from linearity due to coordination to vanadium. The bite angle N1-V-N2 , O1-V-N2 and N2-V-O1 are 76.54°, 84.81°, and 84.65° lower than 90° due to coordination, and The bite angle O1-V-O2 of 94.73° is also more than 90° due to coordination.

L2 1,10 Phenanthorline

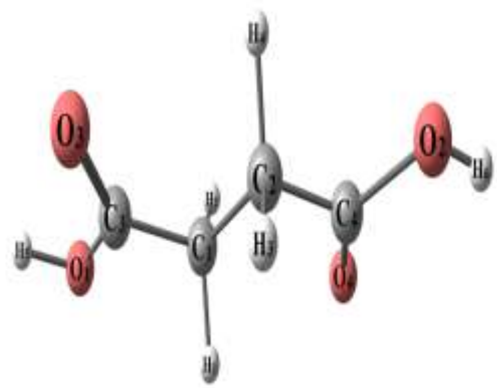

L8 Succanic acid

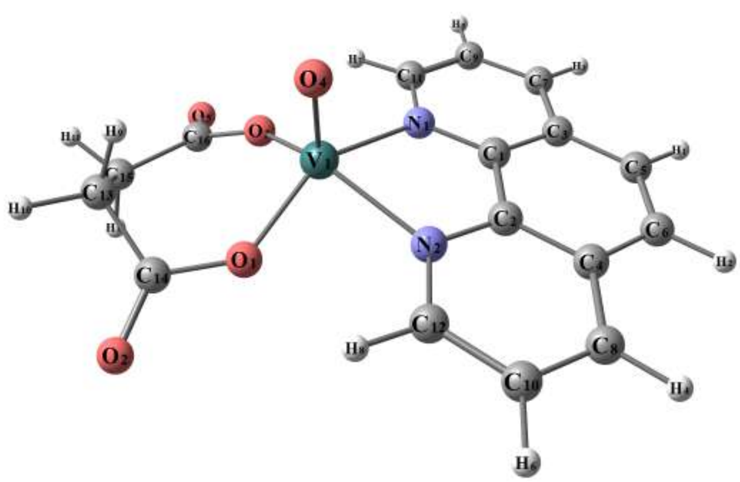

C7 [VO (succ) (phen)]

Figure 3.65 *Optimized structure of **C7** by density function theory B3LYP/LANL2DZ, ligands in upper and complex in lower.*

Table 3.18 Calculated energies, Optimized bond lengths and angles of C7

Ligand	E[a]	HOMO[b]	LUMO[c]	ΔE[d]	Dipole moment [d]
Succinic acide	-456.898	-0.2892	-0.0222	0.267	0.032
1,10 phenanthroline	-571.488	-0.2310	-0.0654	0.1656	4.096
[VO(succ)(phen)]	-1173.983	-0.2361	-0.1204	0.1157	13.880
Type of Angle	Angle (°)	Type of Angle	Angle (°)	Type of bond	Bond length(Å)
	C7		C7		C7
O1-V-O3	94.73	O3-V-N1	84.65	V-O1	1.891
O1-V-O4	110.2	O3-V-N2	145.2	V-O3	1.888
O1-V-N1	144.9	N1-V-O4	102.7	V-O4	1.599
O1-V-N2	84.88	N1-V-N2	76.54	V-N1	2.152
O3-V-O4	110.7	O4-V-N2	102.0	V-N2	2.141

3.3.8 The Molecular modeling of ligand L3, L9 and complex C8:

(Figure 3.66) shows the optimized structures of ligand (L3), (L9) and its complex (C8) as the most stable configurations. The vanadium atom is five-coordinate in a distorted square pyramidal geometry, the bond angles ranging from 79.41 to 152.6°, (Table 3.19).

The distance between donor atoms involved in coordination N2- - - - -O2 decreased upon complex formation from 3.626Å (in free ligand) to 2.611 Å (in the complex). The distance between N1- - - - -O1, is also decreased from 2.588Å (in free ligand) to 2.574Å (in the complex).The bond length of V-O1, V-O2, are 1.932, 1.905 Å longer than V=O4 1.599 Å.

The atoms N1, N2, N3 and O1 are almost in one plane deviated by 15.8°. The axial bond angles of N1-V-N2 and O1-V-O2, 152.6° and 127.5° is deviated from linearity due to coordination to vanadium. The bite angle N1-V-O1 , O2-V-N2 and

N2-V-O1 are 79.40°, 80.49°, and 86.08 lower than 90° due to coordination, and The bite angles of N1-V-O2 of 90.05°are also more than 90° due to coordination.

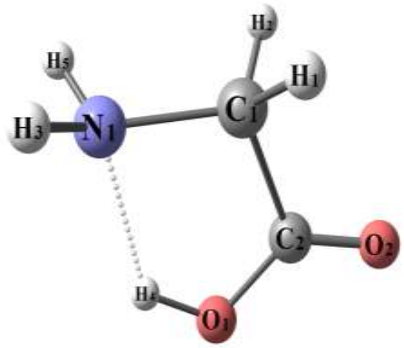

.

L3 Glycine

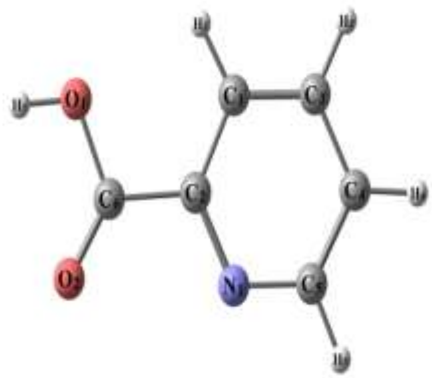

L9 2-Picolinic acid

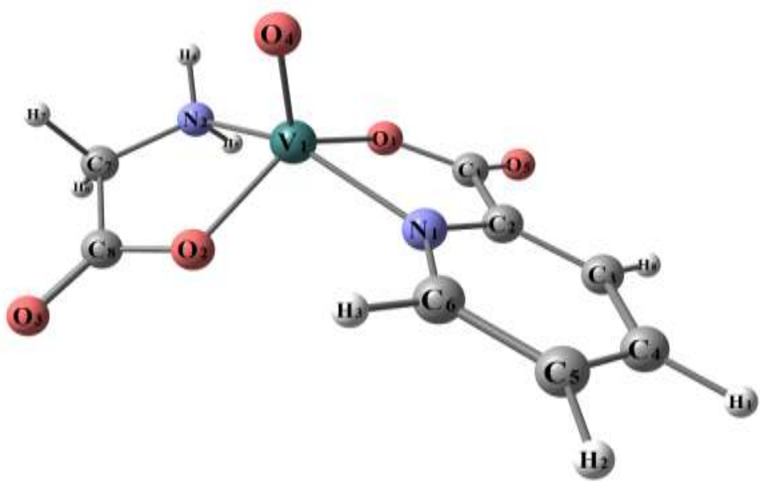

C8 [VO (2.pic) (gly)]

Figure 3.66 *Optimized structure of **C8** by density function theory B3LYP/LANL2DZ, ligands in upper and complex in lower.*

Table3.19 Calculated energies, Optimized bond lengths and angles of C8

Ligand	E[a]	HOMO[b]	LUMO[c]	ΔE[d]	Dipole moment [d]
2-Picolinic acid	-436.774	-0.2672	-0.0807	0.1865	4.456
Glycine	-284.382	-0.2405	-0.0206	0.2199	1.803
[VO (2.PA)(gly)]	-866.756	-0.2514	-0.1069	0.1445	2.227

	Angle (°)	Type of Angle	Angle (°)	Type of bond	Bond length(Å)
	C8		C8		C8
O1-V-O2	127.5	O2-V-N1	90.05	V - O1	1.932
O1-V-O4	117.2	O2-V-N2	80.49	V - O2	1.905
O1-V-N1	79.41	N1-V-O4	105.2	V - O4	1.599
O1-V-N2	86.08	N1-V-N2	152.6	V - N1	2.092
O2-V-O4	115.2	N2-V-O4	100.7	V - N2	2.128

3.3.9The Molecular modeling of ligand L2, L10 and complex C9:

(Figure 3. 67) shows the optimized structures of ligand (L2), (L9) and the complex (C9) as the most stable configurations. The vanadium atom is five-coordinate in a distorted square pyramidal geometry, the bond angles ranging from 79.21° to 162.3°, (Table 3.20)

The distance between donor atoms involved in coordination N1- - - - -S1 decreased upon complex formation from 3.125Å (in free ligand) to 2.942 Å (in the complex). The bond length of V=O1 is 1.586 Å.

The atoms N1, S1, N4 and N5 are almost in one plane deviated by 26.6°. The axial bond angles of N1-V-N5 and N4-V-S1, 162.3°and 125.4° is deviated from linearity due to coordination with vanadium. The bite angles N1-V-S1, S1-V-N5 and N5-V-N4 are 81.46, 86.81, and 79.21° lower than 90° due to coordination, and The bite angles N1-V-N4 of 96.86° are also more than 90° due to coordination.

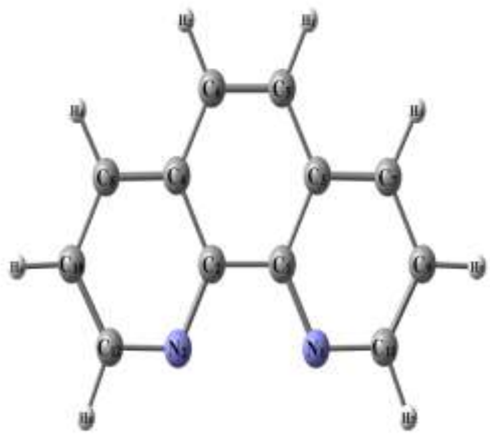

L2 1,10 Phenanthorline

L10 ChlorobenzaldehydeThioSemicarbazone

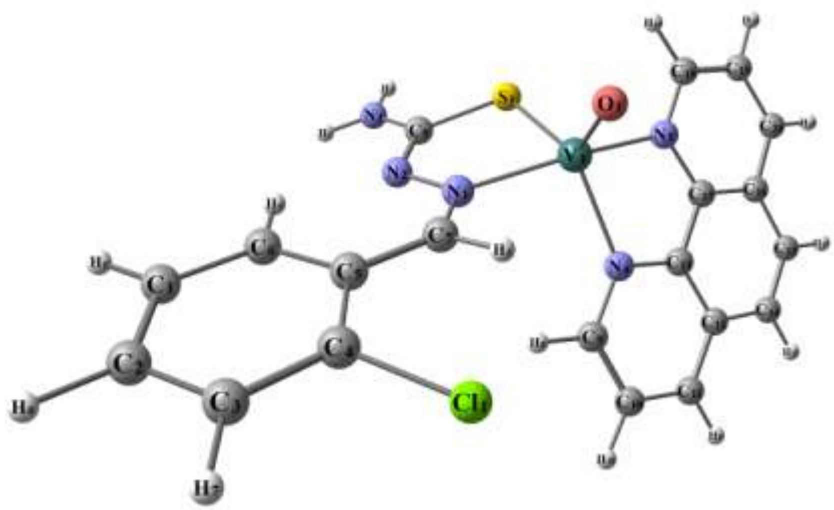

C9 [VO (ClBTSC) (phen)]

Figure 3.67 *Optimized structure of C9 by density function theory B3LYP/LANL2DZ, ligands in upper and complex in lower*

.

Table 3.20 Calculated energies, Optimized bond lengths and angles of C9

Ligand		E^a		$HOMO^b$	$LUMO^c$	ΔE^d	Dipole moment[d]
CLBTSC		-498.835		-0.2060	-0.0662	0.1398	7.9433
1,10 phenanthroline		-571.488		-0.2310	-0.0654	0.1656	4.096
[VO(ClBTSC)(1.10ph)]		-1216.323		-0.3263	-0.2239	0.1024	8.1945
Type of Angle	Angle (°) C9	Type of Angle	Angle (°) C9			Type of bond	Bond length(Å) C9
O1-V-S1	121.1	S1-V-N4	125.4			V - O1	1.610
O1-V-N1	99.29	S1-V-N5	86.81			V - S1	2.388
O1-V-N4	113.1	N1-V-N4	96.89			V - N1	2.109
O1-V-N5	98.11	N1-V-N5	162.3			V - N4	2.116
S1-V-N1	81.46	N4-V-N5	79.21			V - N5	2.105

3.3.10 The Molecular modeling of ligand L10, L11 and complex C10:

(Figure 3.68) shows the optimized structures of ligand (L10), (L11) and the complex (C10) as the most stable configurations. The vanadium atom is five-coordinate in a distorted square pyramidal geometry, the bond angles ranging from 80.53° to 160.0°, (Table 3.21).

The distance between donor atoms involved in coordination N1- - - - -S1 decreased upon complex formation from 3.125Å (in free ligand) to 2.984 Å (in the complex). The bond length of V-O3 is 1.854 Å longer than those of V=O2 1.598 Å.

The atoms N1, S1, O3 and N5 are almost in one plane deviated by 12.40°. The axial bond angles of N1-V-O3 and N5-V-S1, 138.0°and 160.0° is deviated from linearity due to coordination to vanadium. The bite angles N1-V-S1 , S1-V-O3 and N5-V-O3 are 80.35, 88.20, and 83.25° lower than 90° due to coordination, and The bite angles N1-V-N5 is 93.68° are also more than 90° due to coordination.

L10 Chlorobenzaldehyde ThioSemicarbazone

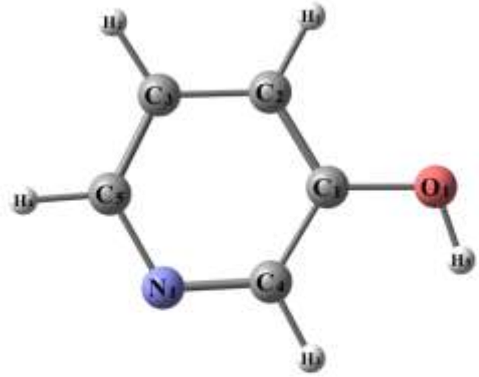

L11 3-Hydroxypyridine

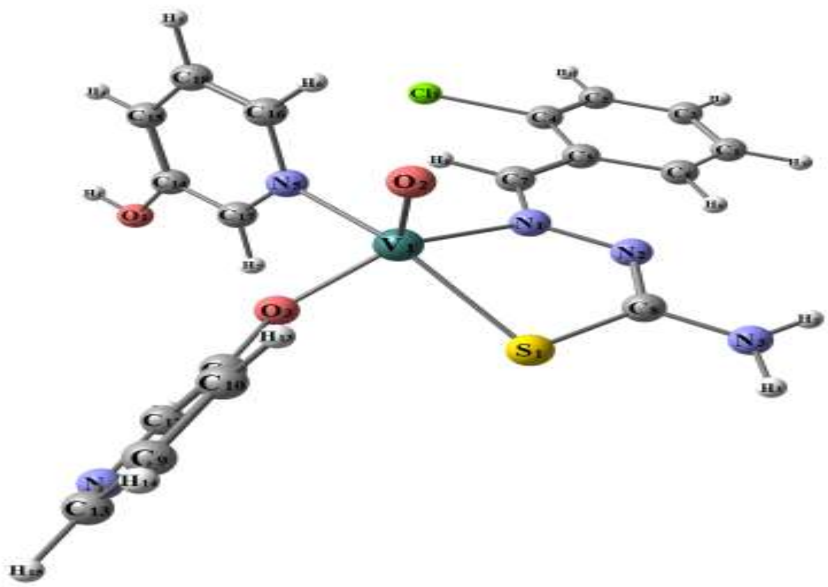

C10: [VO (ClBTSC)(3.HPy)$_2$]

Figure 3.68 *Optimized structure of **C10** by density function theory B3LYP/LANL2DZ, ligands in upper and complex in lower.*

Table3-21 Calculated energies, Optimized bond lengths and angles of C10

Ligand	E[a]	HOMO[b]	LUMO[c]	ΔE[d]	Dipole moment[d]
CLBTSC	-498.835	-0.2060	-0.0662	0.1398	7.9433
3-Hydroxypyridine	-323.446	-0.2517	-0.0388	0.2129	1.207
[VO(ClBTSC)(3.Hyp)]	-1291.322	-0.2042	-0.0926	0.1116	9.566

Type of Angle	Angle (°)	Type of Angle	Angle (°)	Type of bond	Bond length(Å)
	C10		C10		C10
O2-V-O3	116.700	S1-V-N1	80.354	V-O3	1.854
O2-V-N1	105.314	S1-V-N5	159.967	V-O2	1.598
O2-V-N5	95.248	N1-V-O3	137.981	V-N1	2.157
O2-V-S1	104.765	N1-V-N5	93.680	V-N5	2.149
S1-V-O3	88.202	O3-V-N5	83.517	V-S1	2.454

3.3.11 The Molecular modeling of ligand L11, L12 and complex C11:

(Figure 3.69) shows the optimized structures of ligand (L11), (L12) and the complex (C11) as the most stable configurations. The vanadium atom is five-coordinate in a distorted square pyramidal geometry, the bond angles ranging from 77.65° to 170.6°, (Table 3.22).

The distance between donor atoms involved in coordination N1- - - - -S1 decreased upon complex formation from 4.004 Å (in free ligand) to 2.997Å (in the complex). But the distance between N1- - - - -O1, is slightly increased from 2.636 (in free ligand) to 2.797Å (in the complex) this is probably due to the formation of hydrogen bonding between N1---HO1 in L12. The bond length of V-O1 is 1.917 Å longer than those of V=O3 and V=O4, 1.634, 1.620 Å.

The atoms N1, S1, O3 and O1are almost in one plane deviated by 1.99°. The axial bond angle of S1-V-O1 and N1-V-O3, 152.9°and 157.4° is deviated from linearity due to coordination to vanadium. The bite angles N1-V-S1and N1-V-O1 are 76.70 and 83.07, are also lower than 90° due to coordination.

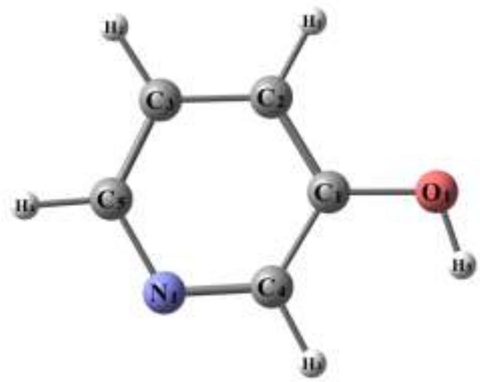

L11 3.Hydroxypyridine

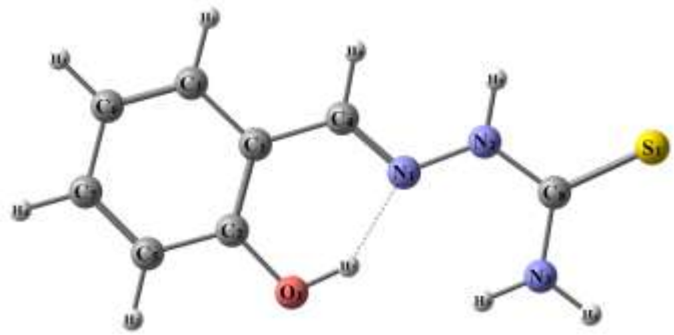

L12 Salicylsaldehydethiosemicarbazone

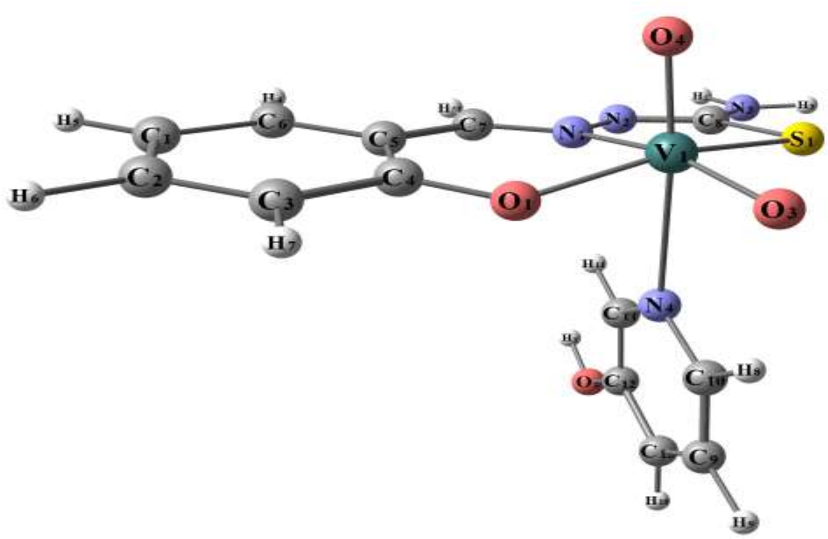

C11- [VO_2 (SALTSC) (3-Hpy)]

Figure 3.69 *Optimized structure of **C11** by density function theory B3LYP/LANL2DZ, ligands in upper and complex in lower.*

Table 3.22 Calculated energies *Optimized bond lengths and angles of C11*

Ligand	E[a]	HOMO[b]	LUMO[c]	ΔE[d]	Dipole moment[d]
3Hydroxypyridine	-323.446	-0.2517	-0.0388	0.2129	1.207
SALTSC	-559.761	-0.2176	-0.0833	0.1076	4.543
$[VO_2(SALTSC)(3.Hpy)]$	-1104.04	-0.0757	0.0570	0.133	9.719

Type of Angle	Angle (°)	Type of Angle	Angle (°)	Type of bond	Bond length(Å)
	C11		C11		C12
O1-V-O3	101.6	O3-V-N4	81.62	V-O1	1.917
O1-V-O4	101.5	O3-V-S1	90.87	V-O3	1.634
O1-V-N1	83.07	N1-V-O4	92.95	V-O4	1.620
O1-V-N4	78.45	N1-V-N4	77.65	V-N1	2.281
O1-V-S1	152.9	N1-V-S1	76.70	V-N4	2.646
O3-V-O4	107.5	N4-V-O4	170.6	V-S1	2.537
O3-V-N1	157.4	N4-V-S1	79.79		
S1-V-O4	97.34				

3.3.12The Molecular modeling of ligand L3, L13 and complex C12:

(Figure 3.70) shows the optimized structures of ligand (L3), (L13) and the complex (C12) as the most stable configurations. The vanadium atom is five-coordinate in a distorted trigonal bipyramidal geometry, the bond angles ranging from 75.48° to 155.1°, (Table 3.23).

The distance between donor atoms involved in coordination S1- - - - -N2 decreased upon complex formation from 3.919Å (in free ligand) to 2.930 Å (in the complex). The bond length of V-O1 is 1.938 Å longer than those of V=O2 and V=O4, 1.621 and 1.623 Å, respectively.

The atoms N1, O2, O4 and V are almost in one plane deviated by 5.38°. The axial bond angle of O1-V-S1, 155.1°, is deviated from linearity due to coordination to vanadium. The bite angles S1-V-N2 is 75.48° lower than 90° due to coordination.

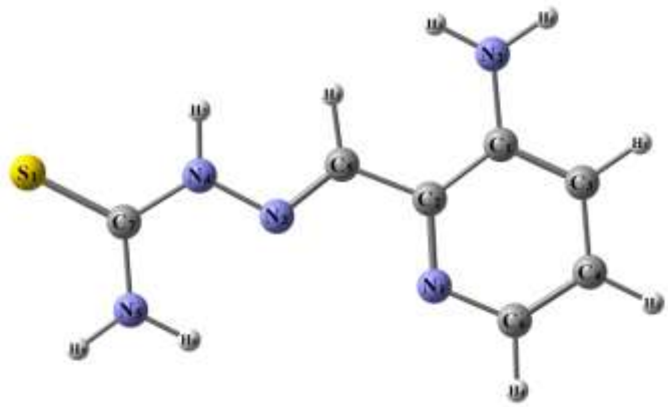

L13 3.Aminopyridinethiosemicarbazone

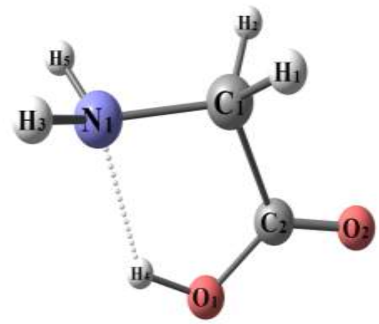

L3 Glycine

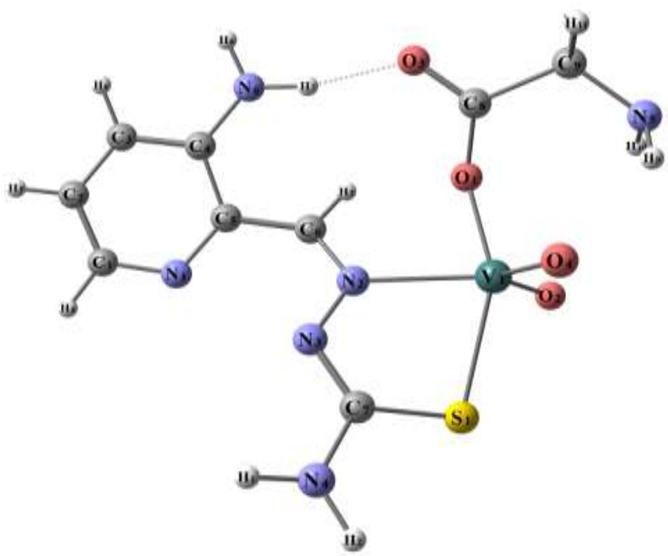

C12 [VO_2 (3-APTSC) (gly)]

Figure 3.70 *Optimized structure of* ***C****12 by density function theory B3LYP/LANL2DZ, ligands in upper and complex in lower.*

Table 3.23 Calculated energies, Optimized bond lengths and angles of C12

Ligand	E[a]	HOMO[b]	LUMO[c]	ΔE[d]	Dipole moment[d]
Glycine	-284.382	-0.2405	-0.0206	0.2199	1.803
3.APTSC	-555.900	-0.2075	-0.0743	0.1332	7.312
[VO(gly)(3.APTSC)]	-1061.145	-0.0921	0.0322	0.0599	9.3163

Type of Angle	Angle (°)	Type of Angle	Angle (°)	Type of bond	Bond length(Å)
	C12		C12		C12
O1-V-O2	99.14	O2-V-N2	136.1	V - O1	1.938
O1-V-O4	100.5	O2-V-S1	90.87	V - O2	1.621
O1-V-N2	81.58	S1-V-O4	97.54	V - O4	1.622
O1-V-S1	155.1	S1-V-N2	75.48	V - S1	2.515
O2-V-O4	109.4	N2-V-O4	97.54	V - N2	2.120

3.3.13The Molecular modeling of ligand L14 and complex C13:

(Figure 3.71) shows the optimized structures of ligand (L14) and its complex (C13) as the most stable configurations. The vanadium atom is five-coordinate in a distorted trigonal bipyramidal geometry, the bond angles ranging from 76.30° to 155.0°, (Table 3.24).

The distance between donor atoms involved in coordination N1- - - - -N2 decreased upon complex formation from 3.756Å (in free ligand) to 2.703 Å (in the complex) and the distance between N2- - - - -O1 is also decreased from 5.922Å (in free ligand) to 3.991 Å (in the complex). But the distance between and N1- - - - -O1 is slightly increased from 2.620 Å (in free ligand) to 2.697Å (in the complex) this is probably due to the formation of hydrogen bonding betweenN1---HO1 in L6, Figure 8. The hydroxyl atom in L6 is hydrogen bonded to the nitrogen atom.

The bond length of V-O1 is 1.886 Å longer than those of V=O2 and V=O3, 1.625 and 1.620 Å, respectively.

The atoms N1, O2, O3 and V are almost in one plane deviated by 11.95°. The axial bond angle of O1-V-N2, 154.9°, is deviated from linearity due to coordination to vanadium. The bite angles N1-V1-N2 and O1-V-N1 are 76.30 and 82.97° lower than 90° due to coordination.

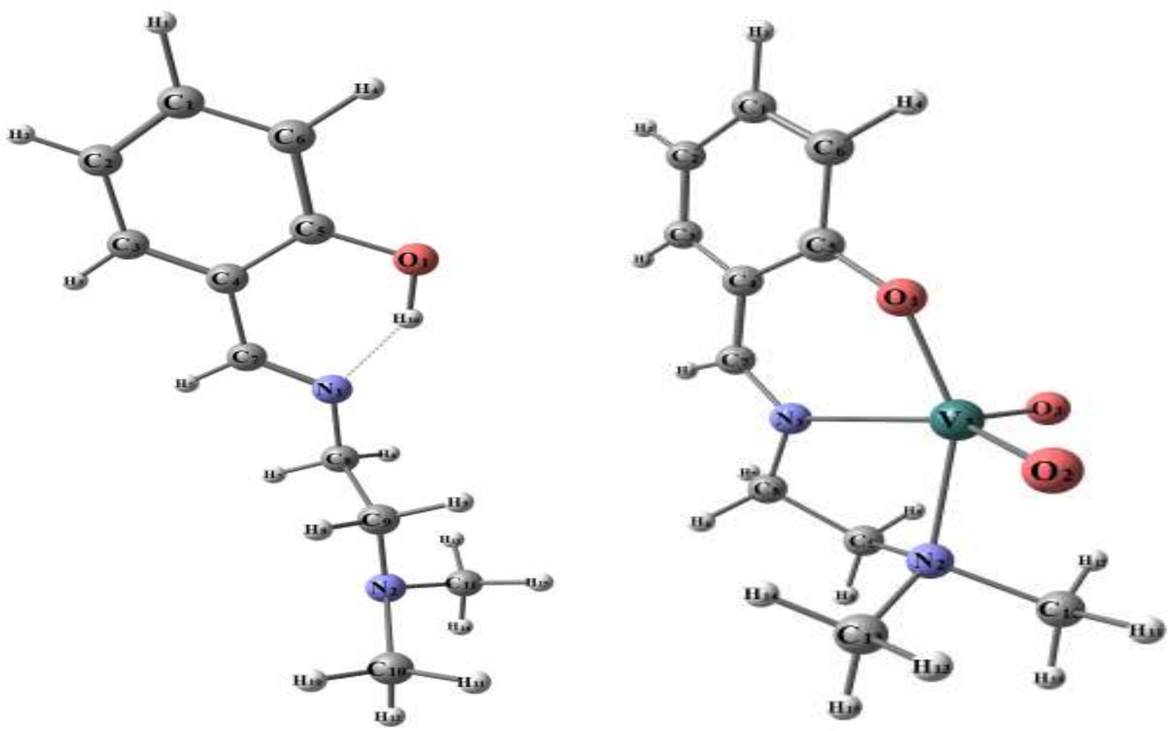

L14 sal-DMEDA   C13 [VO_2(Sal-DMEDA)]

Figure 3.71 *Optimized structure of ligand (L14, left) and complex (C13, right) by density function theory B3LYP/LANL2DZ.*

Table 3.24 Calculated energies, Optimized bond lengths and angles of C13

Ligand		E[a]	HOMO[b]	LUMO[c]	ΔE[d]	Dipole moment[d]
Sal-DMEDA		-613.418	-0.2062	-0.0582	0.148	2.768
[VO_2(Sal-DMEDA)]		-1447.649	-0.0799	0.0592	0.0207	11.4203
Type of Angle	**Angle (°) C13**	**Type of Angle**	**Angle (°) C13**	**Type of bond**	**Bond length(Å) C13**	
O1-V-O2	87.774	O2-V-N3	78.611	V-O1	2.081	
O1-V-O3	153.779	N1-V-O3	87.567	V-O2	1.921	
O1-V-O4	97.276	N1-V-O4	88.455	V-O3	1.630	
O1-V-N1	80.431	N1-V-N3	90.846	V-O4	1.620	
O1-V-N3	76.900	N3-V-O3	80.081	V-N1	2.220	
O2-V-O3	99.878	N3-V-O4	174.168	V-N3	2.519	
O2-V-O4	101.051	O3-V-O4	105.669			
O2-V-N1	165.739					

3.3.14The Molecular modeling of ligand L15 and complex C14:

(Figure 3.72) shows the optimized structures of ligand (L15) and its complex (C14) as the most stable configurations. The vanadium atom is five-coordinate in a distorted trigonal bipyramidal geometry, the bond angles ranging from 76.93° to 158.9°, (Table 3.25).

The distance between donor atoms involved in coordination N1- - - - -N2 decreased upon complex formation from 2.963 Å (in free ligand) to 2.683 Å (in the complex) but the distance between and N1- - - - -O1is slightly increased from 2.618 Å(in free ligand) to 2.676Å (in the complex), this is probably due to the formation of hydrogen bonding betweenN1---HO1 in L1, Figure 8. The two hydroxyl atoms in L1 are hydrogen bonded to the nitrogen atoms. The bond length of V-O1 is 1.900Å longer than those of V=O3 and V=O4, 1.616 and 1.627Å, respectively. The atoms N1, O3, O4and V are almost in one plane deviated by 9.26°. The axial bond angle of O1-V-N2, 158.9°, is deviated from linearity due to coordination to vanadium. The bite angles N1-V1-N2 and O1-V-N1are 76.94 and82.60° lower than 90° due to coordination.

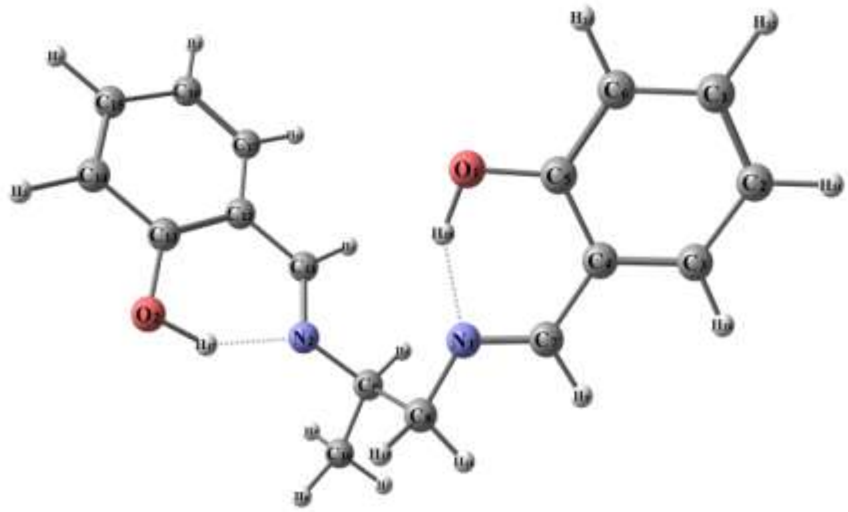

L15 Sal-DAP

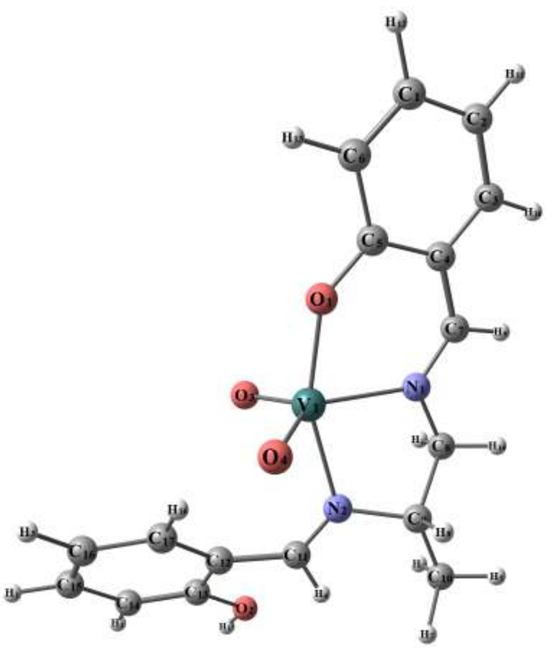

C14 [VO_2 (Sal-DAP)]

Figure 3.72 *Optimized structure of L15 (upper) and its complexC14 (lower) by density function theory B3LYP/LANL2DZ.*

Table3.25 Calculated energies, Optimized bond lengths and angles of C14

Ligand		E^a		$HOMO^b$	$LUMO^c$	ΔE^d	Dipole moment[d]
Sal –DAP		-918.463		-0.2210	-0.0614	0.1596	7.943
$[VO_2$(Sal- DAP)]		-1139.249		-0.0854	0.0549	0.1403	9.6982
Type of Angle	Angle (°)	Type of Angle	Angle (°)		Type of	Bond length(Å)	
	C14		C14		bond	C14	
O1-V-O2	169.155	O2-V-N2	72.691		V-O1	2.032	
O1-V-O3	93.284	N1-V-O3	94.492		V-O2	2.017	
O1-V-O4	92.131	N1-V-O4	152.947		V-O3	1.623	
O1-V-N1	73.677	N1-V-N2	68.133		V-O4	1.624	
O1-V-N2	98.251	N2-V-O3	155.177		V-N1	2.356	
O2-V-O3	92.981	N2-V-O4	92.082		V-N2	2.428	
O2-V-O4	94.109	O3-V-O4	109.502				
O2-V-N1	97.010						

3.3.15 The Molecular modeling of ligand L16 and complex C15:

(Figure 3.73) shows the optimized structures of ligand (L16) and its complex (C15) as the most stable configurations. The vanadium atom is five-coordinate in distorted trigonal bipyramidal geometry, the bond angles ranging from 74.58 to 157.3°, (Table 3.26).

The distance between donor atoms involved in coordination N1- - - - -N2 decreased upon complex formation from 3.677Å (in free ligand) to 2.597 Å (in the complex) and the distance between N1- - - - -O1 , N2- - - - -O1 are also decreased from 7.099 and 4.219Å (in free ligand) to 3.952 and 2.685 Å (in the complex).The bond length of V-O1 is 1.895 Å longer than those of V=O2 and V=O3, 1.619 and 1.623 Å, respectively.

The atoms N1, O2, O3 and V are almost in one plane deviated by 11.85°. The axial bond angle of O1-V-N1, 157.3°, is deviated from linearity due to coordination to vanadium. The bite angles N1-V1-N2 and O1-V-N2 are 74.58 and 82.84° lower than 90° due to coordination.

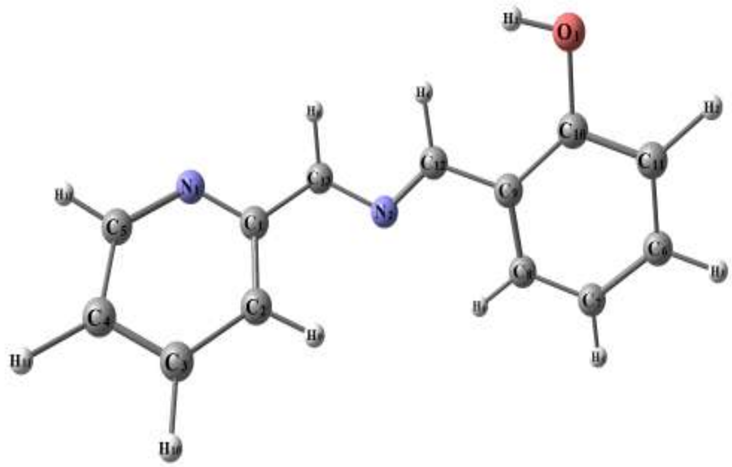

L16 Sal-PA

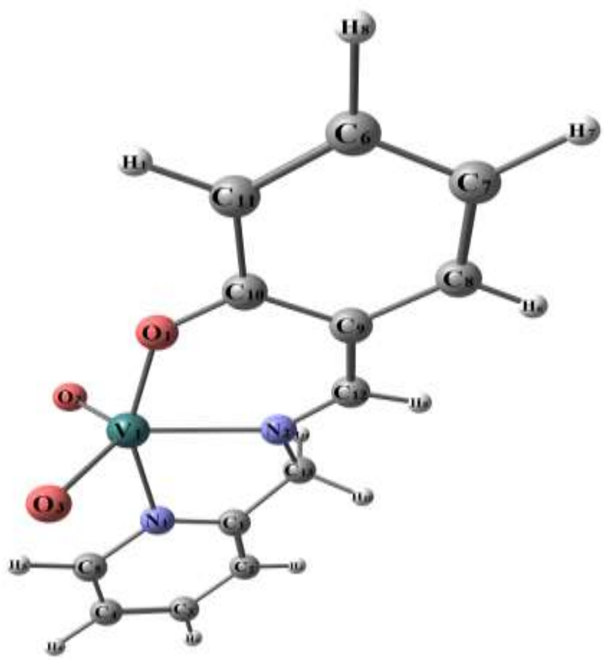

C15 [VO_2 (Sal-2PA)]

Figure 3.73 *Optimized structure of L16 (upper) and its complex C15 (lower) by density function theory B3LYP/LANL2DZ*

Table 3.26 Calculated energies, Optimized bond lengths and angles of C15

Ligand	**E[a]**	**HOMO[b]**	**LUMO[c]**	**ΔE[d]**	**Dipole moment[d]**
SAL-2-Pic	-687.198	-0.2363	-0.0628	0.1735	1.533
$[VO_2(Sal\text{-}2PA)]$	-908.582	-0.2205	-0.0880	0.1325	9.6808
Type of Angle	**Angle (°)**	**Type of Angle**	**Angle (°)**	**Type of**	**Bond length(Å)**
	C15		**C15**	**bond**	**C15**
O1-V-O2	104.100	O2-V-N1	89.770	V-O1	1.895
O1-V-O3	102.709	O2-V-N2	121.329	V-O2	1.614
O1-V-N1	157.311	N1-V-O3	88.595	V-O3	1.622
O1-V-N2	82.844	N1-V-N2	74.575	V-N1	2.135
O2-V-O3	110.742	N2-V-O3	124.547	V-N2	2.151

3.4Biological studies

3.4.1 Animals

80 Female Wistar rats (8 weeks, 180–250g), were kept in climate-controlled room in the animal house of National Research Centre at air conditioned room a maintained temperature and relative humidity (25 ± 5^{0}C- 35– 60%) respectively with12 h light- dark cycle, The rats were fed with pellet diet and water.

Diabetes mellitus (type 2 diabetes) was induced by intraperitoneal (i.p.) single dose of streptozotocin (STZ) in overnight fasted animals. STZ was freshly prepared (40 mg/Kg body weight) dissolved in 0.1M citrate buffer (pH 4.5) immediately before use. (Emerick, et al, 2005) (Milani , et al, 2005) (Punithavathi , et al, 2008) After injection, animals had free access to food and water and were given 5% glucose solution to drink overnight to counter hypoglycemic shock (Bhandari, 2005). After 48hrs, body weights as well as blood glucose concentrations of the STZ-injected rats were measured. The samples were taken from the tail vein after

8hrs fasting conditions. Hyperglycemia was achieved by high glucose level in plasma using a digital glucometer (One Touch Ultra). Rats with blood glucose concentrations greater than 300 mg/dl were considered to be diabetic. Also, blood glucose level and body weights of the rats were measured by the same method every week during the period of experiment (4Week).

These diabetic rats were further grouped (n = 5) and were treated with test/standards for Forth weeks according to the following protocol:

g nc	*healthy rats as normal control (-)*
g dc	*diabetic control (+)*
g in	*diabetic+ insulin*
g or	*diabetic + oral administration* (*Glibenclmide)*
gC1	*diabetic+ [VO (Cys)(Phen)]*
gC2	*diabetic + [VO (2.6Py) (phen)]*
gC3	*diabetic +[VO (ClBTSC) (3-HPy)$_2$]*
gC4	*diabetic+ [VO$_2$ (SAL-DMEN)]*

Complexes were prepared and the dose of test compounds was based on earlier studies on dose optimization 2mg/kg/day. (Itzhak, et al, 2000) STZ rats received daily intra peritoneal administrations of complexes at a dose of 2 mg vanadium/kg body, the blood glucose concentrations and body weights of the rats were measured every week before injection showing in (Fig3.75). For the combined group of all animals tested, hypoglycemic effects were observed on the first week after the complex administration (Fig3.75).

Figure 3.74 Intra peritoneal injection and oral administration on Rats

4.2 Statistical Analysis

Data were analyzed by comparing values for different treatment groups with the values for individual control. All data were expressed as mean ± standard error for 5 rats in each group. Significant differences between the groups were statistically analyzed using one– way analysis of variance, ANOVA using the spss16 computer program. Differences were considered significant at $p \leq 0.05$.

Table3.27: Effect of new vanadium complexes on blood glucose level of STZ – diabetic rats

	Blood glucose level (mg/dl) (Mean ± S.E.M)				
Groups	***After Induction***	***1st Week***	***2nd Week***	***3rd Week***	***4th Week***
g nc	93.6 ± 2.5^{abc}	99.8 ± 1.8^{abc}	98.6 ± 3.6^{abc}	103.0 ± 2.7^{abc}	95.4 ± 1.9^{abc}
g dc	$595.8 \pm 2.8^{*}$	$590.2 \pm 3.6^{*bc}$	$593.0 \pm 1.9^{*bc}$	$589.0 \pm 1.4^{*bc}$	$588.0 \pm 2.0^{*bc}$
Gin	$588.6 \pm 3.9^{*}$	$444.4 \pm 7.7^{*ac}$	$354.2 \pm 6.6^{*ac}$	$289.8 \pm 4.0^{*a}$	$122.8 \pm 8.3^{*a}$
g or	$589.0 \pm 6.1^{*}$	$497.4 \pm 7.4^{*ab}$	$421.8 \pm 7.4^{*ab}$	$302.4 \pm 4.3^{*a}$	$121.2 \pm 7.7^{*a}$
g C1	$593.4 \pm 4.0^{*}$	$479.8 \pm 7.5^{*ab}$	$345.0 \pm 6.1^{*ac}$	$256.4 \pm 5.0^{*ab}$	$122.4 \pm 5.9^{*a}$
g C6	$591.0 \pm 5.8^{*}$	$473.4 \pm 7.9^{*abc}$	$289.0 \pm 6.0^{*abc}$	$187.8 \pm 7.5^{*abc}$	98.8 ± 4.7^{abc}
g C10	$509.2 \pm 4.0^{*abc}$	$391.0 \pm 5.1^{*abc}$	$295.8 \pm 6.9^{*abc}$	$149.4 \pm 4.4^{*abc}$	93.8 ± 1.9^{abc}
g C13	$551.8 \pm 1.3^{*abc}$	$362.2 \pm 6.0^{*abc}$	$247.0 \pm 7.6^{*abc}$	$176.4 \pm 6.7^{*abc}$	107.0 ± 3.1^{ab}

Data are expressed as mean ±SE 5 rats in each group, * is the level of significance at P≤0.05 compared with control group, [a] is the level of significance at P≤0.05 compared with diabetic group, [b] is the level of significance at P≤0.05 compared with insulin group, [c] is the level of significance at P≤0.05 compared with oral drug group.

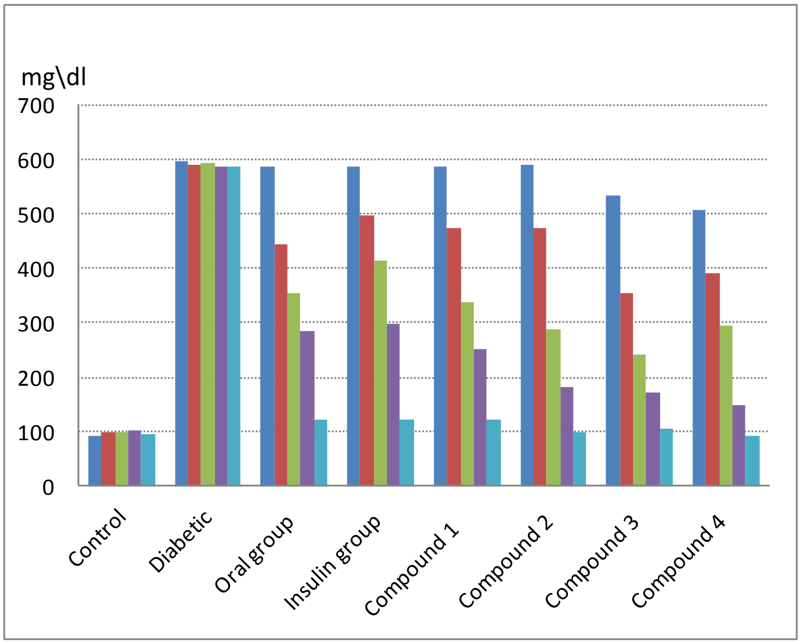

Fig.3.75 B*lood glucose concentration plotted against time*

Chapter Four

4. Discussion and conclusion

4.1 Discussion

The molar conductivities values of the oxovanadium (IV) and dioxovanadium (V) complexes were measured in DMF solution C1─ C15 lie in the range of 18-30 $mScm^2mol^{-1}$ which indicates its non-electrolytic nature while the molar conductivity of C9, C11, C12 lie in the range of 35-64 $mScm^2mol^{-1}$ which indicates univalent electrolytic nature of these complexes the values are given in (Table3-3).

Magnetic moments of oxovanadium (IV) and dioxovanadium (V) complexes were measured at room temperature and the values are given in (Table 3-4), Magnetic studies showed that all the complexes of oxovanadium (IV) C1- C10 are paramagnetic in the range 1.3 -1.77 B.M., which correspond to a single electron of the d^1 -system of square-bipyramidal and octahedral oxovanadium (IV) center. And all the dioxovanadium (V) complexes C11- C15 are diamagnetic in the range 0.3 - 0 B.M as expected for d^0- system of trigonl bipyramidal and octahedral dioxovanadium (V) center.

The electronic spectra of metal complexes in $c = 1.0\times10^{-3}$mol dm^{-3} were recorded in the UV-visible region C1─ C15 from (Table 3.5) to (Table 3.7) showed two high energy absorption bands in the region 255-270 nm **$(\lambda)_{max}$**. Many absorptions appear as unresolved bands resulting from the intra ligand transitions $\pi \rightarrow \pi^*$ and $n \rightarrow \pi^*$ (Figures from 3.1 to 3.15).

To study the binding mode of the ligand to vanadium in the new complexes, IR spectra of the free ligands were compared with the spectra of the vanadium complexes (Figures from 3-16 to 3-30). Selected IR data for complexes (C1- C15) and their free ligands (L1-L16) were given in (Tables 3.8) (Tables 3.9).

For the free ligands L1-L2-L3-L4-L5, characteristic stretching vibration bands appear at 1537cm^{-1} corresponding to the C=N vibration L2. A strong band is observed in the free ligand L1 at 898 cm^{-1} Characteristic of the C=S vibration, 3427cm^{-1}, 3381cm^{-1}, 3425cm^{-1} and 3415cm^{-1} Characteristic of the ν(O─H) vibration, and 3166 cm^{-1}, 3035cm^{-1}, 3206 cm^{-1} and 3411cm^{-1} characteristic of the stretching ν(N─H2) of the free ligands L1-L3-L4-L5 respectively. In the spectra of new complexes C1- C2 - C3 - C4, the band due to ν(C=N) showed a positive shift to 1588cm^{-1},1604cm^{-1},1588cm^{-1},1592cm^{-1}, indicating coordination of the nitrogen to vanadium.ν(O–H) vibration was absent in the complexes indicating deprotonation to coordination .The band due to ν(N–H2) showed a positive shift to 3388cm^{-1}, 3338cm^{-1}, 3328cm^{-1}, 3426cm^{-1}, indicating coordination also of the nitrogen to vanadium. In addition, the complexes exhibit the characteristic ν(V=O) bands at 975 cm^{-1} , 972 cm^{-1}, 851 cm^{-1}966 cm^{-1}, and ν(V–O) bands at 602 cm^{-1}, 682 cm^{-1} , 686 cm^{-1} , 613 cm^{-1}and ν(V–N) bands at 541 cm^{-1} , 548 cm^{-1}, 541 cm^{-1}550 cm^{-1} for complex C 1 ,C2,C3,C4 respectively , and ν(V–S) bands at 732 cm^{-1} for C1.

For the free ligands L2-L3-L6-L7-L8-L9, characteristic stretching vibration bands appear at 1537cm^{-1} ,1567cm^{-1},1574cm^{-1} corresponding to the C=N vibration of L2-L7-L9 respectively. A strong band is observed in the free ligand L3-L6-L7-L8-L9 at 3381cm^{-1}, 3361cm^{-1}, 3411cm^{-1}, 3485cm^{-1}, 3438cm^{-1} respectively characteristic of the (O–H) vibration. The characteristic stretching vibration bands appear at 3035cm^{-1} corresponding to the (N–H_2) vibration L3. In the spectra of new complexes C5- C6 - C7- C8, the band due to ν(C=N) showed a positive shift to 1588cm^{-1}, 1578cm^{-1}, 1588cm^{-1} and 1583cm^{-1} indicating coordination of the nitrogen to vanadium, ν(O–H) vibration was absent in the complexes indicating deprotonation to coordination. The band due to $\nu(N–H_2)$ showed a positive shift to 3421cm^{-1}, indicating coordination of the nitrogen to vanadium C8.In addition, the complexes exhibit the characteristic ν(V=O) bands at 962cm^{-1} , 918cm^{-1}, 969cm^{-1} and 953cm^{-1}, ν(V–O) bands at 652 cm^{-1},686 cm^{-1} ,643 cm^{-1} and 626 cm^{-1}, ν(V–N) bands at 548 cm^{-1} 568 cm^{-1}, 560 cm^{-1}and 517 cm^{-1}for C5-C6-C7-C8 respectively.

For the free ligands L3-L10-L11-L12-L13, characteristic stretching vibration bands appear at 1537cm^{-1} corresponding to the C=N vibration L2. A strong band is observed in the free ligands L10-L12-L13 at 864cm^{-1} 888cm^{-1} 884cm^{-1} Characteristic of the C=S vibration, 3381, 2910cm^{-1},3428cm^{-1}Characteristic of the ν(O–H) vibration of L3- L11-L12. In the spectra of new complexes C9-C10-C11-C12 the bands due to C–S vibration showed a negative shift, 726cm^{-1}, 723cm^{-1}, 753cm^{-1}, 709 cm^{-1}. ν(C=N) showed a positive shift to1584cm^{-1}, indicating coordination of the nitrogen to vanadium of C9. In addition, the complexes exhibit the characteristic ν(V=O) bands at 975 cm^{-1} 968 cm^{-1}, 891-945cm^{-1} and 956-869cm^{-1} of C9-C10-C11-C12, ν(V–O) bands at 674cm^{-1}, 602 cm^{-1}, 692cm^{-1}, of C10-C11-C12, and ν(V–N) bands at 541cm^{-1}, 505cm^{-1}, 538cm^{-1}, 507cm^{-1}, for complex C9-C10-C11-C12 respectively.

The free ligands L14-L15-L16 characteristic stretching vibration bands appear at 1588cm^{-1}, 1581 cm^{-1}, 1594 cm^{-1}, corresponding to the C=N vibration, and 3432cm^{-1}, 3068cm^{-1} and 3310cm^{-1} characteristic of the ν(O–H) vibration respectively. In the spectra of new complexes C13- C14 – C15 the band due to ν(C=N) showed a positive shift to1601cm^{-1},1604cm^{-1} and 1625cm^{-1} indicating coordination of the nitrogen to vanadium, and ν(O–H) vibration was absent in the complexes indicating deprotonation to coordination .

The complexes exhibit the characteristic ν(V=O) bands at 908- 958cm^{-1}, 884-925cm^{-1}, 844-1012cm^{-1}, and ν(V–O) bands at 618cm^{-1},618 cm^{-1} 602cm^{-1}, and ν(V–N) bands at 528 cm^{-1} , 544 cm^{-1}, 544 cm^{-1} for complex C 13 , C14, C15 respectively.

The ^{1}H and ^{13}C NMR data summarized in(Table 3.10) (Figures from 3.31 to 3. 44) confirm the complex formation and the coordination mode of the free ligands (L1-L13) and Schiff-base ligands (L14-L16). In particular the deprotonation of the hydroxyl, phenolate groups and the coordination of amino group is confirmed by the absence or exhibit of their characteristic resonances in the ^{1}H NMR spectra of the complexes (C1- C15).

The percent losses in mass and thermal effects accompanying the changes in the solid complex on heating are shown in (Table 3-11) As shown in the curves (figures 3-46 and 3-47) there is mass lose in 95 – 100 C^{0} which confirm the elemental analysis data that water of crystallization in the complex C2 and C3 and as shown in the curve (Figure 3-45 and Figures from 3-48 to 3-58) there is no mass lose below 180 C^{0} which confirm the elemental analysis data that no water of crystallization in the complexes C1, C4- C15.

The TGA curve showed many steps .The first step shows the loss of ligands and the residue of range (16%-33%) corresponding to VO_2, $NaVO_3$ and V_2O_5.

The density functional theory was applied to calculate the optimized geometries using the Gaussian09 program 114. Full geometry optimization was performed using B3LYP/6-31G (p, d) as a basis set to generate the optimized structure for the ligand and using B3LYP/LANL2DZ for the complex.

(Figures from 3.59 to 3.73) showed the optimized structures of ligands (L1- L16), and their complexes (C1- C15) as the most stable configurations. The vanadium atom is five-coordinate in a distorted square pyramidal geometry, trigonal bipyramidal geometry, and six-coordinate in a distorted octahedral geometry.

The computed total energies, the highest occupied molecular orbital (HOMO) energies, the lowest unoccupied molecular orbital (LUMO) energies and the dipole moment for the ligands (L1-L16), and their complexes (C1-C15) were calculated, (Table from 3.12 to 3.26) shows The more negative value of total energy of the complexes than that of free ligands indicates the extra stabilities of the complexes than the free ligands and the polarities of the complexes are much larger than the free ligands.

Streptozotocin STZ induced diabetes produced marked increase in blood glucose level. the diabetic rats blood glucose level as compared to control and after treatment insulin injection, oral anti diabetic with complexes C1, C6, C10 and C13 showed an anti-hyperglycemic effect and there was significant decrease in blood glucose level ($P<0.05$). (Table 3-27 to Table 3-31).

4.2 Conclusion

Oxovanadium complexes and dioxovanadium complexes were preperd as insulin mimics.The synthesis of the complexes with verified ligands such as 1,10 phenanthorolin ,amino acids thiosemicarbazied carboxylic acid and Schiff-base .The structures of the synthesized compounds were elucidated on the bases of physiochemical and spectroscopic data (IR. ^{1}H and ^{13}C N.M.R, UV-VIS and TGA).

The molecular structure of the complexes was confirmed using the DFT calculation to obtain the optimized geometries using the Gaussian09 program at the B3LYP/LANL2DZ level.

In this study intra peritoneal administration of active anti-diabetic organic vanadium complexes were synthesized, C1, C6, C10, C13 has been further tested on streptozotocin-treated rats, a type 2-like diabetic animal model.

The results showed that 4 weeks of complexes treatment significantly improved hyperglycemia. The complexes had anti-diabetic and insulin-sensitizing effects in the diabetic rats, exhibiting the potential to be developed as a new therapeutic agent for the treatment of type-2 diabetes.

Recommendation for farther work

From the data obtained, we suggest: (1) to couple the vanadium cation with phosphorus.

(2) to complex the synthesis ligand with the cation such as Zn, Ni, and Co.

References

Atkins, P.W. & Shriver, D.F. (1999). *Inorganic chemistry,* 4th ed Oxford University: Oxford.

Berry, R. E., Armstrong, E. M., Beddoes, R., Collison, D., Ertok, S., Nigar,H., Madeleine,G., & David, C. (1999) The *structural characterization of amavadin,* Angewandte Chemie, International Edition, 38(6), pp. 795–797.

Bhandari ,U., Kanojia , R . & Pillai, K.K. (2005) *Effect of ethanolic extract of Zingiber officinale on dyslipidaemia in diabetic rats*. J. Ethnopharmacol., 97, 227-230.

Blanke, S. R., Yi, S. & Hager, L. P. (1989). *Development of Semi Continuous and Continuous Flow Bioreaci'ors for The High Level Production Of Chloroperoxidase,* Biotechnology, Vol 11, pp. 769–770.

Boer, E, Kooyk, Y, Kooyk, Y, Tromp, M, Plat, H, & Wever, *R* (1986) *Bromoperoxidase from Ascophyllum nodosum: a novel class of enzymes containing vanadium as a prosthetic group?,* Biochimica et Biophvsica Acta 869, pp. 48–53.

Boer, E., Tromp, M., Plat, H., Krenn, G., & Wever, R. (1986) *Vanadium(V) as an essential element for haloperoxidase activity in marine brown algae: purification and characterization of a vanadium(V)-containing bromoperoxidase from Laminaria saccharina*, Biochimica et Biophysica Acta 872, pp. 104–115.

Boca Raton, CRC press, FL, (1989), *Chemistry, and Physics*, Handbook, 70th
Edition, p. D-221.

Bryman, Alan; Cramer, Duncan (2011). *Quantitative Data Analysis with IBM SPSS 17, 18 and 19:* A Guide for Social Scientists. New York

Butler, A. (1998) *Acquisition and Utilization of Transition Metal Ions by Marine*

Organisms, Chemistry and Biology of the Oceans, 281(July), pp. 207–210.

Butler, A., and J. Carrano, C. (1991) *Coordination chemistry of vanadium in biological systems*, Coordination Chemistry Reviews, 109(1), pp. 61–105.

Cotton, F.A., Wilkinson, G., Bochmann, M., & Murillo, C. (1998) *Advanced inorganic chemistry*, 6th edn, Wiley, New York, pp.714-737

Crans, D. C., Smee, Jason J., Gaidamauskas, E., & Yang, L. (2004) .*The Chemistry and Biochemistry of Vanadium and the Biological Activities Exerted by Vanadium Compounds*', *Chemical Reviews*, 104(2), pp. 849–902.

Crichton, R. R. (2008) *Biological Inorganic Chemistry*, 1st edn Elsevier, pp. 291-294 UK.

Dalton, J. C., Bonamico, B. M., Dessy, G., Fares, V., Scaramuzza, L., & Elettronica, S. (1972) *Structural Studies of Eight-co-ordinate Metal Complexes. Part 1. Crystal and Molecular Structures of Tetrakis(pheny1dithioacetato)vanad- ium(iv) and Tetrakis(dithiobenzoato)vanadium(iv),* J.C.S Dalton, 33(1258), pp. 1258–1263.

Dobson, J. C., & Taube, H. (1989*) Coordination Chemistry and Redox Properties of Polypyridyl Complexes of Vanadium (II),* Inorganic Chemistry, Vol. 28, No. 7(2), pp. 1310–1315.

Drew, R.E., & Einstein, F.W. (1972) *The Crystal Structure of Ammonium Oxodiperoxoamminevanadate (V),* Inorganic Chemistry., Vol. 11(5), pp. 1079–1083.

Emerick, A.J., Richards, M.P., Kartje, G. L., Neasfsey, E. J & Stubbs, E.B.J.r (2005) *Expermintal diabetes attenuates cerebral cortical – evoked forelimb motor responses* .Diabetes, 54, 2764- 2771

Elvingson, K., Baró, G., & Pettersson, L. (1996) *Speciation in Vanadium Bioinorganic Systems. 2. An NMR, ESR, and Potentiometric Study of the Aqueous H+-Vanadate-Maltol System*, Inorg. Chem., 35(8), pp. 3388–3393.

Figgis, B.N., Lewis, J. In Lewis, J., & Wilkins, R. (1960) *Modern Coordination Chemistry*, Interscience Publishers Inc.: New York, 1960, pp. 400-454

Gengenbach, A. (1996) *Spectroscopic and Functional Modeling Studies of Vanadium Bromoperoxidase,* Litersture Seminar (lys m), pp. 3–6.

Goldwaser, I., Gefel, D., Gershonov, E., Fridkin, M., & Shechter, Y. (2000) *Insulin-like effects of vanadium: Basic and clinical implications*, Journal of Inorganic Biochemistry, 80(1–2), pp. 21–25.

Greenwood, N.N., & Earnshaw, A. (2005) *Chemistry of the Elements,* University of Leeds, 2[ed] edn U.K, pp.977-1001.

Hodge, A., & Nordquest, K. (1971) *Oxovanadium Complexes Containing Bidentate and Oxygen-Sulfur Ligands*, Chemistry Laboratory Bowling Green State University, U.S.A., pp. 491–498.

Housecroft, C. E., & Sharpe, A. G. (2008) *In Inorganic Chemistry*, Pearson Education Limited, , Vol. 3

Hsu, H. F., Chu, W. C., Hung, C. H., & Liao, J. H. (2003) T*he First Example of a Seven-Coordinate Vanadium(III) Thiolate Complex Containing the Hydrazine Molecule, an Intermediate of Nitrogen Fixation*, Inorganic Chemistry, 42(23), pp. 7369–7371.

Itzhak, G.W., Dov, G, Eytan, G, Mati, F., & Yoram, S. (2000) *Insulin –like effect of vanadium basic and clinical implications*.80, 21-25,

Jennifer, L., Esther, G., Rodriguez, & Isupov, M. (2009) *Vanadium containing Bromoperoxidase – Insights into the enzymatic mechanism using X-ray crystallography,* School of Biosciences, University of Exeter, pp. 1–22.

Kanamori, K. Kyotoh, A., Fujimoto, K., Nagata, K., & Suzuki, H. (2001) *Syntheses , Structures , and Properties of Vanadium(III) Complexes with the Hexadentate Ligand , Tetramethylenediamine- N , N , N , N -tetraacetate , Bis (*

2-pyridylmethyl) -1 , 3-propanediamine- N , N -diacetate', *Structure*, The Chemical Society of Japan, pp. 2113–2118.

Kanamori, K., & Tsuge, K. (2012) *Vanadium Biochemical and Molecular Biological Approaches*, Springer Science Business Media B.V, Japan, Chapter 1 pp.3-31

Klich, P. R. Daniher, A. T., Challen, P., Mcconville, D. B., & Youngs, W. J. (1996) *Vanadium (IV) Complexes with Mixed O,S Donor Ligands. Syntheses, Structures, and Properties of the Anions Tris (2-mercapto-4-methylphenolato) vanadate (IV) and Bis (2-mercaptophenolato) oxovanadate (IV),* Inorganic Chemistry, *35*, pp. 347–356.

Korbecki, J., Baranowska, B. I., Gutowska, I., & Chlubek, D. (2012) *Biochemical and medical importance of vanadium compounds*, Acta Biochimica Polonica, 59(2), pp. 195–200.

Ligtenbarg, A.G. J. (2001) *Vanadium and Iron Complexes for Catalytic Oxidation*, University of Groningen Vanadium, Holland, pp.1-13.

Lorber, C., Choukroun, R., & Donnadieu, B. (2003) *Synthesis and crystal structure of unprecedented phosphine adducts of d1-aryl imido-vanadium(IV) complexes* Inorganic Chemistry, 42(3), pp. 673–675.

Messerschmidt, A., & Wever, R. (1996) *X-ray structure of a vanadium-containing enzyme: chloroperoxidase from the fungus Curvularia inaequalis*, Proceedings of the National Academy of Sciences of the United States of America, 93(1), pp. 392–396.

Milani , E ., Nikfar , S., Khorasani , R ., Zamani, M. J. & bdollahi, M. (2005) *Reduction of diabetes induced oxidative stress by phosphodiestrase inhibitors in rats. Comparative Biochemistry and physiology part c*, Toxicology pharmacol, p.p140 251- 255.

Natasha, H. Y. (2004) *Insulin-Mimetic Vanadium IV\V Complexes*, Inorganic

Literature seminar, pp. 52–54

Nakai, M. Sekiguchi, F., Obata, M., Ohtsuki, C., Adachi, Y., Sakurai, H., Orvig, C., Rehder, D., & Yano, S. (2005) *Synthesis and insulin-mimetic activities of metal complexes with 3-hydroxypyridine-2-carboxylic acid*, Journal of Inorganic Biochemistry, 99(6), pp. 1275–1282.

Punithavathi , V. R., Anuthama1, R . & Stanely, M. P. (2008) *Combined treatment with naringin and vitamin C ameliorates streptozotocin-induced diabetes in male Wistar rats. J. Appl. Toxicol., 28, 806–813*

NEJO, A. A. (2009) *Metal (II) Schiff Base Complexes and the Insulin-Mimetic Studies on the Oxovanadium (IV) Complexes*, A Thesis in The Department of Chemistry, University of Zululand, p.17-20.

Rehder, D. (2008) *Bioinorganic vanadium chemistry*, *Department Chemie*, A Wiley Series of Advanced Textbooks, Universty Hamburg, Germany, pp. 1–213.

Santoni, G., & Rehder, D. (2004) *Structural models for the reduced form of vanadate-dependent peroxidases: Vanadyl complexes with bidentate chiral Schiff base ligands*, Journal of Inorganic Biochemistry, 98(5), pp. 758–764.

Sakurai, H., Funakoshi, S. and Adachi, Y. (2005) *New developments of insulinomimetic dinuclear vanadyl(IV)-tartrate complexe*, Pure and Applied Chemistry, 77(9), pp. 1629–1640.

Schijndel, V. Simons, L.H., Vollenbroek, E.G., & Wever, R. (1993) *The vanadium chloroperoxidase from the fungus , Curvularia inaequalis Evidence for the involvement of a histidine residue in the binding of vanadate*, Federation of European Biochemical Societies, 336(2), pp. 239–242.

Thomas, S., Jose, A., Guevara, G., Quoc, T.D., Philippe, B., & Stefan, L. (2016) *Why Antidiabetic Vanadium Complexes are Not in the Pipeline of "Big*

Pharma" Drug Research?, A Critical Review Current Medicinal Chemistry, 23.25pp. 2874–2891.

Tolman, E.L, Barris, M, Burns, M, Pansini, A , & Partidge R.(1979) *Effects of vanadium on glucose metabolism in vitro*, Life sci, 25(13), pp.1159-1164

Vilter, H. (1984) *Peroxidases from Phaeophyceae AVanadium(V) Dependent Peroxidase from Ascophyllum Nodosum*, Phytochemistry, Vol 23(7), pp. 1387–1390.

Wang, D., Ebel, M., Schulzke, C., Grüning, C., Hazari, S., & Rehder, D. (2001) *Vanadium(IV and V) Complexes ContainingSNO (Dithiocarbonylhydrazone; Thiosemicarbazone*, European Journal of Inorganic Chemistry, 2001(4), pp. 935–942.

Wever, R. (2012) *Vanadium Biochemical and Molecular Biological Approache*. Springer Science Business Media B.V, Jaban, Chapter 5, pp.95-123.

Wever, R., Blat. H, & Boer, E.(1985) *Purification of bromoperoxidase*, Biochimica et Biophvsica Acta, 830, pp. 181–186.

Winfried P, (1997) *Vanadium (V) Complexes with Flexible and Hydrolytically Stable Amine Alcohol Ligands and their isomerization in solution: Models for the interaction of Vanadium (V) with biogenic ligands,* Vol 623, journal of Inorganic and General Chemistry ZAAC P.P 461–477.

Wolf, A. V., (1966) *Aqueous Solutions and Body Fluids*, Harper and Row, New York.

Xia, J.B., Cormier, K. W, & Chen, C. (2012) *A highly selective vanadium catalyst for benzylic C–H oxidation*, Chemical Science, 3(7), p.p 2240.